BULLETIN OF
BIOMATHEMATICS

For α=0.9

Editor-in-Chief
Mehmet Yavuz, PhD

BULLETIN OF BIOMATHEMATICS

i

Cabada, Alberto
University of Santiago de Compostela
Spain

Dassios, Ioannis
University College Dublin
Ireland

Eskandari, Zohreh
Shahrekord University
Iran

Flaut, Cristina
Ovidius University of Constanta
Romania

González, Francisco Martínez
Universidad Politécnica de Cartagena
Spain

Gürbüz, Burcu
Johannes Gutenberg-University Mainz, Institute of
Mathematics, *Germany*

Hammouch, Zakia
ENS Moulay Ismail University Morocco;
Thu Dau Mot University Vietnam and China Medical
University, *Taiwan*

Hristov, Jordan
University of Chemical Technology and Metallurgy
Bulgaria

Jafari, Hossein
University of Mazandaran, *Iran*;
University of South Africa, *South Africa*

Jajarmi, Amin
University of Bojnord
Iran

Lupulescu, Vasile
Constantin Brâncuşi University of Târgu-Jiu
Romania

Naik, Parvaiz Ahmad
Department of Mathematics and Computer Science,
Youjiang Medical University for Nationalities, *China*

Owolabi, Kolade
Federal University of Technology
Nigeria

Otero-Espinar, Maria Victoria
University of Santiago de Compostela
Spain

Özdemir, Necati
Balıkesir University
Türkiye

Pinto, Carla M.A.
ISEP, *Portugal*

Povstenko, Yuriy
Jan Dlugosz University in Czestochowa
Poland

Qureshi, Sania
Mehran University of Engineering and Technology
Pakistan

Sabatier, Jocelyn
Bordeaux University
France

Safaei, Mohammad Reza
Florida International University
USA

ii

Salahshour, Soheil
Bahçeşehir University
Türkiye

Sarı, Murat
Yıldız Technical University
Türkiye

Sarris, Ioannis E.
University of West Attica
Greece

Sene, Ndolane
Cheikh Anta Diop University
Senegal

Stamova, Ivanka
University of Texas at San Antonio
USA

Torres, Delfim F. M.
University of Aveiro
Portugal

Townley, Stuart
University of Exeter
United Kingdom

Valdés, Juan Eduardo Nápoles
Universidad Nacional del Nordeste
Argentina

Yang, Xiao-Jun
China University of Mining and Technology
China

Yuan, Sanling
University of Shanghai for Science and Technology
China

Technical Editor

Kerim Sarıgül
Research Information System, Gazi University,
Ankara / TÜRKİYE
kerimsarigul@gazi.edu.tr

English Editors (In Alphabetical Order)

- **Abdulkadir Ünal** - School of Foreign Languages, Foreign Languages, Alanya Alaaddin Keykubat University, Antalya Türkiye.

- **Ahmet Sınak** - Necmettin Erbakan University, Department of Mathematics and Computer Sciences, Konya, Türkiye.

- **Faruk Türk** - Karamanoğlu Mehmetbey University, School of Foreign Languages, Karaman, Türkiye.

Editorial Secretariat

Fatma Özlem Coşar
Department of Mathematics and Computer Sciences,
Faculty of Science, Necmettin Erbakan University,
Meram Yeniyol, 42090 Meram, Konya / TÜRKİYE

Müzeyyen Akman
Department of Mathematics and Computer Sciences,
Faculty of Science, Necmettin Erbakan University,
Meram Yeniyol, 42090 Meram, Konya / TÜRKİYE

iv

Contents

RESEARCH PAPER

Mathematical modeling for the transmission dynamics of cholera with an optimal control strategy

Umar Tasiu Mustapha [ID] 1,*,‡, **Yahaya Adamu Maigoro** [ID] 1,‡, **Abdullahi Yusuf** [ID] 1,2,‡ **and Sania Qureshi** [ID] 3,4,5,‡

[1]Department of Mathematics, Federal University Dutse, 7156 Jigawa, Nigeria, [2]Department of Computer Engineering, Biruni University, 34010 Istanbul, Türkiye, [3]Department of Basic Sciences and Related Studies, Mehran University of Engineering and Technology, Jamshoro 76062, Pakistan, [4]Department of Mathematics, Near East University, 99138 Mersin, Türkiye, [5]Department of Computer Science and Mathematics, Lebanese American University, Beirut, Lebanon

* Corresponding Author
‡ umartasiumustapha@yahoo.com (Umar Tasiu Mustapha); aymaigoro0006@gmail.com (Yahaya Adamu Maigoro); yusufabdullahi@fud.edu.ng (Abdullahi Yusuf); sania.qureshi@faculty.muet.edu.pk (Sania Qureshi)

Abstract

Cholera is an acute diarrheal disease caused by Vibrio cholera, its prevalence occurs in almost all the continents of the world, annually there are about 1.3 to 4.0 million cases of cholera and $21,000$ to $143,000$ deaths worldwide. In this paper, we propose a deterministic model for the transmission dynamics of cholera to assess the impact of vaccines in decreasing the spread of cholera infection in Nigeria. Moreover, we develop an optimal control strategy, in which we consider personal hygiene a control strategy on infection class, with $u(t)$ as the control function. The best values of the fitting parameters have been obtained using least square minimization to validate the model with the help of experimental data obtained from Nigeria. We perform sensitivity analysis to determine the key parameters that have impacts on the control of the spread of cholera infections in the population. In addition, the numerical simulation of the model reveals that the use of vaccines and personal hygiene will effectively control the spread of cholera infection.

Keywords: Basic reproduction number; treatment; model fitting; sensitivity analysis
AMS 2020 Classification: 34C23; 62P10; 92B05; 92D25

1 Introduction

Cholera is a short-term (acute) life-threatening disease caused by a bacterium called Vibrio cholera. The disease attracts the intestine and brings about diarrhea. Cholera exists in different serogroups, but only 01 and 0139 cause outbreaks [1]. Diarrhea is the main symptom of cholera and it is

sometimes called acute diarrheal disease. The diarrhea is accompanied by severe dehydration and can lead to death within hours. The disease is asymptomatic between 12 hours to 5 days after its invasion into humans through ingesting contaminated food or water. However, infected individuals can still shed the bacterium (which can contaminate the environment) and can infect others [2]. People with low immunity "such as malnourished children or people living with HIV have a higher tendency to develop the infection [3].

Cholera is transmitted through ingestion of food or water contaminated with the Vibro cholera bacterium (which implies that unhygienic environments are more susceptible to cholera). The disease can also be transmitted directly through human-to-human contact such as shaking hands [4]. To avoid its transmission, proper sanitation of the environment is required to ensure clean water and food. In addition to ensuring proper hygiene, vaccination is used for the prevention of its prevalence [2]. The disease treatment is by quick replacement of the fluids and salt lost through diarrhea (Oral rehydration solution (ORS) is used) [2]. Recovered cholera patients acquired immunity that prevent them from being infected for many years [5].

Cholera prevalence occurs in almost all the continents of the world. It has been estimated that there are 1.3 to 4.0 million cases of cholera, and $21,000$ to $143,000$ deaths worldwide due to cholera annually [2]. Its pandemic started in 1961 in Indonesia, and it then spread into Europe, the South Pacific, and Japan at the end of 1970*s*. The prevalence reached South America in 1990*s*. Previously, there are many cholera outbreaks in India (2007), Congo, Zimbabwe and Iraq (2008), Zimbabwe and Vietnam (2009), Nigeria and Haiti (2010). In the year 2010 alone, it is estimated that 3–5 million people were infected with cholera which causes the death of $100,000$–$130,000$ people worldwide [6]. In Nigeria, cholera is a recursive disease that occurs annually (during a rainy season). Its first epidemic occurred in 1970 and 1990 with high epidemics in $1992, 1995, 1996$ and 1997. There were 37,289 cholera cases and the disease caused $1,434$ deaths between January and October 2010 as reported by the Federal Ministry of Health. Furthermore, in 2011, $22,797$ cases of cholera with 728 deaths were reported. Nigeria Centre for Disease Control (NCDC) reported 42,466 suspected cases with 830 deaths in 2018 [1]. The NCDC also reported in November 21, 2021 that Nigeria recorded $103,589$ cholera infections and $3,566$ deaths which is greater than the death caused by *covid* -19 (2977) in the same year [7].

Many mathematical models have been developed to study the transmission dynamic of cholera infection and come up with different measures, some of these are: the study by [8] shows that effective control of the epidemic can easily be achieved through vaccination, public health education, and treatment. Hove-Musekwa *et al.*, (2011) recommended that nutritional issues should be addressed in poor communities affected by cholera to reduce the burden of the disease. In order to avoid the cholera outbreak in China, Sun et al. (2017) stated that it might be better to increase the immunization coverage rate and make an effort to improve environmental management, especially for drinking water. Motivated by the aforementioned works, we developed a mathematical model of cholera infection with vaccination as a control measure.

2 Model description

We developed a mathematical model to study the spread of cholera in a human population at time $t > 0$, denoted by $N(t)$, and subdivided into four compartments: Susceptible individuals $S(t)$ (those who are healthy but can acquire the infection) with the infection rate λ; Vaccinated individuals $V(t)$ (those who take the vaccine) but some can acquire the infection at a slower rate $\sigma\lambda$; Infected individuals $I(t)$ (those who are infected with the disease) but can obtain immunity with recovery rate ϕ and Recovered individuals $R(t)$ (those who recovered from the disease). The susceptible individuals are vaccinated at a constant rate ω, while the vaccine wears off at a rate ψ. The population of the bacteria is denoted by $M(t)$ (the concentration of Vibrio Cholerae

(V.C) in contaminating the environment). We use ξ and θ to denote the rate of disinfection and the decay rate of V.C, respectively. We split the transmission rate into two parts. One is environment-to-human transmission rate β_1; and the other is human-to-human transmission rate β_2. The parameter k represents the concentration of the V.C in contaminating the environment which yields 50% chance of acquiring the cholera disease (half-saturation constant of the bacteria population). The force of infection denoted by λ (the rate at which the susceptible individuals acquire the infectious disease) is given by:

$$\lambda = \frac{\beta_1 M}{k + M} + \beta_2 I.$$
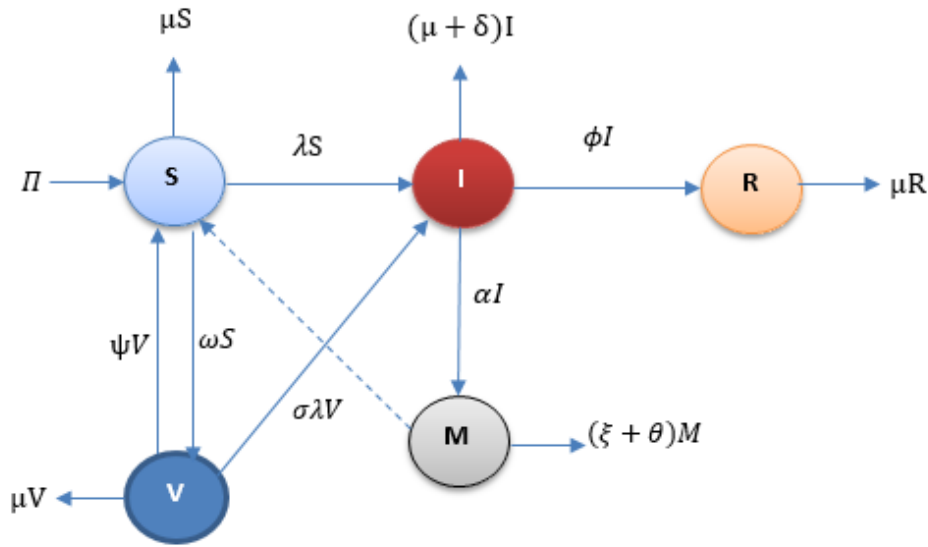
Figure 1. Schematic diagram of the model (1). Solid arrows indicate transitions and expressions next to arrows show the *per ca-pita* flow rate between compartments

According to the diagram above, the dynamics of cholera can be described by the following system of five differential equations.

$$
\begin{aligned}
\frac{dS}{dt} &= \Pi - \lambda S - (\mu + \omega)S + \psi V, \\
\frac{dV}{dt} &= \omega S - (\mu + \psi)V - \sigma \lambda V, \\
\frac{dI}{dt} &= \lambda S - (\mu + \delta + \phi)I + \sigma \lambda V, \\
\frac{dR}{dt} &= \phi I - \mu R, \\
\frac{dM}{dt} &= \alpha I - (\xi + \theta)M.
\end{aligned}
\tag{1}
$$

Table 1. Interpretation of the state variables and parameters used in the model (1)

Variable	Description
N	Total human population
S	Susceptible individuals
I	Infected individuals
V	Vaccinated individuals
R	Recovered individuals
M	Concentration of V.C in contaminating the environment
Parameter	
Π	Recruitment rate
μ	Natural death rate
λ	Force of infection
β_1	Environment to human transmission rate
β_2	Human to human transmission rate
k	Concentration of V.C in the environment
σ	Parameter for decrease of infectiousness in V
δ	V.C induced death rate
ϕ	Recovery rate
α	Rate of human contribution to V.C
θ, ξ	Rate of disinfection in the environment and decay rate of V.C respectively
ω	Vaccination rate
ψ	Vaccine withdrawing period

3 Basic properties of the model

Boundedness and positivity of solutions

The model consists of the human population and bacteria population (V.C). As such the variables and parameters of the model are non-negative.

Theorem 1 *The solution of the model* (1) *within the invariant region are feasible for all $t > 0$,*

$$\Omega = \left\{ (S(t), I(t), V(t), R(t), M(t)) \ \in \ R_+^5 : N \leq \frac{\pi}{\mu}, M \leq \frac{\alpha}{(\xi + \theta)^2} \right\}.$$

Proof It suffices to show that the solution of the model (1) initiated in Ω does not leave the region i.e R_+^5 is positively invariant under the flow of system (1). [9, Theorem 2.1.5]. From the boundedness of Ω it follows that $S(0) > 0, I(0) > 0, V(0) > 0, R(0) > 0$, and $M(0) > 0$. Suppose $S(0)$ and $V(0)$ are not positive, then there exists a time $\tilde{t} > 0$, such that $S(t) > 0$ and $V(t) > 0$ for $t \in [0, \tilde{t})$, and $S(\tilde{t}) = V(\tilde{t}) = 0$. Now, consider the second, and the last part of model (1), we have

$$\frac{dI(t)}{dt} \ \geq \ -(\mu + \delta + \Phi)I(t), \quad \text{for} \ \ t \in [0, \tilde{t}),$$

$$\frac{dM(t)}{dt} \ \geq \ -(\xi + \theta)M(t), \quad \text{for} \ \ t \in [0, \tilde{t}),$$

so that $I(0) > 0$, and $M(0) > 0$ for $t \in [0, \tilde{t})$. Now, from the first and the second part of the model (1), we have

$$\frac{dS(t)}{dt} \ \geq \ -(\mu + \lambda + \omega)S(t), \quad \text{for} \ \ t \in [0, \tilde{t}),$$

$$\frac{dV(t)}{dt} \ \geq \ -(\mu + \psi)V(t), \quad \text{for} \ \ t \in [0, \tilde{t}).$$

Now, $S(0) > 0$, and $V(0) > 0$ which contradict our hypothesis $S(\tilde{t}) = V(\tilde{t}) = 0$. Therefore $S(t)$, and $V(t)$ are positive. To determine the positivity of the remaining variables we can write the remaining part of the model (1) excluding first and the second equation in matrix form as follows:

$$\frac{dY(t)}{dt} = \mathcal{Q}Y(t) + B(t),$$ (2)

with

$$Y(t) = \begin{pmatrix} I & R & M \end{pmatrix}^T,$$

$$\mathcal{Q} = \begin{pmatrix} -(\mu + \delta + \Phi) & 0 & 0 \\ \Phi & \mu & 0 \\ \alpha & 0 & -(\xi + \theta) \end{pmatrix},$$ (3)

$$B(t) = \begin{pmatrix} 0 & 0 & 0 \end{pmatrix}^T.$$

The above matrix $\mathcal{Q}$ is called a Metzler matrix for the fact that $S(t)$ is non-negative. Thus, subsystem (2) is a monotone system [10]. Hence we can conclude that $\mathbb{R}^4_+$ is invariant under the flow of subsystem (2). Therefore, $\mathbb{R}^5_+$ is positively invariant under the flow of system (1).

Disease-free equilibrium

In the absence of the disease, the model system (1) has a disease-free equilibrium which is obtained by setting the right-hand side of the model equations to zero. Thus we have,

$$\epsilon^0 = (S^0, V^0, I^0, R^0, M^0) = \left(\frac{(\mu + \psi)\pi}{\mu(\mu + \omega + \psi)}, \frac{\omega\pi}{\mu(\mu + \omega + \psi)}, 0, 0, 0 \right).$$

Now, the total population at disease-free equilibrium $N(t)$ is,

$$N^0 \le \frac{\pi}{\mu}.$$

Basic reproduction number

The next generation operator method described by [11], was used to determine the basic reproduction number denoted by $R_0 = \rho(FV^{-1})$. The matrices F for the new infection terms and V for the remaining transition terms are given by:

$$F = \begin{bmatrix} \frac{\Pi\beta_2(\mu+\psi)}{(\mu+\omega)(\mu+\psi)-\psi\omega} + \frac{\Pi\beta_2\omega}{(\mu+\omega)(\mu+\psi)-\psi\omega} & \frac{\Pi\beta_1(\mu+\psi)}{k((\mu+\omega)(\mu+\psi)-\psi\omega)} + \frac{\Pi\beta_1\sigma\omega}{k((\mu+\omega)(\mu+\psi)-\psi\omega)} \\ 0 & 0 \end{bmatrix},$$ (4)

$$V = \begin{bmatrix} \mu + \delta + \psi & 0 \\ -\alpha & \xi + \theta \end{bmatrix},$$ (5)

$$V^{-1} = \begin{bmatrix} \frac{1}{\mu+\delta+\phi} & 0 \\ \frac{\alpha}{(\mu+\delta+\phi)(\xi+\theta)} & \frac{1}{\xi+\theta} \end{bmatrix}, \tag{6}$$

$$FV^{-1} = \begin{bmatrix} \frac{\Pi\left((\beta_2(\xi+\theta)k+\alpha\beta_1)\mu+\beta_2\psi\,(\xi+\theta)k+\beta_1\alpha\,(\omega\sigma+\psi)\right)}{k\mu\,(\mu+\psi+\omega)(\mu+\delta+\phi)(\xi+\theta)} & \frac{\Pi\beta_1(\omega\sigma+\mu+\psi)}{k\mu\,(\mu+\psi+\omega)(\xi+\theta)} \\ 0 & 0 \end{bmatrix}. \tag{7}$$

We determine the basic reproduction number as follows:

$$R_0 = \frac{\Pi\left((\beta_2\,(\xi+\theta)\,k+\alpha\,\beta_1)\,\mu+\beta_2\psi\,(\xi+\theta)\,k+\alpha\,\beta_1\,(\omega\,\sigma+\psi)\right)}{k\mu\,(\mu+\psi+\omega)\,(\mu+\delta+\phi)\,(\xi+\theta)}.$$

Using the proof from Theorem 2 of [11], if the reproduction number is less than one, the disease-free equilibrium point is locally stable and the population can not be invaded by the disease. Hence, the proof of the following theorem holds.

Theorem 2 *The disease-free equilibrium (DFE) T_0, of the model* (1), *is locally-asymptotically stable (LAS) in Ω if $R_0 < 1$, and unstable if $R_0 > 1$.*

Interpretation of the basic reproduction number

The threshold parameter (R_0) is interpreted as the number of secondary cases produced by a single cholera-infected individual in a completely susceptible population.

Global stability of disease-free equilibrium

Theorem 3 *The disease-free equilibrium (DFE) ϵ^0, of the model* (1), *is globally-asymptotically stable (GAS) in Ω if $R_0 < 1$, and unstable if $R_0 > 1$.*

Proof To show the GAS of DFE, the two condition $[F_1]$, and $[F_2]$ for $R_0 < 1$, need to be satisfied [12]. The system of (1) is re-write as.

$$\begin{aligned} \frac{dY_1}{dt} &= F_1(Y_1, Y_2), \\ \frac{dY_2}{dt} &= F_2(Y_1, Y_2) : F_2(Y_1, 0) = 0, \end{aligned} \tag{8}$$

where $Y_1 = (S^0, V^0, R^0)$, and $Y_2 = (I^0, M^0)$, with the elements of $Y_1 \in R_+^3$, representing the uninfected population and the elements of $Y_2 \in R_+^2$, representing the infected population. The DFE is now denoted as, $\epsilon^0 = (Y_1^*, 0)$, where $Y_1^* = (N^0, 0)$. Now for the first condition, that is GAS of Y_1^*, gives

$$\frac{dY_1}{dt} = F_1(Y_1, 0) = \begin{bmatrix} \pi - (\mu+\omega)S^0 + \psi V \\ \omega S - (\mu+\psi)V^0 \\ -\mu R \end{bmatrix}. \tag{9}$$

Solving the linear differential equations gives,

$$S^0(t) = \frac{\pi + \psi V}{(\mu + \omega)} - \frac{\pi + \psi V}{(\mu + \omega)}e^{-(\mu+\omega)t} + S^0(0)e^{-(\mu+\omega)t},$$

$$V^0(t) = \frac{\omega S}{\mu + \psi} - \frac{\omega S}{\mu + \psi}e^{-(\mu+\psi)t} + V^0(0)e^{-(\mu+\psi)t},$$

$$R^0(t) = R(0)e^{-(\mu)t}.$$

Now, it is easy to show that $S^0(t) + V^0(t) + R^0(t) \to N^0(t)$, as $t \to \infty$, regardless of the value of $S^0(t), V^0(t)$ and, $R^0(t)$. Thus, $Y_1^* = (N^0, 0)$ is globally asymptotically stable.
Furthermore, for the second condition, that is $\tilde{F}_2(Y_1, Y_2) = BY_2 - F_2(Y_1, Y_2)$, gives:

$$B = \begin{pmatrix} \beta_2 S - (\mu + \delta + \phi) + \sigma\beta_2 V & \frac{\beta_1 Sk}{(k+M)^2} + \frac{\sigma\beta_1 Vk}{(k+M)^2} \\ \alpha & -(\xi + \theta) \end{pmatrix}. \tag{10}$$

This is a Metziller matrix

$$F_2(Y_1, Y_2) = \begin{pmatrix} \lambda S - (\mu + \delta + \phi)I + \sigma\lambda V \\ \alpha I - (\xi + \theta)M \end{pmatrix}. \tag{11}$$

Then,

$$\tilde{F}_2(Y_1, Y_2) = BY_2 - F_2(Y_1, Y_2) = \begin{bmatrix} 0 \\ 0 \end{bmatrix}.$$

Thus, we have

$$\tilde{F}_2(Y_1, Y_2) = \begin{bmatrix} 0 & 0 \end{bmatrix}^T.$$

It is clear that $\tilde{F}_2(Y_1, Y_2) = 0$. Hence, the two conditions are satisfied, guaranteeing the global stability of the disease-free equilibrium.

Endemic equilibrium point

The conditions $I \neq 0$ and $M \neq 0$ imply that the cholera invades the population. As such, setting the vector field of (1) to zero, we obtain the equilibrium point at the endemic state as:

$$\epsilon^* = (S^*, V^*, I^*, R^*, S^*),$$

$$S^* = \frac{\pi(\sigma\lambda + \mu + \psi)}{\sigma\lambda^2 + \sigma\lambda\mu + \sigma\lambda\omega + \mu\lambda + \lambda\psi + \mu^2 + \mu\omega + \mu\psi},$$

$$V^* = \frac{\pi\omega}{\sigma\lambda^2 + \sigma\lambda\mu + \sigma\lambda\omega + \mu\lambda + \lambda\psi + \mu^2 + \mu\omega + \mu\psi},$$

$$I^* = \frac{\lambda\pi(\sigma\lambda + \sigma\omega + \mu + \psi)}{(\mu + \delta + \phi)(\sigma\lambda^2 + \sigma\lambda\mu + \sigma\lambda\omega + \mu\lambda + \lambda\psi + \mu^2 + \mu\omega + \mu\psi)},$$

$$R^* = \frac{\phi\lambda\pi(\sigma\lambda + \sigma\omega + \mu + \psi)}{\mu(\mu + \delta + \phi)(\sigma\lambda^2 + \sigma\lambda\mu + \sigma\lambda\omega + \mu\lambda + \lambda\psi + \mu^2 + \mu\omega + \mu\psi)},$$

$$\tag{12}$$

$$M^* = \frac{\alpha \lambda \pi \left(\sigma \lambda + \sigma \omega + \mu + \psi\right)}{(\xi + \theta)(\mu + \delta + \phi)(\sigma \lambda^2 + \sigma \lambda \mu + \sigma \lambda \omega + \mu \lambda + \lambda \psi + \mu^2 + \mu \omega + \mu \psi)}.$$

Existence of the endemic equilibrium

To determine the existence of the endemic equilibrium, Descartes's rule of sign is used. Now the force of infection at the endemic state is given by,

$$\lambda^* = \frac{\beta_1 M^*}{k + M^*} + \beta_2 I^*.$$

Substituting the endemic equilibrium points into the above force of infection gives $\lambda^* = 0$, and the polynomial of order four is obtained in the form of λ^*

$$A\lambda^{*4} + B\lambda^{*3} + C\lambda^{*2} + D\lambda^* + E = 0,$$

where

$$
\begin{aligned}
A =\ & k(\xi + \theta)(\mu + \delta + \phi)^2\sigma^2 + \Pi\alpha(\mu + \delta + \phi)\sigma^2, \\
B =\ & 2k(\xi + \theta)(\mu + \delta + \psi)^2(\sigma\mu + \mu^2 + \mu\omega + \mu\phi)\sigma + \Pi\alpha\sigma(\mu + \delta + \phi)(\sigma\mu + 2\sigma\omega + 2\mu + 2\psi) \\
& - \Pi\alpha\beta_1\sigma^2(\mu + \delta + \phi) - \Pi\beta_2\alpha k(\xi + \theta)(\mu + \delta + \phi)\sigma^2 - \Pi^2\beta_2\alpha\sigma^2, \\
C =\ & k(\xi + \theta)(\mu + \delta + \phi)[2\sigma(\mu^2 + \mu\omega + \mu\psi) + (\sigma\mu + \sigma\omega + \mu + \psi)^2] + \Pi\alpha(\mu + \delta + \phi)[\sigma(\mu^2 + \mu\omega + \mu\psi) \\
& + (\sigma\omega + \mu + \psi)(\sigma\mu + \sigma\omega + \mu + \psi)] - \Pi\alpha\beta_1(\mu + \delta + \phi)(\sigma\mu + 2\sigma\omega + 2\mu + 2\psi)\sigma \\
& - \Pi\beta_2 k(\xi + \theta)(\mu + \delta + \phi)(\sigma\mu + 2\sigma\omega + 2\mu + 2\psi)\sigma - 2\Pi^2\alpha\beta_2(\sigma\omega + \mu + \psi)\sigma, \\
D =\ & 2k(\xi + \theta)(\mu + \delta + \phi)^2(\sigma\mu + \sigma\omega + \mu + \psi)(\mu^2 + \mu\omega + \mu\psi) + \Pi\alpha\beta_1(\mu + \delta + \phi)[(\mu^2 + \mu\omega + \mu\psi)\sigma \\
& + (\sigma\omega + \mu + \psi)(\sigma\mu + \sigma\omega + \mu + \psi)] - \Pi\beta_2 k(\xi + \theta)(\mu + \delta + \phi)[(\mu^2 + \mu\omega + \mu\psi)\sigma \\
& + (\sigma\omega + \mu + \psi)(\sigma\mu + \sigma\omega + \mu + \psi)] - \Pi^2\alpha\beta_2(\sigma\omega + \mu + \phi)^2, \\
E =\ & k(\xi + \theta)(\mu + \delta + \phi)^2(\mu^2 + \mu\omega + \mu\psi)^2[1 - R_0].
\end{aligned}
$$

$$\text{(13)}$$

Global stability of endemic equilibrium

Theorem 4 *If $R_0 > 1$, the endemic equilibrium ϵ^* is globally asymptotically stable.*

Proof We construct a Lyapunov function

$$
\begin{aligned}
F =\ & \left(S - S^* - S^*ln\left(\frac{S}{S^*}\right)\right) + \left(V - V^* - V^*ln\left(\frac{V}{V^*}\right)\right) + \left(I - I^* - I^*ln\left(\frac{I}{I^*}\right)\right) \\
& + \left(R - R^* - R^*ln\left(\frac{R}{R^*}\right)\right) + \left(M - M^* - M^*ln\left(\frac{M}{M^*}\right)\right).
\end{aligned}
$$

$$\text{(14)}$$

The derivative of along the solution of model Eq. (1) is:

$$
\begin{aligned}
F' =\ & \Pi - \lambda S - (\mu + \omega)S - \frac{S^*}{S}(\Pi - \lambda S - (\mu + \omega)S) + \omega S - \sigma\lambda V - \mu V - \frac{V^*}{V}(\omega S - \sigma\lambda V - \mu V) \\
& + \lambda S - (\mu + \phi)I + \sigma\lambda V - \frac{I^*}{I}(\lambda S - (\mu + \phi)I + \sigma\lambda V) + \phi I - \mu R - \frac{R^*}{R}(\phi I - \mu R) \\
& + \alpha I - (\xi + \theta)M - \frac{M^*}{M}(\alpha I - (\xi + \theta)M).
\end{aligned}
$$

At steady state:

$$\Pi = \lambda S^* + (\mu + \omega)S^*,$$
$$(\mu + \phi)I^* = \lambda S^* + \sigma \lambda V^*,$$
$$\omega S^* = (\mu + \psi)V^* + \sigma \lambda V^*,$$
$$\phi I^* = \mu R^*,$$
$$\alpha I^* = (\xi + \theta)M^*.$$

Using the above relation we have:

$$F' \leqslant (\mu + \omega)S^* \left(2 - \frac{S}{S^*} - \frac{S^*}{S}\right) + \lambda S^* \left(3 - \frac{S^*}{S} - \frac{I}{I^*} - \frac{I^*}{I}\right) + \mu V^* \left(2 - \frac{V}{V^*} - \frac{V^*}{V}\right)$$
$$+ \sigma \lambda V^* \left(3 - \frac{I}{I^*} - \frac{I^*}{I} - \frac{V^*}{V}\right) + \mu R^* \left(2 - \frac{R}{R^*} - \frac{R^*}{R}\right) + M^*(\xi + \theta) \left(2 - \frac{M}{M^*} - \frac{M^*}{M}\right).$$

Since the arithmetic mean is greater than the geometric mean we have:

$$\left(2 - \frac{S}{S^*} - \frac{S^*}{S}\right) \leqslant 0, \left(3 - \frac{S^*}{S} - \frac{I}{I^*} - \frac{I^*}{I}\right) \leqslant 0, \left(2 - \frac{V}{V^*} - \frac{V^*}{V}\right) \leqslant 0,$$
$$\left(3 - \frac{I}{I^*} - \frac{I^*}{I} - \frac{V^*}{V}\right) \leqslant 0, \left(2 - \frac{R}{R^*} - \frac{R^*}{R}\right) \leqslant 0, \left(2 - \frac{M}{M^*} - \frac{M^*}{M}\right) \leqslant 0,$$

thus, we have that $F' \leqslant 0$ for $R_0 > 1$, since the relevant variables in the equations for $S(t)^*, V(t)^*$, $I(t)^*, R(t)^*, M(t)^*$ are at endemic steady state, it follows that these can be substituted into the equations for $S(t), V(t), I(t), R(t)$ and $M(t)$. Therefore, the result follows by applying the LaSalle's invariance principle [13]. Hence the endemic equilibrium (EE) ϵ^* of model (1) is globally asymptotically stable (GAS).

4 Designing the optimal control problem

Optimal control involves the determination of a piece-wise control variable $u(t)$, and the associated state variables $x(t)$, that minimize the number of infectious individuals and the cost of controlling the infection. In this paper, we use personal hygiene as a control strategy on the basic model of cholera transmission which symbolizes $u(t)$. Moreover, the controlled system is as follows:

$$\frac{dS}{dt} = \Pi - u(t)\lambda S - (\mu + \omega)S + \psi V,$$
$$\frac{dV}{dt} = \omega S - (\mu + \psi)V - u(t)\sigma \lambda V,$$
$$\frac{dI}{dt} = u(t)\lambda S - (\mu + \delta + \phi)I + u(t)\sigma \lambda V, \qquad (15)$$
$$\frac{dR}{dt} = \phi I - \mu R,$$
$$\frac{dM}{dt} = \alpha I - (\xi + \theta),$$

with $S(0) = S_0, V(0) = V_0, I(0) = I_0, R(0) = R_0, M(0) = M_0$.
The single-objective function called the cost functional $J[x(t), u(t)]$ to be minimized for our

problem is given by:

$$J[x(t), u(t)] = \int_0^{t_f} \left(aI + \frac{1}{2}wu^2 \right) dt, \tag{16}$$

where $a > 0$, $w > 0$, and the terms aI and $\frac{1}{2}wu^2$ represent the cost of infection and the cost of personal hygiene, respectively. The condition associated with the cost is nonlinear, and therefore we perceive the cost expression to be quadratic ($\frac{1}{2}w_i u_i^2$). $u(t)$ is a piece-wise continuous in the set of admissible control $U = \{(u(t)) : 0 \leq u(t) \leq 1\}$. The aim is to determine the optimal control u^* such that

$$J(u^*) = \min_{(u(t)) \in U} J(u(t)).$$

Thus, we show that an optimal control u^* for system (15) exists. Also, we are to highlight that the system (15) is bounded for finite time [14]. We extend to find the upper bound solutions (super solutions) of S, V, I, R and M in model (15). Now, we consider the first equation of (15).

Existence of an optimal control on the system

We can prove the existence of optimal control by using the method used by [15]. For more details, see [[16], Theorem 6, pp. 6].

Let S_{max}, be the super solution associated with S. Given that $S(t) \geq 0$, and $V(t) \geq 0$ as proved in Theorem 1, then

$$\frac{dS_{max}}{dt} = \Pi + \psi V.$$

Similarly, Let V_{max}, I_{max}, R_{max}, and M_{max} be the super solution associated with V, I, R, and M respectively in (15). Given that $I(t) \geq 0$, $R(t) \geq 0$, and $I(t) \geq 0$ then,

$$\frac{dV_{max}}{dt} = \omega S,$$
$$\frac{dI_{max}}{dt} = \lambda S + \sigma \lambda V,$$
$$\frac{dR_{max}}{dt} = \phi I,$$
$$\frac{dM_{max}}{dt} = \alpha S.$$

We can formulate a set of super solutions for system (15), by using the bounds. Denoting these super solutions by $\overline{S}, \overline{V}, \overline{I}, \overline{R}$, and $\overline{M}$ such as:

$$\begin{bmatrix} \frac{d\overline{S}}{dt} \\ \frac{d\overline{V}}{dt} \\ \frac{d\overline{I}}{dt} \\ \frac{d\overline{R}}{dt} \\ \frac{d\overline{M}}{dt} \end{bmatrix} = \begin{pmatrix} 0 & \psi & 0 & 0 & 0 \\ \omega & 0 & 0 & 0 & 0 \\ \lambda_{max} & \sigma\lambda_{max} & 0 & 0 & 0 \\ 0 & 0 & \psi & 0 & 0 \\ 0 & 0 & \alpha & 0 & 0 \end{pmatrix} \begin{pmatrix} \overline{S} \\ \overline{V} \\ \overline{I} \\ \overline{R} \\ \overline{M} \end{pmatrix} + \begin{pmatrix} \pi \\ 0 \\ 0 \\ 0 \\ 0 \end{pmatrix} = \begin{pmatrix} 0 \\ 0 \\ 0 \\ 0 \\ 0 \end{pmatrix}. \tag{17}$$

It shows that this is a linear system in finite time with bounded coefficients, hence, the super-

solutions $\overline{S}, \overline{V}, \overline{I}, \overline{R}$, and $\overline{M}$ are uniformly bounded. Likewise, our original system is ultimately bounded. It shows that an optimal control exists.

Hamiltonian and optimality of the system

We used Pontryagin's Maximum Principle, which provides the necessary and sufficient conditions for optimality, to prove the optimality of the system. To obtain that, we need to write in detail, the Hamiltonian. The Hamiltonian (H) is generally symbolized as:

$$H = L + \lambda_1 \frac{dS}{dt} + \lambda_2 \frac{dV}{dt} + \lambda_3 \frac{dI}{dt} + \lambda_4 \frac{dR}{dt} + \lambda_5 \frac{dM}{dt}, \tag{18}$$

where L is the Lagrangian, obtained from the objective function. The Hamiltonian associated with the system under study is given by:

$$\begin{aligned} H =& aI + \frac{1}{2}wu^2 + \lambda_1 \left(\Pi - u(t)\lambda S - (\mu + \omega)S + \psi V\right) + \lambda_2 \left(\omega S - (\mu + \psi)V - u(t)\sigma\lambda V\right) \\ &+ \lambda_3 \left(u(t)\lambda S - (\mu + \delta + \phi)I + u(t)\sigma\lambda V\right) + \lambda_4 \left(\phi I - \mu R\right) + \lambda_5 \left(\alpha I - (\xi + \theta)\right), \end{aligned} \tag{19}$$

where $\lambda_1, \lambda_2, \lambda_3, \lambda_4$, and λ_5 are called the adjoint variables to be determined. We now state the following theorem.

Theorem 5 *Given the optimal control set $u(t)$ together with the corresponding solution, S, V, I, R, and M which minimize $J(u(t))$ over U, then there exist adjoint variables $\lambda_1, \lambda_2, \lambda_3, \lambda_4$, and λ_5 such that*

$$\begin{aligned} \frac{d\lambda_1}{dt} &= \lambda_1 \left(u(t)\lambda + \mu + \omega\right) - \lambda_2\omega - \lambda_3 u(t)\lambda, \\ \frac{d\lambda_2}{dt} &= -\lambda_1\psi + \lambda_2(\mu + \psi + u(t)\sigma\lambda) - \lambda_3 u(t)\sigma\lambda, \\ \frac{d\lambda_3}{dt} &= -a + u(t)\beta_2[\lambda_1 S + \lambda_2\sigma V - \lambda_3(S + \sigma V)] + (\mu + \sigma + \phi)\lambda_3 - \phi\lambda_4 - \alpha\lambda_5, \\ \frac{d\lambda_4}{dt} &= \mu\lambda_4, \\ \frac{d\lambda_5}{dt} &= -\frac{\beta_1 k}{(k + M)^2}[S\lambda_1 + u(t)\sigma\lambda_2 V - (S + \sigma V)u(t)\lambda_3] + (\xi + \theta)\lambda_5, \end{aligned} \tag{20}$$

with transversality conditions $\lambda_i(t_f) = 0, i = 1, ..., 5$. Moreover,

$$u^* = \min\left(\max\left(\frac{\lambda[\lambda_1 S + \lambda_2\sigma V - \lambda_3(S + \sigma V)]}{w}, 0\right), 1\right). \tag{21}$$

Proof As stated above, we applied the Pontraygin's Maximum Principle to determine the adjoint variables and the representations of the control functions Since the control functions exist. For the adjoint variables we proceed as follows:

$$\begin{aligned} \frac{d\lambda_1}{dt} &= -\frac{\partial H}{\partial S} = -[\lambda_1(-u(t)\lambda - (\mu + \omega)) + \lambda_2\omega + \lambda_3 u(t)\lambda] = \lambda_1\left(u(t)\lambda + \mu + \omega\right) - \lambda_2\omega - \lambda_3 u(t)\lambda, \\ \frac{d\lambda_2}{dt} &= -\frac{\partial H}{\partial V} = -[-\lambda\psi - \lambda_2(\mu + \psi + u(t)\sigma\lambda) + \lambda_3 u(t)\sigma\lambda] \\ &= -\lambda_1\psi + \lambda_2(\mu + \psi + u(t)\sigma\lambda) - \lambda_3 u(t)\sigma\lambda, \end{aligned}$$

$$\frac{d\lambda_3}{dt} = -\frac{\partial H}{\partial I} = -a + u(t)\beta_2[\lambda_1 S + \lambda_2 \sigma V - \lambda_3(S + \sigma V)] + (\mu + \sigma + \phi)\lambda_3 - \phi\lambda_4 - \alpha\lambda_5,$$

$$\frac{d\lambda_4}{dt} = -\frac{\partial H}{\partial R} = -(-\mu\lambda_4) = \mu\lambda_4,$$

$$\frac{d\lambda_5}{dt} = \frac{\partial H}{\partial M} = -\left(-\frac{\lambda_1\beta_1 Sk}{(k+M)^2} - \frac{\lambda_2\beta_1\sigma u(t)Vk}{(k+M)^2} + \frac{\lambda_3\beta_1 u(t)Sk}{(k+M)^2} + \frac{\lambda_3\beta_1\sigma u(t)Vk}{(k+M)^2} - (\xi+\theta)\lambda_5\right)$$

$$= -\frac{\beta_1 k}{(k+M)^2}[S\lambda_1 + u(t)\sigma\lambda_2 V - (S+\sigma V)u(t)\lambda_3] + (\xi+\theta)\lambda_5.$$

$$(22)$$

The illustrations of the controls is given by:

$$\frac{\partial H}{\partial u(t)} = 0,$$

at $u(t) = u(t)^*$. Thus, the standard optimality argument is:

$$u(t)^* = \min\left(\max\left(\frac{\lambda[\lambda_1 S + \lambda_2\sigma V - \lambda_3(S+\sigma V)]}{w}, 0\right), 1\right). \tag{23}$$

Based on the results of the above Theorem 5, which imply that after obtaining the terms for the control function u^*, as well as the adjoint equations with their transversality conditions. We suggest the optimal control terms for minimizing the spread of cholera transmission.

5 Model fitting and parameter estimation

This section is devoted to fitting some unavailable biological parameters of the proposed five-dimensional epidemic model for cholera disease. It also assists one to have built confidence in the model proposed, for the validation comes along. Such vital analyses are possible only when some authentic information for the real experimental data for the disease under investigation is available. When the data set for the actual infected cases is arranged, there comes the question of a method that could be chosen for validation of the model with the help of an experimental data set. It may be noted that several methods exist in the present literature for the fitting of a nonlinear system of ordinary differential equations to the experimental results, we resort to least-squares minimization. Under this method, the best values of the fitting parameters can be obtained, including respective standard errors, statistical estimators (like the t-statistic and p-value), and confidence intervals.

The available parameters of the model (1) are shown in Table 2 wherein their units and the sources where-from they are taken are also mentioned. The two most important parameters β_1, and β_2 are fitted with their best estimates as shown in Table 3 that accompanies some statistical estimators as well. The p-values are < 0.05 with 95% confidence intervals for both estimated parameters, including reasonably small standard error with acceptable t-statistic.

Moreover, the descriptive statistical measures for both real and predicted cases are shown in Table 4 where minimum, three quartiles, mean, maximum and standard deviation can be observed. Each value from the real cases is found to have good agreement with what is obtained via simulations for the I compartment including the smaller standard deviation in the predicted cases. It may also be noted the interquartile range (IQR) for both cases is identical to be 5.7750×10^2, thereby containing middle 50% of the data. Figure 2 further confirms the better agreement of the predicted cholera cases with the real cases of the disease having R-squared (coefficient of determination) value to be about 0.9376, including some residuals which are uniformly distributed as shown in

multiple types of residuals in Figure 3. Some outliers are observed in the cholera cases (real and predicted) as shown by the box and whisker plot in Figure 4.

Table 2. Baseline values, units, and references for parameters of model (1)

Parameter	Baseline	Units	Sources
N	20616716	Persons	[17]
μ	$1/(11.4 \times 52)$	week^{-1}	[18]
Π	$36.855 \times \mu$	week^{-1}	[17]
k	1	$Cells.mL^{-1}$	[18]
σ	0.127	week^{-1}	[17]
δ	0.47	week^{-1}	[17]
ϕ	1.4	week^{-1}	[18]
α	2000	$Cells.mL^{-1}.week^{-1}$	[18]
θ	0.07	week^{-1}	[18]
ξ	0.2331	week^{-1}	[18]
ω	0.149	week^{-1}	[8]
ψ	0.021	week^{-1}	[8]

Table 3. The best fit parameters of the model (1) with the respective statistical estimators

	Estimate	Standard Error	t-Statistic	P-Value	Confidence Interval
β_1	4.3208×10^{-5}	1.2003×10^{-5}	3.5998	2.0480×10^{-3}	$(1.7991 \times 10^{-5}, 6.8425 \times 10^{-5})$
β_2	7.0320×10^{-8}	6.6760×10^{-9}	1.0533×10^{1}	3.9918×10^{-9}	$(5.6294 \times 10^{-8}, 8.4345 \times 10^{-8})$

Table 4. The descriptive statistical summary for both real experimental data and the simulations predicted from model (1) for I compartment

	Min	Q1	Q2	Q3	Mean	Max	SD
Real	4.600×10^{1}	7.800×10^{1}	2.540×10^{2}	6.330×10^{2}	5.535×10^{2}	2.127×10^{3}	6.406×10^{2}
Predicted	1.554×10^{2}	1.821×10^{2}	2.661×10^{2}	6.145×10^{2}	5.783×10^{2}	2.127×10^{3}	6.077×10^{2}
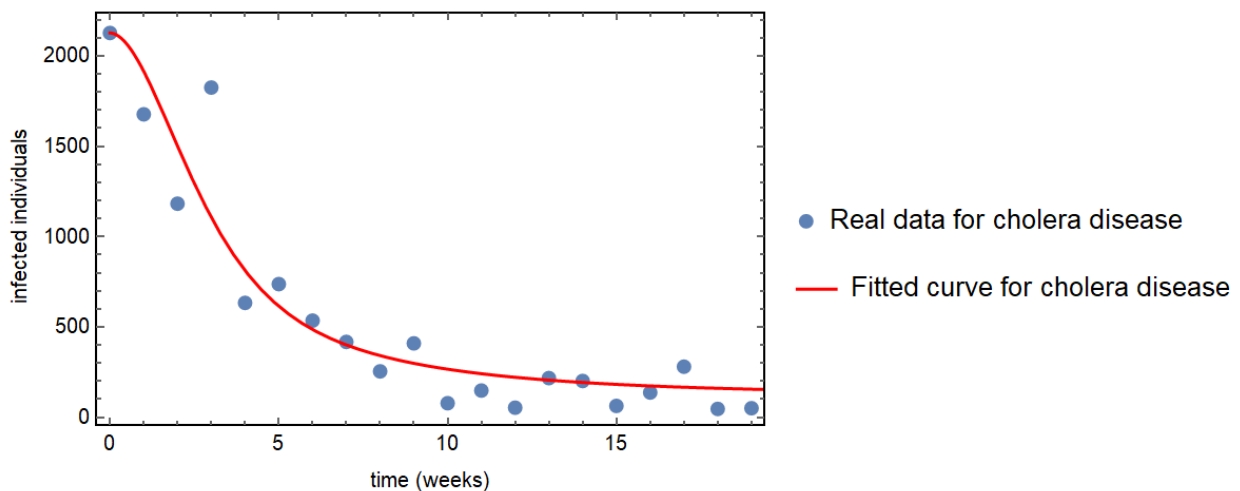
Figure 2. The best curve fitting for the real cases of the infected individuals from the proposed cholera model (1)
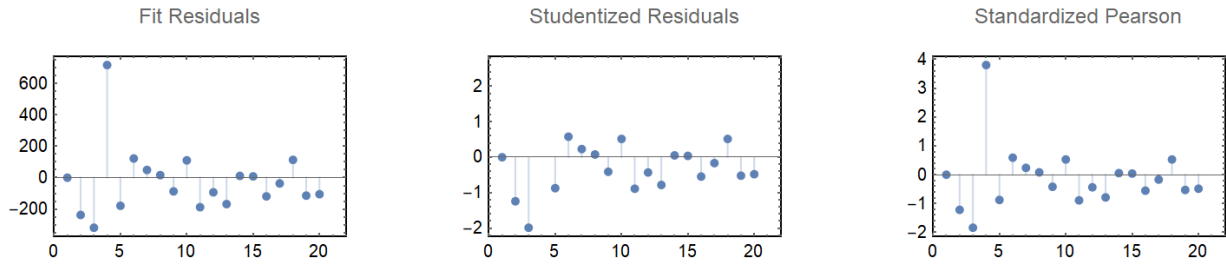
Figure 3. The residuals for the real cases of the infected individuals from the proposed cholera model (1)
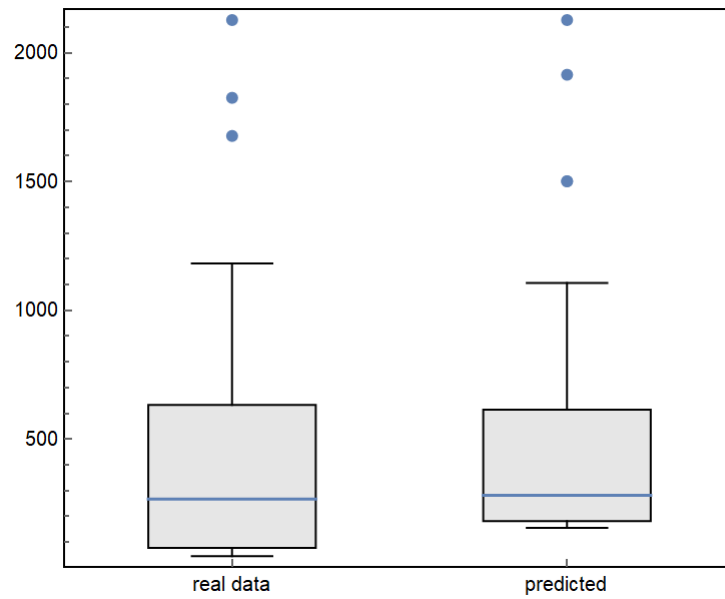
Figure 4. The comparison between real and predicted symptomatically infected individuals via BoxWhisker plot
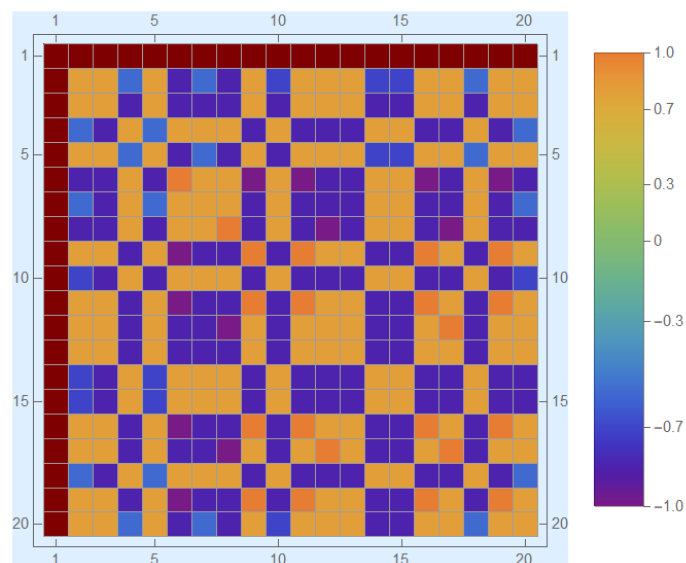
Figure 5. Contour plots of the basic reproduction number in terms of parameter values

6 Sensitivity analysis

In this section, the proposed cholera model associated with the basic reproduction number R_0 with respect to the biological parameters of the model is analyzed using the forward sensitivity index. This method is applied to determine the most sensitive parameters of the model, parameters with positive signs are considered the most sensitive for increasing the value of R_0 while those with negative signs are sensitive to the decrease of R_0 [15, 19]. We determine the sensitivity status of each parameter and their impacts on the control of the spread of cholera infections in the population to obtain the optimal result [20, 21]. The normalized local sensitivity index of R_0 with respect to ξ is denoted by $\chi_\xi^{R_0}$ which is written as

$$\chi_\xi^{R_0} = \frac{\xi}{R_0} \times \frac{\partial R_0}{\partial \xi}, \tag{24}$$

Table 5 shows the indices for R_0 with respect to parameters.

Table 5. Forward normalized sensitivity indices

Parameter	Elasticity Indices	Values of the Elasticity index
β_1	$\chi_{\beta_1}^{R_0}$	1.0000
k	$\chi_k^{R_0}$	-1.0000
ω	$\chi_\omega^{R_0}$	-0.4132
α	$\chi_\alpha^{R_0}$	1.0000
ξ	$\chi_\xi^{R_0}$	-0.7691
ϕ	$\chi_\phi^{R_0}$	-0.7480
θ	$\chi_\theta^{R_0}$	-0.2310
δ	$\chi_\delta^{R_0}$	-0.2511
ψ	$\chi_{\beta_2}^{R_0}$	0.3822
σ	$\chi_\sigma^{R_0}$	0.4546

7 Numerical scenarios

This is the section in which the behavior of the model is examined. The transmission dynamics of the governing model may be effectively explored using numerical simulations with the aid of state variables of interest. The numerical simulations are used to understand the behavior of the model under investigation. The parameters generated by the nonlinear minimum-squares fitting technique are used in the immediate section to determine different types of time series graphs. $S[0] = 20614589, I[0] = 2127, V[0] = 0, R[0] = 0, M[0] = 0.$

8 Discussion and conclusions

This research describes a deterministic model for the transmission dynamics of cholera infection incorporating vaccine and personal hygiene as strategies for controlling its spread. Analysis of the model shows that the disease-free equilibrium is locally and globally asymptotically stable when $R_0 < 1$, and unstable when $R_0 > 1$. Lyapunov function method is used in verifying the stability of the endemic equilibrium point which is found to be globally asymptotically stable when $R_0 > 1$, and unstable when $R_0 < 1$. The numerical simulations have been carried out using the data published by the Nigeria Centre for Disease Control [17]. A detailed explanation of the
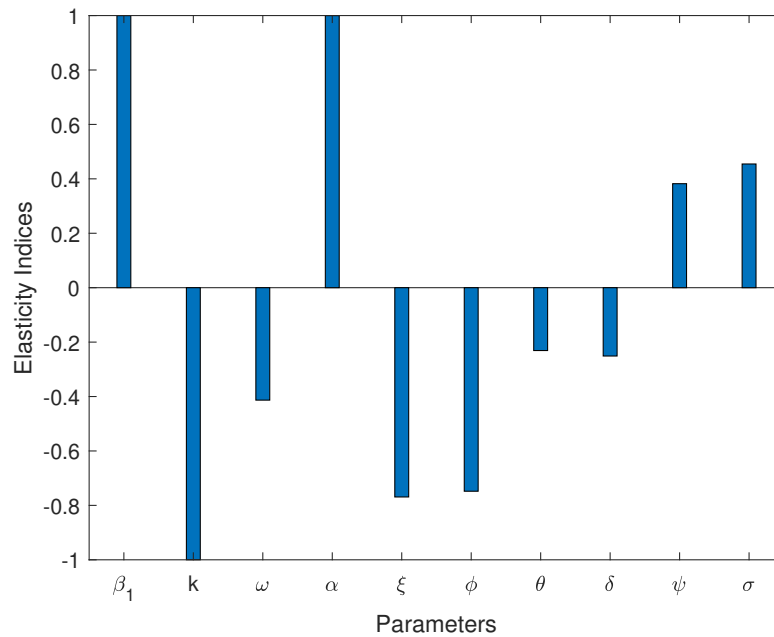
Figure 6. Elasticity indices versus parameters
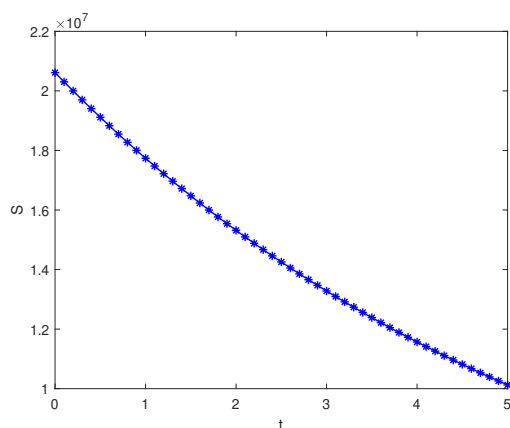
(a) Behavior of the state variable susceptible individual S
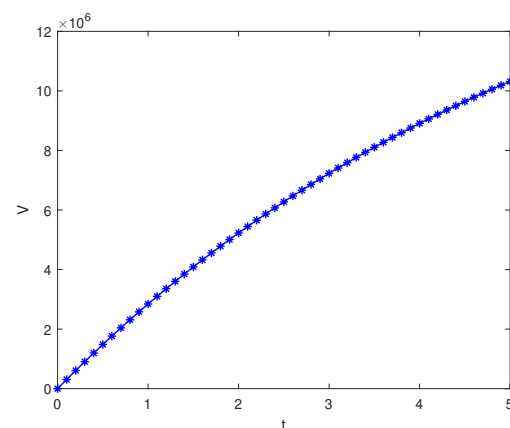
(b) Behavior of the state variable vaccinated individual V

method followed for the model fitting was described in Section 4. The fitted parameters of the model are summarized in Table 2. The most sensitive parameters for controlling the spread of cholera infection are determined using the forward sensitivity index method, these parameters with their elasticity index are summarized in Table 5. Patterns of the susceptible, vaccinated, infected, recovered and concentration of V.C in contaminating the environment are described in Figure 7a, Figure 7b, Figure 8a, Figure 8b and Figure 9, respectively. The effect of the rate of human contribution to V.C on the concentration of V.C in contaminating the environment is shown in Figure 10a. The figure shows that a decrease in contaminating the environment can reduce environmental transmission. Figure 10b shows that as the chance of becoming infected by vaccinated individuals decreases, the number of infected individuals also decreases, which implies that the disease control is dependent on the efficacy of the vaccine. Figure 11a shows that an increase in the rate of disinfection of the environment results to the decrease in the environmental cholera transmission. This implies that proper sanitation can control the environmental transmission of V.C. Nevertheless, the optimal control described in Section 4 shows that proper sanitation will
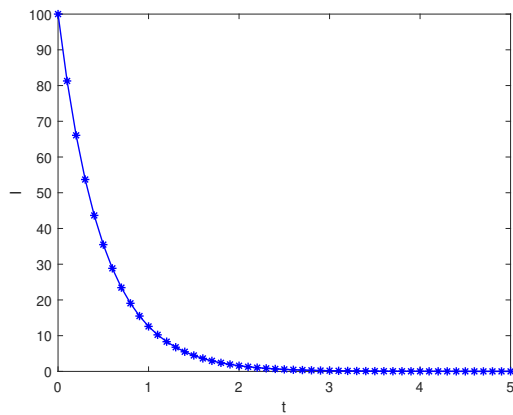
(a) Behavior of the state variable infected individual I
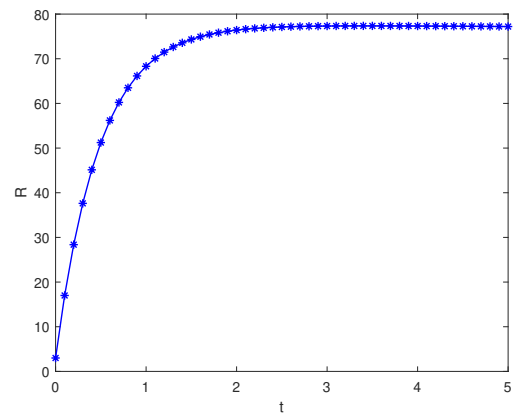
(b) Behavior of the state variable recovered individual R
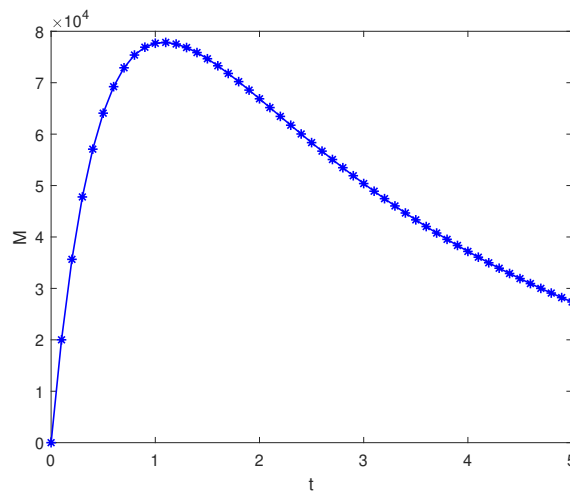
Figure 9. Behavior of the state variable Concentration of V.C in Contaminating the Environment M
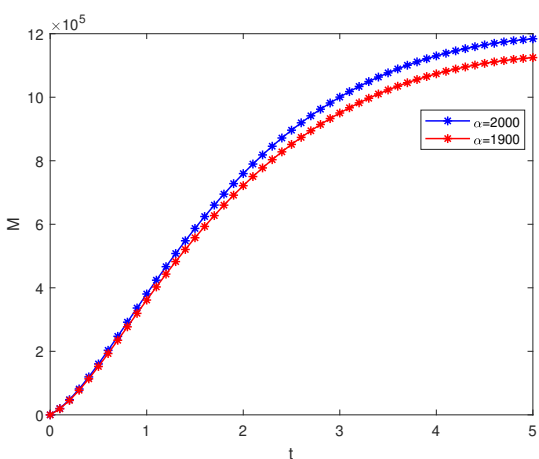
(a) pattern of M with different values of the rate of human contribution to V.C
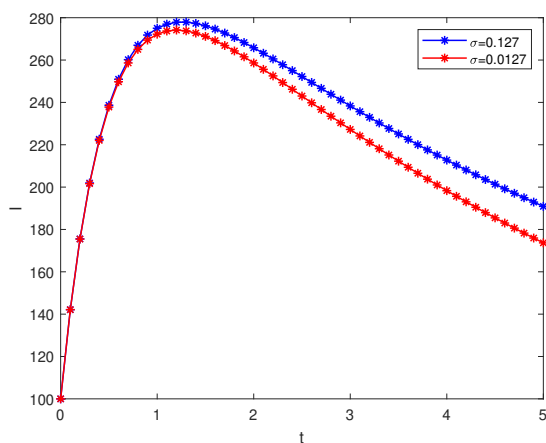
(b) pattern of I with different values of the modification parameter that decreases the infectiousness of V

cost less and the same time effective in controlling the recurrence of the disease. So to eradicate cholera disease in Nigeria, an efficient vaccine and proper sanitation should be enhanced.
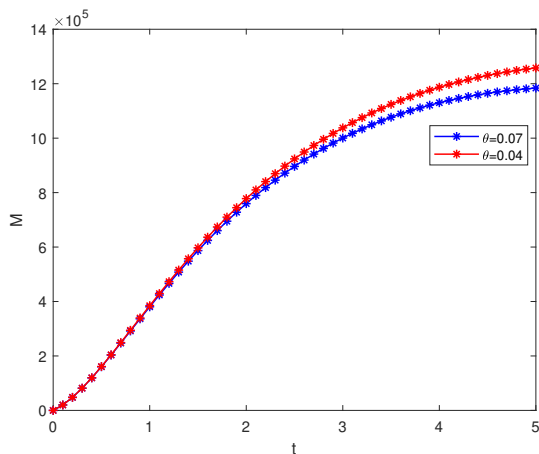
(a) pattern of M with different values of the rate of disinfection of environment
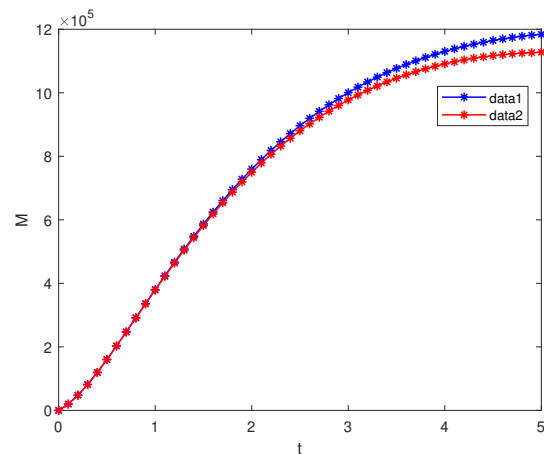
(b) Behavior of the state variables (A) Infected individuals with undetectable viral load I_3, (B) Infected individuals under treatment I_t

Declarations

Use of AI tools

The authors declare that they have not used Artificial Intelligence (AI) tools in the creation of this article.

Data availability statement

All data generated or analyzed during this study are included in this article.

Ethical approval

The authors state that this research complies with ethical standards. This research does not involve either human participants or animals.

Consent for publication

Not applicable

Conflicts of interest

The authors declare that they have no conflict of interest.

Funding

Not applicable

Author's contributions

U.T.M.: Methodology, Software, Validation, Y.A.M.: Formal Analysis, Investigation, Writing - Original Draft, Visualization, A.Y. and S.Q.: Software, Validation, Supervision, Project Administration. The authors have read and agreed to the published version of the manuscript.

Acknowledgements

Not applicable

References

[1] Center for Disease Control and Prevention (CDC), Cholera-Vibrio Cholerae infection, (2019). https://www.cdc.gov/cholera/index.html.

[2] World Health Organization (WHO), Cholera world health organization, (2021). http://apps.www.who.org.

[3] Hove-Musekwa, S.D., Nyabadza, F., Chiyaka, C., Das, P., Tripathi, A. and Mukandavire, Z. Modelling and analysis of the effects of malnutrition in the spread of cholera. *Mathematical and Computer Modelling*, 53(9-10), 1583-1595, (2011). [CrossRef]

[4] Yang, C., Wang, X., Gao, D. and Wang, J. Impact of awareness programs on cholera dynamics: two modeling approaches. *Bulletin of Mathematical Biology*, 79, 2109-2131, (2017). [CrossRef]

[5] Harris, J.B., LaRocque, R.C., Kadri, F., Ryan, E.T. and Calderwood, S.B. Cholera. *Lancet*, 379(9835), 2466-2476, (2012). [CrossRef]

[6] Tian, J.P. and Wang, J. Global stability for cholera epidemic models. *Mathematical Biosciences*, 232(1), 31-41, (2011). [CrossRef]

[7] Center for Disease Control, (2021). https://www.premiumtimesng.com.

[8] Mwasa, A. and Tchuenche, J.M. Mathematical analysis of a cholera model with public health interventions. *Biosystems*, 105(3), 190-200, (2011). [CrossRef]

[9] Stuart, A. and Humphries, A.R. *Dynamical Systems and Numerical Analysis* (Vol. 2). Cambridge University Press: United Kingdom, (1998).

[10] Smith, H.L. *Monotone Dynamical Systems, An Introduction to the Theory of Competitive and Cooperative Systems* (Vol. 41). American Mathematical Society: ABD, (1995).

[11] Van den Driessche, P. and Watmough, J. Reproduction numbers and sub-threshold endemic equilibria for compartmental models of disease transmission. *Mathematical Biosciences,* 180(1-2), 29-48, (2002). [CrossRef]

[12] Castillo-Charez, C. and Song, B. Dynamical models of tuberculosis and their applications. *Mathematical Biosciences & Engineering,* 1(2), 361-404, (2004). [CrossRef]

[13] La Salle, J.P. *The Stability of Dynamical Systems* (Vol. 25). SIAM: Philadelphia, (2002).

[14] Fleming, W.H. and Rishel, R.W. *Deterministic and Stochastic Optimal Control* (Vol. 1). Springer Verlag: New York, (1975).

[15] Mustapha, U.T. and Hincal, E. An optimal control of hookworm transmissions model with differential infectivity. *Physica A: Statistical Mechanics and its Applications,* 545, 123625, (2020). [CrossRef]

[16] Saad, F.T. and Hincal, E. An optimal control approach for the interaction of immune checkpoints, immune system, and BCG in the treatment of superficial bladder cancer. *The European Physical Journal Plus,* 133, 241, (2018). [CrossRef]

[17] Nigeria Centre for Disease Control and Prevention, (2022). https://ncdc.gov.ng/diseases/sitreps/?cat=7&name=An%20update%20of%20Choler%20out\break%20in%20Nigeria

[18] Sun, G.Q., Xie, J.H., Huang, S.H., Jin, Z., Li, M.T. and Liu, L. Transmission dynamics of cholera: Mathematical modeling and control strategies. *Communications in Nonlinear Science and Numerical Simulation*, 45, 235-244, (2017). [CrossRef]

[19] Yusuf, A., Mustapha, U.T., Sulaiman, T.A., Hincal, E. and Bayram, M. Modeling the effect of horizontal and vertical transmissions of HIV infection with Caputo fractional derivative.

Chaos, Solitons & Fractals, 145, 110794, (2021). [CrossRef]

[20] Usaini, S., Mustapha, U.T. and Sabiu, S.M. Modelling scholastic underachievement as a contagious disease. *Mathematical Methods in the Applied Sciences,* 41(18), 8603-8612, (2018). [CrossRef]

[21] Mustapha, U.T., Qureshi, S., Yusuf, A. and Hincal, E. Fractional modeling for the spread of Hookworm infection under Caputo operator. *Chaos, Solitons & Fractals,* 137, 109878, (2020). [CrossRef]

Bulletin of Biomathematics (BBM)
(https://bulletinbiomath.org)

RESEARCH PAPER

Dynamical analysis of HIV-TB co-infection transmission model in the presence of treatment for TB

Bolarinwa Bolaji [1,3,‡], **Thomas Onoja** [1,3,‡], **Celestine Agbata** [2,‡],
Benjamin Idoko Omede [1,3,‡] **and Udoka Benedict Odionyenma** [4,‡,*]

[1]Mathematical Sciences Department, Prince Abubakar Audu (Formerly, Kogi State) University, Anyigba, Nigeria, [2]Mathematics Department, Confluence University of Science and Technology, Osara, Nigeria, [3]Laboratory of Mathematical Epidemiology and Applied Sciences (LOMEAS), Prince Abubakar Audu University, Anyigba, Nigeria, [4]African University of Science and Technology, Abuja, Nigeria

[*] Corresponding Author
[‡] bolarinwa.s.bolaji@gmail.com (Bolarinwa Bolaji); tuonoja@gmail.com (Thomas Onoja); abcinfotech08@gmail.com (Celestine Agbata); benjaminomede197@gmail.com (Benjamin Idoko Omede); oudoka@aust.edu.ng (Udoka Benedict Odionyenma)

Abstract

The immense disease burden of tuberculosis (TB) infection is well-documented, particularly among those co-infected with HIV and TB. To better understand the transmission dynamics of HIV-TB co-infection in the absence of readily available HIV treatment, we develop a deterministic compartmental co-infection model. Our model helps to identify the effects of TB infection on the co-infection dynamics of the two diseases, especially when treatment for TB is readily available. We find that susceptibility to TB reinfection after a previous infection leads to backward bifurcation in the TB-only model when the associated reproduction number (R_0) is less than unity. However, when we make the susceptibility to TB re-infection insignificant in the model, the disease-free equilibrium of the TB-only model is locally asymptotically stable when the associated R_0 is less than unity. We conduct sensitivity and uncertainty analyses to identify the key parameters driving TB infection dynamics, using the R_0 as the response function. We discover that the transmission rate for TB, the modification parameters accounting for the infectiousness of infected individuals with TB-only, and the treatment rates for singly infected individuals with latently infected TB are the top drivers of TB infection in the given population. Our numerical simulations suggest that concentrating treatment on TB-infected individuals in the diagnosed latently infected stage (singly or dually infected with HIV) could effectively reduce the co-infection disease burden and HIV incidence in the population under study.

Keywords: Tuberculosis; HIV; co-infection; symptoms; stability; simulations

AMS 2020 Classification: 92D25; 92D30; 37C75

---

1 Introduction

HIV, the Human Immunodeficiency Syndrome, is a virus that attacks cells aiding human resistance to infections, thus increasing vulnerability to numerous other infections and diseases [1–3]. When a person is infected with the virus, it targets and destroys CD4 cells of the immune system. As the HIV infection progresses within the human system, the viral load increases, weakening the immune system. Without antiretroviral treatment, the infection advances to Acquired Immune Deficiency Syndrome (AIDS), the advanced stage of HIV infection, where the immune system becomes severely compromised. The virus was initially identified among homosexuals in the United States of America in 1983, though other reports claim its discovery among apes in 1982 in Kenya [4]. Causes of HIV include vaginal intercourse with an HIV-positive individual without using a condom or pre-exposure prophylaxis (PrEP), as well as sharing equipment for injectable illicit drugs, hormones, and steroids with someone infected with HIV [5]. The virus can be transmitted through blood, semen, pre-seminal fluid, vaginal fluids, rectal fluids, and breast milk [4]. HIV can be prevented by avoiding risky behaviors, using condoms during sex, and receiving regular vaccinations for potential opportunistic infections. An individual with an undetectable level of HIV cannot transmit the virus to another individual [5].

Tuberculosis, also known as TB, is a bacterial infection caused by Mycobacterium tuberculosis bacteria [6]. It primarily affects the lungs but can also affect other parts of the body. Transmission occurs through the air when a person inhales droplet nuclei containing the bacteria. Active TB manifests with symptoms such as coughing up mucus or blood, chest pain, fever, night sweats, loss of appetite, fatigue, and persistent coughing for three or more weeks [3, 7]. The disease can be prevented and treated with medication. TB/HIV co-infection presents special diagnostic and therapeutic challenges and places a significant burden on healthcare systems in many countries [8–10]. TB remains one of the leading causes of death worldwide in the era of HIV, with both diseases collectively responsible for the deaths of 4 million people annually [8]. Studies indicate that while not all HIV patients develop TB disease, those co-infected with both HIV and TB have a higher risk of progressing from TB infection to TB disease due to weakened immune systems. Unlike HIV, TB is entirely preventable, treatable, and curable. While treatment is a fraction of the cost of medications used for HIV, TB co-infection accelerates HIV progression to AIDS [11]. Infected HIV patients are at a heightened risk of contracting tuberculosis [8]. Therefore, adequate attention to the prevention and control of TB/HIV co-infections in a population is crucial.

Several studies have investigated the co-infection of HIV and TB, developing models to understand their epidemics' dynamics. These studies emphasize the importance of incorporating each disease's effects and formulating models for their transmission mechanisms. Wang et al. [12] proposed a dynamic epidemiological model of HIV-TB co-infection incorporating latent age, emphasizing the significance of assessing each disease's effects on co-infection dynamics. Kaur et al. [13] formulated a simple compartmental deterministic model for HIV-TB co-infection, highlighting the existence of an unstable co-infection equilibrium point under certain parameter restrictions. Azeez et al. [1] developed a deterministic compartmental epidemiological model to study the transmission mechanism of HIV-TB co-interaction, revealing that individuals with HIV infection are at greater risk of TB co-infection compared to those without HIV infection. Fatmawati et al. [14] formulated an optimal control co-infection model of HIV-TB, demonstrating that combining anti-TB and antiretroviral treatment is optimal for reducing the burden of co-infection. Omale et al. [15] developed a deterministic co-infection model incorporating control measures to study the scenario where both HIV and tuberculosis infect the same individual, finding that the infectiousness of one disease increases the risk of infectiousness of the other and that the implemented control measures significantly reduce tuberculosis infection, ultimately reducing co-infection rates.

In general, epidemiological models, such as those in [16–25], are valuable tools for studying the transmission dynamics of infectious diseases. Therefore, this research study aims to develop and analyze a mathematical model for HIV/TB co-infection in the presence of treatment. The study has six specific objectives, including:

- Demonstrating the stability of the disease-free equilibrium.
- Analyzing the reproduction number to identify parameters that can reduce the spread of the disease.
- Conducting sensitivity analysis to identify key parameters that drive infectiousness.
- Validating theoretical results with numerical simulations.
- Creating contour plots involving key parameters and the reproduction numbers for the diseases with the aim of determining the threshold for control measures that can help eradicate the diseases from the human population.
- Providing qualitative and empirically-based recommendations to policymakers in the health sector to assist them in controlling the spread of the two diseases and obtaining necessary and sufficient conditions for their eradication in the human population.

In general, from this study, it is anticipated that its findings will significantly contribute to the body of knowledge that informs health policymakers, planners, project implementers, and future researchers by providing strategies for the prevention and control of HIV/TB co-infections through the dynamic analysis of our model.

The manuscript is organized into six sections, including a description of the model formulation, theoretical analysis, sensitivity analysis, numerical simulations, discussion of the plots, and conclusion.

2 Model formulation

The total human population $N(t)$, at any time t is divided into 13 compartments, as listed in Table 1, to obtain:

$$N(t) = S(t) + E(t) + E_L(t) + E_{UL}(t) + I_{UA}(t) + T(t) + R(t) + I_H(t) + E_{TH}(t) + I_{HU}(t) \\ + I_{HUA}(t) + I_{HDA}(t) + T_{HT}(t).$$

It is assumed that individuals who are dually infected can only transmit one of the diseases at a time. The equations for the new co-infection model are formulated as follows.

Transmissions by singly infected individuals

Individuals acquire HIV infection $I_H(t)$, from effective contact with those infected with HIV only, at a rate given by:

$$\dot{\lambda}_H = \beta_H \frac{I_H(t)}{N}, \tag{1}$$

where β_H represents the transmission rate for HIV.

Likewise, the acquisition of TB infection by individuals from those in I_{UA}, and T, compartments, at a rate λ_T, is given as:

$$\lambda_T = \beta_T \frac{(I_{UA} + \eta_1 T)}{N}. \tag{2}$$

Here, the rate of TB transmission is β_T, where the modification parameter $\eta_1 \geq 1$, accounts for the

relative infectiousness of individuals with diagnosed actively infected TB compared to those with undiagnosed actively infected TB infection. The assumption is that those individuals diagnosed as actively infected with TB are more infectious than those undiagnosed [9].

Transmissions by dually infected individuals

TB is transmitted by dually infected individuals at a rate given by:

$$\lambda_{TH} = \frac{\beta_T(\eta_2 I_{HUA} + \eta_3 I_{HDA})}{N}. \tag{3}$$

The transmission rate for TB is modified by the parameters η_2, while η_3, accounts for the increased infectiousness of dually infected individuals with HIV and undiagnosed active TB infection compared to those with dually infected HIV diagnosed TB only. It is assumed that $\eta_3 \geq \eta_2 > 1$. HIV transmission by those infected with both diseases occurs at the following rate:

$$\lambda_{HT} = \frac{\beta_H(E_{HT} + \phi_1 I_{HU} + \phi_2 I_{HUA} + \phi_3 I_{HDA} + \phi_4 I_{HT})}{N}. \tag{4}$$

Here, the relative infectiousness of HIV-infected individuals with primary, secondary, early latent, and late latent TB, respectively, compared to HIV-only infected individuals is accounted for by parameters ϕ_1, ϕ_2, ϕ_3, and ϕ_4.

Description of model equation formation

The rate of recruitment for susceptible individuals to the two diseases occurs at the rate π. Those that acquire HIV and TB infection do so at the rates λ_H, and λ_T, respectively. Likewise, HIV and TB are transmitted by dually infected individuals at rates given by λ_{TH}, and λ_{HT} (where λ_H, λ_T, λ_{TH}, and λ_{HT}, are as initially defined in Section 2. The natural death rate for individuals in all compartments occurs at the uniform rate μ. The contact rates for HIV and tuberculosis are given by β_H, and β_T, respectively. Singly infected individuals with latently infected TB, undiagnosed latently infected TB, undiagnosed actively infected, and diagnosed actively infected individuals with TB on prompt treatment are treated at rates σ_1, σ_2, σ_3, and σ_4, respectively.

On the other hand, treatment rates for dually infected individuals with HIV and latently infected TB, HIV and undiagnosed latently infected TB, HIV and undiagnosed actively infected TB, and HIV and diagnosed actively infected individuals with TB are σ_{T1}, σ_{T2}, σ_{T3}, and σ_{T4} respectively, while the modification parameters that account for the infectiousness of dually infected individuals are ϕ_1, ϕ_2, ϕ_3, and ϕ_4. Individuals who are singly infected progress from exposed class, diagnosed latently infected class, undiagnosed latently infected class, undiagnosed actively infected class, diagnosed actively infected with TB on prompt treatment class to classes E_L, E_{UL}, I_{UA}, T, and R, at the rates ψ_1, ψ_2, ψ_3, and ψ_4, respectively. Likewise, individuals that are infected with the two diseases in the classes E_{HT}, I_{HU}, I_{HUA}, I_{HDA}, and T_{HT}, progress to classes I_{HU}, I_{HUA}, I_{HDA}, and T_{HT}, at the rates ψ_{HU}, ψ_{HUA}, ψ_{HDA}, and ψ_{HT}, respectively.

The modification parameters accounting for variability in the susceptibility of recovered individuals to TB infection are given by ε_1, and ε_2, while those accounting for the susceptibility of recovered individuals to TB infection are represented by γ_1, and γ_2. Similarly, the modification parameters accounting for the susceptibility of TB-infected individuals to HIV infection are given as θ_1, θ_2, θ_3, θ_4, θ_5, θ_6, θ_7, and θ_8, respectively, while those accounting for the infectiousness of infected individuals with TB only, HIV and undiagnosed actively infected TB, HIV and diagnosed actively infected TB are η_1, η_2, and η_3, respectively. It should be noted that the disease-induced

death rate in each of the disease-infected compartments occurs at uniform rates δ_1, δ_2, δ_3, δ_4, δ_5, and δ_6, respectively.

Table 1. Description of the model variables and parameters

Variable	Description
S_h	Group of individuals that are susceptible to the two infections
E	Group of exposed individuals to TB
E_L	Group of diagnosed latently infected individuals to TB
E_{UL}	Group of undiagnosed latently infected individuals to TB
I_{UA}	Group of undiagnosed actively infected individuals to TB
T	Group of diagnosed actively infected individuals to TB on prompt treatment
R	Group of recovered individuals
I_H	Group of HIV infected individuals
E_{HT}	Group of dually infected individuals with diagnosed latent HIV and TB
I_{HU}	Group of dually infected individuals with HIV and undiagnosed latently infected TB
I_{HUA}	Group of dually infected individuals with HIV and undiagnosed active TB
I_{HDA}	Group of dually infected individuals with HIV and diagnosed active TB
T_{HT}	Group of dually infected individuals with HIV and TB on prompt treatment for both diseases
Parameter	**Description**
π	Recruitment rate into the susceptible class
μ	Rate at which individuals die naturally
β_T (β_H)	Contact rates for tuberculosis (HIV)
$\sigma_1, \sigma_2, \sigma_3, \sigma_4$	Treatment rates for singly infected individuals with latently-infected TB, undiagnosed latently-infected TB, undiagnosed actively-infected and diagnosed actively-infected individuals with TB on prompt treatment
$\sigma_{T1}, \sigma_{T2}, \sigma_{T3}, \sigma_{T4}$	Treatment rates for dually infected individuals with HIV and latently-infected TB, HIV and undiagnosed latently-infected with TB, HIV and undiagnosed actively-infected with TB, HIV and diagnosed actively-infected individuals with TB
$\psi_1, \psi_2, \psi_3, \psi_4$	Rate of progression for singly infected individuals from exposed, diagnosed latently-infected, undiagnosed latently-infected, undiagnosed actively infected, diagnosed actively infected with TB on prompt treatment to classes E_L, E_{UL}, I_{UA}, T, and R, respectively
$\varepsilon_1, \varepsilon_2$	Modification parameters accounting for variability in susceptibility of recovered individuals to TB infection
$\psi_{HU}, \psi_{HUA}, \psi_{HDA}, \psi_{HT}$	Rate of progression for dually infected individuals from classes E_{HT}, I_{HU}, I_{HUA}, I_{HDA}, and T_{HT}, to classes I_{HU}, I_{HUA}, I_{HDA}, and T_{HT}, respectively
γ_1, γ_2	Modification parameters accounting for the susceptibility of recovered individuals to TB infection
$\theta_1, \theta_2, \theta_3, \theta_4, \theta_5, \theta_6, \theta_7, \theta_8$	Modification parameters accounting for the susceptibility of TB-infected individuals to HIV infection
η_1, η_2, η_3	Modification parameters accounting for the infectiousness of infected individuals with TB only, HIV, and undiagnosed actively infected TB, HIV, and diagnosed actively-infected TB respectively
$\phi_1, \phi_2, \phi_3, \phi_4$	Modification parameters accounting for the infectiousness of dually infected individuals
$\delta_1, \delta_2, \delta_3, \delta_4, \delta_5, \delta_6$	Disease-induced death rates due to HIV with TB co-infection

Based on the description above, the model assumptions, and the schematic diagram below, we formulate the following system of non-linear differential equations as that which captures the transmission dynamics of HIV-TB co-infection in a given population:

$$\frac{dS}{dt} = \pi - \lambda_T S - \lambda_H S - \lambda_{TH} S - \lambda_{HT} S - \mu S,$$

$$\frac{dE}{dt} = \lambda_T S + \lambda_{TH} S + \varepsilon_1 \lambda_T R + \varepsilon_2 \lambda_{TH} R - \lambda_H E - \lambda_{HT} E - (\psi_1 + \mu) E,$$

$$\frac{dE_L}{dt} = \psi_1 E - \theta_1 \lambda_H E_L - \theta_2 \lambda_{HT} E_L - (\psi_2 + \sigma_1 + \mu) E_L,$$

$$\frac{dE_{UL}}{dt} = \psi_2 E_L - \theta_3 \lambda_H E_{UL} - \theta_4 \lambda_H E_{UL} - (\psi_3 + \sigma_2 + \mu) E_{UL},$$

$$\frac{dI_{UA}}{dt} = \psi_3 E_{UL} - \theta_5 \lambda_H I_{UA} - \theta_6 \lambda_{HT} I_{UA} - (\psi_4 + \sigma_3 + \mu) I_{UA},$$

$$\frac{dT}{dt} = \psi_4 I_{UA} - \theta_7 \lambda_H T - \theta_8 \lambda_{HT} T - (\psi_5 + \sigma_4 + \mu) T,$$

$$\frac{dR}{dt} = \sigma_1 E_L + \sigma_2 E_{UL} + \sigma_3 I_{UA} + \sigma_4 T - \varepsilon_1 \lambda_T R - \lambda_H R - \varepsilon_2 \lambda_{TH} R - \lambda_{HT} R - \mu R,$$

$$\frac{dI_H}{dt} = \lambda_H S + \lambda_{HT} S + \lambda_H R + \lambda_{HT} R - \gamma_1 \lambda_T I_H - \gamma_2 \lambda_{TH} I_H + \sigma_{T1} E_{HT} + \sigma_{T2} I_{HU}$$
$$\qquad + \sigma_{T3} I_{HUA} + \sigma_{T4} I_{HDA} + \sigma_{T5} T_{HT} - (\mu + \delta_1) I_H,$$

$$\frac{dE_{HT}}{dt} = \sigma_1 \lambda_T I_H + \sigma_2 \lambda_{TH} I_H + \lambda_{HT} E - (\psi_{HU} + \sigma_{T1} + \delta_2 + \mu) E_{HT},$$

$$\frac{dI_{HU}}{dt} = \psi_{HU} E_{HT} + \theta_1 \lambda_H E_L + \theta_2 \lambda_{HT} E_L - (\psi_{HUA} + \delta_3 + \sigma_{T2} + \mu) I_{HU},$$

$$\frac{dI_{HUA}}{dt} = \psi_{HUA} I_{HU} + \theta_3 \lambda_H E_{UL} + \theta_4 \lambda_{HT} E_{UL} - (\psi_{HDA} + \sigma_{T3} + \delta_4 + \mu) I_{HUA},$$

$$\frac{dI_{HDA}}{dt} = \psi_{HDA} I_{HUA} + \theta_5 \lambda_H I_{UA} + \theta_6 \lambda_{HT} I_{UA} - (\psi_{HT} + \sigma_{T4} + \delta_5 + \mu) I_{HDA},$$

$$\frac{dT_{HT}}{dt} = \psi_{HU} I_{HDA} + \theta_7 \lambda_H T + \theta_8 \lambda_{HT} T - (\sigma_{T5} + \delta_6 + \mu) T_{HT},$$

$$(5)$$

where

$$\lambda_H = \frac{\beta_H I_H}{N}, \quad \lambda_T = \frac{\beta_T (I_{UA} + \eta_1 T)}{N}, \quad \lambda_{TH} = \frac{\beta_T (\eta_2 I_{HUA} + \eta_3 I_{HDA})}{N},$$

and

$$\lambda_{HT} = \frac{\beta_H (E_{HT} + \phi_1 I_{HU} + \phi_2 I_{HUA} + \phi_3 I_{HDA} + \phi_4 I_{HT})}{N}.$$

It is pertinent to note that due to the fact that model (5) is monitoring the human population, consequently, we assumed that all variables and parameters in the model are non-negative. Therefore, we shall carry out the analysis of model (5) in the invariant region given as follows:

$$\Omega_1 = \Big\{ (S(t), E(t), E_L(t), E_{UL}(t), I_{UA}(t), T(t), R(t), I_H(t), E_{TH}(t), I_{HU}(t), I_{HUA}(t),$$
$$I_{HDA}(t), T_{HT}(t)) \in \mathfrak{R}_+^{13} : N \leq \frac{\pi}{\mu} \Big\}.$$

Model assumptions

In formulating our model, some assumptions have been considered which are listed as follows:

- Individuals infected with tuberculosis can recover through treatment, but there is no treatment-induced recovery for those infected with HIV [14, 19].
- Natural death occurs uniformly for all individuals in each class of the model at a constant rate μ.
- The disease-induced death rate in all the infected compartments is uniform.
- We have not included in the model those individuals who progress from being infected with HIV to being infected with AIDS after some time.
- In cognizance of the fact that findings show that 80% of individuals afflicted with HIV infection are practically bound to suffer from TB infection [19], we assume that only those suffering from TB affliction are infected with HIV infection.
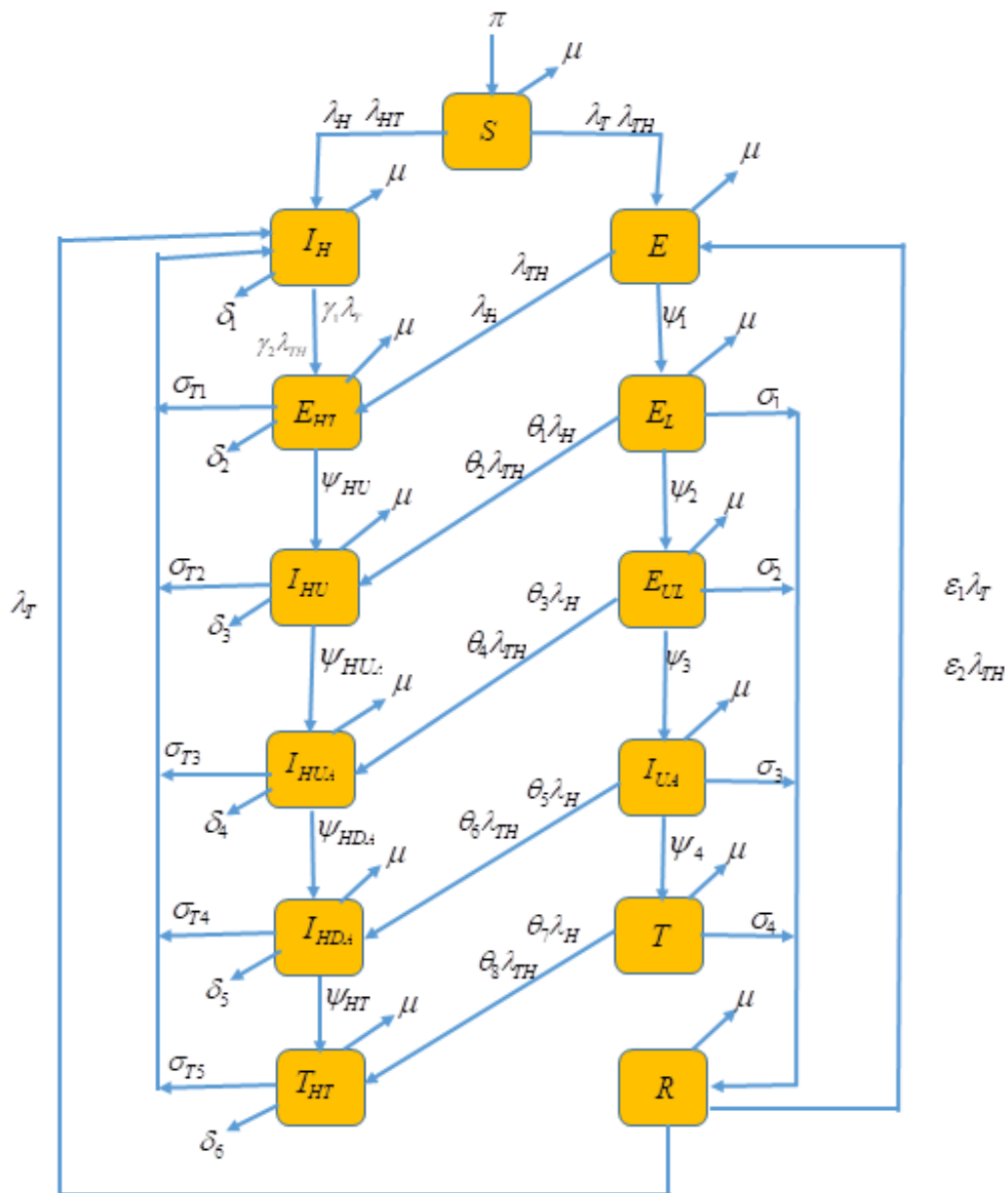
Figure 1. Flow chart of co-infection model (5) where λ_H, λ_T, λ_{HT}, and λ_{TH}, are as defined in Eqs. (2) and (3), respectively

Invariance region

Lemma 1 *The solution of the model equations is feasible for all $t > 0$, if they are contained in the invariant region:*

$$\Omega_1 = \{S(t) + E(t) + E_L(t) + E_{UL}(t) + I_{UA}(t) + T(t) + R(t) + I_H(t) + E_{TH}(t) + I_{HU}(t) \\ + I_{HUA}(t) + I_{HDA}(t) + T_{HT}(t)\} \in \mathfrak{R}_+^{13}\}. \tag{6}$$

Proof Suppose

$$\Omega_1 = \{S(t) + E(t) + E_L(t) + E_{UL}(t) + I_{UA}(t) + T(t) + R(t) + I_H(t) + E_{TH}(t) + I_{HU}(t) \\ + I_{HUA}(t) + I_{HDA}(t) + T_{HT}(t)\} \in \mathfrak{R}_+^{13}\},$$

be any solution of model Eq. (5) with non-negative initial conditions.

In the absence of disease-induced death rate, $\frac{dN}{dt}$ becomes:

$$\frac{dN}{dt} \le \pi - \mu N,$$

we have

$$\frac{dN}{dt} + \mu N \le \pi.$$

Solving the equation above by multiplying both sides by $e^{\mu t}$, the integrating factor

$$\frac{dN}{dt}(e^{\mu t}) + \mu N(e^{\mu t}) \le \pi(e^{\mu t}).$$

From the above equation, we obtain

$$d(Ne^{\mu t}) \le \pi e^{\mu t} dt,$$

by integrating both sides of the above equation, we have that

$$Ne^{\mu t} \le \frac{\pi e^{\mu t}}{\mu} + k_0.$$

Dividing all through by $e^{\mu t}$, we have

$$N(t) \le \frac{\pi}{\mu} + k_0 e^{-\mu t}. \tag{7}$$

Applying the initial conditions $t(0) = N(0)$, we have

$$N(0) \le \frac{\pi}{\mu} + k_0,$$

$$N(0) - \frac{\pi}{\mu} \leq k_0.$$

Eq. (7) becomes

$$N(t) \leq \frac{\pi}{\mu} + \left(N(0) - \frac{\pi}{\mu} \right) e^{-\mu t}. \tag{8}$$

Therefore, the human population approaches the carrying capacity $\frac{\pi}{\mu}$, as $t \to \infty$. Obviously, the feasible solution set of the model Eq. (5) enters the invariant region:

$$\Omega_1 = \{ (S(t) + E(t) + E_L(t) + E_{UL}(t) + I_{UA}(t) + T(t) + R(t) + I_H(t) + E_{TH}(t) + I_{HU}(t)$$
$$+ I_{HUA}(t) + I_{HDA}(t) + T_{HT}(t)) \in \mathfrak{R}_+^{13} : N < \frac{\pi}{\mu} \},$$

where $S(0) > 0$, $E(0) > 0$, $E_L(0) > 0$, $E_{UL}(0) > 0$, $I_{UA}(0) > 0$, $T(0) > 0$, $R(0) > 0$, $I_H(0) > 0$, $E_{TH}(0) > 0$, $I_{HU}(0) > 0$, $I_{HUA}(0) > 0$, $I_{HDA}(0) > 0$, $T_{HT}(0) > 0$. Therefore, model (5) is biologically and mathematically feasible. Hence whenever $N > \frac{\pi}{\mu}$, then $N < 0$, which means that the population reduces asymptotically to the carrying capacity. Whenever $N \leq \frac{\pi}{\mu}$, every solution with an initial condition in Ω_1, remains positive for all $t > 0$, and the model is said to be mathematically well-posed and biologically meaningful.

Lemma 2 *Let the initial condition be:*

$$\{ S(0) > 0, E(0) > 0, E_L(0) > 0, E_{UL}(0) > 0, I_{UA}(0) > 0, T(0) > 0, R(0) > 0, I_H(0) > 0,$$
$$E_{TH}(0) > 0, I_{HU}(0) > 0, I_{HUA}(0) > 0, I_{HDA}(0) > 0, T_{HT}(0) > 0 \}. \tag{9}$$

Consequently, the solution set:

$$\{ S(t), E(t), E_L(t), E_{UL}(t), I_{UA}(t), T(t), R(t), I_H(t), E_{TH}(t), I_{HU}(t), I_{HUA}(t), I_{HDA}(t), T_{HT}(t) \},$$

of the system of model Eq. (5) is positive for all $t > 0$.

Proof From the first equation of the model system (5), we have

$$\frac{dS}{dt} = \pi - (\lambda_T + \lambda_H + \lambda_{TH} + \lambda_{HT} + \mu) S,$$

$$\frac{dS}{dt} = \pi - (\lambda_T + \lambda_H + \lambda_{TH} + \lambda_{HT} + \mu) S \geq - (\lambda_T + \lambda_H + \lambda_{TH} + \lambda_{HT} + \mu) S.$$

Which can be re-written as

$$\frac{dS}{S} \geq - (\lambda_T + \lambda_H + \lambda_{TH} + \lambda_{HT} + \mu) dt.$$

Integrating the equation above, we have

$$\ln S \geq - (\lambda_T + \lambda_H + \lambda_{TH} + \lambda_{HT} + \mu) t + k_1,$$

$$S(t) \geq e^{-(\lambda_T + \lambda_H + \lambda_{TH} + \lambda_{HT} + \mu)t + k_1},$$

$$S(t) \geq k_1 e^{-(\lambda_T + \lambda_H + \lambda_{TH} + \lambda_{HT} + \mu)t}.$$

Applying the initial conditions $t = 0$, $S(0) = k_1$ gives

$$S(t) \geq S(0)e^{-(\lambda_T + \lambda_H + \lambda_{TH} + \lambda_{HT} + \mu)t}, \quad \text{and} \quad (\lambda_T + \lambda_H + \lambda_{TH} + \lambda_{HT} + \mu) > 0.$$

Similarly, the above integration can be shown for other state variables, for $E(t) > 0$, $E_L(t) > 0$, $E_{UL}(t) > 0$, $I_{UA}(t) > 0$, $T(t) > 0$, $R(0) > 0$, $I_H(t) > 0$, $E_{TH}(t) > 0$, $I_{HU}(t) > 0$, $I_{HUA}(t) > 0$, $I_{HDA}(t) > 0$, and $T_{HT}(t) > 0$.

3 Theoretical analysis of the model

To conduct the analysis of the model, we first analyze the singly infected system before proceeding to analyze the dually infected system.

HIV-only model

To obtain the HIV-only model, we set all the TB components to zero as follows:

$$E = 0, E_L = 0, E_{UL} = 0, I_{HU} = 0, T = 0, E_{HT} = 0, I_H = 0, I_{HUA} = 0, I_{HDA} = 0, I_{HT} = 0.$$

Therefore, the HIV-only model is given by:

$$\begin{aligned} \frac{dS}{dt} &= \pi - (\lambda_H + \mu)S, \\ \frac{dI_H}{dt} &= \lambda_H S - (\mu + \delta_1)I_H, \end{aligned} \tag{10}$$

where

$$\lambda_H = \frac{\beta_H I_H}{N}, \quad \text{and} \quad N(t) = S(t) + I_H(t).$$

HIV-only disease-free equilibrium (DFE)

The DFE of the HIV-only model (10) is:

$$(S^+, I_H^+) = (\frac{\pi}{\mu}, 0). \tag{11}$$

Existence of endemic equilibrium point (EEP) of HIV-only model

The endemic equilibrium (S^{++}, I_H^{++}), of the model Eq. (10) is given by:

$$(S^{++}, I_H^{++}) = (\frac{\pi}{\lambda_H^{++} + \mu}, \frac{\pi \lambda_H^{++}}{(\lambda_H^{++} + \mu)(\mu + \delta_1)}).$$

The basic reproduction number

The threat posed by any infectious disease on humans depends on the rate at which it invades a population. The measure of the potential for disease to spread in a population is the basic

reproduction number ($\mathcal{R}_0$). It represents the average number of secondary cases of infection that will be generated by the influx of just one infected person into a healthy population [18]. If the reproduction number of the disease is less than unity ($\mathcal{R}_0 < 1$), when there is an influx of at least one infected individual into a healthy population, then it means that, on average, each infected individual produces less than one newly infected individual throughout an infection period. In this case, the disease might gradually die out over time. On the other hand, if $\mathcal{R}_0 > 1$, each infected individual produces, on average, more than one new infection, and the infection will continue to spread rapidly in the given population. The basic reproduction number of the HIV-only model (10) follows from [20] and is given by:

$$\mathcal{R}_{0H} = \rho\left(\frac{\beta_H}{\mu + \delta_1}\right).$$

Local stability of disease-free equilibrium of HIV-only model

Theorem 1 *If $\omega_1, \omega_2, \ldots, \omega_n$ are the eigenvalues of the Jacobian matrix of the HIV-only model (10), its disease-free equilibrium is locally asymptotically stable (LAS) whenever $\omega_1, \omega_2, ..., \omega_n < 0$.*

Proof Let $A = \pi - (\lambda_H + \mu)S$, and $B = \lambda_H S - (\mu + \delta_1)I_H$, we have that

$$\frac{\partial A}{\partial S} = (\lambda_H + \mu), \quad \frac{\partial A}{\partial I_H} = 0,$$

$$\frac{\partial B}{\partial S} = \lambda_H, \quad \frac{\partial B}{\partial I_H} = -(\mu + \delta_1).$$

The Jacobian matrix is given as:

$$J(\varepsilon f) = \begin{vmatrix} \frac{\partial A}{\partial S} & \frac{\partial A}{\partial I_H} \\ \frac{\partial B}{\partial S} & \frac{\partial B}{\partial I_H} \end{vmatrix}.$$

So that

$$J(\varepsilon f) = \begin{vmatrix} -(\lambda_H + \mu) & 0 \\ \lambda_H & -(\mu + \delta_1) \end{vmatrix},$$

$$J(\varepsilon f - \lambda I) = \begin{vmatrix} -(\lambda_H + \mu) - \lambda & 0 \\ \lambda_H & -(\mu + \delta_1) - \lambda \end{vmatrix}.$$

The characteristic equation of the matrix $J(\varepsilon f - \lambda I)$ is given by:

$$P(\lambda) = (-(\lambda_H + \mu) - \lambda)(-(\mu + \delta_1) - \lambda) = 0.$$

The eigenvalues of the characteristic equation $P(\lambda)$, are

$$\omega_1 = \lambda_1 = -(\lambda_H + \mu), \quad \text{and} \quad \omega_2 = \lambda_2 = -(\mu + \delta_1).$$

Observe that the eigenvalues $\omega_1 < 0$, and $\omega_2 < 0$. Hence, arising from Theorem 1, the disease-free equilibrium of the model is locally asymptotically stable.

Local stability of endemic equilibrium point (EEP) of HIV-only model

The endemic equilibrium of the HIV-only model (10) is obtained by solving for the force of infection (λ_H^{++}), at steady-state, giving:

$$(S^{++}, I_H^{++}) = \left(\frac{\pi}{\lambda_H^{++} + \mu}, \frac{\pi \lambda_H^{++}}{(\lambda_H^{++} + \mu)(\mu + \delta_1)} \right). \tag{12}$$

In terms of the total subpopulation, we have:

$$N^{++} = \frac{\pi(\mu + \delta_1 + \lambda_H^{++})}{(\lambda_H^{++} + \mu)(\mu + \delta_1)}.$$

Substituting N^{++}, and I_H^{++}, into:

$$\lambda_H^{++} = \beta_H \frac{I_H^{++}}{N^{++}},$$

we have:

$$\lambda_H^{++} + (\mu + \delta_1)(1 - \mathcal{R}_{0H}) = 0.$$

It implies that $\lambda_H^{++} = (\mu + \delta_1)(\mathcal{R}_{0H} - 1)$. Hence, if $\mathcal{R}_{0H} > 1$, then $\lambda_H^{++} > 0$. Therefore, the HIV-only model (10) has a unique endemic equilibrium if $\mathcal{R}_{0H} > 1$. Next is to investigate the local asymptotic stability (LAS) of the HIV-only model (10). We evaluate the Jacobian matrix of model (10) at the EEP as follows:

$$J_{/EEP} = \begin{vmatrix} -\beta_H \frac{I_H^{++2}}{N^{++2}} & -\beta_H \frac{S^{++2}}{N^{++2}} \\ \beta_H \frac{I_H^{++2}}{N^{++2}} & \beta_H \frac{S^{++2}}{N^{++2}} - \mu - \sigma_1 \end{vmatrix}.$$

Evaluating the determinant, we have:

$$Det(J_{/EEP}) = \beta_H \frac{I_H^{++2}}{N^{++2}}(\mu + \sigma_1) + \frac{\mu \beta_H S^{++2}}{\mathcal{R}_{0H}}\left(1 - \frac{1}{\mathcal{R}_{0H}}\right).$$

The trace of the Jacobian matrix is given as:

$$Tr(J_{/EEP}) = -\mu - \frac{\beta_H}{\mathcal{R}_{0H}}(\mathcal{R}_{0H} - 1).$$

It is clear that $Det(J_{/EEP}) > 0$, and $Tr(J_{/EEP}) > 0$, if $\mathcal{R}_{0H} > 1$. Using the Routh-Hurwitz criterion, the conditions derived in the previous section indicate that the endemic equilibrium of the HIV-only model (10) is locally and asymptotically stable if $\mathcal{R}_{0H} > 1$, provided that all the model parameters remain positive. This means that HIV infection will invade the subpopulation.

Global asymptotic stability of DFE of HIV-only model

To demonstrate that the model Eq. (10) do not undergo a backward bifurcation at $\mathcal{R}_{0H} = 1$, we need to prove the global asymptotic stability (GAS) of the disease-free equilibrium (DFE) of the model (10).

Theorem 2 *The disease-free equilibrium (DFE) of model (10) is globally asymptotically stable (GAS) if $\mathcal{R}_{0H} \leq 1$, and it is unstable if $\mathcal{R}_{0H} \geq 1$.*

Proof We construct a linear Lyapunov function as follows:

$$\mathcal{L}_1 = I_H. \tag{13}$$

Differentiating (13) with respect to time (t) (where the dot represents derivative with respect to time) we have:

$$\dot{\mathcal{L}}_1 = \dot{I}_H = I_H \left(\beta_H \frac{S}{N} - (\mu - \delta_1) \right). \tag{14}$$

Recall that $S \leq N$, and $N \leq \frac{\pi}{\mu}$, for all $t > 0$, Eq. (14) becomes

$$\dot{\mathcal{L}}_1 \leq I_H (\mu - \delta_1) (\mathcal{R}_{0H} - 1). \tag{15}$$

Therefore $\dot{\mathcal{L}}_1 = 0$, if $\mathcal{R}_{0H} \leq 1$, with $\dot{\mathcal{L}}_1 = 0$, if and only if $I_H = 0$. Hence, it follows from Driessche and Watmough in [20] that every solution to the HIV-only model (10) with non-negative initial conditions converges to DFE as $t \to 0$. At point $I_H = 0$, in the first Eq. (10) yields $S(t) \to \frac{\pi}{\mu}$, as $t \to \infty$. Thus $(S, I_H) \to \left(\frac{\pi}{\mu}, 0 \right)$. As $t \to \infty$ for $R_H \leq 1$. Therefore, the disease-free equilibrium of HIV-only model (10) is globally asymptotically stable in the region $\mathcal{R}_{0H} \leq 1$.

Implication of Theorem 1 and Theorem 2:

Theorem 1 and Theorem 2, which center on the local stability of the disease-free equilibrium, form the basis by which we obtained the threshold for disease control and are able to confirm that the conditions for disease control have been met. As shown in the two theorems, the threshold for disease control is that the reproduction number of the disease must be less than one. This means that the introduction of a single infected individual into the susceptible human population, considered to be free from HIV and TB infection, will fail to generate an average of a single infected individual, resulting in the disease ultimately dying out in no time.

Global asymptotic stability of the EEP of HIV-only model

In this section, we consider the asymptotic stability of the endemic equilibrium point of HIV-only model (10).

Theorem 3 *The unique EEP of model (10) is globally asymptotically stable (GAS) in Ω_1 / Ω_2, whenever $\bar{\mathcal{R}}_{0H} > 1$, and unstable whenever $\bar{\mathcal{R}}_{0H} < 1$, and $\mathcal{L}_2 = 0$.*

Proof Consider HIV-only model (10), with the conditions: $\bar{\mathcal{R}}_{0H} = \bar{\mathcal{R}}_{0H} > 1$, when $\mathcal{L}_2 = 0$, for existence of unique equilibrium, therefore we construct the non-linear Lyapunov function of the Goh-Volterra type as follows:

$$\mathcal{L}_2 = S - S^{++} - S^{++} \ln \left(\frac{S}{S^{++}} \right) + I_H - I_H^{++} \ln \left(\frac{I_H}{I_H^{++}} \right). \tag{16}$$

Differentiating (16) with respect to time, yields

$$\dot{\mathcal{L}}_2 = \dot{S} - \frac{S^{++}}{S}\dot{S} + \left(\dot{I}_H - \frac{I_H^{++}}{I_H}\dot{I}_H \right). \tag{17}$$

From Eqs. (10) and (17), we have:

$$\dot{\mathcal{L}}_2 = \pi - \bar{\beta}_H I_H S - \mu S - \frac{S^{++}}{S}\left(\pi - \bar{\beta}_H I_H S - \mu S \right) + \bar{\beta}_H I_H S - \mu I_H - \frac{I_H^{++}}{I_H}\left(\bar{\beta}_H I_H S - \mu I_H \right), \tag{18}$$

$$\pi = \bar{\beta}_H I_H^{++} S^{++} + \mu S^{++}, \tag{19}$$

where

$$\mu = \bar{\beta}_H S^{++}. \tag{20}$$

Putting (19) and (20) into (18) we have:

$$\dot{\mathcal{L}}_2 = \mu S^{++}\left(2 - \frac{S^{++}}{S} - \frac{S}{S^{++}} \right) + \bar{\beta}_H I_H^{++} S^{++}\left(2 - \frac{S^{++}}{S} - \frac{S}{S^{++}} \right). \tag{21}$$

Observe that $\dot{\mathcal{L}}_2$, is a Lyapunov function in Ω_1/Ω_2, and the endemic equilibrium of HIV-only model (10) is unique under these conditions.

TB - only model

The TB-only model is obtained by setting all HIV components to zero in the co-infection model (5), that is, setting: $I_H = 0, I_{HT} = 0, I_{HU} = 0, I_{HDA} = 0, I_{TH} = 0$, to give TB-only model:

$$\frac{dS}{dt} = \pi - \lambda_T S - \mu S,$$
$$\frac{dE}{dt} = \lambda_T S + \varepsilon_1 \lambda_T R - (\psi_1 + \mu) E,$$
$$\frac{dE_L}{dt} = \psi_1 E - (\psi_2 + \sigma_1 + \mu) E_L,$$
$$\frac{dE_{UL}}{dt} = \psi_2 E_L - (\psi_3 + \sigma_2 + \mu) E_{UL},$$
$$\frac{dI_{UA}}{dt} = \psi_3 E_{UL} - (\psi_4 + \sigma_3 + \mu) I_{UA},$$
$$\frac{dT}{dt} = \psi_4 I_{UA} - (\psi_5 + \sigma_4 + \mu) T,$$
$$\frac{dR}{dt} = \sigma_1 E_L + \sigma_2 E_{UL} + \sigma_3 I_{UA} + \sigma_4 T - \varepsilon_1 \lambda_T R - \mu R,$$

with

$$\lambda_T = \beta_T \frac{(I_{UA} + \eta_1 T)}{N},$$

where

$$N(t) = S(t) + E(t) + E_L(t) + E_{UL}(t) + I_{UA}(t) + T(t) + R(t). \tag{22}$$

It can equally be shown that the solution set of TB-only model (22) are all positive when they enter the invariant region Ω_3, defined as:

$$\Omega_3 = \left\{ S(t) + E(t) + E_L(t) + E_{UL}(t) + I_{UA}(t) + T(t) + R(t) \in \Re_+^7 : N \leq \frac{\pi}{\mu} \right\}.$$

Therefore, we can conclude that it is appropriate to analyze the transmission dynamics of the TB-only model (22) within the domain Ω_3. This allows us to consider the model as biologically and mathematically well-posed, as indicated by previous studies [18].

Disease–free equilibrium (DFE) of TB-only model

To find the disease-free equilibrium of the TB-only model, we set all the disease components to zero at a steady-state. Thus, we have:

$$\Omega_3 = (S^+, E^+, E_L^+, E_{UL}^+, I_{UA}^+, T^+, R^+) = \left(\frac{\pi}{\mu}, 0, 0, 0, 0, 0, 0 \right).$$

Local stability of disease-free equilibrium of TB-only model

To determine the local asymptotic stability (LAS) of the disease-free equilibrium (DFE) in the TB-only model (22), we can use the next-generation matrix method. This approach is based on the method proposed by Van den Driessche and Wartmough [20], which involves defining a next-generation matrix where the new infection terms and the remaining transfer terms are represented by, respectively.

$$\mathcal{F}_2 = \begin{pmatrix} 0 & 0 & 0 & \beta_T & \eta_1\beta_T \\ 0 & 0 & 0 & 0 & 0 \\ 0 & 0 & 0 & 0 & 0 \\ 0 & 0 & 0 & 0 & 0 \\ 0 & 0 & 0 & 0 & 0 \end{pmatrix}, \quad \mathcal{V}_2 = \begin{pmatrix} c_1 & 0 & 0 & 0 & 0 \\ -\psi_1 & c_2 & 0 & 0 & 0 \\ 0 & -\psi_2 & c_3 & 0 & 0 \\ 0 & 0 & -\psi_3 & c_4 & 0 \\ 0 & 0 & 0 & -\psi_4 & c_5 \end{pmatrix},$$

where

$c_1 = (\psi_1 + \mu), c_2 = (\psi_2 + \sigma_1 + \mu), c_3 = (\psi_3 + \sigma_2 + \mu), c_4 = (\psi_4 + \sigma_3 + \mu),$ and $c_5 = (\psi_5 + \sigma_4 + \mu).$ ρ is the spectral radius of $(\mathcal{F}_2 \mathcal{V}_2^{-1})$. It follows from [26] that, the effective reproduction number of TB-only model (22) is given as

$$\mathcal{R}_T = \rho \left(\mathcal{F}_2 \mathcal{V}_2^{-1} \right),$$

$$\Rightarrow \mathcal{R}_T = \frac{\beta_T \psi_1 \psi_2 \psi_3 (c_5 + \eta_1 \psi_4)}{(\psi_1 + \mu)(\psi_2 + \sigma_1 + \mu)(\psi_3 + \sigma_2 + \mu)(\psi_4 + \sigma_3 + \mu)(\psi_5 + \sigma_4 + \mu)}. \tag{23}$$

Lemma 3 *The disease-free equilibrium (DFE) of the TB-only model (22) is locally asymptotically stable whenever $\mathcal{R}_T < 1$, and unstable whenever $\mathcal{R}_T > 1$.*

The threshold parameter, denoted by $\mathcal{R}_T$, is the basic reproduction number for the TB-only model (22), representing the average number of secondary TB infections caused by an infected individual introduced to a population completely free of TB infections [26].

Based on Lemma 3, TB can be eradicated from the population if the initial sizes of the subpopulation of the submodel are in the region of attraction of the DFE.

Analysis of the reproduction number for the TB-only model

It is important to analyze the basic reproduction number with respect to the treatment parameters, in order to determine the sufficient and necessary conditions required to control and eradicate the disease in the population. By taking the following limits, we can obtain:

$$\lim_{\sigma_1 \to \infty} \mathcal{R}_T = 0, \tag{24}$$

$$\lim_{\sigma_2 \to \infty} \mathcal{R}_T = 0, \tag{25}$$

$$\lim_{\sigma_3 \to \infty} \mathcal{R}_T = 0, \tag{26}$$

and

$$\lim_{\sigma_4 \to \infty} \mathcal{R}_T = \frac{\beta_T \psi_1 \psi_2 \psi_3}{(\psi_1 + \mu)(\psi_2 + \sigma_1 + \mu)(\mu + \sigma_2 + \psi_3)(\psi_4 + \sigma_3 + \mu)} > 0. \tag{27}$$

It can be inferred from the Eqs. (24)-(27) that implementing a control strategy that emphasizes high treatment rates for undiagnosed and diagnosed latent TB infections, as well as undiagnosed and diagnosed active TB infections, can lead to effective control of the disease in the population, provided that the right-hand sides of these equations are reduced to less than one.

However, it should be noted that near-total eradication of TB can only be achieved if high treatment rates are applied to all stages of the disease, rather than just focusing on the treatment of diagnosed active cases, as the limit in Eq. (27) does not approach zero. Furthermore, the effect of the treatment parameters and on the control of TB in the population can be determined by computing the partial derivatives of the reproduction number with respect to these parameters. This analysis will shed light on how changes in and impact the control of TB. Specifically, we obtain:

$$\frac{\partial \mathcal{R}_T}{\partial \sigma_1} = -\frac{\beta_T \psi_1 \psi_2 \psi_3 (\mu + \sigma_4 + \psi_5 + \eta_1 \psi_3 \psi_4)}{(\psi_1 + \mu)(\psi_2 + \sigma_1 + \mu)^2(\psi_3 + \sigma_2 + \mu)(\psi_4 + \sigma_3 + \mu)(\psi_5 + \sigma_4 + \mu)} < 0, \tag{28}$$

$$\frac{\partial \mathcal{R}_T}{\partial \sigma_2} = -\frac{\beta_T \psi_1 \psi_2 \psi_3 (\mu + \sigma_4 + \psi_5 + \eta_1 \psi_3 \psi_4)}{(\psi_1 + \mu)(\psi_2 + \sigma_1 + \mu)(\psi_3 + \sigma_2 + \mu)^2(\psi_4 + \sigma_3 + \mu)(\psi_5 + \sigma_4 + \mu)} < 0, \tag{29}$$

$$\frac{\partial \mathcal{R}_T}{\partial \sigma_3} = -\frac{\beta_T \psi_1 \psi_2 \psi_3 (\mu + \sigma_4 + \psi_5 + \eta_1 \psi_3 \psi_4)}{(\psi_1 + \mu)(\psi_2 + \sigma_1 + \mu)(\psi_3 + \sigma_2 + \mu)(\psi_4 + \sigma_3 + \mu)^2(\psi_5 + \sigma_4 + \mu)} < 0, \tag{30}$$

and

$$\frac{\partial \mathcal{R}_T}{\partial \sigma_4} = -\frac{\beta_T \psi_1 \psi_2 \psi_3 (\mu + \sigma_4 + \psi_5 + \eta_1 \psi_3 \psi_4)}{(\psi_1 + \mu)(\psi_2 + \sigma_1 + \mu)^2(\psi_3 + \sigma_2 + \mu)(\psi_4 + \sigma_3 + \mu)(\psi_5 + \sigma_4 + \mu)} < 0. \tag{31}$$

The results of the previous analysis indicate that effective treatment of undiagnosed and diagnosed latently infected individuals, as well as undiagnosed and diagnosed actively infected individuals, can have a positive impact on reducing the spread of TB in the population. This is supported by the fact that the partial derivatives of the reproduction number with respect to the treatment parameters were found to be negative. However, the analysis also revealed that a treatment strategy that places a higher emphasis on the treatment of diagnosed actively-infected individuals is more effective for controlling the disease than focusing on other stages of the disease.

Theorem 4 *The treatment of individuals infected with TB, regardless of the stage of infection, will have a positive impact on the dynamics of TB in the population.*

Further analysis of the relationship between the reproduction number and treatment rates for singly infected individuals with latent TB, as well as undiagnosed cases of latent TB, reveals that increasing the values of the treatment parameters would lead to a corresponding decrease in the value of the reproduction number. It was also found that a high treatment rate for individuals with latent TB can compensate for a lower treatment rate for undiagnosed cases of latent TB by reducing the value of the reproduction number to below unity. However, it is important to note that this conclusion was based on the specific parameter values used in the analysis.
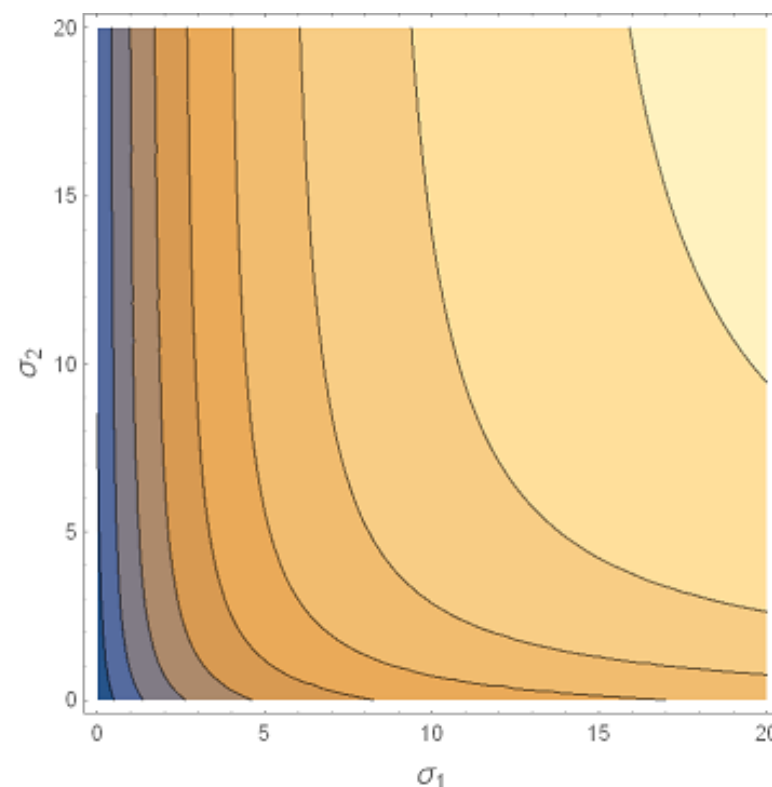
Figure 2. A contour plot of $\mathcal{R}_T$, as a function of σ_1, and σ_2, where parameter values are as given in Table 3

Existence of endemic equilibrium for the TB-only model

To find the endemic equilibrium point (EEP) of TB-only model (22) in the TB-only model (20) context, we can set each equation of model (22) to zero and solve for the force of infection. This

gives us:

$$
S^{++} = \left(\frac{\pi}{\lambda_T^{++} + \mu} \right), \ E^{++} = \left(\frac{\pi c_2 c_3 c_4 c_5 \lambda_T^{++} (\mu + \eta_1 \lambda_T^{++})}{P} \right),
$$

$$
E_L^{++} = \left(\frac{\pi \psi_1 c_1 c_3 c_4 c_5 \lambda_T^{++} (\mu + \eta_1 \lambda_T^{++})}{P} \right), E_{UL}^{++} = \left(\frac{\pi \psi_1 c_3 c_4 c_5 \lambda_T^{++} (\mu + \eta_1 \lambda_T^{++})}{P} \right),
$$

$$
I_{UA}^{++} = \left(\frac{\pi c_1 c_2 c_3 c_5 \lambda_T^{++} (\mu + \eta_1 \lambda_T^{++})}{P} \right), \ T^{++} = \left(\frac{\pi c_1 c_2 c_3 c_4 \lambda_T^{++} (\mu + \eta_1 \lambda_T^{++})}{P} \right),
$$

$$
R^{++} = \frac{Q}{P}, \quad \text{and} \quad N^{++} = \frac{R}{P}, \tag{32}
$$

where

$$
\begin{aligned}
P &= (\mu + \lambda_T^{++})(c_1 c_2 c_3 c_4 c_5 (\mu + \eta_1 \lambda_T^{++}) \\
&\quad - \eta_1 \lambda_T^{++} \psi_1 (\sigma_1 c_3 c_4 c_5 + \sigma_2 \psi_2 c_4 c_5 + \sigma_3 \psi_2 \psi_3 c_5 + \sigma_4 \psi_2 \psi_3 \psi_4 c_5 + \sigma_4 \psi_2 \psi_3 \psi_4)), \\
Q &= \pi \psi_1 \lambda_T^{++} (\sigma_1 c_3 c_4 c_5 + \sigma_2 \psi_2 c_4 c_5 + \sigma_3 \psi_2 \psi_3 c_4 + \sigma_4 \psi_2 \psi_3 \psi_4 c_5 + \sigma_4 \psi_2 \psi_3), \\
R &= c_1 c_2 c_3 c_4 c_5 (\mu + \eta_1 \lambda_T^{++}) \pi c_2 c_3 c_4 c_5 \lambda_T^{++} (\mu + \eta_1 \lambda_T^{++}) + \pi c_1 c_2 c_4 c_5 \lambda_T^{++} (\mu + \eta_1 \lambda_T^{++}) \\
&\quad + \pi c_1 c_2 c_3 c_5 \lambda_T^{++} (\mu + \eta_1 \lambda_T^{++}) - \pi \psi_1 \eta_1 \lambda_T^{++} (\sigma_1 c_3 c_4 c_5 + \sigma_2 \psi_2 c_4 c_5 + \sigma_3 \psi_2 \psi_3 c_5 + \sigma_4 \psi_2 \psi_3 \psi_4 c_5 + \sigma_4 \psi_2 \psi_3) \\
&\quad + \pi c_1 c_2 c_3 c_4 c_5 \lambda_T^{++} (\mu + \eta_1 \lambda_T^{++}) + \pi c_1 c_2 c_3 c_4 c_5 \lambda_T^{++} (\mu + \eta_1 \lambda_T^{++}) \\
&\quad + \pi c_1 \lambda_T^{++} (\sigma_1 c_3 c_4 c_5 + \sigma_2 \psi_2 c_4 c_5 + \sigma_3 \psi_2 \psi_3 c_4 + \sigma_4 \psi_2 \psi_3 \psi_4 c_5 + \sigma_4 \psi_2 \psi_3 \psi_4).
\end{aligned}
$$

It is important to note that on expansion, it can be shown that $P > 0$, and $R > 0$, likewise. By letting the TB force of infection at a steady state by:

$$
\lambda_T^{++} = \beta_T^{++} \frac{(I_{UA}^{++} + \eta_1 T^{++})}{N^{++}}. \tag{33}
$$

By substituting the values I_{UA}^{++}, T^{++}, and N^{++}, above into the force of infection in (33), we obtain:

$$
P_0 \lambda_T^{++2} + P_1 \lambda_T^{++} + P_2 = 0, \tag{34}
$$

where

$$
\begin{aligned}
P_0 &= \eta_1 (c_2 c_3 c_4 c_5 + \psi_1 c_3 c_4 c_5 + \psi_1 \psi_2 c_4 c_5 + \psi_1 \psi_2 \psi_3 c_3 c_5 + \psi_1 \psi_2 \psi_3 \psi_4 c_5 + \psi_1 \psi_2 \psi_3 \psi_4), \\
P_1 &= \eta_1 c_1 c_2 c_3 c_4 c_5 (1 - R_T) - \eta_1 \sigma_1 \psi_1 c_3 c_4 c_5 - \eta_1 \sigma_2 \psi_1 c_3 c_4 c_5 - \eta_1 \sigma_3 \psi_1 \psi_2 \psi_3 c_4 c_5 - \eta_1 \sigma_4 \psi_1 \psi_2 \psi_3 \psi_4 c_5 \\
&\quad - \eta_1 \sigma_4 \psi_1 \psi_2 \psi_3 \psi_4 + \mu c_2 c_3 c_4 c_5 + \mu \psi_1 c_3 c_4 c_5 + \mu \psi_1 \psi_2 c_4 c_5 + \mu \psi_1 \psi_2 \psi_3 c_5 + \mu \psi_1 \psi_2 \psi_3 \psi_4 c_5 \\
&\quad + \mu \psi_1 \psi_2 \psi_3 \psi_4 + \sigma_1 \psi_1 c_3 c_4 c_5 + \sigma_2 \psi_1 \psi_2 c_4 c_5 + \sigma_3 \psi_1 \psi_2 \psi_3 c_5 + \sigma_4 \psi_1 \psi_2 \psi_3 \psi_4 + \sigma_4 \psi_1 \psi_2 - 3 \psi_3 \psi_4, \\
P_2 &= \mu c_1 c_2 c_3 c_4 c_5 (1 - \mathcal{R}_T).
\end{aligned}
$$

A careful look at the quadratic equation in (34) shows that P_0, has a positive coefficient while P_1 has a positive (negative) coefficient which depends on whether the basic reproduction number $\mathcal{R}_T$ is less (greater) than unity. From this, we establish the following results:

Lemma 4 *The TB-only model* (22) *has:*

- *A unique endemic equilibrium if $A_2 < 0 \leftrightarrow \mathcal{R}_T > 1$;*
- *A unique endemic equilibrium if $A_2 < 0$, and $A_0 = 0$, or $A_1^2 - 4 A_2 A_0 = 0$;*
- *Two endemic equilibria if $A_0 > 0$, $A_1 < 0$, and $A_{21} - 4 A_2 A_0 > 0$, and $\mathcal{R}_T < 1$;*

- *No endemic equilibrium otherwise.*

From the above, the occurrence of item (22) gives rise to the suggestion of the possibility of the existence of backward bifurcation in the TB-only model (22), where there is coexistence of locally asymptotically stable DFE and locally asymptotically stable endemic equilibrium whenever the basic reproduction number $\mathcal{R}_T < 1$. The causes of this kind of phenomenon in epidemiological models were extensively discussed in the works of [9, 16, 27–29]. Biologically, the existence of backward bifurcation in a model implies that the classical epidemiological requirement, that for the effective control of a disease in a population, the basic reproduction number of the disease must be less than unity, though necessary, in this circumstance, it is not sufficient for the effective control of such a disease. Consequently, we now explore the existence of backward bifurcation in the TB-only model (22).

Analysis of bifurcation

Consequently, it becomes highly imperative to explore the possibility of backward bifurcation in the TB-only model (22) as follows:

Theorem 5 *For the TB-only model (22) there is the exhibition of the phenomenon of backward bifurcation at $\mathcal{R}_T = 1$, whenever the inequality $\varepsilon_1 > \frac{(\omega_2+\omega_3+\omega_4+\omega_5+\omega_6+\omega_7)(\omega_3+\eta_1\omega_4)}{\omega_8(\omega_3+\eta_1\omega_4)}$ holds.*
It should be noted that ε_1, stands for the modification parameter accounting for reduced susceptibility to tuberculosis reinfection after an individual has been successfully treated for a previous tuberculosis infection.

Proof Let

$$\Delta_3 = \left(S^{++}, E^{++}, E_L^{++}, E_{UL}^{++}, I_{UA}^{++}, T^{++}, R^{++}\right), \tag{35}$$

denote an arbitrary endemic equilibrium point of the TB-only model (22). We then investigate whether a backward bifurcation exists in the model by using the 'center manifold theory' [30]. For convenience, we carry out the following change of variables before applying the theory: Let $S = x_1$, $E = x_2$, $E_L = x_3$, $E_{UL} = x_4$, $I_{UA} = x_5$, $T = x_6$, and $R = x_7$. Consequently, we rewrite model (22) as follows:

$$
\begin{aligned}
\dot{x}_1 \equiv f_1 &= \pi - \frac{\beta_T(x_5 + \eta_1 x_6)x_1}{\sum_{i=1} x_i} - \mu x_1, \\
\dot{x}_2 \equiv f_2 &= \frac{\xi_1 \beta_T(x_5 + \eta_1 x_6)x_7}{\sum_{i=1}^7 x_i} - c_1 x_2, \\
\dot{x}_3 \equiv f_3 &= \phi_1 x_2 - c_2 x_3, \\
\dot{x}_4 \equiv f_4 &= \phi_2 x_3 - c_3 x_4, \\
\dot{x}_5 \equiv f_5 &= \phi_3 x_4 - c_4 x_5, \\
\dot{x}_6 \equiv f_6 &= \phi_4 x_5 - c_5 x_6, \\
\dot{x}_7 \equiv f_7 &= \sigma_1 x_3 + \sigma_2 x_5 + \sigma_3 x_5 + \sigma_5 x_6 - \frac{\beta_T(x_5 + \eta_1 x_6)x_2}{\sum_{i=1} x_i} - \mu x_7.
\end{aligned}
\tag{36}
$$

Considering a bifurcation parameter $\beta_T = \beta_T^*$. By solving for $\beta_T = \beta_T^*$, from R_T, yields

$$\beta_T^* = \frac{c_1 c_2 c_3 c_4 c_5}{\phi_1 \phi_2 \phi_3 (1 + \sigma_1)(c_5 + \mu \eta \phi_4 + \eta \phi_3 \phi_4)},$$

where

$c_1 = (\phi_1 + \mu)$, $c_2 = (\phi_2 + \sigma_1 + \mu)$, $c_3 = (\phi_3 + \sigma_2 + \mu)$, $c_4 = (\phi_4 + \sigma_3 + \mu)$, and $c_5 = (\varphi_5 + \sigma_4 + \mu)$. We then evaluate the Jacobian of the transformed system (36) evaluated at DFE (Δ_3) with $\beta_T = \beta_T^*$, to obtain

$$
J(\Delta_3) = \begin{bmatrix}
-\mu & 0 & 0 & 0 & -\beta_T^* & -\eta_1\beta_T^* & 0 \\
0 & -c_1 & 0 & 0 & \beta_T^* & \eta_1\beta_T^* & 0 \\
0 & \phi_1 & -c_1 & 0 & 0 & 0 & 0 \\
0 & 0 & \phi_2 & -c_3 & 0 & 0 & 0 \\
0 & 0 & 0 & \phi_3 & -c_4 & 0 & 0 \\
0 & 0 & 0 & 0 & \phi_4 & 0 & 0 \\
0 & 0 & \sigma_1 & \sigma_2 & \sigma_3 & \sigma_4 & -\mu
\end{bmatrix}.
$$

The matrix J^* has a simple zero eigenvalue and the remaining eigenvalues have real parts indicating that "center manifold theory" is applicable. It is noted that matrix J^* has a right eigenvector given by $\omega = (\omega_1, \omega_2, ..., \omega_7)^T$, where $\omega_1 = \frac{-(\beta_T^*\omega_5 - \eta_1\beta_T^*\omega_5)}{\mu}$, $\omega_2 > 0$, $\omega_3 = \frac{\phi_1\phi_2}{c_2}$, $\omega_5 = \frac{\phi_1\phi_2\phi_3\omega_3}{c_2c_3c_4}$, $\omega_6 = \frac{\phi_1\phi_2\phi_3\phi_4\omega_2}{c_2c_3c_4c_5}$, and $\omega_7 = \frac{\sigma_1\omega_3 + \sigma_2\omega_4 + \sigma_3\omega_5 + \sigma_4\omega_6}{\mu}$. Similarly, J^* has left eigenvectors $V = (v_1, v_2, ..., v_7)$, satisfying $v.\omega = 1$, with $v_1 = 0$, $v_2 = \frac{\phi_1v_3}{c_1}$, $v_3 > 0$, $v_4 = \frac{c_2v_3}{\phi_2}$, $v_5 = \frac{c_2c_3\omega_2}{\phi_3}$, $v_6 = \frac{\eta_1\beta_T^*\phi_3\phi_1}{c_1c_5}$, and $v_7 = 0$.

Arising from Theorem 4.1 in [30] computation of the associated non-zero partial derivatives of $f(x)$, evaluated at DFE (Δ_3), the associated bifurcation coefficients a, and b defined as

$$
a = \sum v_k\omega_i\omega_j \frac{\partial^2 f_k}{\partial x_i \partial x_j}(0,0), \quad \text{and} \quad b = \sum v_k\omega_i \frac{\partial^2 f_k}{\partial x_i \partial \beta_T^*}(0,0),
$$

are: $a = 2v_2\eta_1\beta_T\frac{\mu}{\pi}(\omega_3\omega_7 + \omega_4\omega_7) - 2v_2\eta_1\beta_T\frac{\mu}{\pi}(\omega_2\omega_3 + \omega_3\omega_5 + \omega_3\omega_6 + \omega_3^2 + \omega_3\omega_7 + \omega_3\omega_4) - 2v_2\eta_1\beta_T * \frac{\mu}{\pi}(\omega_2\omega_4 + \omega_4\omega_5 + \omega_3\omega_4 + \omega_4\omega_7 + \omega_4^2 + \omega_4\omega_5 + \omega_4\omega_6)$, and $b = v_2\omega_3 + \eta_1v_2\omega_4 > 0$, with $v_2, \omega_2, \omega_3, \omega_4, \omega_5, \omega_6$, and ω_7, being positive. Consequently, due to the fact that the bifurcation coefficient $b > 0$, it can be deduced from Theorem 4.1 in [30] that the TB-only model (22) undergoes the phenomena of a backward bifurcation whenever the backward bifurcation coefficient $a > 0$. This is so if

$$
\epsilon_1 > \frac{(\omega_2 + \omega_3 + \omega_4 + \omega_5 + \omega_6 + \omega_7)(\omega_3 + \eta_1\omega_4)}{\omega_8(\omega_3 + \eta_1\omega_4)} = \epsilon^* \tag{37}
$$

holds. It should be recalled that ϵ_1, stands for the modification parameter accounting for the reduction in susceptibility to tuberculosis reinfection after an infected individual has been successfully treated for a previous tuberculosis infection. It should be noted that all parameters of model (22) are non-zero, and $\beta_T^* > 0$. Setting $\epsilon_1 = 0$, the bifurcation coefficient a, is reduced to

$$
\begin{aligned}
a = -[2v_2\beta_T^*\frac{\mu}{\pi}(\omega_2\omega_3 + \omega_3\omega_5 + \omega_3\omega_6 + \omega_3^2 + \omega_3\omega_6 + \omega_3\omega_4) \\
+ 2v_2\eta_1\beta_T^*\frac{\mu}{\pi}(\omega_2\omega_4 + \omega_4\omega_5 + \omega_3\omega_4 + \omega_4\omega_7\omega_4^2 + \omega_4\omega_6 + \omega_4\omega_6)],
\end{aligned} \tag{38}
$$

with $v_2 > 0$, $\omega_2 > 0$, $\omega_3 > 0$, $\omega_4 > 0$, $\omega_5 > 0$, $\omega_6 > 0$, and $\omega_7 > 0$, where each of them are as defined earlier. Consequently, since $b > 0$, it can be deduced from Theorem 4.1 in [30] that the TB-only model (22) does not undergo a backward bifurcation if $\epsilon = 0$, since the backward bifurcation coefficient $a < 0$. The revelation from here is that the cause of backward bifurcation in

the model (22) is the susceptibility to tuberculosis reinfection after a successful treatment from a previous infection. Obviously, for the TB-only model (22) to undergo backward bifurcation at $R_T = 1$, requires that the bifurcation coefficient $a > 0$, for ϵ_1, is of greater value than the quantity on the right-hand side of (37), that is $\epsilon_1 > \epsilon^*$. On the other hand, if $\epsilon_1 < \epsilon^*$, model (22) will not undergo backward bifurcation at $R_T = 1$. As a matter of fact, if $\epsilon_1 = 0$, for the TB-model (22), there will be the existence of the phenomenon of backward bifurcation. See Figure 3 for the schematic diagram of the phenomenon of backward bifurcation that the TB-only model (22) undergoes.
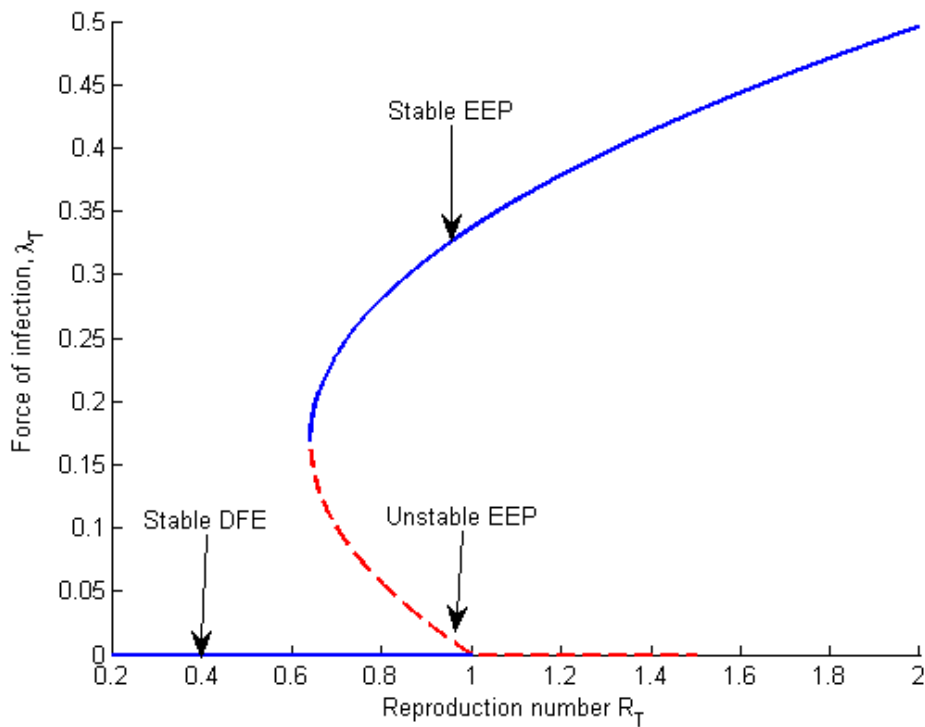

Figure 3. Bifurcation diagram of the TB-only model

Global asymptotic stability of DFE of TB-only model

In this section, we remove the cause of backward bifurcation, by setting $\varepsilon_1 = 0$, and then show that the given model (22) is globally asymptotically stable.

By considering model (22) with $\varepsilon_1 = 0$, the following is claimed:

Theorem 6 *The DFE of TB-only model (22) is globally asymptotically stable in Ω_3, whenever the reproduction number $\mathcal{R}_T < 1$.*

See the proof of this theorem in ''Appendix A''. The implication of Theorem 6 epidemiologically is that a previous infection of the disease covers a lifelong immunity to reinfection of susceptible individuals to tuberculosis. Thus, tuberculosis can ultimately be eradicated from the given human population when the reproduction number $\mathcal{R}_T < 1$.

Furthermore, since with $\varepsilon_1 = 0$, the global stability of the DFE of the TB-only model (22) follows if $\mathcal{R}_T < 1$, from here, we carry out the estimates of the range of values of the treatment parameters σ_1, σ_2, σ_3, and σ_4, for which the objectives of tuberculosis eradication is possible. When we set $\mathcal{R}_T < 1$, and make the treatment parameters σ_1, σ_2, σ_3, and σ_4, the subject of the expression in the

reproduction number of the model (22), we obtain the following:

$$
\begin{aligned}
\sigma_1 &> \beta_T \psi_1 \psi_2 \psi_3 \frac{(c_5 + \eta_1 \psi_4)}{(\psi_1 + \mu)(\psi_3 + \sigma_2 + \mu)(\psi_4 + \sigma_3 + \mu)(\psi_5 + \sigma_4 + \mu)} - (\psi_2 + \mu), \\
\sigma_2 &> \beta_T \psi_1 \psi_2 \psi_3 \frac{(c_5 + \eta_1 \psi_4)}{(\psi_1 + \mu)(\psi_2 + \sigma_1 + \mu)(\psi_4 + \sigma_3 + \mu)(\psi_5 + \sigma_4 + \mu)} - (\psi_3 + \mu), \\
\sigma_3 &> \beta_T \psi_1 \psi_2 \psi_3 \frac{(c_5 + \eta_1 \psi_4)}{(\psi_1 + \mu)(\psi_2 + \sigma_1 + \mu)(\psi_3 + \sigma_2 + \mu)(\psi_5 + \sigma_4 + \mu)} - (\psi_4 + \mu), \\
\sigma_4 &> \beta_T \psi_1 \psi_2 \psi_3 \frac{(c_5 + \eta_1 \psi_4)}{(\psi_1 + \mu)(\psi_2 + \sigma_1 + \mu)(\psi_3 + \sigma_2 + \mu)(\psi_4 + \sigma_3 + \mu)} - (\psi_5 + \mu).
\end{aligned} \tag{39}
$$

If the inequalities in (39) above are satisfied, then the reproduction number $\mathcal{R}_T < 1$, and tuberculosis can be completely eradicated in the human population.
However, from the first inequalities in (39), if

$$
\beta_T \psi_1 \psi_2 \psi_3 \frac{(c_5 + \eta_1 \psi_4)}{(\psi_1 + \mu)(\psi_3 + \sigma_2 + \mu)(\psi_4 + \sigma_3 + \mu)(\psi_5 + \sigma_4 + \mu)} < (\psi_2 + \mu),
$$

then treating individuals that are latently-infected with TB is not necessary as $\sigma_1 = 0$, will result in $\mathcal{R}_T < 1$. Likewise, the same results are obtained from other inequalities in (39).

4 Analysis of the co-infection model of TB-HIV

We carry out the analysis of the HIV-TB Co-infection model (5) for its basic properties as follows:

Local asymptotic stability of the DFE of the TB-HIV co-infection model

The disease free equilibrium of the TB-HIV co-infection model (5) is as given below:

$$
\begin{aligned}
D_4 &= \left(S^+, E^+, E_L^+, E_{UL}^+, I_{UA}^+, T^+, R^+, I_H^+, E_{HT}^+, I_{HU}^+, I_{HUA}^+, I_{HDA}^+, T_{HT}^+ \right) \\
&= \left(\frac{\pi}{\mu}, 0, 0, 0, 0, 0, 0, 0, 0, 0, 0, 0, 0, \right).
\end{aligned} \tag{40}
$$

By using the next-generation matrix method, we obtain the Local Asymptotic Stability (LAS) of the DFE of co-infection model (5). It follows from Driessche and Watmough in [20] which is defined by FV^{-1}. Where F, and V, are the terms for new infection and the terms for the remainder respectively, given as:

$$
F = \begin{bmatrix}
0 & 0 & 0 & \beta_T & \eta_1 \beta_T & 0 & 0 & 0 & \eta_2 \beta_T & \eta_3 \beta_T & 0 \\
0 & 0 & 0 & 0 & 0 & 0 & 0 & 0 & 0 & 0 & 0 \\
0 & 0 & 0 & 0 & 0 & 0 & 0 & 0 & 0 & 0 & 0 \\
0 & 0 & 0 & 0 & 0 & 0 & 0 & 0 & 0 & 0 & 0 \\
0 & 0 & 0 & 0 & 0 & \beta_H & \beta_H & \phi_1 \beta_H & \phi_2 \beta_H & \phi_3 \beta_H & \phi_4 \beta_H \\
0 & 0 & 0 & 0 & 0 & 0 & 0 & 0 & 0 & 0 & 0 \\
0 & 0 & 0 & 0 & 0 & 0 & 0 & 0 & 0 & 0 & 0 \\
0 & 0 & 0 & 0 & 0 & 0 & 0 & 0 & 0 & 0 & 0 \\
0 & 0 & 0 & 0 & 0 & 0 & 0 & 0 & 0 & 0 & 0 \\
0 & 0 & 0 & 0 & 0 & 0 & 0 & 0 & 0 & 0 & 0 \\
0 & 0 & 0 & 0 & 0 & 0 & 0 & 0 & 0 & 0 & 0
\end{bmatrix},
$$

and

$$
V = \begin{bmatrix}
c_1 & 0 & 0 & 0 & 0 & 0 & 0 & 0 & 0 & 0 & 0 \\
-\psi_1 & c_2 & 0 & 0 & 0 & 0 & 0 & 0 & 0 & 0 & 0 \\
0 & -\psi_2 & c_3 & 0 & 0 & 0 & 0 & 0 & 0 & 0 & 0 \\
0 & 0 & -\psi_3 & c_4 & 0 & 0 & 0 & 0 & 0 & 0 & 0 \\
0 & 0 & 0 & -\psi_4 & c_5 & 0 & 0 & 0 & 0 & 0 & 0 \\
0 & 0 & 0 & 0 & 0 & c_6 & -\sigma_{T1} & -\sigma_{T2} & -\sigma_{T3} & -\sigma_{T4} & 0 \\
0 & 0 & 0 & 0 & 0 & 0 & c_7 & 0 & 0 & 0 & 0 \\
0 & 0 & 0 & 0 & 0 & 0 & 0 & c_8 & 0 & 0 & 0 \\
0 & 0 & 0 & 0 & 0 & 0 & 0 & -\psi_{HUA} & c_9 & 0 & 0 \\
0 & 0 & 0 & 0 & 0 & 0 & 0 & 0 & -\psi_{HDA} & c_{10} & 0 \\
0 & 0 & 0 & 0 & 0 & 0 & 0 & 0 & 0 & -\psi_{HU} & c_{11}
\end{bmatrix},
$$

where

$c_1 = (\psi_1 + \mu), c_2 = (\psi_2 + \sigma_1 + \mu), c_3 = (\psi_3 + \sigma_2 + \mu), c_4 = (\psi_4 + \sigma_3 + \mu), c_5 = (\psi_5 + \sigma_4 + \mu), c_6 = (\delta_1 + \mu), c_7 = (\psi_{HU} + \sigma_{T1} + \delta_2 + \mu), c_8 = (\psi_{HUA} + \delta_3 + \sigma_{T2} + \mu), c_9 = (\psi_{HDA} + \sigma_{T3} + \delta_4 + \mu), c_{10} = (\psi_{HT} + \sigma_{T4} + \delta_5 + \mu),$ and $c_{11} = (\sigma_{T5} + \delta_6 + \mu)$.

Consequently, arising from [26], the basic reproduction number for the disease is obtained as:

$$
\mathcal{R}_C = \rho\left(FV^{-1}\right) = \max\{\mathcal{R}_H, \mathcal{R}_T\},
$$

where

$$
\mathcal{R}_H = \frac{\beta_H}{(\mu + \sigma_1)}, \quad \text{and} \quad \mathcal{R}_T = \frac{\beta_T \psi_1 \psi_2 \psi_3 (c_5 + \eta_1 \psi_4)}{(\psi_1 + \mu)(\psi_2 + \sigma_1 + \mu)(\psi_3 + \sigma_2 + \mu)(\psi_4 + \sigma_3 + \mu)(\psi_5 + \sigma_4 + \mu)}.
$$

That is,

$$
\mathcal{R}_C = \frac{\beta_T \psi_1 \psi_2 \psi_3 (c_5 + \eta_1 \psi_4)}{(\psi_1 + \mu)(\psi_2 + \sigma_1 + \mu)(\psi_3 + \sigma_2 + \mu)(\psi_4 + \sigma_3 + \mu)(\psi_5 + \sigma_4 + \mu)}. \tag{41}
$$

It should be noted that Theorem 2 in [20] gives rise to the result below.

Lemma 5 *The disease-free equilibrium, (DFE), D_4 of the co-infection model (5), is locally asymptotically stable (LAS) whenever the reproduction number of the model is less than unity ($\mathcal{R}_C < 1$), and unstable when $\mathcal{R}_C > 1$.*

It is pertinent to note that the quantity $\mathcal{R}_C = max\{\mathcal{R}_H, \mathcal{R}_T\}$, is the effective reproduction number of the co-infection model (5), in which case is previously defined. By adopting the same approach as we did in Section 3, it can be shown that there is an exhibition of the phenomenon of backward bifurcation at $\mathcal{R}_C = 1$, for co-infection model (5). It is pertinent to note that the same conclusion is arrived at for TB-only model (22) in the previous section, that susceptibility to tuberculosis reinfection after a successful treatment of the disease is the cause of this backward bifurcation in the co-infection model (5).

Theorem 7 *There is an exhibition of backward bifurcation at $\mathcal{R}_C = 1$, for co-infection model (5) whenever*

$$
\varepsilon_1 > \frac{(\omega_2 + \omega_3 + \omega_4 + \omega_5 + \omega_6 + \omega_7 + \omega_8)(\omega_3 + \eta_1 \omega_4)}{\omega_8 (\omega_3 + \eta_1 \omega_4)}
$$

holds.

For the proof of this theorem, see ''Appendix B''.

5 Sensitivity analysis and uncertainty analysis of TB-only model

In the TB-only model, many parameters are involved in its formulation. Therefore, expectedly, uncertainties do arise in the estimation of the values of these parameters adopted for the numerical simulations of the model. By adopting the approach in [16, 26, 31], using Latin hypercube sampling (LHS), we carried out in this section, uncertainty analysis with a view to accounting for the effect that such uncertainties have on the numerical simulation results obtained in this work. Additionally, by using partial rank correlation coefficients (PRCC), we equally carried out a global sensitivity analysis to quantify the impact of the variations or sensitivity of each parameter on the associated numerical simulations.

The Latin hypercube sampling (LHS) method is adopted here by defining baseline values and ranges for each of the parameters of the TB-only model (22), as stated in Table 3, where multiple runs for $NR = 1000$, are done for the sample data for the response output [26, 31]. In this case, it is the control reproduction number $\mathcal{R}_T$. It is worth mentioning that each parameter is assumed to obey a uniform distribution [32].

On the other hand, we computed the sensitivity of the parameters in the Tuberculosis-only model (22) by finding PRCC between each parameter and the control reproduction number $\mathcal{R}_T$. The values of these PRCC values making up the effective reproduction number of the model (22) are as given in Table 2, while Figure 4 gives the distribution of PRCC values. From the PRCC distribution in Figure 4, it could be seen that the transmission rate for tuberculosis β_T, the modification parameters that account for the infectiousness of infected individuals with TB-only η_1, and the treatment rates for singly infected individuals with latently-infected TB, σ_1, are the parameters that play a dominant role in driving the dynamics of tuberculosis with respect to the response function $\mathcal{R}_T$. It is worth mentioning that while β_T, and η_1, are positively correlated with the response function $\mathcal{R}_T$, on the other hand, σ_1, is negatively correlated with the response function $\mathcal{R}_T$. The epidemiological implication of this is that tuberculosis can be effectively controlled and eradicated by procuring all strategies that can help minimize the transmission rate of the disease, such as measures like public awareness and educational enlightenment campaigns for susceptible individuals always to cover their mouth when coughing or sneezing, and the need for infants to be vaccinated against tuberculosis.

Likewise, the infectiousness of individuals with latent tuberculosis can be minimized by testing and adequate treatment of latently infected individuals.

Table 2. PRCC values of the parameters of TB-only model (22), with $\mathcal{R}_T$, as the output (response function). Parameter values and ranges used are as given in Table 3

| S/N	Parameters	PRCC (R_T)
1.	β_T	0.9013
2.	σ_1	0.0412
3.	u_2	-0.03712
4.	σ_2	-0.3124
5.	ψ_3	-0.4021
6.	ψ_2	-0.4202
7.	η_1	0.5633
8.	σ_3	-0.6234
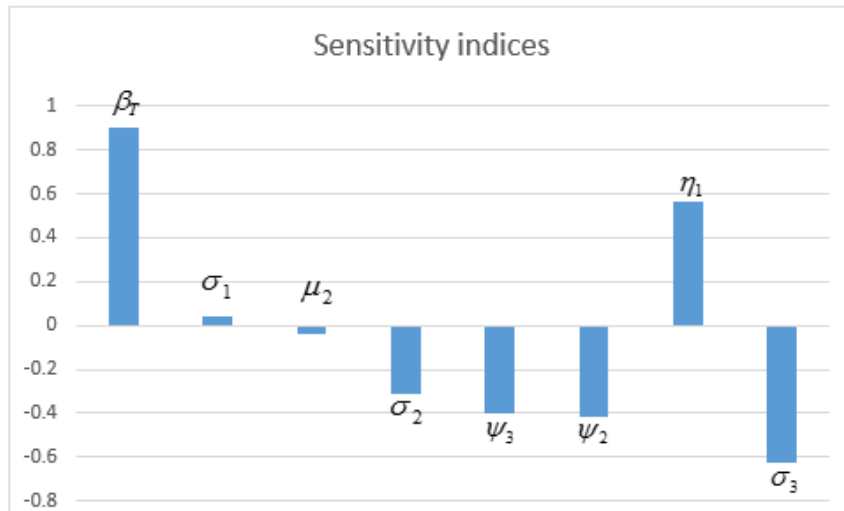
Figure 4. Schematic diagram of the sensitivity indices for the TB-only model (22). Values and ranges of parameters used are as given in Table 3

6   Numerical simulation

For the illustration of some of the theoretical results obtained earlier in this study, it is necessary to conduct numerical simulations of the co-infection model. We performed numerical simulations of the model using the parameter values presented in the table below. The numerical simulation of the model was carried out using MATLAB's ODE45 solver, which is well-known for its high convergence, consistency, and stability. The embedded numerical scheme in MATLAB, like other computing software such as Maple, Mathematica, and Scientific Workplace, is known for its reliability and efficiency in numerical simulations of epidemiological models.

Table 3. Values of parameters of the co-infection model (5) with the total population of Nigeria as of January 1st, 2023 estimated at 200,000,000 (real-life data as obtained from National Population Commission (NPC) of Nigeria)

| Parameter	Baseline (Range)	Sources
π	5,000 [3,500 - 6500] year^{-1}	[1]
μ	0.02043 [0.02034 - 0.02052] year^{-1}	[16]
$\beta_T(\beta_H)$	0.1 year^{-1}	[1]
$\sigma_1, \sigma_2, \sigma_3, \sigma_4$	0.7, 0.7, 0.7, 0.7 year^{-1}	[15]
$\sigma_{T1}, \sigma_{T2}, \sigma_{T3}, \sigma_{T4}$	0.7, 0.7, 0.7, 0.7 year^{-1}	[15]
$\psi_1, \psi_2, \psi_3, \psi_4$	6, 4.18, 2.5, 3 year^{-1}	[16]
$\psi_{HU}, \psi_{HUA}, \psi_{HDA}, \psi_{HT}$	6, 4.5, 3, 3 year^{-1}	[16]
$\varepsilon_1, \varepsilon_2$	1, 1.2 [0.8-1.2, 1-1.5]	Assumed
γ_1, γ_2	0.6, 0.8 [0-1, 0-1]	Assumed
$\theta_1, \theta_2, \theta_3, \theta_4, \theta_5, \theta_6, \theta_7, \theta_8$	3.2, 3, 3.2, 2, 2, 2, 2, 2 [2.8-3.6, 2.5-3.5, 1.7 -2.3]	[16]
η_1, η_2, η_3	1.2, 1.3, 1.5 [1-2, 0.9-1.7, 1-2.3]	[16]
$\phi_1, \phi_2, \phi_3, \phi_4$	1.3, 1.7, 1.2, 1.1 [1-1.6, 1-2.4, 0.8-1.6, 0.7-1.5, 0.75-1.25]	[16]
$\delta_1, \delta_2, \delta_3, \delta_4, \delta_5, \delta_6$	0.08, 0.05, 0.8, 0.1, 0.1, 0.01 year^{-1}	[15]
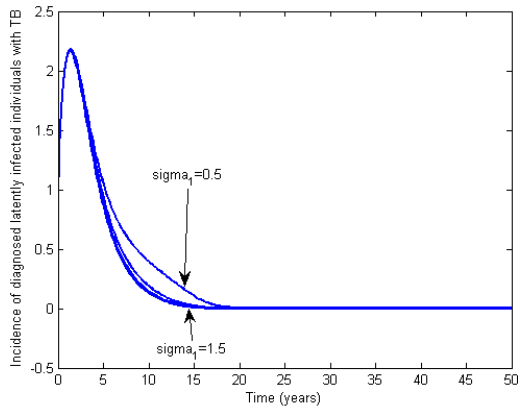
(a) Incidence of diagnosed latently infected individuals with TB with the effect of σ_1
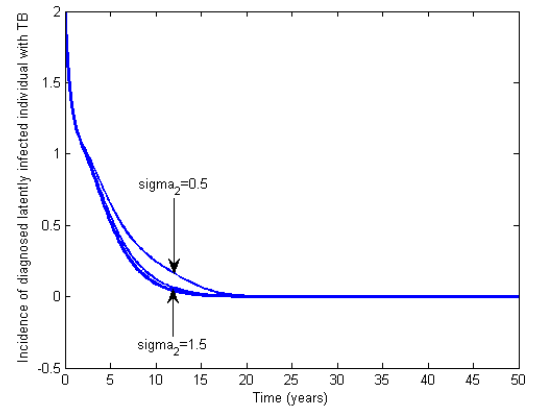
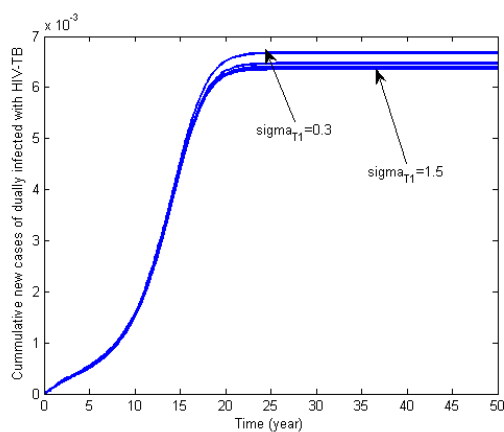**(b)** Incidence of diagnosed latently infected individuals with TB with the effect of σ_2
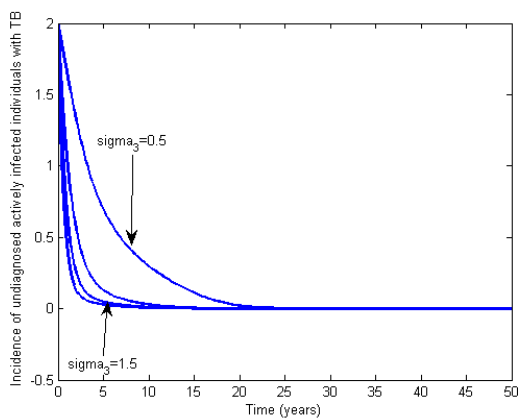
(c) Incidence of diagnosed latently infected individuals with TB with the effect of σ_3
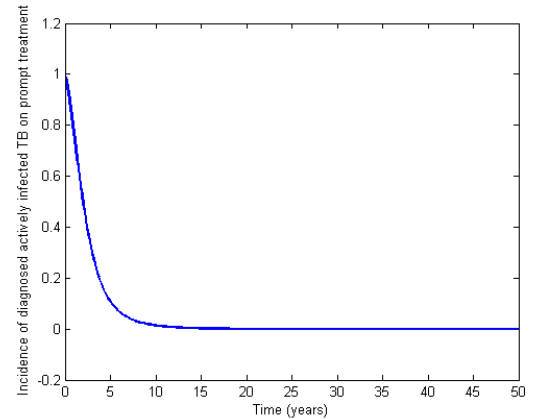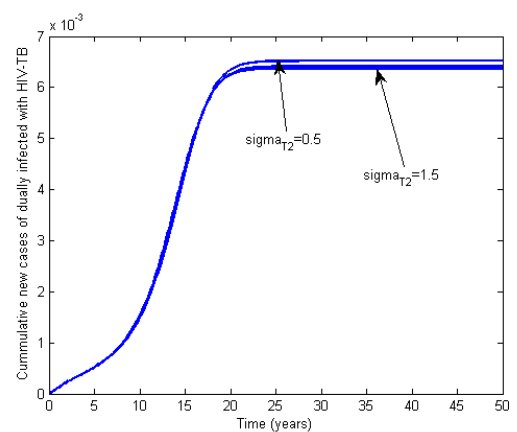
(d) Incidence of diagnosed latently infected individuals with TB with the effect of σ_4

Figure 5. Incidence of diagnosed latently infected individuals with TB with the effect of σ

(a) Cumulative number of new cases of dually infected HIV-TB with the effect of σ_{T3}

(b) Cumulative number of new cases of dually infected HIV-TB with the effect of σ_{T4}

Figure 6. Cumulative number of new cases of dually infected HIV-TB with the effect of σ
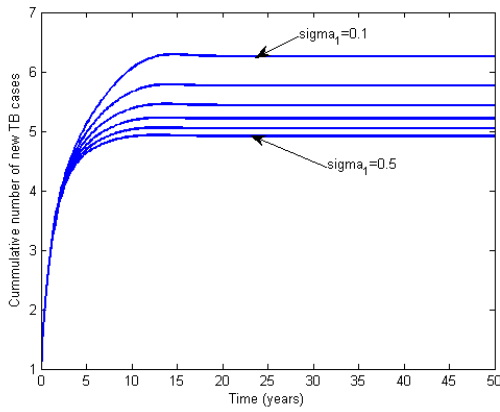
(a) Cumulative number of new cases of TB with the effect of σ_1
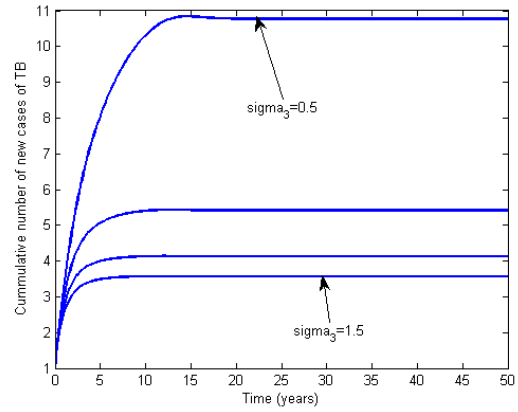
(b) Cumulative number of new cases of Tuberculosis with the effect of σ_3
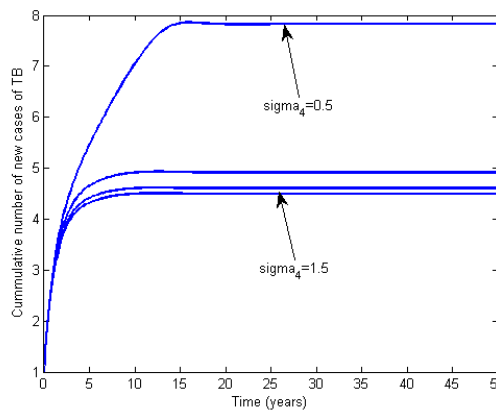
(c) Cumulative number of new cases of TB with the effect of σ_4

Figure 7. Cumulative number of new cases of TB with the effect of σ

Discussion of numerical simulation of the model

For the simulation of the co-infection model for dually infected individuals with the two diseases TB and HIV, from Figure 5a, it is observed that there is a steady rise in the number of cumulative cases for dual infection until day eighteen when it flattens out with a slight drop in its values as the treatment rate σ_{T1} increases. Likewise, from Figure 5b, it is observed that there is a steady rise in the number of cumulative cases of dually infected individuals with the two diseases until about day twenty, for an increase in treatment rate σ_{T2}, accompanied by a slight drop in the values of the cumulative number of new cases of dually infected individuals. However, as observed from Figure 5c, there is a significant effect of the treatment rate σ_{T3} on the cumulative number of new cases of dually infected individuals of HIV-TB. As the treatment rate increases, it is accompanied by a drop in the values of the cumulative number of new cases of infections of individuals infected with both diseases. The same effect is observed for the treatment rate σ_{T4} on the cumulative number of new cases of individuals infected with both diseases, as seen in Figure 5d.

From Figure 6a, it can be seen that the cumulative number of new cases of TB rises steadily until day three when it flattens out with an increase in the values of the treatment rates σ_1. In Figure 6b, we observe that the cumulative number of new cases of TB rises generally and starts flattening out almost immediately with a drop in the values of the cumulative number of new cases of TB as the

treatment rate σ_2 increases. Similarly, there is a significant effect of treatment rate σ_4 on the value of the cumulative number of new cases of TB, which drops as the treatment rate is increased. The reproduction number $\mathcal{R}_C$ for the TB-HIV co-infection model (5) is 0.0715997. As shown in Figure 7a, where we plotted the incidence of diagnosed latently infected individuals with TB with the effect of treatment rate σ_1, there was a general steady rise in the first two days followed by a decline until day ten, when it flattens out as the treatment rate increases. From Figure 7b, it can be observed that the incidence of diagnosed latently infected individuals decreases steadily until day seven when it flattens out as the treatment rate σ_2 decreases in value. Similarly, in Figure 7c, the incidence of diagnosed latently infected individuals decreases from day one and flattens out immediately as the treatment rate σ_3 increases. The implication of this is that as the values of the treatment rates σ_1, σ_2, and σ_3 increase, there is a decrease in the incidence of the disease, ultimately bringing the disease under control.

7 Findings from the research work

The major findings from this work are:

- The HIV-only model possesses a locally asymptotically stable disease-free equilibrium whenever the associated reproduction number $\mathcal{R}_H$ is less than unity.
- The co-infection model (5) and the TB-only model (22) undergo the phenomenon of backward bifurcation due to susceptibility to TB re-infection after recovery from previous tuberculosis infection. The implication of this is that the classical requirement that the reproduction number of the disease be less than unity, though still necessary for disease control, is no longer sufficient for its control, meaning that more strategies are needed to be procured for effective control of the disease in the given population.
- When the cause of backward bifurcation is removed from the TB-only model and the co-infection model, the disease-free equilibrium of the TB-only model and co-infection model is shown to be locally asymptotically stable when the associated reproduction number $\mathcal{R}_T$ is less than unity.
- The disease-free equilibrium of the TB-only model and that of the co-infection model are each shown to be locally asymptotically stable when the associated reproduction number $\mathcal{R}_T$ and $\mathcal{R}_C$ respectively are not up to unity.
- From the sensitivity and uncertainty analysis of the TB model, it could be seen that the transmission rate for tuberculosis β_T, the modification parameters accounting for the infectiousness of infected individuals with TB-only η_1, and the treatment rates for singly infected individuals with latently-infected TB, σ_1 are the three top drivers of tuberculosis infection in the given population.
- From the numerical simulation of the model, it could be seen that different treatment rates have a significant effect on the reduction of the incidence of tuberculosis infection and on the cumulative number of new cases of TB-HIV co-infection.

Of importance is the revelation that through this work, it has been shown that with adequate treatment of tuberculosis, even though there is currently no treatment available for HIV, the burden of the co-infection of the two diseases will be significantly reduced in the population. It is pertinent to note that this work has made a modest contribution to the control of the spread of tuberculosis and HIV in a population where both diseases are co-circulating.

8 Recommendations

The primary purpose of research in mathematical epidemiology is to provide healthcare policy-makers with evidence-based recommendations that can guide the formulation of effective policies for controlling the spread of contagious diseases and reducing the burden of disease in both

human and animal populations. With this objective in mind, it is essential to present actionable recommendations that can be readily utilized by healthcare policymakers. Below are some crucial recommendations:

- Every effort must be made to launch a comprehensive educational campaign aimed at individuals who are susceptible to TB. The campaign should emphasize the importance of consistently covering their mouths when coughing or sneezing in public spaces. Additionally, ensuring that infants receive vaccination against the disease should be a priority.
- It is essential to implement a highly visible awareness program targeting all members of communities. This program should stress the significance of practicing safe sexual activities by consistently using condom protection during sexual encounters.
- A comprehensive educational awareness campaign is crucial for educating all individuals about the importance of being cautious to avoid contact with bodily secretions and droplets from infected patients. Additionally, it is essential to implement appropriate measures to prevent the vertical transmission of these diseases.
- A campaign should be initiated to encourage regular screening for both diseases among individuals. It is imperative that infected individuals seek prompt medical attention as soon as they are aware of their status.

9   Conclusion

In this research work, we developed a co-infection model to gain insights into the transmission of HIV-Tuberculosis in a human population where HIV treatment is not readily available but tuberculosis treatment is accessible. We rigorously analyzed both the HIV-only and TB-only models to understand their fundamental properties. Subsequently, we extended our analysis to the co-infection model.
The key contributions in this work are:

- We show that the disease-free equilibrium of the sub-models and the full co-infection model were locally asymptotically stable.
- We conducted a rigorous analysis of the reproduction number to identify parameters that can reduce the spread of the disease.
- We conducted the sensitivity analysis to identify key parameters that drive the infectiousness of each of the diseases and that which is of great influence on the co-infection of both diseases.
- The theoretical results were validated appropriately with numerical simulations, and the plots from the simulations were extensively interpreted.
- We plotted contour plots involving key parameters and the reproduction numbers for the diseases with a view to determining the threshold for control and measures that can help eradicate the disease from the human population.

Specifically, by using parameter values sourced from existing literature and employing the MATLAB programming language, we conducted numerical simulations of the model, allowing us to validate the theoretical results obtained from the model analysis. Our findings revealed that a specific subgroup of individuals, those with varying treatments for tuberculosis, plays a pivotal role in significantly reducing the disease burden caused by co-infection. Notably, our simulations highlighted that targeting treatment towards individuals with tuberculosis in the diagnosed latent infection stage (whether singly or dually infected with HIV) is an effective strategy for reducing both the co-infection disease burden and HIV incidence within the studied population. This work's merit lies in demonstrating the promising potential for controlling co-infection when HIV treatment is not readily accessible.
Furthermore, the outcomes of this study can be valuable for healthcare policymakers, especially

in regions with limited healthcare resources. In societies where tuberculosis treatment, albeit occasionally scarce, is available while HIV treatment is not, our results suggest that careful application of these findings can aid in formulating robust public awareness campaigns and disease control strategies. Ultimately, this approach has the potential to reduce the incidence and prevalence of both HIV and tuberculosis in populations where these diseases co-circulate.

The formulation of our model has a notable limitation: it does not account for the simultaneous transmission of both diseases from the same source. We acknowledge that this is a potential scenario, as suggested by the findings of Ciesielski et al. [33], where they demonstrated the possibility of an individual acquiring both HIV and Hepatitis C virus (HCV) from a single source. As an area for further contribution to knowledge by other researchers, this work can be extended by incorporating time-dependent control functions into the proposed model. This extension would yield a model with optimal control, facilitating the development of optimal strategies for preventing the spread of the disease within the given population and implementing other strategies to mitigate the disease burden. Furthermore, the model proposed herein can be reformulated as a fractional-order model, incorporating fractional-order derivatives. The resulting system of nonlinear fractional-order derivatives can be solved using appropriate methods, such as Laplace Adomian decomposition or other techniques commonly employed for solving fractional-order models.

Declarations

Ethical approval

The authors hereby state that the project is in compliance with ethical standards. This research does not involve human or animal participants.

Consent for publication

Not applicable

Conflict of Interest

The authors hereby declare that there are no known competing interests.

Data availability statement

Data availability is not applicable to this research work, as no new data was created or analyzed in the work.

Authors' contributions

B.B.: Conceptualization, Project administration, supervision, Model analysis. T.O.: Compliment in model formulation, Joined in model analysis. AC: Coding for numerical simulation, Script writing, O.U. and O.B.: Model validation, Interpretation of plots. The authors have read and agreed to the published version of the manuscript.

Acknowledgements

Appendix A: Proof of Theorem 6

Proof Consider the following linear Lyapunov function

$$g_2 = \psi_1 (c_3 + \psi_2 \eta_1) E + c_1 (c_3 + \psi_2 \eta_1) I_{UA} + c_3 c_3 c_3 T.$$

With Lyapunov derivatives

$$\dot{g}_2 = (I_{UA} + \eta_1 T) \left[\frac{\beta_T S}{N} (\psi_1 (c_3 + \psi_2 \eta_1) - c_1 c_2 c_3) \right],$$

$$\dot{g}_2 = c_1 c_2 c_3 (I_{UA} + \eta_1 T) \left[{}^S/_N R_T - 1 \right].$$

By taking note that $S(t) \leq N(t)$, and $N(t) \leq {}^\pi/_\mu$, in Ω_2, for all $t > 0$, it follow from the above that $\dot{g}_2 = c_1 c_2 c_3 (I_{UA} + \eta_1 T)(R_T - 1)$.

Hence, $\dot{g}_2 \leq 0$, if $R_T \leq 1$, with $\dot{g}_2 = 0$, if and only if $E = E_L = E_{UL} = I_{UA} = T = R = 0$. Therefore, $\dot{g}_2$, is a Lyapunov function in Ω_2, and it follows from Lasalle's invariance principle [34] that every solution to the equations in TB-only model (22) with initial conditions in Ω_2, converges to ξ, as $t \to \infty$. That is, $(E(t), E_L(t), E_{UL}(t), I_{UA}(t), T(t), R(t)) \to (0,0,0,0,0,0)$, as $t \to \infty$. By substituting $E = E_L = E_{UL} = I_{UA} = T = R = 0$, into the first equation in model (22) with $S(t) \to {}^\pi/_\mu$, as $t \to \infty$. Therefore $(S(t), E(t), E_L(t), E_{UL}(t), I_{UA}(t), T(t), R(t)) \to \left({}^\pi/_\mu, 0,0,0,0,0,0 \right)$, as $t \to \infty$, for $R_T \leq 1$, so that the DFE, ξ, of TB-only model (22) is locally asymptotically stable in Ω_2, when $R_T \leq 1$.

Appendix B: Proof of Theorem 7

Proof For convenience, let $S = x_1$, $E = x_2$, $E_L = x_3$, $E_{UL} = x_4$, $I_{UA} = x_5$, $T = x_6$, $R = x_7$, $I_H = x_8$, $E_{HT} = x_9$, $I_{HU} = x_{10}$, $I_{HUA} = x_{11}$, $I_{HDA} = x_{12}$, and $T_{HT} = x_{13}$. It then follows that the model (22) can be rewritten as:

$$\dot{x}_1 \equiv f_1 = \pi - \frac{\beta_T (x_5 + \eta_1 x_6) x_1}{N} - \frac{\beta_H x_8 x_1}{N} - \frac{\beta_T (\eta_2 x_{11} + \eta_3 x_{12}) x_1}{N}$$
$$- \frac{\beta_H (x_9 + \phi_1 x_{10} + \phi_2 x_{11} + \phi_3 x_{12} + \phi_4 x_{13}) x_1}{N} - \mu x_1,$$

$$\dot{x}_2 \equiv f_2 = \frac{\beta_T (x_5 + \eta_1 x_6) x_1}{N} - \frac{\beta_T (\eta_2 x_{11} + \eta_3 x_{12}) x_1}{N} + \frac{\varepsilon_1 \beta_T (x_5 + \eta_1 x_6) x_7}{N} + \frac{\beta_T (\eta_2 x_{11} + \eta_3 x_{12}) x_7}{N}$$
$$- \frac{\beta_H x_8 x_2}{N} - \frac{\varepsilon_2 \beta_H (x_9 + \phi_1 x_{10} + \phi_2 x_{11} + \phi_3 x_{12} + \phi_4 x_{13}) x_2}{N} - c_1 x_2,$$

$$\dot{x}_3 \equiv f_3 = \psi_1 x_2 - \frac{\phi_1 \beta_H x_8 x_3}{N} - \frac{\phi_2 \beta_T (\eta_2 x_{11} + \eta_3 x_{12}) x_3}{N} - c_2 x_3,$$

$$\dot{x}_4 \equiv f_4 = \psi_2 x_3 - \frac{\phi_3 \beta_H x_8 x_4}{N} - \frac{\phi_4 \beta_H x_8 x_4}{N} - c_3 x_4,$$

$$\dot{x}_5 \equiv f_5 = \psi_3 x_4 - \frac{\phi_5 \beta_H x_8 x_5}{N} - \frac{\phi_6 \beta_H (x_9 + \phi_1 x_{10} + \phi_2 x_{11} + \phi_3 x_{12} + \phi_4 x_{13}) x_5}{N} - c_4 x_5,$$

$$\dot{x}_6 \equiv f_6 = \psi_4 x_5 - \frac{\theta_7 \beta_H x_8 x_6}{N} - \frac{\phi_8 \beta_H (x_9 + \phi_1 x_{10} + \phi_2 x_{11} + \phi_3 x_{12} + \phi_4 x_{13}) x_6}{N} - c_5 x_6,$$

$$(42)$$

$$\dot{x}_7 \equiv f_7 = \sigma_1 x_3 + \sigma_2 x_4 + \sigma_3 x_5 + \sigma_4 x_6 - \frac{\varepsilon_1 \beta_T (x_5 + \eta_1 x_6) x_7}{N} - \frac{\varepsilon_2 \beta_T (\eta_2 x_{11} + \eta_3 x_{12}) x_7}{N}$$
$$- \frac{\beta_H x_8 x_7}{N} - \frac{\varepsilon_2 \beta_H (x_9 + \phi_1 x_{10} + \phi_2 x_{11} + \phi_3 x_{12} + \phi_4 x_{13}) x_6}{N} - \mu x_7,$$

$$\dot{x}_8 \equiv f_8 = \frac{\beta_H x_8 x_1}{N} + \frac{\beta_H (x_9 + \phi_1 x_{10} + \phi_2 x_{11} + \phi_3 x_{12} + \phi_4 x_{13}) x_1}{N} - \frac{\psi_1 \beta_T (x_5 + \eta_1 x_6) x_7}{N}$$
$$+ \frac{\beta_H x_8 x_1}{N} + \frac{\beta_H (x_9 + \phi_1 x_{10} + \phi_2 x_{11} + \phi_3 x_{12} + \phi_4 x_{13}) x_6}{N} - \frac{\psi_2 \beta_T (\eta_2 x_{11} + \eta_3 x_{12}) x_8}{N}$$
$$+ \sigma_{T1} x_9 + \sigma_{T2} x_{10} + \sigma_{T3} x_{11} + \sigma_{T4} x_{12} + \sigma_{T5} x_{13} - c_6 x_8,$$

$$\dot{x}_9 \equiv f_9 = \frac{\sigma_1 \beta_T (x_5 + \eta_1 x_6) x_8}{N} + \frac{\sigma_2 \beta_T (\eta_2 x_{11} + \eta_3 x_{12}) x_8}{N}$$
$$+ \frac{\beta_H (x_9 + \phi_1 x_{10} + \phi_2 x_{11} + \phi_3 x_{12} + \phi_4 x_{13}) x_6}{N} - c_7 x_9,$$

$$\dot{x}_{10} \equiv f_{10} = \psi_{HU} x_9 + \frac{\theta_1 \beta_H x_8 x_3}{N} + \frac{\theta_2 \beta_H (x_9 + \phi_1 x_{10} + \phi_2 x_{11} + \phi_3 x_{12} + \phi_4 x_{13}) x_3}{N} - c_8 x_{10},$$

$$\dot{x}_{11} \equiv f_{11} = \psi_{HUA} x_{10} + \frac{\theta_3 \beta_H x_8 x_4}{N} + \frac{\theta_4 \beta_H (x_9 + \phi_1 x_{10} + \phi_2 x_{11} + \phi_3 x_{12} + \phi_4 x_{13}) x_4}{N} - c_9 x_{11},$$

$$\dot{x}_{12} \equiv f_{12} = \psi_{HDA} x_{11} + \frac{\theta_5 \beta_H x_8 x_5}{N} + \frac{\theta_6 \beta_H (x_9 + \phi_1 x_{10} + \phi_2 x_{11} + \phi_3 x_{12} + \phi_4 x_{13}) x_5}{N} - c_{10} x_{12},$$

$$\dot{x}_{13} \equiv f_{13} = \psi_{HU} x_{12} + \frac{\theta_7 \beta_H x_8 x_6}{N} + \frac{\theta_8 \beta_H (x_9 + \phi_1 x_{10} + \phi_2 x_{11} + \phi_3 x_{12} + \phi_4 x_{13}) x_6}{N} - c_{11} x_{13},$$

$$(43)$$

where $N = x_1 + x_2 + x_3 + x_4 + x_5 + x_6 + x_7$. The Jacobian of the transformed system evaluated at DFE is given by:

$$J^* (\xi_0) = \begin{pmatrix} J1_{(7 \times 7)} & J2_{(7 \times 6)} \\ J3_{(6 \times 7)} & J4_{(6 \times 6)} \end{pmatrix},$$

where

$$J1 = \begin{bmatrix} -\mu & 0 & 0 & 0 & -\beta_T^* & -\eta_1 \beta_T^* & 0 \\ 0 & -c_1 & 0 & 0 & \beta_T^* & \eta_1 \beta_T^* & 0 \\ 0 & \psi_1 & -c_2 & 0 & 0 & 0 & 0 \\ 0 & 0 & \psi_2 & -c_3 & 0 & 0 & 0 \\ 0 & 0 & 0 & \psi_3 & -c_4 & 0 & 0 \\ 0 & 0 & 0 & 0 & \psi_4 & -c_5 & 0 \\ 0 & 0 & \sigma_1 & \sigma_2 & \sigma_3 & \sigma_4 & -\mu \end{bmatrix},$$

$$J2 = \begin{bmatrix} \beta_H^* & \beta_H^* & -(\eta_2 \beta_T^* + \phi_2 \beta_H^*) & -(\eta_3 \beta_T^* + \phi_3 \beta_H^*) & -\eta_2 \beta_T^* & -\eta_3 \beta_T^* \\ 0 & 0 & \eta_2 \beta_T^* & \eta_2 \beta_T^* & 0 & 0 \\ 0 & 0 & 0 & 0 & 0 & 0 \\ 0 & 0 & 0 & 0 & 0 & 0 \\ 0 & 0 & 0 & 0 & 0 & 0 \\ 0 & 0 & 0 & 0 & 0 & 0 \\ 0 & 0 & 0 & 0 & 0 & 0 \end{bmatrix},$$

$$J3 = \begin{bmatrix} 0 & 0 & 0 & 0 & 0 & 0 & 0 \\ 0 & 0 & 0 & 0 & 0 & 0 & 0 \\ 0 & 0 & 0 & 0 & 0 & 0 & 0 \\ 0 & 0 & 0 & 0 & 0 & 0 & 0 \\ 0 & 0 & 0 & 0 & 0 & 0 & 0 \\ 0 & 0 & 0 & 0 & 0 & 0 & 0 \end{bmatrix},$$

$$J4 = \begin{bmatrix} \beta_H^* - c_6 & \beta_H^* & \phi_1\beta_H^* + \sigma_{T1} & \phi_2\beta_H^* + \sigma_{T2} & \phi_3\beta_H^* + \sigma_{T3} & \phi_4\beta_H^* + \sigma_{T4} \\ 0 & -c_7 & 0 & 0 & 0 & 0 \\ 0 & \psi_{HU} & -c_8 & 0 & 0 & 0 \\ 0 & 0 & \psi_{HUA} & -c_9 & 0 & 0 \\ 0 & 0 & 0 & \psi_{HDA} & -c_{10} & 0 \\ 0 & 0 & 0 & 0 & \psi_{HT} & -c_{11} \end{bmatrix}.$$

We consider the case with $\beta_T = \beta_T^*$, a bifurcation parameter. By solving for $\beta_T = \beta_T^*$, from R_T, yields:

$$\beta_T^* = \frac{c_1 c_2 c_3 c_4 c_5}{\psi_1 \psi_2 \psi_3 (1 + \sigma_1)(c_5 + \mu\eta\psi_4 + \eta\sigma_2\psi_4 + \eta\psi_3\psi_4)},$$

where $c_1 = (\psi_1 + \mu)$, $c_2 = (\psi_2 + \sigma_1 + \mu)$, $c_3 = (\psi_3 + \sigma_2 + \mu)$, $c_4 = (\psi_4 + \sigma_3 + \mu)$, and $c_5 = (\psi_5 + \sigma_4 + \mu)$.

It is noted that matrix $J^*(\xi_0)$, has a right eigenvector given by: $w = (w_1, w_2, ...w_{13})^T$, where
$w_1 = \frac{-(\beta_T^* w_5 - \eta_1 \beta_T^* w_5)}{\mu}$, $w_2 > 0$, $w_3 = \frac{\psi_1 w_2}{c_2}$, $w_4 = \frac{\psi_1 \psi_2 w_2}{c_2 c_3}$, $w_5 = \frac{\psi_1 \psi_2 \psi_3 w_2}{c_2 c_3 c_4}$, $w_6 = \frac{\psi_1 \psi_2 \psi_3 \psi_4 w_2}{c_2 c_3 c_4 c_5}$,
$w_7 = \frac{\sigma_1 w_3 + \sigma_2 w_4 + \sigma_3 w_5 + \sigma_4 w_6}{\mu}$, $w_8 = w_9 = w_{10} = w_{11} = w_{12} = w_{13} = 0$.
Similarly, the component of the left eigenvectors of $J^*(\xi_0)|_{\beta_T = \beta_T^*}$, $v = (v_1, v_2, ...v_{13})$, satisfying $v.w = 1$, are
$v_1 = 0$, $v_2 = \frac{\psi_1 v_3}{c_1}$, $v_3 > 0$, $v_4 = \frac{c_2 v_3}{\psi_2}$, $v_5 = \frac{c_2 c_3 w_2}{\psi_3}$, $v_6 = \frac{\eta_1 \beta_T^* \psi_3 \psi_1}{c_1 c_5}$, $v_7 = v_8 = v_9 = 0$, $v_{10} = \frac{\psi_{UA} v_{11}}{c_8}$, $v_{11} = \frac{\psi_{HUA} v_{12} + \phi_2 \beta_T^* v_2}{c_9}$, $v_{12} = v_{13} = 0$. It then follows from Theorem 4.1 in [30] that by computing the associated nonzero partial derivatives of $f(x)$, evaluated at the DFE (D_3), the associated bifurcation coefficients a, and b, are defined as: $a = \sum_{k,i,j=1}^n v_k w_i w_j \frac{\partial^2 f_k}{\partial x_i \partial x_j}(0,0)$, and $b = \sum_{k,i,j=1}^n v_k w_i \frac{\partial^2 f_k}{\partial x_i \partial \beta_T^*}(0,0)$, are computed to be:

$$a = 2v_2 \varepsilon_1 \beta_T^* \frac{\mu}{\pi}(w_3 w_7 + \phi_1 w_4 w_7)$$

$$-2v_2 \beta_T^* \frac{\mu}{\pi}\left(w_2 w_3 + w_3 w_5 + w_3 w_6 + w_3 w_7 + w_3^2 + w_3 w_7 + w_3 w_4\right)$$

$$-2v_2 \eta_1 \beta_T^* \frac{\mu}{\pi}\left(w_2 w_4 + w_4 w_5 + w_3 w_4 + w_3 w_7 + w_4^2 + w_4 w_5 + w_3 w_6\right),$$

and

$$b = v_2 w_3 + \eta_1 v_2 w_4 > 0,$$

with $v_2, w_2, w_3, w_4, w_5, w_6$, and w_7, being positive. Consequently, since the bifurcation coefficient $b > 0$, it can be deduced from Theorem 4.1 in [30] that TB-only model (22) undergoes a backward bifurcation if the backward bifurcation coefficient $a > 0$. This is so if,

$$\varepsilon_1 > \frac{(\omega_2 + \omega_3 + \omega_4 + \omega_5 + \omega_6 + \omega_7)(\omega_3 + \eta_1\omega_4)}{\omega_8(\omega_3 + \eta_1\omega_4)}.$$

Obviously, if $\varepsilon_1 = 0$, then $a < 0$, and HIV and TB co-infection model (5) will not undergo backward bifurcation at $\mathcal{R}_C = 1$.

References

[1] Azeez, A., Ndege, J., Mutambayi, R. and Qin, Y. A mathematical model for TB/HIV co-infection in treatment and transmission mechanism. *Asian Journal of Mathematics and Computer Research*, 22(4), 180-192, (2017). [CrossRef]

[2] David, J.F. *Mathematics epidemiology of HIV/AIDS and tuberculosis co-infection*. Ph.D. Thesis, Department of Mathematics, Faculty of Sciences, University of British Columbia, (2015). [CrossRef]

[3] Silva, C.J. and Torres, D.F.M. Modeling TB-HIV syndemic and treatment. *Journal of Applied Mathematics*, 2014, 248407, (2014). [CrossRef]

[4] Agbata, B.C, Ode, O.J., Ani, B.N., Odo, C.E. and Olorunishola O.A. Mathematical assessment of the transmission dynamics of HIV/AIDS with treatment effects. *International Journal of Mathematics and Statistics Studies (IJMSS)*, 7(4), 40-52, (2019).

[5] Chun, T.W. and Fauci, A.S. HIV reservoirs: pathogenesis and obstacles to viral eradication and cure. *Aids*, 26(10), 1261-1268, (2012). [CrossRef]

[6] World Health Organization (WHO), Tuberculosis, (2023). https://www.who.int/news-room/fact-sheets/detail/tuberculosis, [Accessed: 11/02/2024].

[7] Agbata, B.C., Omale, D., Ojih, P.B. and Omatola, I.U. Mathematical analysis of Chickenpox transmission dynamics with control measures. *Continental Journal of Applied Sciences*, 14(2), 6-23, (2019). [CrossRef]

[8] Centre for Disease Control (CDC), Basic TB facts, (2016). https://www.cdc.gov/tb/topic/basics/default.htm, [Accessed: 11/02/2024].

[9] Shah, N.H. and Gupta, J. Mathematical modelling of pulmonary and extra-pulmonary tuberculosis. *International Journal of Mathematics Trends and Technology*, 4(9), 158-162, (2013).

[10] World Health Organization (WHO), Global tuberculosis report, (2023). https://www.who.int/teams/global-tuberculosis-programme/tb-reports, [Accessed: 19/08/2023].

[11] Mitku, A.A., Dessie, Z.G., Muluneh, E.K. and Workie, D.L. Prevalence and associated factors of TB/HIV co-infection among HIV infected patients in Amhhara region Ethiopia. *African Health Sciences*, 16(2), 588-595, (2016). [CrossRef]

[12] Wang, X., Yang, J. and Zhang, F. Dynamic of a TB-HIV coinfection epidemic model with latent age. *Journal of Applied Mathematics*, 2013, 429567, (2013). [CrossRef]

[13] Kaur, N., Ghosh, M. and Bhatia, S.S. HIV-TB co-infection: a simple mathematical model. *Journal of Advanced Research in Dynamical and Control Systems*, 7(1), 66-81, (2015).

[14] Fatmawati and Tasman, H. An optimal treatment control of TB-HIV coinfection. *International Journal of Mathematics and Mathematical Sciences*, 2016, 8261208, (2016). [CrossRef]

[15] Omale, D., Ojih, P.B., Atokolo, W., Omale, A.J and Bolaji, B. Mathematical model for transmission dynamics of HIV and tuberculosis co-infection in Kogi State, Nigeria. *Journal of Mathematical and Computational Science*, 11(5), 5580-5613, (2021). [CrossRef]

[16] Nwankwo, A. and Okuonghae, D. Mathematical analysis of the transmission dynamics of HIV syphilis co-infection in the presence of treatment for syphilis. *Bulletin of Mathematical Biology*, 80, 437-492, (2018). [CrossRef]

[17] Agbata, B.C., Emmanuel, O., Bashir, T. and William, O. Mathematical analysis of COVID-19 transmission dynamics with a case study of Nigeria and its computer simulation. *medRxiv*, (2020). [CrossRef]

[18] Diekman, O. and Heesterbeck, J.A.P. *Mathematical Epidemiology of Infectious Diseases: Model Building, Analysis and Interpretation*. John Wiley & Sons: New York, (2000).

[19] Naresh, R., Sharma, D. and Tripathi, A. Modelling the effect of tuberculosis on the spread of HIV infection in a population with density-dependent birth and death rate. *Mathematical and Computer Modelling*, 50(7-8), 1154-1166, (2009). [CrossRef]

[20] Van den Driessche, P. and Watmough, J. Reproduction number and sub-threshold endemic equilibria for compartmental models of disease transmission. *Mathematical Biosciences*, 180(1-2), 29–48, (2002). [CrossRef]

[21] Naim, M., Sabbar, Y. and Zeb, A. Stability characterization of a fractional-order viral system with the non-cytolytic immune assumption. *Mathematical Modelling and Numerical Simulation with Applications*, 2(3), 164-176, (2022). [CrossRef]

[22] Sabbar, Y., Din, A. and Kiouach, D. Influence of fractal–fractional differentiation and independent quadratic Lévy jumps on the dynamics of a general epidemic model with vaccination strategy. *Chaos, Solitons & Fractals*, 171, 113434, (2023). [CrossRef]

[23] Ammi, M.R.S., Zinihi, A., Raezah, A.A. and Sabbar, Y. Optimal control of a spatiotemporal SIR model with reaction–diffusion involving p-Laplacian operator. *Results in Physics*, 106895, (2023). [CrossRef]

[24] Odionyenma, U.B., Omame, A., Ukanwoke, N.O. and Nometa, I. Optimal control of Chlamydia model with vaccination. *International Journal of Dynamics and Control*, 10, 332-348, (2022). [CrossRef]

[25] Omame, A., Okuonghae, D., Nwafor, U.E. and Odionyenma, B.U. A co-infection model for HPV and syphilis with optimal control and cost-effectiveness analysis. *International Journal of Biomathematics*, 14(07), 2150050, (2021). [CrossRef]

[26] Blower, S.M. and Dowlatabadi, H. Sensitivity and uncertainty analysis of complex models of disease transmission: an HIV model, as an example. *International Statistical Review/Revue Internationale de Statistique*, 62(2), 229–243, (1994). [CrossRef]

[27] Okuonghae, D. and Omosigho, S.E. Analysis of a mathematical model for tuberculosis: what could be done to increase case detection. *Journal of Theoretical Biology*, 269(1), 31–45, (2011). [CrossRef]

[28] Gumel, A.B. Causes of backward bifurcations in some epidemiological models. *Journal of Mathematical Analysis and Applications*, 395(1), 355-365, (2012). [CrossRef]

[29] Iboi, E. and Okuonghae, D. Population dynamics of a mathematical model for syphilis. *Applied Mathematical Modelling*, 40(5-6), 3573–3590, (2016). [CrossRef]

[30] Castillo-Chavez, C. and Song, B. Dynamical models of tuberculosis and their applications. *Mathematical Biosciences and Engineering*, 1(2), 361–404, (2004). [CrossRef]

[31] Sanchez, M.A. and Blower, S.M. Uncertainty and sensitivity analysis of the basic reproductive rate: tuberculosis as an example. *American Journal of Epidemiology*, 145(12), 1127–1137, (1997). [CrossRef]

[32] Elbasha, E.H. Model for hepatitis C virus transmission. *Mathematical Biosciences and Engineering*, 10(4), 1045–1065, (2013). [CrossRef]

[33] Ridzon, R., Gallagher, K., Ciesielski, C., Mast, E.E., Ginsberg, M.B., Robertson, B.J. et al. Simultaneous transmission of human immunodeficiency virus and hepatitis C virus from a needle-stick injury. *The New England Journal of Medicine*, 336(13), 919–922, (1997). [CrossRef]

[34] La Salle, J.P. and Lefschetz, S. *The stability of dynamical systems.* SIAM: Philadelphia, (1976).

Bulletin of Biomathematics (BBM)
(https://bulletinbiomath.org)

RESEARCH PAPER

The impact of the COVID-19 pandemic on education in Bangladesh and its mitigation

Md. Kamrujjaman [1,‡,*], **Sadia Shihab Sinje** [1,‡], **Tanni Rani Nandi** [1,‡], **Fariha Islam** [1,‡], **Md. Atikur Rahman** [1,‡], **Asma Akter Akhi** [1,‡], **Farah Tasnim** [2,‡] and **Md. Shah Alam** [3,‡]

[1]Department of Mathematics, University of Dhaka, Dhaka 1000, Bangladesh, [2]Department of Mathematics and Statistics, University of North Carolina at Charlotte, NC 28223, USA, [3]Department of Mathematics, University of Houston, Houston, Texas-77204, USA

* Corresponding Author
‡ kamrujjaman@du.ac.bd (M. Kamrujjaman); sadiashihab41@gmail.com (S.S. Sinje); tanni2250@gmail.com (T.R. Nandi); farihaislam415@gmail.com (F. Islam); atik.splash@gmail.com (M.A. Rahman); akhiasma752@gmail.com (A.A. Akhi); ftasnim@uncc.edu (F. Tasnim); malam20@cougarnet.uh.edu (M.S. Alam)

Abstract

The global COVID-19 pandemic disrupted various facets of societal functioning, with the education sector facing unprecedented challenges. The sudden closure of schools and universities, coupled with the shift towards remote learning, created a dynamic educational environment. It significantly affected academic performance, psychological health, dropout rates, school closures, and even increased early marriage rates in Bangladesh. In 2021, the dropout rate stood at 14.15 percent. This study delves into the specific repercussions of the pandemic on the education landscape in Bangladesh. The research reveals the disparities in access to online education, shedding light on the socio-economic factors influencing digital learning engagement. Through a comprehensive analysis of quantitative and qualitative data, we explore the multifaceted effects on educational institutions, students, and educators. We present the impact of COVID-19 on education graphically using interpolation polynomials. Mitigating the impact of COVID-19 on the education sector in Bangladesh necessitates a multifaceted approach that addresses various interconnected challenges. Moreover, prioritizing mental health support for students, teachers, and parents is paramount in navigating the emotional toll of the pandemic. Collaboration and partnerships with international organizations, non-government organizations (NGOs), and private sector entities are indispensable for mobilizing resources and expertise. Bangladesh can effectively manage the pandemic's complications and ensure the continued viability of its educational system by implementing such an all-encompassing approach.

Keywords: COVID-19; education; learning loss; interpolation; data analysis

AMS 2020 Classification: 37N25; 49J15; 92D30

1 Introduction

Every few hundred years or so, something happens on the planet that permanently alters the way things have been for humanity up until that point. In late December 2019, a novel infectious disease, COVID-19, emerged in the human population. This disease, caused by a previously unidentified coronavirus, was first detected in the city of Wuhan, located in China's Hubei province [1]. By January 2020's end, it was officially designated as a global public health emergency. Subsequently, on March 11, 2020, the World Health Organization classified it as a pandemic [2, 3]. Bangladesh announced its first three confirmed coronavirus cases in the country on 8 March 2020. Institute of Epidemiology, Disease Control, and Research (IEDCR) Director Meerjady Sabrina Flora said at a press conference in Dhaka that two men and a woman tested positive for the coronavirus and that the three were admitted to a hospital [4–6]. As a result of the COVID-19 pandemic, numerous nations and regions worldwide have implemented several non-pharmaceutical precautions known as lockdowns [7]. By April 2020, approximately half of the global population was subjected to different degrees of lockdowns. More than 3.9 billion people were instructed or required to stay at home by governments in more than 90 countries and territories [8–10]. Semlali et al. developed a new delayed SIR epidemic model to examine COVID-19's behavior, considering immigration, vaccination, and general incidence. They found that vaccination reduces confirmed cases, but the disease persists due to the immigration of infected people. They recommended controlling the immigration of infected individuals or eradicating the disease in all regions to eliminate infection [11]. The mathematical model can be used to describe the dynamics of RNA viruses such as SARS-CoV-2 within the human body. This model relies on two key threshold parameters to define its dynamics: the basic reproduction number and the reproduction number for humoral immunity. These parameters are crucial for identifying biologically plausible equilibria within the SARS-CoV-2 infection model [12].

Among many other sectors of day-to-day life, the lockdown took a great toll on our education sector, as educational institutions remained closed for a longer period. The government of Bangladesh announced the first all educational institutions closure from 17 March 2020 to 31st March 2020 and enhanced the closure many times in an attempt to reduce the spread of COVID-19. This closure of educational institutions continued on and off till the first half of 2022. The pandemic has affected all facets of life globally for people, and the education system is experiencing its worst crisis in a century. Such as permanently closed schools, dropouts, staff shortages, unemployment of teachers, etc. Furthermore, students and educators continue to struggle with mental health challenges, high rates of violence and misbehavior, and concerns about lost instructional time. Due to the COVID-19 pandemic, about 38 million students were affected when schools closed on March 17, 2020, and they remained closed for a long time. But the government acted fast to keep learning going. They used TV and the internet to teach students with pre-recorded classes starting in April 2020. The Ministry of Primary and Mass Education set up teams to make learning materials and share them on TV, phones, radio, and the internet [13].

Like other countries, Bangladesh has experienced educational challenges as a consequence of the COVID-19 pandemic. Public and private universities have struggled to keep up with teaching and learning because of this. Numerous inquiries have been conducted to address the challenges encountered by universities and to examine their responses. General and engineering university students experienced difficulties including insufficient equipment, stress, and financial difficulties [14]. COVID-19 compelled educational institutions worldwide to switch from in-person to virtual teaching. This change posed a threat to humanity as a whole, requiring everyone in the education sector to modify and adapt their usual practices. Hosen et al. surveyed to explore the impact of COVID-19 on tertiary educational institutions and students in Bangladesh. Their analysis

showed that 60% of respondents didn't have separate reading rooms, and 21% didn't have personal electronic gadgets for online classes. Also, 55% reported spending less time studying during the pandemic. Moreover, 88% of respondents faced mental health-related stress, anxiety, and depression issues. To lessen the impact of COVID-19 on the education sector, authorities must prioritize underprivileged students. This can be achieved by providing interest-free loans, ensuring access to high-speed internet, and organizing online webinars designed to alleviate the mental stress experienced by both students and staff [15].

In addressing the challenges posed by the COVID-19 pandemic in the education sector of an emerging economy like Bangladesh, it is important to adopt flexible strategies. The opening and closure of educational institutions can give rise to various risks, encompassing economic, health, social, mental, and behavioral changes for students. To assist students in overcoming these challenges and attaining Sustainable Development Goals (SDGs), it is imperative to embrace and develop innovative techniques for navigating the evolving and dynamic educational landscape [16]. A qualitative study was conducted using thematic analysis to investigate the impact of COVID-19 on tertiary education in Bangladesh from the student's perspective. The study focused on themes including university closure, disruptions in learning, loss of social interaction, physical health problems, mental health problems, shifting to online education, and financial crisis and parental involvement. Findings underscored that transitioning to online education for tertiary studies induced stress, anxiety, and disappointment due to various challenges associated with virtual learning strategies [17].

With a particular focus on Moroccan high schools, the study investigated how mathematical biology might be incorporated into the teaching of mathematics in high school. Emphasis was placed on the significance of mathematical modeling in recent advancements in epidemiology. The goal was to evaluate the extent to which mathematical applications in biology are incorporated into the high school mathematics curriculum. After examining two bachelor textbooks used in the second year, it was determined that the Moroccan mathematics curriculum is not sufficiently accessible to experimental sciences, especially ignoring biology, as demonstrated by the lesson on differential equations. There is a need to shape students' perspectives on mathematics, mathematical biology and enhance their competencies [18].

Some research highlighted the positive outcomes of the COVID-19 pandemic, contrasting the prevailing focus on its negative impacts. Researchers collected data via online Focus Group Discussions (FGD) conducted from April 2021 to June 2021, involving final-year undergraduate students from the Sylhet division of Bangladesh. During this period, people spent valuable time with their families, pursued personal interests, acquired new skills, and gained a heightened awareness of sanitation, hygiene, and social distancing. Reduced energy use and greenhouse gas emissions improved the environment and helped to preserve ecosystems [19].

We can get more knowledge about education reform in the areas of equity, access, and inclusion; curriculum and assessment; teacher preparation; and higher education. Together, these researches offer a comprehensive view of Bangladesh's educational past, present, and future, including comparisons to other developing nations [20]. With over 100 million cases and 2 million recorded fatalities worldwide, the new coronavirus (COVID-19) pandemic has had a terrible effect on humanity. The educational, economic, medical, and public health infrastructure of China as well as other countries, particularly the neighbors, has been put to the test by this unique virus outbreak. How the virus will affect our life here in Bangladesh will only become clear with time [21, 22]. The coronavirus disease pandemic, as well as the methods taken to stop the virus's spread, have hurt education. These actions included closing schools, which significantly disrupted the lives of children. Long-term school closures will have an impact on the skills that kids can learn during their formative years, as well as on their work prospects and earning potential for many years after

school ends. Due to school closures caused by the epidemic, more than 1.5 billion kids and young people worldwide have been impacted, with major earning and learning losses being widespread in all economies indexed by United Nations Educational, Scientific and Cultural Organization [UNESCO 2021a] [23].

The study included the following objectives and their alignment:

- The aim is to analyze the educational system in Bangladesh in contrast to global standards and delineate their structural disparities.
- The repercussions of extended school closures and strategies to mitigate their effects in educational institutions.
- The impact of learning loss on student mental health and well-being.
- An examination of early marriage among female students resulting from school dropouts and measures for its prevention.
- Examining how polynomial interpolation techniques interact with the available data.

This article is organized as follows: a general structure of Bangladesh's education system is presented in Section 2. The long-term impacts of COVID-19 on education sectors are discussed in Section 3. Section 4 explores COVID-19's effect on the education system in Bangladesh by using polynomial interpolation. Section 5 of the study covers potential strategies for reducing COVID-19's effects on the education sector. Finally, a fruitful conclusion is included in Section 6.

2 Educational structure of Bangladesh

Education in the twenty-first century is truly a worldwide phenomenon. Getting a good education is seen as both a right and a responsibility in most countries today. The future of a country depends on the products of its current educational systems. Every country in the world has some kind of educational system in place, although these systems differ widely. The primary factors influencing educational systems are the financial and material means available to support them in various countries. Education policies, including a country's cultural attitudes toward education, the amount of time and resources allocated to it, and how it is distributed throughout the country also contribute to these variations.

Education in Bangladesh is heavily subsidized and is overseen by the Ministry of Education (MOE) [24]. The foundation of the educational system in Bangladesh was laid long ago. Over the last decade, Bangladesh has made notable progress in expanding access to education. The government of Bangladesh has made it a priority to ensure that all citizens, regardless of their background or gender, have access to quality education, and as such, they have implemented several programs, and initiatives aimed at doing just that. Apart from having some drawbacks, the educational system has only progressed over time.

General education, madrasah education, English medium education, and technical-vocational education are the four main educational tracks in Bangladesh. Bangladeshi Educational structure has three main levels: primary level, secondary level, and tertiary level. As of 2022, the total literacy rate of Bangladesh is 74.66 percent [25], where the Female and Male students' literacy is presented in Figure 1.
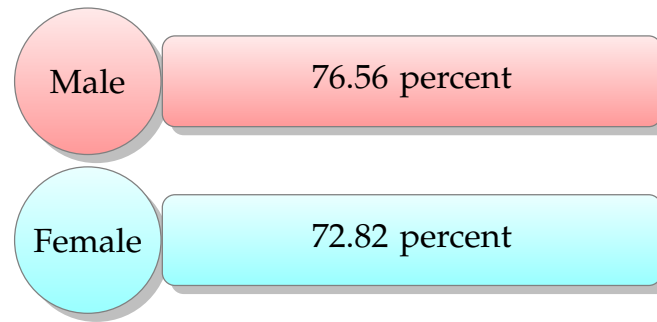
Figure 1. Female and male students distribution

In the national budget of 2017-18, a total amount of Tk 50,432 crore was allocated in the budget for education, which was groomed and boosted up to improve the education and human resources [26]. The budget distribution for three different sectors in 2017-2018 is depicted in the map referenced as Figure 2.
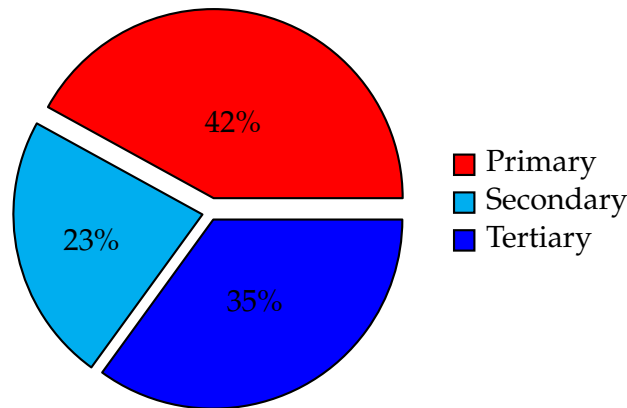

Figure 2. The educational national budget for different education sub-sectors in the fiscal year 2017-18

Primary education

Primary education is the ground floor of formal schooling. It usually marks the beginning of the educational process, coming after preschool or kindergarten and before secondary school. The Ministry of Primary and Mass Education holds the responsibility of implementing primary education programs and government-funded schools at the grassroots level [27]. Primary education is free. Children between the ages of 6 and 11 are served by elementary education, which lasts five years (from grades I through V). Its primary goal is to develop children's literacy and numeracy abilities, which include speaking, listening, reading, and computational abilities. It also aims to build additional competencies and understanding that equip young people for meaningful engagement in society [28].

Based on the Primary Education Census of 2018, there were 20.8 million students enrolled in pre-primary through grade five across all types of primary schools [29–31]. Here, a simple list is given in Table 1 which shows the list of primary schools in Bangladesh, the total number of students and female students, the total number of teachers, and female teachers in the primary sector [32].

Table 1. The number of students and teachers in different types of schools in Bangladesh

School type	Students (total)	Students (female)	Teachers (total)	Female
Government School	14671914	7530261	319112	191830
Experimental School	10652	5250	282	246
Ebtadaee Madrasah	372277	181341	11673	2300
Kindergarten	1988365	914016	93799	54813
*NGO School	210170	107898	5454	3764
Community School	16747	8679	405	322
Attached to High Madrasah	871047	427341	19764	2812
Primary Sections of High School	572751	295659	8301	4450
*BRAC	324438	185873	7798	7277
*ROSC School	106884	53751	3591	2867
Sishu Kollyan Primary	15665	8284	410	277
Others School	97519	48808	4875	2967
Grand total	**19,258,429**	**9,767,161**	**475,464**	**274,143**

*NGO School stands for Non-government Organization School; BRAC represents Bangladesh Rehabilitation Assistance Committee; and ROSC stands for Reaching Out of School Children.

Secondary education

Secondary education is managed and administered by the Ministry of Education (MOE) which is charged with policy formation, planning, monitoring, evaluation, and execution of plans and programs. At present, secondary education consists of three sub-stages such as:

- Lower secondary (grade 6 to 8).
- Junior secondary (grade 9 to 10).
- Higher secondary (grade 11 to 12).

The goals of secondary education in Bangladesh were established following the suggestions outlined by the Bangladesh Education Commission of 1974, the National Curriculum and Syllabus Committee of 1975, and the National Curriculum and Coordination Committee of 1993. Its primary purpose was to facilitate learners in acquiring new knowledge and competencies, utilize the possibilities of contemporary science and technology, foster a constructive perspective and scientific mindset, equip them with self-employment abilities, and instill a sense of patriotism alongside religious, ethical, cultural, and societal values [33]. At this level, each student must attain two public examinations named Secondary School Certificate (SSC) and Higher Secondary Certificate (HSC) under the supervision of nine Boards of Intermediate and Secondary Education. They are Dhaka, Chottogram, Barishal, Comilla, Dinajpur, Jashore, Mymensingh, Rajshahi, and Sylhet Education Board. Every high school has a particular education board. The number of high schools for every educational board is listed in Table 2 [34]. In 2021, the total enrolment of students in secondary level was 10.19 million, and the total teachers were 266568. In 2021, the Teacher-Student Ratio (TSR) was 1:38, and the average number of teachers per institution was only 13.

Higher secondary education

The Higher Secondary Education (HSE) serves an essential purpose as a connection point between secondary and tertiary education in Bangladesh. Grades 11 and 12 make up Bangladesh's system of higher secondary education. At this level, most students choose a stream of education (e.g.

Table 2. Education Boards and their corresponding number of High Schools

Education Boards	Number of High Schools
Dhaka	3549
Rajshahi	4607
Comilla	1483
Jeshore	2274
Chottogram	248
Barishal	1396
Sylhet	645

pre-engineering, pre-medicine, business management, or arts/humanities) that will serve as the cornerstone of their career throughout their lives.

The rates of HSE enrollment and completion have significantly increased recently, and there has been some improvement in the gender equity of HSE enrollment. Data reveal there are significant enrollment gaps between urban and rural colleges, which makes it difficult to advance socioeconomic development and equity. Although there has been a notable progression in achieving gender equality in HSE enrollment, there exists a significant task of enhancing and sustaining female participation. Data highlights substantial disparities between urban and rural enrollment. According to research outcomes, enrolment in HSE has significantly increased, necessitating improvements in many areas within this sector [35].
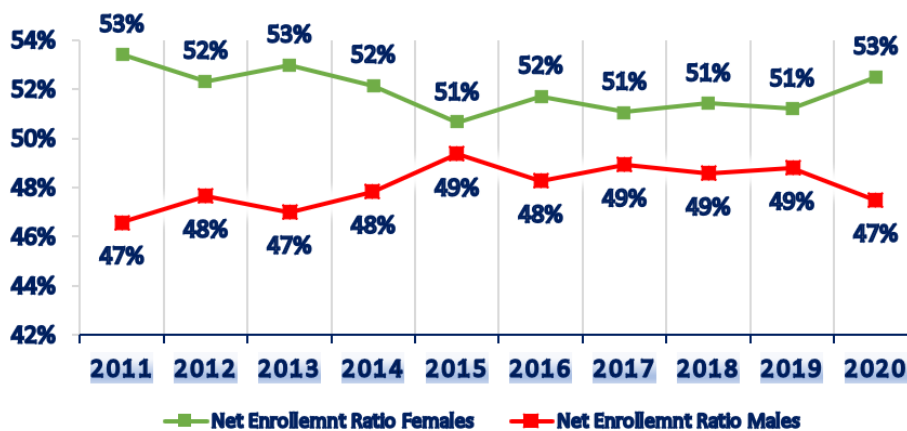
Figure 3. Enrollment ratio comparison between boys and girls [36]

According to BANBEIS 2021 data [36], the net enrollment ratio (NER) for male students at the HSE level could never beat the NER of female students in the last decade from Figure 3. This pattern can be linked to heightened parental awareness of the significance of enrolling girls in higher education and attaining an HSE diploma. Moreover, over the past five years, the Bangladesh government has amplified the stipend/scholarship initiative to expand greater participation of girls in higher education. The Bangladesh government has implemented specific policies to address the challenges of the 21st century in various sectors, including education. Some of these policies include:

National Education Policy: The government has formulated and implemented a National Education Policy aimed at modernizing and improving the quality of education in Bangladesh. This policy focuses on enhancing access to education, improving the quality of teaching and learning,

and promoting lifelong learning opportunities for all citizens.

Digital Bangladesh Initiative: The government has launched the Digital Bangladesh initiative to promote the use of information and communication technology (ICT) in education. This initiative includes programs to provide digital literacy training to students and teachers, promote e-learning platforms, and integrate ICT into the curriculum.

Science, Technology, Engineering, and Mathematics (STEM) Education: Recognizing the importance of STEM education in the 21st century, the government has prioritized initiatives to promote STEM education in schools and colleges. This includes the establishment of STEM-focused schools and the introduction of STEM-related curriculum and extracurricular activities.

3 Cumulative impact of COVID-19 on education

Learning loss

The phrase "learning loss" is frequently used in the literature to characterize declines in student knowledge and skills. Learning loss describes the deterioration or regression of students' academic knowledge and skills over extended periods of interrupted or inadequate learning opportunities. Historical data, which is frequently obtained through regular testing, gives academics insight into where student learning should be on an annual basis. When educational advancement is not made at the same rate that it has historically compared to previous years, learning loss occurs.

COVID-19 has disrupted the education of an entire generation of children. The pandemic has caused one of the lengthiest school closures worldwide, affecting the education of 37 million children in Bangladesh [37]. At the height of school closures, globally 168 million children were out of school. Furthermore, around 214 million children, or 1 in 7 have missed more than three-quarters of their in-person learning [38].

The impact of school closures was particularly challenging for all children, with girls and children from underprivileged homes suffering the greatest difficulties. They experienced noticeable learning setbacks and confronted intensified risk of dropping out of their education. Before the pandemic, as early as 2017, more than half of Bangladeshi children who completed primary school struggled to read and comprehend basic texts. Current simulations indicate that due to the extended school closures, a staggering seventy-six percent of children will likely not achieve the essential reading proficiency level by the end of primary school. While some countries managed to limit the losses, the actual impact of COVID-19 on learning progress shows that school closures frequently have a large, persistent, and unequal effect on learning. Online education is not a good enough substitute for in-person learning, particularly for children from low-income families. An examination of 35 rigorous studies from 20 countries reveals three key issues:

  i. The majority of studies (32) discover evidence of learning loss. 27 of the 35 studies that reported learning loss findings did so in a format with a similar effect size. In most research, learning losses were reported to range between 0.25 and 0.12 standard deviations (SDs). Losses in learning were even higher in five studies. The average amount of learning lost across all studies is 0.17 standard deviations or more than half a school year.

  ii. The studies consistently find different levels of learning loss by student socioeconomic status, past academic learning, and the subject of knowledge. By socioeconomic position, learning loss was studied in 20 research. 15 of them demonstrate a statistically significant difference between children or schools with lower socioeconomic levels and greater learning loss, whereas 5 do not. Numerous studies have also revealed that pupils who had academic difficulties before the epidemic suffer more from learning loss. In the studies that used this measure, 11 showed that students with lower levels of academic achievement experienced larger learning losses, while 3 showed that students with higher levels of prior academic achievement experienced greater

learning losses.

iii. Learning losses increased in proportion to the length of school closures. The average length of school closures for the 19 nations for which we have reliable learning loss data was 15 weeks, resulting in an average learning loss of 0.18 standard deviations. In other words, learning decreased on average by 1.2 points, or 0.01 standard deviations, for each week that schools were closed. These nations show compelling evidence that the pandemic-induced school closures were responsible for learning deficits. Average learning losses in these European nations were 0.16 standard deviations, and average school closures lasted 11 weeks on average. As a result, learning losses were roughly 1.5 points, or 0.015 standard deviations, per month, for each week that schools were closed.

Here, results presented in months of loss are converted to standard deviations, with 1 school year of learning equal to 0.33 standard deviations [39].
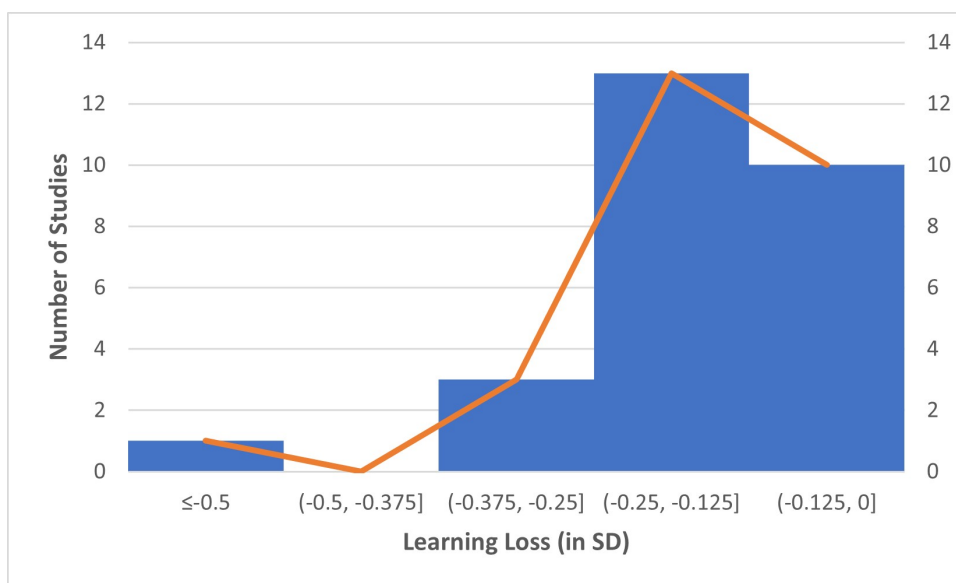
Figure 4. Range of learning loss (in SDs) in the 27 studies reporting comparable effect sizes

In Figure 4, learning equal to 0.33 standard deviations. Negative SDs represent learning loss. According to Figure 4, most studies indicate a loss of approximately one academic year in learning. However, one study showed 1.5 school years of learning loss. In 2020, the Bangladeshi government decided to cancel one of the nation's significant public examinations due to concerns related to the COVID-19 pandemic. The Ministry of Education declared that approximately 1.4 million candidates who were supposed to appear for the HSC and equivalent examinations that year would instead be assessed based on their performance in two of their preceding public exams, namely the JSC (Junior School Certificate) and SSC. As a result, all candidates were granted an 'Auto-pass' [40]. Furthermore, various countries postponed their major public exams due to rising cases of COVID-19.

The crisis-induced learning deficits will exploit a substantial economic cost. According to the World Bank's estimations, today's generation of school children could face a lifetime earnings reduction of USD 17 trillion in current value. This amount equates to approximately 14 percent of the existing global Gross Domestic Product (GDP) [41].

Effect on student's mental health

Since the start of the COVID-19 pandemic in early 2020, school closures have affected the education of around 37 million children in Bangladesh and approximately 800 million children worldwide including Asia, encompassing South Asia, Southeast Asia, and East Asia [42]. In Bangladesh, schools were closed throughout the entire pandemic until 12 September 2021, when they reopened again after an 18-month closure. A whole generation's future is on the line. The pandemic has provided parents, teachers, and kids with several difficulties. We are just now beginning to understand the far-reaching effects of school closures, isolation policies, and other abrupt changes on students. The COVID-19 pandemic has had a significant impact on student mental health, and several quotes shed light on the situation. From a student: "I miss going to school every day and seeing my friends. Learning from home is challenging because I don't have access to a computer or internet connection. Sometimes, I feel like I'm falling behind in my studies" and from another educator: "It's heartbreaking to see how the pandemic has disrupted the education of so many students. We're doing our best to provide support and resources to help them continue learning, but it's challenging without the structure of regular school days."

COVID-19 has significantly affected primary school students and children. The effects on children of the disruption of educational services cannot be disregarded. Children lose the largest chance to learn and grow to their full potential when schools are closed. Children who already deal with mental health issues have been particularly susceptible to the changes. When school restarts, some depressed children may have a difficult time returning to their regular routines. Approximately 29% of parents report that their children are presently grappling with emotional or mental health challenges due to the effects of social distancing and closures. An additional 14% of parents suggest that their children can endure a few more weeks of social distancing before their mental health begins to deteriorate [43].

The consequences on high school students or teenagers as a result of the COVID-19 pandemic are notable. The year 2020 proved challenging for everyone, but it had an especially significant effect on the mental well-being of teenagers and young adults. A recent study involving 5,400 participants reported that 25% of individuals aged 18 to 24 had thoughts of doing suicide in the preceding 30 days. Moreover, a recent survey revealed that 80% of students faced adverse effects on their mental health as a result of the pandemic, with 20% indicating a substantial deterioration in their mental well-being [44].

The impact on college students is evident due to COVID-19. 20% of college students say their mental health has significantly worsened under COVID-19. 48% have experienced financial setbacks due to COVID-19. Among all students, 38% said having trouble focusing on their studies. 74% are challenged in maintaining a routine [45]. A data table of the impact on mental health due to COVID-19 is listed in Table 3 according to types of mental problems [45].

Table 3. Impacts of COVID-19 on students' mental health [45]

Type	All students	College students	High school students
Stress or anxiety	87%	91%	74%
Disappointment or sadness	78%	80%	74%
Loneliness or isolation	42%	48%	26%
Financial setback	42%	48%	26%
Relocation	39%	56%	2%
Illness (myself or loved one)	7%	5%	9%
Loss of a loved one	4%	3%	5%
None of the above	4%	2%	8%

COVID-19's influence on university students is discernible. There has been an upswing in concern about the mental health of undergrads in recent years. Since COVID-19, the educational landscape in Bangladesh has undergone significant change. All university campuses were closed during the pandemic. There was a problem with the student's mental health. University students are now more likely to have mental health problems due to the pandemic's stressors and constraints, which could seriously harm their academic performance, social connections, and future careers. University students indicated normal levels of depression 30.41%, anxiety 43.29%, and stress 47.40% during COVID-19 [46]. Many of them committed suicide due to mental issues. Male students reported lower levels of anxiety and stress compared to female students. Furthermore, students living in the urban area of Dhaka displayed higher levels of depression and anxiety in comparison to students residing outside the city [46]. Table 4 displays the frequencies and percentages of depression, anxiety, and stress labels among university students in Bangladesh [46].

Table 4. Labels indicating depression, anxiety, and stress levels among university students in Bangladesh [46]

Rating	Depression (n%)	Anxiety (n%)	Stress (n%)
Normal	111 (30.41)	158 (43.29)	173 (47.40)
Mild	53 (14.52)	25 (6.85)	43 (11.78)
Moderate	84 (23.01)	82 (22.47)	54 (14.79)
Severe	33 (9.04)	25 (6.85)	49 (13.42)
Extremely Severe	84 (23.01)	75 (20.55)	46 (12.60)

Consequently, there was a discernible escalation in mental health distress when students indicated the experience of COVID-19-related symptoms. For instance, in cases where individuals reported experiencing one or more symptoms, the risk of stress elevated by a factor of 1.60, while the presence of at least one symptom amplified this risk to 3.06 times. Similarly, anxiety's risk factor increased to 3.02 times with the presence of one or more symptoms and further to 4.96 times with at least one symptom [47]. Moreover, a different research investigation revealed that undergoing symptoms such as fever, dry cough, fatigue, sore throat, and difficulty breathing played a pivotal role in the emergence of mental diseases.

The concern about contracting COVID-19 emerged as a noteworthy indicator of depression, anxiety, and stress in multiple studies. Likewise, incidents, where family members or friends had been affected by COVID-19, were also associated with heightened levels of anxiety. According to a study, students who expressed high levels of anxiety about coming into contact with individuals infected with COVID-19 faced 3.5 and 2.75 times greater risks of experiencing anxiety and depression compared to those who had no or minimal contact. Likewise, students who had been in contact with confirmed COVID-19 cases were found to be at 4 and 3.17 times higher risk of experiencing stress and anxiety, respectively [47].

The duration of internet browsing has been considered a predictive element for psychological disorders in one study. According to this study, students who spent 5 to 6 hours or more than 6 hours browsing the internet were at a high risk of experiencing psychological problems, in contrast to those who spent less than 2 hours. Furthermore, experiencing sleep difficulties was also associated with an elevated risk of mental health issues. Another study asserted that students who reported dissatisfaction with their sleep patterns experienced higher levels of psychological distress compared to those who were satisfied with their sleep quality. The habit of smoking was reported as a significant factor in evaluating mental health problems. The students who were

engaged in smoking were more prone to psychological suffering [47].

Economical impact of COVID-19 related school closures

The economic impact of school closures in Bangladesh can be significant and multifaceted, affecting individuals, teachers, and students in various ways: loss of income, increased household expenses, reduced productivity, professional challenges, disrupted education and emotional impact. All these issues somehow connected with the individuals, teachers, and students.

Education helps people to be more effective at their jobs, especially in today's knowledge-based industries. Education also gives people the information and abilities they need to create and use novel ideas and breakthroughs that advance technology and boost the nation's economy completely. The coronavirus disease (COVID-19) and related school closures substantially disrupted children's education. Long-term school closures will affect the students' learning and potential professional productivity. The COVID-19 pandemic has seriously disrupted educational systems around the world. According to UNESCO (2021b), a total of 210 economies have experienced either full or partial school closures, with 84 of them enduring closures lasting over 40 weeks, equivalent to a full school year. Due to prolonged school closures during COVID-19, Bangladesh has endured substantial declines in gross domestic product (GDP) and employment [23].

Especially in developing economies, where students frequently suffer from reliable access to high-speed internet connectivity, online education might not yield the same effectiveness as traditional in-person teaching and learning. While online learning can lessen the effects of an interrupted school year, its success depends on the accessibility of learning resources and their effectiveness in promoting learning. To address the learning deficit, one frequently proposed solution is online education. However, the transition to online learning is not currently a feasible solution for Bangladesh. Approximately 5 percent of households lack access to a mobile phone, and when it comes to computers/tablets, only 5.60 percent of households possess one. However, merely owning a computer/tablet is insufficient. With only 37.60 percent of households having internet connectivity at home (with urban areas at 53.10 percent and rural areas at 33.20 percent), the feasibility of this option appears dimmer. Additionally, clear regional and income disparities are evident: rural and economically disadvantaged regions have significantly less access to Information and Communications Technology (ICT) compared to urban and wealthier areas. This inequality extends to poorer households as well. Based on the most recent Household Income and Expenditure Survey (HIES) data, updated to 2020, it can be estimated that approximately 12.70 percent of impoverished households lack access to even a single mobile phone [48]. The poorest and second lowest percentiles of wealth have faced the hardest hit in economies with a noticeable presence of students from rural areas. The primary causes of this are the lack of dependable internet connections and the difficulties associated with online learning, which hurt these students' chances of obtaining a degree. Furthermore, economies with a high percentage of unskilled laborers within the workforce also experience significant limitations in terms of both learning and earning potential. For this reason, the closure of schools leads a significant portion of the affected students towards opportunities in unskilled employment.

The closure of schools has generated an impact on labor productivity as well. Since the start of the pandemic, there has been a significant decrease in the participation of women in the workforce, particularly among working mothers who have had to care for their children. The increased dependency on virtual learning due to school closures has arisen in a situation where women having young children have chosen to step back from their jobs. While the eventual return to traditional in-person schooling could potentially boost labor force participation rates, the possibility of this outcome remains uncertain. This uncertainty is especially relevant in developing

economies, where many kids have not received vaccinations. When a considerable proportion of the working force is employed in unskilled labor, both learning and earning are significantly impacted. Forecasts for Bangladesh indicate that skilled employment may experience a decline of 3.18 percent, and unskilled labor employment may see a decline of 3.16 percent by the year 2030. Regarding the magnitude of the change, Bangladesh is projected to encounter a notable decline in GDP in South Asia, following India, with an estimated decrease of approximately $13.84 billion by 2030. Meanwhile, India is anticipated to undergo the most substantial GDP decline in South Asia, with a projected decrease of about $98.84 billion by 2030. Moreover, the country's skilled employment is expected to decrease by 0.244 percent in 2023 and further by 0.759 percent in 2025 [49].

According to the report, school closures cause a decline in the global GDP and employment possibilities. The research titled "Potential Economic Impact of COVID-19-Related School Closures," done by the Asian Development Bank (ADB), reports that the GDP has shrunk by 3.1 percent as compared to the baseline scenario without COVID-19 because of the lost revenue from these closures. This reduction amounts to a global decline in GDP of 0.19 percent in 2024, 0.64 percent in 2028, and 1.11 percent in 2030. By the year 2030, it is estimated that the world economy will have lost 943 billion dollars due to school closures caused by the COVID-19 epidemic [49].

Due to financial hardships brought on by pandemic control measures, the COVID-19 pandemic may have a more significant effect on schooling. The South Asian Network on Economic Modeling (SANEM) used the latest Household Income Expenditure Survey (HIES) to calculate that, before the crisis, 8.4 million students' families (23.90 percent) lived in poverty. With a prolonged crisis and a three-month lockdown starting from March 25, 2020, causing a 25.0 percent drop in yearly per capita income, SANEM predicts that the number of student families below the poverty line could increase to 43.90 percent. This implies that an additional 7.70 million student families could fall into poverty during this crisis, bringing the total to 16 million students living in the poverty line [48].
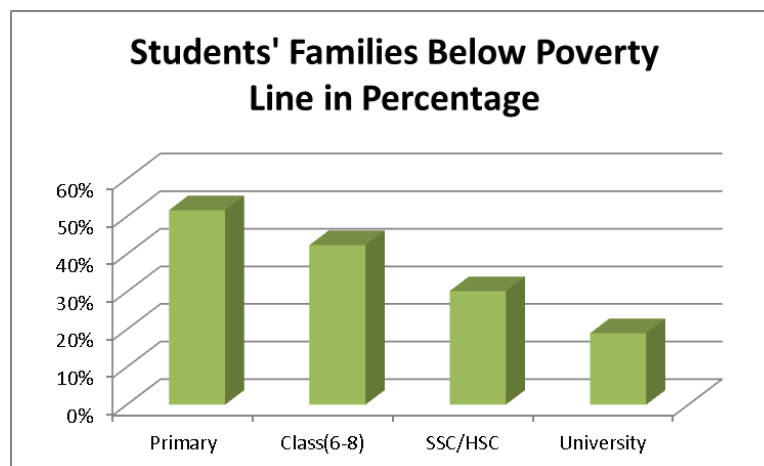
Figure 5. Students' families below the poverty line

In Figure 5, the horizontal axis shows the educational levels, and the vertical axis shows the percentage of children whose families earned less than the poverty line in COVID-19. The percentage is high at the primary school level and low at the university level. The primary students are unable to work and be paid. Thus, their livelihood is only managed by the guardians. Nevertheless, university students can work and support their families.

Many teachers lost their employment after the closure of the schools. Some departed because

they were stressed and struggled with technology, while others lost jobs due to insufficient money. Even after two years of closures, most teachers in the study still didn't have jobs, demonstrating the uncertain nature of the teaching job market.

Influence on early marriage

Amidst the COVID-19 pandemic, the incidence of child marriage in Bangladesh has seen a disturbing increase, predominantly due to girls spending more time at home as a result of the closure of educational institutions. It's worth noting that Bangladesh holds the unfortunate distinction of having the fourth highest prevalence of child marriage globally [50]. The pandemic has further exacerbated this critical situation for countless girls. Bangladesh ranks among the top 10 countries in terms of child marriage rates [51].

Disturbingly, over 50% of Bangladeshi women currently in their mid-20s were wed before their 18th birthday, and nearly 18% were married off before the age of 15 [50]. Moreover, the rate of child marriages has surged by up to 220% during the July-September period amid the ongoing pandemic [51]. Even before the COVID-19 outbreak, approximately 100 million girls remained at risk of child marriage over the next decade, despite notable reductions in several countries in recent years [52].

According to a Financial Express report, a girl had eight friends in a village school prior to the outbreak. When the school resumed on September 12, she was alone in her class. She waited for her friends for a few days, but they didn't come back. It turns out that all her friends got married while the school was closed. This violates the laws against child marriage. Many newspapers have written about numerous instances during the pandemic where people violated this guideline [53]. Girls' general well-being, education, and health are severely harmed by child marriage. Beyond the immediate physical risks associated with early pregnancies, such unions often curtail educational opportunities, perpetuating cycles of poverty and reinforcing gender disparities. Moreover, the psychological toll of forced marriages can lead to anxiety, depression, and trauma, hindering girls' mental well-being and long-term prospects. To break this cycle of harm, concerted efforts are needed to promote gender equality, protect girls' rights, and provide comprehensive support to those affected by child marriage.

Case study of dropouts

The most severely affected of all educational institutions were the kindergartens. During the pandemic, thousands of kindergartens have shuttered, and unfortunately, the majority of them are unlikely to resume business. Teachers of these kindergartens have been forced to take menial or odd jobs to survive during the pandemic. Inquiries into household intentions regarding the return of their children, who were attending school before the government-imposed closures in March 2020, reveal that over 13% of current enrollees are considering discontinuing their education. Additionally, approximately two-thirds of these potential dropouts have no intentions of resuming their education after leaving. This trend of dropping out is prevalent across various grade levels. It's worth noting that male students exhibit a slightly higher likelihood of discontinuing their education (14%) compared to female students (13%). Furthermore, among students residing in slum areas, a significant 17% are contemplating dropping out. In contrast, in August 2020, only less than 1% of the students planned to drop out [54]. From the BANBEIS data [36], a comparison of the dropout rates in the primary level for the last six years is shown in Figure 6.
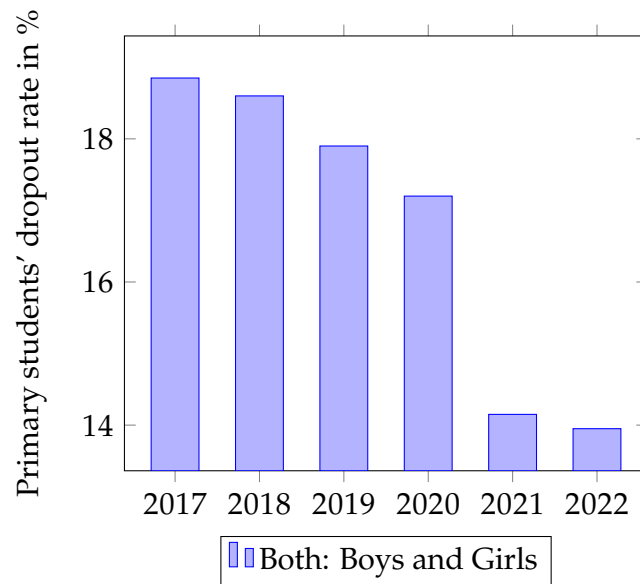
Figure 6. Primary-level student dropout rates, 2017-2022

From the BANBEIS data [36], a comparison of the dropout rates in the secondary level for the last six years is mapped in Figure 7.
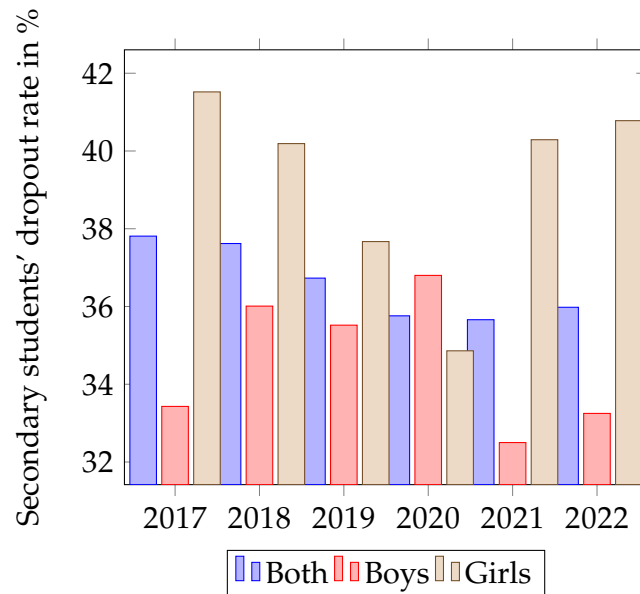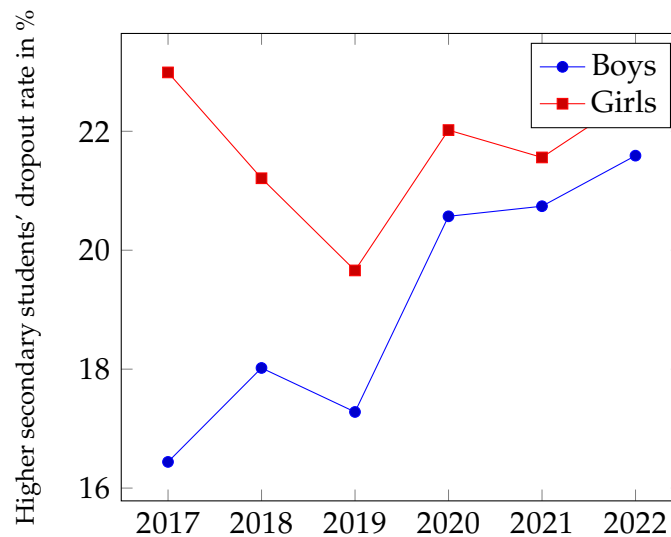

Figure 7. Secondary-level student dropout rates, 2017-2022

Due to the inability to commence their college sessions, students are grappling with concerns about the potential truncation of their academic year. Consequently, many students are forced to juggle multiple unstable jobs such as construction work, garment sector employment, bus driving, auto-rickshaw driving, and so on. This has led to a regrettable situation where numerous students have dropped out of school, leaving them unprepared for the HSC examination.

Throughout 2022, plenty of factors combined to elevate the dropout rates among girls in higher secondary schools. Economic hardships exacerbated by the COVID-19 pandemic, unequal access

to technology for remote learning, societal pressures forcing girls to shoulder domestic duties, increased risks of early marriage and pregnancy, and elevated mental health challenges all converged to hinder girls' educational aspirations. These hurdles underscore the critical necessity for focused interventions aimed at improving females' educational achievements and eliminating long-standing institutional disparities.

In particular, a comparison between boys' and girls' dropout rates in the higher secondary level for the same time interval is displayed in Figure 8.

Figure 8. Higher secondary-level dropout rate comparison: Boys vs Girls

Bangladesh's dropout rate is declining as a result of the government consistently strengthening the educational system. Due to the start of COVID-19 in 2020, students were admitted to schools and colleges early. Thus, the dropout rate does not increase. Dropout rates decreased in 2021 due to auto passes, online courses, etc. However, in 2022, all families experience financial hardship, girls get married, and males begin working to support the family, which causes a small increase in dropout rates. Since girls got married, the dropout rate for females from second to higher secondary schools is particularly high in 2022. They are unable to enroll in college anymore.

4   COVID-19's impact on education with polynomial interpolation

With the help of polynomial interpolation, we plot the number of students who took the Secondary School Certificate (SSC) and Higher Secondary Certificate (HSC) exams in the relevant years to demonstrate the impact of COVID-19 on Bangladesh's educational system. For SSC students:

Year (x)	2018	2019	2020	2021	2022
Students (y)	20,31,899	16,94,652	20,40,28	22,27,113	20,21,006

For calculation, we convert the above data into the Table 5.

Table 5. SSC students participated in Final Exams in 2018-2022

x	18	19	20	21	22
y	2.031899	1.694652	2.040028	2.227113	2.021006

The corresponding Lagrange interpolating polynomial for SSC students is

$$p_1(x) = 2.031899 \frac{(x-19)(x-20)(x-21)(x-22)}{24} + 1.694652 \frac{(x-18)(x-20)(x-21)(x-22)}{-6}$$

$$+ 2.040028 \frac{(x-18)(x-19)(x-21)(x-22)}{4} + 2.227113 \frac{(x-18)(x-19)(x-20)(x-22)}{-6}$$

$$+ 2.021006 \frac{(x-18)(x-19)(x-20)(x-21)}{24}$$

$$= 0.02525054166666664x^4 - 2.109694583333329x^3 + 65.87597895833312x^2$$

$$- 9.110671099166661x + 4710.460643.$$

For HSC students:

Year (x)	2017	2018	2019	2020	2021
Students (y)	11,83,686	13,11,457	13,36,629	13,67,377	11,15,705

For simplicity, we convert the above data into the following list (Table 6).

Table 6. HSC students participated in Final Exams in 2018-2022

x	17	18	19	20	21
y	1.183686	1.311457	1.336629	1.367377	1.115705

The corresponding Lagrange interpolating polynomial for HSC students is

$$p_2(x) = 1.183686 \frac{(x-18)(x-19)(x-20)(x-21)}{24} + 1.311457 \frac{(x-17)(x-19)(x-20)(x-21)}{-6}$$

$$+ 1.336629 \frac{(x-17)(x-18)(x-20)(x-21)}{4} + 1.367377 \frac{(x-17)(x-18)(x-19)(x-21)}{-6}$$

$$+ 1.115705 \frac{(x-17)(x-18)(x-19)(x-20)}{24}$$

$$= -0.01651129166666667x^4 + 1.239881416666671x^3 - 34.89048370833336x^2$$

$$+ 436.0935415833342x - 2041.554638000004.$$

Now, plotting these polynomials, $p_1(x)$ and $p_2(x)$ using MATLAB, we get
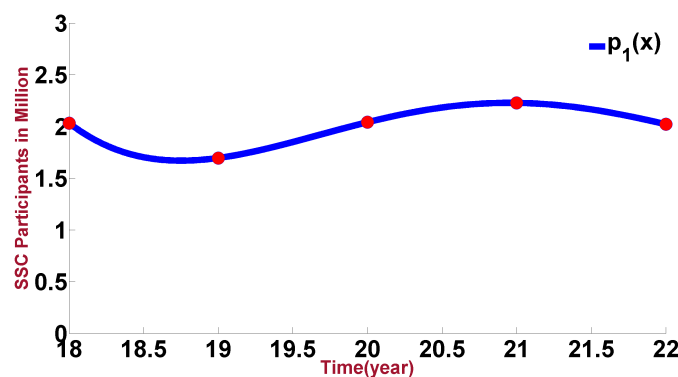
Figure 9. Participants in SSC examination

In Figure 9, participants in the SSC examination from the year 2018 to 2022 have been shown graphically. The number of students that have taken in millions and years has been converted from 2018 (equivalent to 18), 2019 (equivalently 19 in the plot), and likewise. Clearly, in the year 2022, the number of participants has dropped significantly.
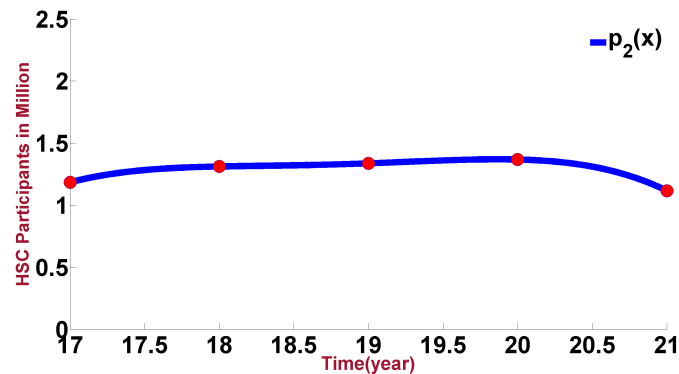

Figure 10. Participants in HSC examination

The number of students taking the HSC exam each year from 2017 through 2021 is graphically represented in Figure 10. The number of students is reported in millions and the years have been converted from 2018 to 18, 2019 to 19. The year 2021 shows a dramatic decline in participation from the previous years.

The devastating impact COVID-19 has had on education in Bangladesh is shown at a glance in declining enrollment in the country's two most important public exams, the Secondary School Certificate (SSC) and Higher Secondary Certificate (HSC) tests. Many pupils dropped out of school in 2020 as the onset of COVID distracted them. Long-term effects were visible in SSC 2022 and HSC 2021. Since they live in a third-world country, not all kids have access to the necessary resources to continue their education. Those who were in Class 10, in college, or previously registered for the HSC when COVID-19 began managed to keep studying, hence the number of students taking the tests did not drop much. But many children who had been inspired to continue their education by passing the JSC or JDC, SSC, or equivalent exams at the beginning of COVID-19, couldn't continue much after that and gave up on their plans to enroll in secondary school or higher secondary school. This explains the dramatic swing in turnout for the SSC 2022 and the HSC 2021.

5 Mitigate the impacts of COVID-19 on education

It's been two and a half years since COVID-19 was declared a global pandemic. The COVID-19 virus was a catastrophic event that has changed the course of human history in numerous ways. Major changes in people's daily routines, places of employment, educational opportunities, and access to medical treatment have resulted from the pandemic. The pandemic has inflicted significant damage on the educational sector. To mitigate its devastating impact, unique and innovative strategies were implemented during and after the crisis.

Minimization of the lost learning

After it became clear that there was no chance of schools reopening any time soon, educational institutions all around the world started to shift their focus to online education. Even before the onset of COVID-19, the field of educational technology had been experiencing substantial growth and widespread adoption. Global tech investments in this sector had surged to $18.66 billion in

2019, and the entire online education market was anticipated to reach a substantial $350 billion by the year 2025 [55]. Learning online has been demonstrated to improve retention and reduce time spent studying, suggesting that the changes brought about by the coronavirus may be here to stay. In many nations, the widespread availability of television has led to the introduction of television and even radio-based programs designed to motivate students to study. Regarding Bangladesh, MoE, and MoPME launched remote learning programs via "Sangsad TV" and on their web platforms: e-connect, Facebook, and YouTube to guarantee learning continuity during school closures. The first TV-based broadcast under this initiative aired on March 29, 2020 [56]. Many universities have reduced the length of their semester from six to four months to cope with the lost time. While in the yearly system, it was reduced to eight months. Bangladesh's government administered its SSC and HSC examinations in 2021 and 2022 on a shortened curriculum to make up for lost instructional time, and it plans to do the same in 2023.

For the government of Bangladesh to get pupils back into the classroom, the first thing they did was begin the vaccination process for those students. A university vaccination program was launched to vaccinate university students. On November 2, the campaign to vaccinate 12-17 year old in school started. They had to register through their schools to be vaccinated [57]. Shortcomings of the measures taken:

The lack of access to technology and the internet is the main barrier to e-learning for pupils from low-income families. So it was not a remedy for all students and contributed to inequality. Those lucky enough to have access to online instruction eventually grew bored with it due to a lack of stimulation and the isolation that came from not having regular one-on-one instruction. Examiners were severely harmed due to the truncated public examination curriculum. They are deprived of the opportunity to learn about the subject matter that was cut from the curriculum, even though it is crucial to their future education.

Based on these findings, some interventions can be proposed aimed at preventing the long-term effect of lost learning. One of the most cost-effective ways to boost academic performance and learning recovery is through a school-wide high-dose, one-on-one tutoring program. Adapt lessons to meet the requirements of individual students and place an emphasis on building essential skills. Lengthening the school year, adding make-up days, and expanding instructional blocks are all potential strategies for helping students to aid in their academic recovery. Develop a schedule for keeping tabs on each student's development. Persistent professional development that emphasizes the individual needs of teachers in terms of both methodology and expertise. Instead of arbitrarily removing topics from the public test curriculum, we must emphasize keeping in place the most foundational topics to ensure that students are not left struggling in the future. Since many universities have shortened their academic year, hybrid learning is a great way to help students manage the added workload and yet finish the required coursework in a reasonable amount of time, assuring that all students can participate in hybrid classes.

Hypothetical solutions are presented to show the window of opportunity available to educational systems to recover learning loss. These methods may prove crucial in reversing the damage done by the pandemic and preventing similar catastrophes in the future.

Mitigation of the negative impact on economy

To address the economic crisis, many low- to middle-income countries have employed various solution methodologies to mitigate the economic challenges brought about by the COVID-19 pandemic. Governments have implemented measures such as cash transfers, tax relief, and increased spending on infrastructure and social welfare programs to boost economic activity and support affected individuals and businesses. Central banks have lowered interest rates,

expanded liquidity support programs, and implemented quantitative easing to stabilize financial markets and stimulate lending and investment. Middle-income countries have sought support from international financial institutions, bilateral partners, and multilateral organizations to access additional funding and technical expertise to address the economic fallout of the pandemic.

When the pandemic lasts a long time, spending less on education goes against what this field needs. Insufficient spending in this field to lessen the effects of COVID-19 will have long-term consequences. The lack of resources in the nation could cause education to be negatively impacted by the epidemic than in other nations. If the government doesn't step in with effective short-term and long-term strategies, young people now might be less productive and earn less money in the future. The country should make a plan of action to solve this. For example:

Ensuring that every student returns to their educational institutions. Prioritizing proactive governmental measures, such as updating existing stipend programs, investigating opportunities for "education loans", running communication campaigns, actively engaging with families in need, etc. The government should establish an "Education Loan" program. If students' families can qualify for the 'Education loan' then they won't have to worry about money. So, there won't be any monetary barriers to pupils attending schools. Furthermore, we can employ several tactics aimed at getting students back into the classroom. We could, for instance, broadcast TV commercials intended to raise public consciousness. To raise awareness and get parents to take their kids back to school, we can re-promote cartoons like the Meena cartoons, village theater productions, and announcing campaigns. Investing in the education of its citizens strengthens the country as a whole. Now, the country risks seeing a decline in its educated population if many children and teenagers do not return to school or enroll in higher education. Workers with little education and skills will be produced. The country's gross domestic product will fall.

There is a pressing need for the government to boost its allocation for education in Bangladesh. Currently, the country's spending on education, both in terms of its proportion to GDP and as a percentage of total tax revenue, ranks among the lowest globally. Regrettably, the allocation for education as a portion of GDP has dwindled, dropping from 2.18 percent in the revised budget of FY20 to a mere 2.09 percent in FY21 (Financial Year 2021) [48]. A budget to spend 2.5 percent of GDP on education should be passed. Spending on education must account for a sizable amount of our total budget. Reopening schools that have been forced to close or compensating those in financial distress should both receive funding from this plan. Also, it's important to allocate funds to raise educators' pay. Take action to re-engage the teaching workforce in our schools. Motivating former educators to return to the classroom is important. A national teaching shortage is possible if many current educators decide not to work in schools again. This will harm the education of the pupils, especially those in distant areas. They won't be able to finish school. Once again, schools will be closed. As a result, the national economy will suffer.

'Unemployment' is a curse. We have to work to eliminate unemployment. 'Job-oriented' education should be provided for unemployed students. Work space should also be arranged for them. Students who want to start a business have to arrange 'Student Loans' so that they can get financial support. Those who want to do something themselves should be encouraged. For them 'Student Loan' should be arranged. Students should develop a mindset where they don't approach any task lightly. They can earn their livelihood by engaging in self-reliant activities like agriculture, animal husbandry, fishing, sewing, cottage industry, etc. Thus the unemployment rate of the country will decrease. If the issues are not properly addressed, the demographic dividend for Bangladesh could eventually become a demographic burden in the future. George Laryea-Adjei, UNICEF Regional Director for South Asia, emphasized the importance of collaborative efforts among governments, partners, and the private sector. He emphasized the need to not only align strategies and investment levels correctly but also to construct more robust, efficient, and inclusive

systems capable of fulfilling the fundamental human right of education for all children. This commitment to education should remain steadfast, whether schools are open or closed [58].

Actions required to counter early marriage

During the 2014 Global Girl Summit, Bangladesh declared to reduce the number of girls marrying between the ages of 15 and 18 by less than one-third By 2021. Bangladesh also committed to ending child marriage by 2041. Since then Bangladesh Government has started to develop a National Action Plan. The following steps can reduce child marriage in the context of the hit of the pandemic.

In recent decades, Bangladesh has been making promising improvements in reducing the occurrence of child marriage. Impressive progress was underway with the Child Marriage Restraint Act of 1929 [59] being reformed in 2017 [60]. It has been illegal for a girl under 18 and a boy under 21 to be wed. The new law increases the punishment for committing or assisting in child marriage. As per the recent legislation, in the case of an adult accused, the prescribed penalty entails imprisonment for a maximum of two years, a fine not exceeding BDT 1 lakh, or both. This legal consequence will also extend to guardians, relatives, or the marriage registrar who are implicated in child marriage.

Since Eve-teasing and even rape threats are frequent in the country, marriage is typically seen as a haven for young girls by their parents. The appropriate law enforcement agencies should keep a vigilant eye out for these types of threats and act swiftly if necessary. Many closed-circuit television cameras should be installed in public areas, including roadways, school entrances, and other key locations, to protect the girls. We must ensure that no criminal escapes justice. Government officials should step forward with a sizable budget and well-thought-out plans to protect the families of poor, at-risk girls. Families can be given a monthly stipend, or even a set amount of money, based on their financial situation, so that they are not in a position where they have to sell their daughters off for poverty. Muslim-dominated Bangladesh has intricate cultural dynamics. Emams in mosques should use their platforms to educate the public on the harms of child marriage at a young age. Leaders in rural communities, such as the Union Parishad Chairman, a member of the Union Parishad, or a Word Commissioner have a unique opportunity to speak out against child marriage and educate the populace.

Efforts to re-engage dropout students in education

The government should have prepared a comprehensive long-term strategy to prevent students from dropping out during the pandemic when the likelihood of them doing so was high. In the aftermath of a pandemic, the government can still take the following measures to reduce dropouts and get former dropouts back into school.

Every student who fell behind or quit studying because of the pandemic has to be contacted. It's impossible to do without a thorough survey. A survey detailing their present family, financial, and mental health issues can help to direct the next steps in their care. The high rates of dropout among children from low-income families highlight the need for continuous financial assistance for these households. Monthly payment in addition to possible additional forms of assistance. Without a system of corruption-free, open, and equitable distribution of funds, the good intentions behind this initiative would go to waste and fewer deserving students would be able to complete their education. Teachers should schedule regular meetings with parents to encourage both students and their families to resume their educational pursuits. For kids who come from such impoverished families that they cannot even provide for themselves with a daily meal, the midday meal might be an extremely important factor. The implementation of creative new teaching

strategies can boost the student's engagement in the learning process. Educators throughout the country must receive specialized training on fascinating topics so that students can return to their regularly scheduled lessons with a greater sense of vigor once the pandemic has run its course. Thus, COVID-19 has adversely affected our education sector. We have to take initiatives at the government and private levels to reduce the impacts of COVID-19.

6 Conclusion

Education is the cornerstone of societal advancement, unlocking individuals' potential to shape a better future for themselves and their communities. The negative consequences of the COVID-19 pandemic have disrupted our educational institutions. The closure of many schools has resulted in widespread job loss among teachers and hindered students' pursuit of talent development. Moreover, economic pressures have made things more difficult for students and their families, highlighting the urgent need to address these issues to ensure equitable access to education and enhance national advancement. This study aimed to underscore the detrimental repercussions of COVID-19 on the education sector and examine potential measures to lessen these consequences. Learning loss can have substantial and enduring consequences, particularly for students from underprivileged circumstances who do not have access to resources for remote learning or other educational support. Proactive steps are required to stop more learning loss and promote educational equity.

Strong educational policies and resources are essential to support all learners in achieving their full potential. Extended periods of isolation, disruptions to daily routines, and the uncertainty brought by the pandemic have led to increased anxiety, depression, and loneliness among students. Authorities must raise awareness about mental health, cultivate a supportive school environment, encourage physical activity and healthy habits, and integrate mindfulness and stress-reduction techniques into the curriculum to enhance students' mental well-being. Economic hardships faced by families as a result of the pandemic have increased the risk of early marriage for some students, particularly girls, as families consider marriage as a way to relieve financial strain or secure their daughters' futures.

By promoting economic independence and ensuring access to quality education, girls can get the freedom to reject early marriage and shape their destinies. The pandemic-induced challenges, such as unreliable internet access and technology, financial hardships, lack of in-person interactions, loss of support networks, and general stress, have led to a rising number of students opting out of education. Meeting these challenges requires collaborative endeavors aimed at narrowing the digital divide, offering specialized assistance to at-risk students, providing sustainable financial support, and reimagining resilient education delivery methods for potential future disruptions. We graphed the drop in the number of students in various board exams due to COVID-19 in Bangladesh and observed the outcomes by using the interpolation method. Our graphical analysis demonstrates the profound effects of COVID-19 on education in Bangladesh, particularly through the noticeable decrease in enrollment for the country's primary public exams, the Secondary School Certificate (SSC), and Higher Secondary Certificate (HSC) tests. In this research, we comprehensively examined the multifaceted effects of COVID-19 on the education sector in Bangladesh and explored potential strategies to mitigate the disruptions due to COVID-19.

Declarations

Use of AI tools

The authors declare that they have not used Artificial Intelligence (AI) tools in the creation of this article.

Abbreviations

Terms	Description
JSC	Junior School Certificate.
SSC	Secondary School Certificate.
HSC	Higher Secondary Certificate.
IEDCR	Institute of Epidemiology, Disease Control, and Research.
WHO	World Health Organization.
UNESCO	United Nations Educational, Scientific and Cultural Organization.
MOE	Ministry of Education.
NGO	Non-government Organization.
BRAC	Bangladesh Rehabilitation Assistance Committee.
ROSC	Reaching Out of School Children.
TSR	Teacher-Student Ratio.
HSE	Higher Secondary Education.
NER	Net Enrollment Ratio.
GDP	Gross Domestic Product.
BANBEIS	Bangladesh Bureau of Educational Information & Statistics.
SD	Standard Deviation.
ICT	Information and Communications Technology.
HIES	Household Income and Expenditure Survey.
ADB	Asian Development Bank.
SANEM	South Asian Network on Economic Modeling.

Data availability statement

The data used in this study is publicly available.

Ethical approval

The authors state that this research complies with ethical standards. This research does not involve either human participants or animals.

Consent for publication

Not applicable

Conflicts of interest

The authors declare that they have no conflict of interest.

Funding

Not applicable

Author's contributions

M.K.: Conceptualization, Formal analysis, Original draft preparation, Review and editing, Supervision, S.S.S.: Conceptualization, Software, Formal analysis, Original draft preparation, T.R.N.: Software, Original draft preparation, F.I.: Methodology, Data curation, M.A.R.: Software, Data curation, A.A.A.: Validation, Investigation, Original draft preparation, F.T.: Investigation, Review and editing, M.S.A.: Validation, Resources. All authors have read and agreed to the published version of the manuscript.

Acknowledgements

References

[1] Baloch, S., Baloch, M.A., Zheng, T. and Pei, X. The coronavirus disease 2019 (COVID-19) pandemic. *The Tohoku Journal of Experimental Medicine,* 250(4), 271-278, (2020). [CrossRef]

[2] Liu, Y.C., Kuo, R.L. and Shih, S.R. COVID-19: the first documented coronavirus pandemic in history. *Biomedical Journal,* 43(4), 328-333, (2020). [CrossRef]

[3] Kamrujjaman, M., Mahmud, M.S. and Islam, M.S. Coronavirus outbreak and the mathematical growth map of COVID-19. *Annual Research & Review in Biology,* 35(1), 72–78, (2020). [CrossRef]

[4] Islam, T., Talukder, A.K., Siddiqui, N. and Islam, T. Tackling the COVID-19 pandemic: the Bangladesh perspective. *Journal of Public Health Research,* 9(4), (2020). [CrossRef]

[5] Bodrud-Doza, M., Shammi, M., Bahlman, L., Islam, A.R.M.T. and Rahman, M.M. Psychosocial and socio-economic crisis in Bangladesh due to COVID-19 pandemic: a perception-based assessment. *Frontiers in Public Health,* 8, 341, (2020). [CrossRef]

[6] Anwar, S., Nasrullah, M. and Hosen, M.J. COVID-19 and Bangladesh: challenges and how to address them. *Frontiers in Public Health,* 8, 154, (2020). [CrossRef]

[7] Islam, M.S., Ira, J.I., Kabir, K.A. and Kamrujjaman, M. Effect of lockdown and isolation to suppress the COVID-19 in Bangladesh: an epidemic compartments model. *Journal of Applied Mathematics and Computation,* 4(3), 83-93, (2020). [CrossRef]

[8] Jesus, T.S., Bhattacharjya, S., Papadimitriou, C., Bogdanova, Y., Bentley, J., Arango-Lasprilla, J.C. et al. Lockdown-related disparities experienced by people with disabilities during the first wave of the COVID-19 pandemic: scoping review with thematic analysis. *International Journal of Environmental Research and Public Health,* 18(12), 6178, (2021). [CrossRef]

[9] Kruizinga, M.D., Peeters, D., van Veen, M., van Houten, M., Wieringa, J., Noordzij, J.G. et al. The impact of lockdown on pediatric ED visits and hospital admissions during the COVID19 pandemic: a multicenter analysis and review of the literature. *European Journal of Pediatrics,* 180, 2271-2279, (2021). [CrossRef]

[10] Mahmud, M.S., Kamrujjaman, M., Jubyrea, J., Islam, M.S. and Islam, M.S. Quarantine vs social consciousness: a prediction to control COVID-19 infection. *Journal of Applied Life Sciences International,* 23(3), 20-27, (2020). [CrossRef]

[11] Semlali, M., Hattaf, K., Sadik, M. and El Gourari, A. Stability analysis of a delayed COVID-19 transmission model involving immigration and vaccination. *Communications in Mathematical Biology and Neuroscience,* 2023, (2023). [CrossRef]

[12] Hattaf, K., El Karimi, M.I., Mohsen, A.A., Hajhouji, Z., El Younoussi, M. and Yousfi, N. Mathematical modeling and analysis of the dynamics of RNA viruses in presence of immunity and treatment: a case study of SARS-CoV-2. *Vaccines,* 11(2), 201, (2023). [CrossRef]

[13] Rahman, T. and Sharma, U. A simulation of COVID-19 school closure impact on student learning in Bangladesh. *The World Bank,* 1-10, (2021).

[14] Huque, S.M.R., Aziza, T., Farzana, T. and Islam, M.N. Strategies to mitigate the COVID-19 challenges of universities in Bangladesh. In *Handbook of Research on Strategies and Interventions*

to Mitigate COVID-19 Impact on SMEs (pp. 563-587). USA: IGI Global, (2021). [CrossRef]

[15] Hosen, M., Uddin, M.N., Hossain, S., Islam, M.A. and Ahmad, A. The impact of COVID-19 on tertiary educational institutions and students in Bangladesh. *Heliyon,* 8(1), (2022). [CrossRef]

[16] Ahmed, S., Taqi, H.M.M., Farabi, Y.I., Sarker, M., Ali, S.M. and Sankaranarayanan, B. Evaluation of flexible strategies to manage the COVID-19 pandemic in the education sector. *Global Journal of Flexible Systems Management,* 22, 81-105, (2021). [CrossRef]

[17] Dutta, S. and Smita, M.K. The impact of COVID-19 pandemic on tertiary education in Bangladesh: students' perspectives. *Open Journal of Social Sciences,* 8(09), 53, (2020). [CrossRef]

[18] Beqqali, N., Hattaf, K. and Achtaich, N. Mathematical biology in high school mathematics education. *Journal of Educational and Social Research,* 13(6), 326-337, (2023). [CrossRef]

[19] Rahman, M.M., Rahaman, S.M., Salamzadeh, A. and Jantan, A.H. Positive consequences of COVID-19 pandemic: reflections based on university students community in Bangladesh. *International Review,* (3-4), 83-92, (2021).

[20] Chowdhury, R. and Sarkar, M. Education in Bangladesh: changing contexts and emerging realities. In *Engaging in Educational Research: Revisiting Policy and Practice in Bangladesh, Education in the Asia-Pacific Region: Issues, Concerns and Prospects* (Vol. 44) (pp. 1-18). Singapore: Springer, (2018). [CrossRef]

[21] Khan, N.N., Begum, S.A., Afeef, R. and Kamrujjaman, M. Vaccine efficacy of COVID-19 in Bangladesh: does vaccination prevent the pandemic?. *Ganit: Journal of Bangladesh Mathematical Society,* 43(1), 45-62, (2023). [CrossRef]

[22] Kamrujjaman, M., Mahmud, M.S., Ahmed, S., Qayum, M.O., Alam, M.M., Hassan, M.N. et al. SARS-CoV-2 and Rohingya refugee camp, Bangladesh: uncertainty and how the government took over the situation. *Biology,* 10(2), 124, (2021). [CrossRef]

[23] Cohen, S., Chakravarthy, S., Bharathi, S., Narayanan Gopalakrishnan, B. and Park, C.Y. Potential economic impact of COVID-19-related school closures. *Asian Development Bank Economics Working Paper Series,* 657, (2022). [CrossRef]

[24] Ministry of Education in Bangladesh, (2024). `https://www.moedu.gov.bd`.

[25] Literacy Rate in Bangladesh-Rising bd.com, Risingbd.com (2022). `https://www.risingbd.com/english/national/news/88254`.

[26] The Daily Star, Budget 2017-2018: education gets a boost, (2017). `https://www.thedailystar.net/country/bangladesh-national-budget-2017-18-education-gets-boost-1414009`.

[27] Prodhan, M. The educational system in Bangladesh and scope for improvement. *Journal of International Social Issues,* 4(1), 11-23, (2016).

[28] Peterson, P., Baker, E. and McGaw, B. *International Encyclopedia of Education (Third Edition).* Elsevier Science: USA, (2010).

[29] ADRA Internation, Primary education in Bangladesh, (2019). `https://www.adrabangladesh.org/single-post/2019/12/31/primary-education-in-bangladesh`.

[30] Gustavsson, S. *Primary Education in Bangladesh: for whom?.* University Press: Dhaka, Bangladesh, (1990).

[31] Mousumi, M.A. and Kusakabe, T. School education system in Bangladesh. In *Handbook of Education Systems in South Asia, Global Education Systems* (pp. 443-477). Singapore: Springer, (2021). [CrossRef]

[32] Education in Bangladesh, (2024). `https://www.dsce.edu.bd/`.

[33] National Encyclopedia of Bangladesh, Banglapedia, Secondary education, (2021). https://en.banglapedia.org/index.php?title=Secondary_Education.

[34] Alam, M.M. Comparative acceptability of GTM and CLT to the teachers of rural secondary high schools in Bangladesh. *Global Journal of Human-Social Science Research,* 15(4), 1-8, (2015).

[35] The Business Standard, 2,716 new educational institutes brought under MPO, (2022). https://www.tbsnews.net/bangladesh/education/2616-new-educational-institutes-brought-under-mpo-453878.

[36] Bangladesh Bureau of Educational Information & Statistics (BANBEIS), Bangladesh education statistics, (2022). https://banbeis.portal.gov.bd/sites/default/files/files/banbeis.portal.gov.bd/npfblock//Bangladesh.

[37] UNICEF, Learning loss must be recovered to avoid long-term damage to children's well-being, new report says, (2022). https://www.unicef.org/bangladesh/en/press-releases/learning-loss-must-be-recovered-avoid-long-term-damage-childrens-well-being-new.

[38] UNICEF, COVID-19: schools for more than 168 million children globally have been completely closed for almost a full year, says UNICEF, (2021). https://www.unicef.org/press-releases/schools-more-168-million-children-globally-have-been-completely-closed#:~:text=NEW.

[39] World Bank Blogs, COVID-19 school closures fueled big learning losses, especially for the disadvantaged, (2022). https://blogs.worldbank.org/developmenttalk/covid-19-school-closures-fueled-big-learning-losses-especially-disadvantaged.

[40] XINHUANET, Bangladesh cancels major public examination amid COVID-19 fears, (2020). http://www.xinhuanet.com/english/2020-10/07/c_139424338.htm.

[41] The World Bank, Learning losses from COVID-19 could cost this generation of students close to $17 trillion in lifetime earnings, (2021). https://www.worldbank.org/en/news/press-release/2021/12/06/learning-losses-from-covid-19-could-cost-this-generation-of-students-close-to-17-trillion-in-lifetime-earnings.

[42] UNICEF, The future of 37 million children in Bangladesh is at risk with their education severely affected by the COVID-19 pandemic, (2021). https://www.unicef.org/bangladesh/en/press-releases/future-37-million-children-bangladesh-risk-their-education-severely-affected-covid.

[43] National Alliance in Mental Illness (NAMI), California, School during the pandemic: mental health impacts on students, (2020). https://namica.org/blog/impact-on-the-mental-health-of-students-during-covid-19/.

[44] Health Central, The growing mental health effects of COVID-19 for young adults, (2020). https://www.healthcentral.com/article/mental-health-effects-of-covid-19-on-students.

[45] Active Minds, The impact of COVID-19 on student mental health, (2020). https://www.activeminds.org/studentsurvey/.

[46] Rahman, M.M., Asikunnaby, Khan, S.J., Arony, A., Mamun, Z.A., Procheta, N.F. et al. Mental health condition among university students of Bangladesh during the critical COVID-19 period. *Journal of Clinical Medicine,* 11(15), 4617, (2022). [CrossRef]

[47] Al Mamun, F., Hosen, I., Misti, J. M., Kaggwa, M.M. and Mamun, M.A. Mental disorders of Bangladeshi students during the COVID-19 pandemic: a systematic review. *Psychology Research and Behavior Management,* 14, 645-654, (2021). [CrossRef]

[48] Uddin, M. Effects of the pandemic on the education sector in Bangladesh. *The Financial Express*, 13(1), (2020).

[49] The Financial Express, BD school closure eats up 3.1pc of GDP: study, (2022). `https://thef inancialexpress.com.bd/national/bd-school-closure-eats-up-31pc-of-gdp-study-1 653791288`.

[50] UNICEF, Ending child marriage in Bangladesh, (2017). `https://www.unicef.org/banglades h/en/reports/ending-child-marriage-bangladesh`

[51] BRAC, School closure during COVID-19 pandemic: concerns over rising rate of school dropouts, child marriages, (2020). `https://www.brac.net/latest-news/item/1291-schoo l-closure-during-covid-19-pandemic-concerns-over-rising-rate-of-school-dropo uts-child-marriages`.

[52] UNICEF, 10 million additional girls at risk of child marriage due to COVID-19 – UNICEF, (2021). `https://www.unicef.org/bangladesh/en/press-releases/10-million-additiona l-girls-risk-child-marriage-due-covid-19-unicef`.

[53] The Financial Express, Getting covid-time dropouts back to classes, (2021). `https://thefin ancialexpress.com.bd/views/columns/getting-covid-time-dropouts-back-to-class es-1632067207`.

[54] Li, Z., Sharma, U. and Matin, M. Impact of COVID-19 on primary school students in disadvantaged areas of Bangladesh. *ADB Briefs*, 200, 1-8, (2021). [CrossRef]

[55] World Economic Forum, The COVID-19 pandemic has changed education forever, (2020). `https://www.weforum.org/agenda/2020/04/coronavirus-education-global-covid19-o nline-digital-learning/`.

[56] The World Bank, TV-based learning in Bangladesh: is it reaching students?, (2020). `https: //www.ungei.org/publication/tv-based-learning-bangladesh-it-reaching-students`.

[57] Mahmud, S., Mohsin, M., Khan, I.A., Mian, A.U. and Zaman, M.A. Knowledge, beliefs, attitudes and perceived risk about COVID-19 vaccine and determinants of COVID-19 vaccine acceptance in Bangladesh. *PloS One*, 16(9), e0257096, (2021). [CrossRef]

[58] UNICEF, The future of 37 million children in Bangladesh is at risk with their education severely affected by the COVID-19 pandemic, (2021). `https://www.unicef.org/banglades h/en/press-releases/future-37-million-children-bangladesh-risk-their-educati on-severely-affected-covid`.

[59] Laws of Bangladesh, Government of the People's Republic of Bangladesh, Legislative and Parliamentary Affairs Division, The child marriage restraint act, 1929, (2019). `http://bdlaws .minlaw.gov.bd/act-details-149.html`.

[60] Laws of Bangladesh, Government of the People's Republic of Bangladesh, Legislative and Parliamentary Affairs Division, The child marriage restraint act, 2017, (2017). `https://www. unicef.org/bangladesh/sites/unicef.org.bangladesh/files/2018-10/Child%20Marria ge%20Restraint%20Act%202017%20English.pdf`.

RESEARCH PAPER

Study of fractional order SIR model with M-H type treatment rate and its stability analysis

Subrata Paul [ID] [1,‡], **Animesh Mahata** [ID] [2,*,‡], **Supriya Mukherjee** [ID] [3,‡], **Meghadri Das** [ID] [4,‡], **Prakash Chandra Mali** [ID] [5,‡], **Banamali Roy** [ID] [6,‡], **Poulami Mukherjee** [ID] [7,‡] and **Pramodh Bharati** [ID] [8,9,‡]

[1]Department of Mathematics, Arambagh Govt. Polytechnic, Arambagh-712602, West Bengal, India, [2]Department of Mathematics, Sri Ramkrishna Sarada Vidya Mahapitha, Kamarpukur, Hooghly-712612, India, [3]Department of Mathematics, Gurudas College, 1/1 Suren Sarkar Road, Kolkata-700054, West Bengal, India, [4]Indian Institute of Engineering Science and Technology, Shibpur, Howrah-711103, West Bengal, India, [5]Department of Mathematics, Jadavpur University, 188 Raja S.C. Mallik Road, Kolkata-700032, West Bengal, India, [6]Department of Mathematics, Bangabasi Evening College, Kolkata-700009, West Bengal, India, [7]Department of Mathematics, Calcutta Girls' B.T. College, Ballygunge, Kolkata-700019, West Bengal, India, [8]Department of Mathematics, Ramnagar College, Purba Medinipur-721453, West Bengal, India, [9]Department of Mathematics, Swami Vivekananda University, Telinipara, Barasat-Barrackpore Rd, Bara Kanthalia, West Bengal-700121, India

* Corresponding Author
‡ paulsubrata564@gmail.com (Subrata Paul); animeshmahata8@gmail.com (Animesh Mahata); supriyaskbu2013@gmail.com (Supriya Mukherjee); dasmeghadri@gmail.com (Meghadri Das); pcmali1959@gmail.com (Prakash Chandra Mali); banamaliroy@yahoo.co.in (Banamali Roy); poulamimukherjee2023@gmail.com (Poulami Mukherjee); pramodbharatinilu@gmail.com (Pramodh Bharati)

Abstract

In this manuscript, we analyze a fractional-order susceptible-infected-recovered (SIR) mathematical model with a nonlinear incidence rate and nonlinear treatment rate for the control of infectious illness. The incidence rate of infection is considered as Holling type II and the treatment rate is considered as Monod-Haldane (MH) type. The existence and uniqueness criteria for the new model, as well as the non-negativity and boundedness, have been established. We also provide an ideal control strategy for the SIR model using the treatment rate as a control parameter. The solution of the suggested model is approximated using the fractional-order Taylor's method. With the help of MATLAB (2018a), we perform numerical simulations and illustrate the results through graphical representations.

Keywords: SIR model; Monod-Haldane type treatment rate; optimal control; Caputo derivative
AMS 2020 Classification: 92D25; 92D30; 26A33; 49J15; 65L07

---

1 Introduction

Epidemiology, sometimes compared to the biological study of public health, focuses on the prevalence and underlying causes of infection susceptibility among the general population. The use of mathematical models to study such communicable diseases makes it easier to comprehend how diseases spread, to identify elements that affect transmission for efficient control efforts, and to assess goals and intervention approaches. Systematically introducing deterministic models for infectious illnesses, Kermack and McKendrick [1, 2]. To better understand the process of disease transmission, a number of researchers have investigated various epidemic systems by looking at various models, such as those developed by SI [3], SIS [4], SIR [5–10], SIRS [9], SEIR [11–14], SIQR [15], SEIRV [16, 17]. Infectious disease management has been harder during the last several decades. One of the most important health measures for avoiding infectious diseases is vaccination because of its safety and cost. Indeed, high vaccination rates have resulted in dramatic reductions or even elimination of a variety of infectious illnesses, such as smallpox [18], SARS-CoV-2 infection [19, 20]. In the modeling of infectious illnesses [21–27], the incidence rate is crucial in determining the behavior at phenomena. In 1927, Kermack and Mckendrick [1] proposed the transmission rate as βSI. The interaction effect is a linearly rising count of the amount of pathogens in this incidence rate, which is unsuitable for a vast population. As a result, Capasso and Serio [28] proposed a nonlinear occurrence $g(I)S$ for $g'(I) < 0$ that permits particular "behavioral" effects. With behavioral modifications, Capasso and Serio inspired their approach. The potential damage of infection may become extraordinarily high during times of high occurrence, leading to major behavioral modifications that minimize the actual risk of illness [29]. Goel and Nilam [8], Wei and Chen [30], Capasso et al. [31, 32], Zhang et al. [33], Anderson and May [34], Li et al. [35], including Kumar and Nilam [9, 10]. A few writers [36–38], have drawn attention to the significance of taking nonlinear incidence rates into account when studying the relationships between infectious transmission and illness. Li et al. [35] presented a SIR model with $f(S, I) = \dfrac{\beta SI}{1 + \gamma I}$.

It is well known that treatment rates are crucial in avoiding and limiting the spread of illnesses. We are aware that the therapy resources in any community are insufficient. As a result, selecting an effective treatment rate is critical for limiting disease transmission. Due to a lack of efficient treatment options and vaccinations, epidemic prevention methods focus on efficient preventative measures. Wang and Ruan [39] proposed the following SIR transmission dynamics with a fixed treatment rate:

$$h(I) = \begin{cases} n & \text{for } I > 0, \\ 0 & \text{for } I = 0. \end{cases}$$

Zhang and Liu [40], who also provided a superior treatment rate (Holling type II) as a continuously differentiable function that populates at the largest benefit, as shown below: $h(I) = \frac{mI}{1+nI}$ for $I \geq 0, m > 0, n > 0$, where m represents the cure rate and n represents the limitation rate in treatment availability. Zhang et al. [41], Zhou et al. [42] and Dubey et al. [43] have investigated this nonlinear saturation treatment rate in a somewhat different manner. Kumar [44] proposed a dynamical model of epidemic along with time delay; Holling Type II incidence rate and Monod–Haldane type treatment rate.

Motivation and research background

A particularly useful tool for modelling an infectious disease system that includes past illness states, a memory of past disease patterns, a profile of genetic diversity, etc. is fractional calculus

[45–48]. When compared to an integer order model, using fractional order derivatives to fine-tune complicated dynamics within a disease system produces a more accurate picture. Because it expands the possibilities of integer-order derivatives, fractional-order modelling is a useful tool for analyzing disease features. The integer order derivative is limited to local characteristics, but the fractional order derivative has a broad scope. When the system's consistency domain is improved, the fractional derivative likewise does better. In this paper, three potential categories using the Caputo technique are studied using the fractional order SIR compartmental model with a nonlinear incidence rate and nonlinear treatment rate. The saturated incidence rate of infection is considered as Holling type II and the treatment rate is considered as Monod-Haldane (MH) type. The existence and uniqueness criteria for the new models, as well as the solution's positivity, have been established, among other conclusions. Both at E_0 and E_1, we have covered the stability analysis of our suggested model. For estimating the system solution, Taylor's approach is also used. We used the MATLAB (2018a) program to run numerical simulations and analyze the graphical significance.

Paper structure

Section 2 introduces a pre-requisite concept. We developed the SIR epidemic model in Section 3 in an environment of the Caputo derivative. In Section 4, the model's solution has been examined in terms of its existence, uniqueness, non-negativity, boundedness criteria, and stability analysis. Using the control parameter treatment rate, we also provide an ideal control strategy for a SIR model in Section 5. The suggested model's approximate solution is discussed in Section 6 using the fractional-order Taylor's technique in the Caputo derivative. In Section 7, the MATLAB-based numerical analysis is presented. Section 8 is where the paper comes to a conclusion.

2 Preliminaries

Definition 1 *[49] Let $f \in C^n([t_0, \infty+), \mathbb{R})$, the Caputo derivative of fractional order $\alpha > 0$ is defined by*

$$
{}_{t_0}^{C} D_t^{\alpha} f(t) = \frac{1}{\Gamma(n-\alpha)} \int_{t_0}^{t} \frac{f^{(n)}(s)}{(t-s)^{\alpha-n+1}} ds,
$$

where $\Gamma(\cdot)$ represent the Gamma function, $t \geq t_0$, $n \in \mathbb{Z}^+$ and $\alpha \in (n-1, n)$.

Lemma 1 *[50] Consider the system*

$$
{}_{t_0}^{C} D_t^{\alpha} u(t) = g(t, x), t_0 > 0,
$$

with initial condition $u(t_0) = u_{t_0}$, where $\alpha \in (0, 1]$, $g : [t_0, \infty) \times \Omega \rightarrow \mathbb{R}^n, \Omega \in \mathbb{R}^n$, if Lipschitz condition is satisfied by $g(t, x)$ with respect to x, then there exists a solution of (3.2) on $[t_0, \infty) \times \Omega$ which is unique.

Lemma 2 *[51] Let $0 < \alpha \leq 1$, $\phi(t) \in C[a, b]$. If ${}_{t_0}^{C} D_t^{\alpha} f(t) \geq 0 \left({}_{t_0}^{C} D_t^{\alpha} f(t) \leq 0 \right), t \in (a, b)$ then $\phi(t)$ is a increasing (decreasing) function for $t \in [a, b]$.*

Lemma 3 *[52] The Laplace transform of the Caputo derivative is given by:*

$$
\mathscr{L} \left\{ {}_{t_0}^{C} D_t^{\alpha} f(t) \right\} = p^{\alpha} F(p) - \sum_{j=0}^{n-1} p^{\alpha-j-1} f^j(t_0),
$$

where $F(p) = \mathscr{L}\{f(t)\}$.

Lemma 4 [53] *For any $B \in \mathbb{C}^{n \times n}$ where $\mathbb{C}$ be the complex plane and $c, d > 0$, the Laplace transform of Mittag-Leffler function is defined as*

$$\mathscr{L}\left\{t^{d-1}E_{c,d}(Bt^c)\right\} = s^{c-d}(s^c - B)^{-1},$$

for $\mathscr{R}(s) > \|B\|^{\frac{1}{c}}$, where $\mathscr{R}(s)$ denotes the real portion of s.

Lemma 5 [53] *Consider the following fractional-order system:*

$$_{t_0}^{C}D_t^\alpha X(t) = \Phi(X), X_{t_0} = (x_{t_0}^1, x_{t_0}^2, ..., x_{t_0}^n), x_{t_0}^i > 0, \quad i = 1, 2, ..., n,$$

with $0 < \alpha \leq 1$, $X(t) = (x^1(t), x^2(t), ..., x^n(t))$ and $\Phi(X) : [t_0, \infty) \to \mathbb{R}^{n \times n}$. The equilibrium points of the above system are evaluated by solving the following system of equations: $\Phi(X) = 0$. These equilibrium points are locally asymptotically stable iff each eigenvalue λ of the Jacobian matrix $J(X) = \dfrac{\partial(\Phi_1, \Phi_2, ..., \Phi_n)}{\partial(x^1, x^2, ..., x^n)}$ calculated at the equilibrium points satisfy $|\arg(\lambda_i)| > \frac{\alpha\pi}{2}$.

Lemma 6 [54] *Suppose $g(t) \in \mathbb{R}_+$ be a differentiable function. Then, for any $t \geq t_0$,*

$$_{t_0}^{C}D_t^\alpha\left[g(t) - g^* - g^* \ln\frac{g(t)}{g^*}\right] \leq \left(1 - \frac{g^*}{g(t)}\right)_{t_0}^{C}D_t^\alpha g(t), \; g^* \in \mathbb{R}_+, \forall \alpha \in (0, 1).$$

Lemma 7 [54] *One parametric and two parametric Mittag-Leffler functions are described as follows:*

$$E_\alpha(z) = \sum_{j=0}^{\infty}\frac{z^j}{\Gamma(\alpha j + 1)}, \; and \; E_{a_1, a_2}(z) = \sum_{j=0}^{\infty}\frac{z^j}{\Gamma(a_1 j + a_2)}, \; where \; \alpha, a_1, a_2 \in \mathbb{R}_+.$$

3 Formulation of the model system

We have introduced a mathematical framework that posits the division of the entire population, denoted as N, into three distinct categories: susceptible individuals denoted as S, infected individuals denoted as I, and individuals who have recovered, represented as R at a time t.

The sub-populations at different times may vary, but the total of all sub-populations remains constant, denoted as N. This can be expressed as $S(t) + I(t) + R(t) = N$. The term $\frac{\beta SI}{1 + \gamma I}$ is the Holling type II functional response representing the saturated incidence rate of infection among susceptible where β is the transmission rate between susceptible and infected population. Also, the term $\frac{mI}{1 + n^2 I}$ represents the Monod-Haldane type treatment rate, which describes the non-monotonic behavior of the treatment rate due to limitations in the availability of effective treatments. Table 1 provides a summary of the symbols used in the proposed model system.

$$\begin{aligned}
_{t_0}^{C}D_t^\alpha S(t) &= \Lambda - \mu S(t) - \frac{\beta S(t)I(t)}{1 + \gamma I(t)}, \; S(t)|_{t=0} = S(0) > 0, \\
_{t_0}^{C}D_t^\alpha I(t) &= \frac{\beta S(t)I(t)}{1 + \gamma I(t)} - \frac{mI(t)}{1 + nI^2(t)} - (\mu + r + \delta)I(t), \; I(t)|_{t=0} = I(0) > 0, \\
_{t_0}^{C}D_t^\alpha R(t) &= \frac{mI(t)}{1 + nI^2(t)} + \delta I(t) - \mu R(t), \; R(t)|_{t=0} = R(0) > 0,
\end{aligned} \tag{1}$$

where $0 < \alpha < 1$, and $^C_{t_0} D^\alpha_t$ denotes the Caputo operator.
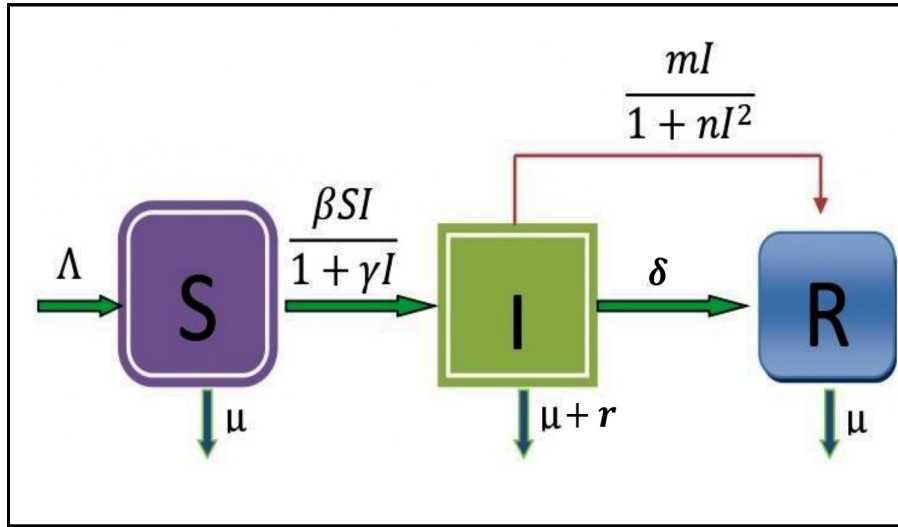
Figure 1. The proposed SIR model's flow diagram

Table 1. Significance of the relevant parameters

Parameters	Biological meaning
Λ	recruitment rate
μ	death rate
β	transmission rate
γ	inhibitory rate
m	treatment rate
n	limitation rate in resources availability
δ	recovery rate
r	disease-induced mortality rate

4   Analysis of the system

Model existence and model uniqueness

Theorem 1 *The model* (1), *with an initial condition of* $(S(t_0), I(t_0), R(t_0))$ *belonging to the positive region* Γ^+, *invariably exhibits a singular solution within the domain* Γ^+ *for all time points* $t \geq t_0$.

Proof Let $\Omega = \{(S, I, R) \in \mathbb{R}^3 : \max(|S|, |I|, |R|) \leq M\}$ where τ and M are finite positive real numbers for the region $\Omega \times [t_0, \tau]$. Let $Y = (S, I, R)$ and $\overline{Y} = (\bar{S}, \bar{I}, \bar{R})$.
Consider a mapping $F(Y) = (F_1(Y), F_2(Y), F_3(Y))$, where

$$F_1(Y) = \Lambda - \mu S(t) - \frac{\beta S(t) I(t)}{1 + \gamma I(t)},$$
$$F_2(Y) = \frac{\beta S(t) I(t)}{1 + \gamma I(t)} - \frac{m I(t)}{1 + n I^2(t)} - (\mu + \delta + r) I(t),$$
$$F_3(Y) = \frac{m I(t)}{1 + n I^2(t)} + \delta I(t) - \mu R(t).$$

For any $Y, \overline{Y} \in \Omega$:

$$\left\| F(Y) - F(\overline{Y}) \right\|$$

$$= \left| F_1(Y) - F_1(\overline{Y}) \right| + \left| F_2(Y) - F_2(\overline{Y}) \right| + \left| F_3(Y) - F_3(\overline{Y}) \right|$$

$$= \left| \Lambda - \mu S - \frac{\beta SI}{1 + \gamma I} - \left(\Lambda - \mu \bar{S} - \frac{\beta \bar{S} \bar{I}}{1 + \gamma \bar{I}} \right) \right|$$

$$+ \left| \frac{\beta SI}{1 + \gamma I} - \frac{mI}{1 + nI^2} - (\mu + \delta + r) I - \left(\frac{\beta \bar{S} \bar{I}}{1 + \gamma \bar{I}} - \frac{m\bar{I}}{1 + n\bar{I}^2} \right) + (\mu + \delta + r) \bar{I} \right|$$

$$+ \left| \frac{mI}{1 + nI^2} + \delta I - \mu R - \left(\frac{m\bar{I}}{1 + n\bar{I}^2} + \delta \bar{I} - \mu \bar{R} \right) \right|$$

$$\leq \mu \left| (S - \bar{S}) \right| + 2\beta \left| \left(\frac{SI}{1 + \gamma I} - \frac{\bar{S} \bar{I}}{1 + \gamma \bar{I}} \right) \right| + 2m \left| \left(\frac{I}{1 + nI^2} - \frac{\bar{I}}{1 + n\bar{I}^2} \right) \right|$$

$$+ (\mu + 2\delta + r) \left| (I - \bar{I}) \right| + \mu \left| (R - \bar{R}) \right|$$

$$\leq \mu \left| (S - \bar{S}) \right| + 2\beta \left| \left(\frac{SI(1 + \gamma \bar{I}) - \bar{S} \bar{I}(1 + \gamma I)}{(1 + \gamma I)(1 + \gamma \bar{I})} \right) \right| + 2m \left| \left(\frac{I(1 + n\bar{I}^2) - \bar{I}(1 + nI^2)}{(1 + nI^2)(1 + n\bar{I}^2)} \right) \right|$$

$$+ (\mu + 2\delta + r) \left| (I - \bar{I}) \right| + \mu \left| (R - \bar{R}) \right|$$

$$\leq \mu \left| (S - \bar{S}) \right| + 2\beta K[M \left| (S - \bar{S}) \right| + \left| (I - \bar{I}) \right| + \gamma M^2 \left| (I - \bar{I}) \right|] + 2mL(1 + nM^2) \left| (I - \bar{I}) \right|$$

$$+ (\mu + 2\delta + r) \left| (I - \bar{I}) \right| + \mu \left| (R - \bar{R}) \right|$$

$$\leq (\mu + 2\beta MK)) \left| (S - \bar{S}) \right| + \left(\mu + 2\delta + r + 2mL(1 + nM^2) + 2\beta K(1 + \gamma M^2) \right) \left| (I - \bar{I}) \right| + \mu \left| (R - \bar{R}) \right|$$

$$\leq G_1 \left| S - \bar{S} \right| + G_2 \left| I - \bar{I} \right| + G_3 \left| R - \bar{R} \right|$$

$$\leq G \left\| Y - \overline{Y} \right\|,$$

where $G = \max\{G_1, G_2, G_3\}$, $G_1 = (\mu + 2\beta M)$, $G_2 = \left(\mu + 2\delta + r + 2mL(1 + nM^2) + 2\beta K(1 + \gamma M^2) \right)$ and $G_3 = \mu$, where $\left| (1 + \gamma I)(1 + \gamma \bar{I}) \right| \geq K$ and $\left| (1 + nI^2)(1 + n\bar{I}^2) \right| \geq L$. Thus, $F(Y)$ satisfies Lipschitz's criteria. So $Y(t)$ is a unique solution of model (1), with the help of Lemma 1.

Boundedness and non-negativity

Theorem 2 *Any solutions originating from the initial condition $(S(t_0), I(t_0), R(t_0))$ in model (1) are characterized by non-negative values.*

Proof Let $Y(t_0) = (S(t_0), I(t_0), R(t_0)) \in \Gamma_+$ be the initial solution of (1). Firstly, we shall prove that $S(t) \geq 0$ for all $t \geq 0$. For this, we assume that $S(t) \geq 0$ is not true. Then there exists a $\tau_1 > 0$, such that

$$\begin{cases} S(t) > 0 \text{ for } t_0 \leq t < \tau_1, \\ S(t) = 0 \text{ for } t = \tau_1, \\ S(t) < 0 \text{ for } \tau_1 < t < \tau_1 + \epsilon_1 \text{ for } \epsilon_1 > 0. \end{cases}$$

With the help of system (1), we have

$$_{t_0}^{C} D_t^\alpha S(t) |_{S(\tau_1) = 0} = \Lambda > 0.$$

Using Lemma 2, for any $0 < \epsilon_1 << 1$, we have $S(\tau_1 + \epsilon_1) = S(\tau_1) + \frac{1}{\alpha} \frac{d^\alpha}{dt^\alpha} S(t) \epsilon_1^\alpha$. As a result, $S(\tau_1 + \epsilon_1) \geq 0$, contradicts our assumption that $S(t) < 0$ for $\tau_1 < t < \tau_1 + \epsilon_1$. Therefore, we get $S(t) \geq 0, \forall t \in [t_0, \infty)$. Secondly, we shall prove that $I(t) \geq 0$ for all $t \geq 0$. For this, we assume

that $I(t) \geq 0$ is not true. Then there exists a $\tau_2 > 0$, such that

$$
\begin{cases}
I(t) > 0 \text{ for } t_0 \leq t < \tau_2, \\
I(t) = 0 \text{ for } t = \tau_2, \\
I(t) < 0 \text{ for } \tau_2 < t < \tau_2 + \epsilon_2 \text{ for } \epsilon_2 > 0.
\end{cases}
$$

With the help of system (1), we have

$$
{}^{C}_{t_0}D^\alpha_t I(t)|_{I(\tau_2)=0} = 0.
$$

Using Lemma 2, for any $0 < \epsilon_2 << 1$, we have $I(\tau_2 + \epsilon_2) = I(\tau_2) + \frac{1}{\alpha}\frac{d^\alpha}{dt^\alpha}I(t)\epsilon_2{}^\alpha$. As a result, $I(\tau_2 + \epsilon_2) = 0$, contradicts our assumption that $I(t) < 0$ for $\tau_2 < t < \tau_2 + \epsilon_2$. Therefore, we get $I(t) \geq 0, \forall t \in [t_0, \infty)$. Lastly, we shall prove that $R(t) \geq 0$ for all $t \geq 0$. For this, we assume that $R(t) \geq 0$ is not true. Then there exists a $\tau_3 > 0$, such that

$$
\begin{cases}
R(t) > 0 \text{ for } t_0 \leq t < \tau_3, \\
R(t) = 0 \text{ for } t = \tau_3, \\
R(t) < 0 \text{ for } \tau_3 < t < \tau_3 + \epsilon_3 \text{ for } \epsilon_3 > 0.
\end{cases}
$$

With the help of system (1), we have

$$
{}^{C}_{t_0}D^\alpha_t R(t)|_{R(\tau_3)=0} = \frac{mI(\tau_3)}{1 + nI^2(\tau_3)} + \delta I(\tau_3) > 0.
$$

Using Lemma 2, for any $0 < \epsilon_3 << 1$, we have $R(\tau_3 + \epsilon_3) = R(\tau_3) + \frac{1}{\alpha}\frac{d^\alpha}{dt^\alpha}R(t)\epsilon_3{}^\alpha$. As a result, $R(\tau_3 + \epsilon_3) \geq 0$, contradicts our assumption that $R(t) < 0$ for $\tau_3 < t < \tau_3 + \epsilon_3$. Therefore, we get $R(t) \geq 0, \forall t \in [t_0, \infty)$.

Theorem 3 *All solutions of system* (1) *are bounded.*

Proof Now $N(t) = S(t) + I(t) + R(t)$, then

$$
\begin{aligned}
{}^{C}_{t_0}D^\alpha_t N(t) &= {}^{C}_{t_0}D^\alpha_t S(t) + {}^{C}_{t_0}D^\alpha_t I(t) + {}^{C}_{t_0}D^\alpha_t R(t) \\
&= \Lambda - \mu N(t) - rI(t).
\end{aligned}
$$

Therefore,

$$
{}^{C}_{t_0}D^\alpha_t N(t) + \mu N(t) \leq \Lambda \quad (\text{as } I \geq 0).
$$

We get (using Lemma 3):

$$
\begin{aligned}
z^\alpha F(z) - z^{\alpha-1}N(0) + \mu F(z) &\leq \frac{\Lambda}{z}, \text{ where } F(z) = \mathcal{L}\{N(t)\} \\
\Rightarrow F(z)(z^{\alpha+1} + z\mu) &\leq z^\alpha N(0) + \Lambda \\
\Rightarrow F(z) &\leq \frac{z^\alpha N(0) + \Lambda}{z^{\alpha+1} + z\mu} \\
&= \frac{z^\alpha N(0)}{z^{\alpha+1} + z\mu} + \frac{\Lambda}{z^{\alpha+1} + z\mu}.
\end{aligned}
$$

Using inverse Laplace transform:

$$N(t) \leq N(0)E_{\alpha,1}(-\mu t^{\alpha}) + \Lambda t^{\alpha} E_{\alpha,\alpha+1}(-\mu t^{\alpha}).$$

From the properties of Mittag-Leffler function [55], we get

$$E_{c,d}(x) = x E_{c,c+d}(x) + \frac{1}{\Gamma(d)}.$$

Hence,

$$N(t) \leq (N(0) - \frac{\Lambda}{\mu})E_{\alpha,1}(-\mu t^{\alpha}) + \frac{\Lambda}{\mu}.$$

As a result, the system solutions are bounded. It completes the proof of the theorem. The impact of $R(t)$ on the first two equations in system (1) is unaltered. System (1) might be converted to a two-dimensional system on the presumption that the whole population N is constant. The third equation of the system (1) is traditionally omitted. As a result, we have:

$$\begin{aligned}
{}^{C}_{t_0}D^{\alpha}_t S(t) &= \Lambda - \mu S(t) - \frac{\beta S(t)I(t)}{1+\gamma I(t)}, \ S(t)|_{t=0} = S(0) > 0, \\
{}^{C}_{t_0}D^{\alpha}_t I(t) &= \frac{\beta S(t)I(t)}{1+\gamma I(t)} - \frac{mI(t)}{1+nI^2(t)} - (\mu + r + \delta)I(t), \ I(t)|_{t=0} = I(0) > 0.
\end{aligned} \tag{2}$$

Equilibrium points of the model (2)

Let ${}^{C}_{t_0}D^{\alpha}_t S(t) = 0$ and ${}^{C}_{t_0}D^{\alpha}_t I(t) = 0$. The model (2) has two equilibrium points namely,

i. The infection free equilibrium is $E_0(\frac{\Lambda}{\mu}, 0)$.
ii. The endemic equilibrium is $E_1(S^*, I^*)$, where
$S^* = \frac{\Lambda + I^*(-m-\mu-\delta-r) + I^{*2}(\Lambda n) - n(\mu+\delta+r)I^{*3}}{\mu(1+nI^{*2})}$ and $XI^{*3} + YI^{*2} + ZI^* + W = 0$, where $X = n(\mu\gamma + \beta)(\mu+\delta+r)$, $Y = \mu n(\mu+\delta+r) - \beta\Lambda n$, $Z = (\mu\gamma+\beta)(m+\mu+\delta+r)$ and $W = \mu(\mu+m+\delta+r) - \Lambda\beta$.

The basic reproduction number

The next-generation matrix [56] technique is used to calculate the model's basic reproduction number R_0, which may be determined from the biggest eigenvalue of the matrix FV^{-1} where,

$$F = \begin{bmatrix} \frac{\beta\Lambda}{\mu} & 0 \\ 0 & 0 \end{bmatrix}, \quad \text{and} \quad V = \begin{bmatrix} m+\mu+\delta+r & 0 \\ \frac{\beta\Lambda}{\mu} & \mu \end{bmatrix}.$$

Therefore, $R_0 = \frac{\beta\Lambda}{\mu(m+\mu+\delta+r)}.$

Stability analysis at E_0

Let us consider $J_0(S, I) = F$ where,

$$F = \begin{bmatrix} F_{11} & F_{12} \\ 0 & F_{22} \end{bmatrix},$$

where

$$F_{11} = -\mu, F_{22} = -(m + \mu + \delta + r), F_{12} = -\frac{\beta\Lambda}{\mu}.$$

Theorem 4 *The point E_0 of system* (2) *is locally asymptotically stable.*

Proof At E_0 the Jacobian matrix is given by

$$J_0(\frac{\Lambda}{\mu}, 0) = \begin{bmatrix} -\mu & -\frac{\beta\Lambda}{\mu} \\ 0 & -(m + \mu + \delta + r) \end{bmatrix}.$$

The eigenvalues of the system are $\lambda_1 = -\mu, \lambda_2 = -(m + \mu + \delta + r)$. It follows that $|\arg(\lambda_i)| = \pi > \frac{\alpha\pi}{2}$ $(i = 1, 2)$ where $0 < \alpha < 1$. Therefore E_0 is asymptotically stable locally by Lemma 5.

To discuss the global stability at E_0 of system (2), first we assume that $G((S(t), I(t)) = \frac{\beta S(t)I(t)}{1+\gamma I(t)}$, is always positive, monotonically increasing and continuously differentiable for all $S > 0$ and $I > 0$. That satisfies the following conditions [9, 57]:

$C1 : G((S(t), I(t)) > 0, G'_S((S(t), I(t)), G'_I((S(t), I(t))$ for $S > 0$ and $I > 0$.

$C2 : G((S(t), 0) = G((0, I(t)) = 0, G'_S((S(t), 0) = 0, G'_I((S(t), 0) > 0$ for $S > 0$ and $I > 0$.

$C3 : G'_I((S(t), 0)$ is increasing with respect to $S(t) > 0$.

$C4 : \frac{G'_S((S_0, 0)}{G'_I((S(t), 0)} < 1$ for $S(t) > S_0$; $\frac{G'_S((S_0, 0)}{G'_I((S(t), 0)} > 1$ for $S(t) \in (0, S_0)$.

Theorem 5 *Suppose that (C1) to (C4) are satisfied, the point E_0 of system* (2) *is globally asymptotically stable.*

Proof Let L be the Lyapunov function defined as:

$$L = (S - S_0 - \int_{S_0}^{S} \lim_{t \to 0^+} \frac{G(S_0, I)}{G(g, I)} dg) + I.$$

The aforementioned function's time derivative is

$$\begin{aligned} {}^{C}_{t_0}D^{\alpha}_t L \quad &= (1 - \frac{S}{S_0}){}^{C}_{t_0}D^{\alpha}_t S + {}^{C}_{t_0}D^{\alpha}_t I \\ &= -\frac{\mu(S - S_0)^2}{S} + \frac{\beta S_0 I}{1 + \gamma I} - \frac{mI}{1 + nI^2} - (\mu + \delta + r)I \\ &\quad -\frac{\mu(S - \frac{\Lambda}{\mu})^2}{S} + \frac{(\mu + \delta + r + m)(R_0 - 1)I}{1 + \gamma I} \\ &\quad -\frac{[-\gamma(\mu + \delta + r + m) + mnI - n\gamma(\delta + r + m)I^2]I^2}{(1 + \gamma I)(1 + nI^2)}. \end{aligned}$$

Since all parameters of the system are positive, then $^{C}_{t_0}D^{\alpha}_t L \leq 0$ if $R_0 \leq 1$ and $^{C}_{t_0}D^{\alpha}_t L = 0$ if $S = S_0 = \frac{\Lambda}{\mu}, I = I_0 = 0$. The point E_0 is asymptotically stable globally.

Stability analysis at E_1

At $E_1(S^*, I^*)$, we get

$$J(S^*, I^*) = \begin{bmatrix} E & F \\ G & H \end{bmatrix},$$

where

$$E = -\mu - \frac{\beta I^*}{1 + \gamma I^*},$$
$$F = -\frac{\beta S^*}{(1 + \gamma I^*)^2},$$
$$G = \frac{\beta I^*}{(1 + \gamma I^*)},$$
$$H = \frac{\beta S^*}{(1 + \gamma I^*)^2} - \frac{m(1 - nI^{*2})}{(1 + nI^{*2})^2} - (\mu + \delta + r).$$

Theorem 6 *The point $E_1(S^*, I^*)$ of system* (2) *is asymptotically stable locally.*

Proof The characteristic equation is $\lambda^2 + (E + H)\lambda + (EH - FG) = 0$. We have $-(E + H) < 0$ and the roots of the characteristic equation are

$$\lambda_{1,2} = \frac{-(E + H)}{2} \pm \frac{\sqrt{(E + H)^2 - 4(EH - FG)}}{2}.$$

If $EH > FG$ then $\left|\arg(\lambda_{1,2})\right| = \pi > \frac{\alpha\pi}{2}; 0 < \alpha < 1$, since $(E + H)^2 - 4(EH - FG) = (E - H)^2 + 4FG$. Using Lemma 5, the point E_1 is locally asymptotically stable in SI plane.

Theorem 7 *The point $E_1(S^*, I^*)$ of system* (2) *is globally asymptotically stable.*

Proof Let us consider the following hypothesis:

$$H(1) \quad : \quad \frac{mI^*}{1 + nI^{*2}} + \frac{(1 + I)\beta S^* I^*}{1 + I\gamma I^*} + \frac{m}{1 + nI^{*2}}$$
$$\leq [\frac{mI}{1 + nI^2} + \frac{\beta S^{*2}}{S + S\gamma I^*} + I^*(\frac{S\beta}{1 + \gamma} + \frac{m}{1 + nI^2 I^{*2}})].$$

Since (S^*, I^*) is the endemic equilibrium point of model (2), then

$$\Lambda - \mu S^* = \frac{\beta S^* I^*}{1 + \gamma I^*}, \frac{\beta S^* I^*}{1 + \gamma I^*} = \frac{mI^*}{1 + nI^{*2}} + (\mu + \delta + r)I^*. \tag{3}$$

Let us consider the Goh-Volterra form as

$$W(S, I) = \left(S - S^* - S^* \ln \frac{S}{S^*}\right) + \left(I - I^* - I^* \ln \frac{S}{S^*}\right). \tag{4}$$

Now, along the integral curves of (2):

$$
\begin{aligned}
{}^{C}_{t_0}D^{\alpha}_t W(S, I) \;&\leq\; \frac{S - S^*}{S}{}^{C}_{t_0}D^{\alpha}_t S(t) + \frac{I - I^*}{I}{}^{C}_{t_0}D^{\alpha}_t I(t) \quad \text{(using Lemma 6)} \\
&= \frac{mI^*}{1 + nI^{*2}} + \frac{(1 + I)\beta S^* I^*}{1 + I\gamma I^*} + \frac{m}{1 + nI^{*2}} \\
&\quad -[\frac{mI}{1 + nI^2} + \frac{\beta S^{*2}}{S + S\gamma I^*} + I^*(\frac{S\beta}{1 + \gamma} + \frac{m}{1 + nI^2 I^{*2}})] \quad \text{(using (4))}.
\end{aligned}
$$

Hence, by $H(1)$, we have

$$
{}^{C}_{t_0}D^{\alpha}_t W(S, I) \leq 0, \forall (S, I) \in \Omega, \tag{5}
$$

and ${}^{C}_{t_0}D^{\alpha}_t W(S, I) = 0$ if $(S, I) = (S^*, I^*)$. So, the point $E_1(S^*, I^*)$ is globally asymptotically stable.

5 SIR model with optimal control

One of the most important tools in the fight against infectious illnesses is the treatment rate. On the subject of optimal control theory in fractional derivatives, Ding et al. [58] and Agarwal et al. [59] have contributed. The fractional optimum control principle is fundamentally challenged by Pontryagin's maximum principle [60]. Our goal is to utilize the control measure v ($0 \leq v(t) \leq 1$) to account for the value of immunization and to choose the optimum control $v*$ to reduce the cost function $J(v)$ of the control strategy. The cost function:

$$
J(v^*) = \min\left(J(v(t))\right) \text{ with } J(v) = \left(\int_0^{t_f}[I + A_1 v^2]\,dt\right), \tag{6}
$$

subject to

$$
\begin{aligned}
{}^{C}_{t_0}D^{\alpha}_t S(t) &= \Lambda - \mu S(t) - \frac{\beta S(t)I(t)}{1 + \gamma I(t)}, S(0) > 0, \\
{}^{C}_{t_0}D^{\alpha}_t I(t) &= \frac{\beta S(t)I(t)}{1 + \gamma I(t)} - \frac{vI(t)}{1 + nI^2(t)} - (\mu + \delta + r)I(t), I(0) > 0, \\
{}^{C}_{t_0}D^{\alpha}_t R(t) &= \frac{vI(t)}{1 + nI^2(t)} + \delta I(t) - \mu R(t), R(t)|_{t=0} = R(0) > 0, \tag{7}
\end{aligned}
$$

where $0 \leq v(t) \leq 1$.

Theorem 8 *Let $v(t)$ be a measurable control function on $[0, t_f]$, with $v(t) \in [0, 1]$. Then there exists an optimal control v^* to minimize $J(v)$ of (6) with $v^*=\max\left[\min(\overline{v}, 1), 0\right], \overline{v} = \dfrac{(\epsilon_2 - \epsilon_3)I}{2A_1(1 + nI^2)}.$*

Proof The following method has been used to study the Hamiltonian:

$$
\begin{aligned}
H &= [I + A_1 v^2] + \epsilon_1(\Lambda - \mu S(t) - \frac{\beta S(t)I(t)}{1 + \gamma I(t)}) + \epsilon_2(\frac{\beta S(t)I(t)}{1 + \gamma I(t)} - \frac{vI(t)}{1 + nI^2(t)} - (\mu + \delta + rI(t)) \\
&\quad + \epsilon_3(\frac{vI(t)}{1 + nI^2(t)} + \delta I(t) - \mu R(t)),
\end{aligned}
$$

with adjoint variables $\epsilon_i(t), i = 1, 2, 3$ expressed as:

$$
{}^{RL}_{t_0}D_t^\alpha \epsilon_1(t)(t) = -\frac{\partial H}{\partial S} = -\epsilon_1(-\mu S(t) - \frac{\beta I}{1+\gamma I}) - \epsilon_2\frac{\beta I}{1+\gamma I},
$$

$$
{}^{RL}_{t_0}D_t^\alpha \epsilon_2(t)(t) = -\frac{\partial H}{\partial I} = -1 - \epsilon_1(-\frac{\beta S}{(1+\gamma I)^2}) - \epsilon_2(-\frac{\beta S}{(1+\gamma I)^2} - \frac{v(1-nI^2)}{(1+nI^2)^2}
$$

$$
-(\mu+\delta+r)) - \epsilon_3(\frac{v(1-nI^2)}{(1+nI^2)^2} + \delta),
$$

$$
{}^{RL}_{t_0}D_t^\alpha \epsilon_3(t)(t) = -\frac{\partial H}{\partial R} = \epsilon_3\mu.
$$

As a result, the issue of decreasing the Hamiltonian with regard to the control is now the problem of finding $v*$ that minimizes H in the context of (7). The Pontryagin principle is then used to produce the following ideal circumstance:

$$
\frac{\partial H}{\partial v} = 2A_1 v + (\epsilon_2 - \epsilon_3)(\frac{I}{1+nI^2}).
$$

It may be solved with adjoint variables and state variables to produce:

$$
\overline{v} = \frac{(\epsilon_2 - \epsilon_3)I}{2A_1(1+nI^2)}.
$$

Consider the control restrictions and the sign of the function $\frac{\partial H}{\partial v}$ for the best control v^*. As a result, we get

$$
v^* = \begin{cases} 0 & if \quad \frac{\partial H}{\partial v} < 0, \\ \overline{v} & if \quad \frac{\partial H}{\partial v} = 0, \\ 1 & if \quad \frac{\partial H}{\partial v} > 0. \end{cases}
$$

The ideal circumstance for the model system may be obtained by applying $v*$ to the equation above (7).

6 Numerical procedure

The model system (2), as stated in Theorem 1, has a single solution. Taylor's theorem will be used to find the model's numerical solution [60]. Then,

$$
{}^C_{t_0}D_t^\alpha S(t) = u_1(t, S, I), S(0) = S_0, t > 0. \tag{8}
$$

Consider the set of points $[0, A]$ as the points on which we are prepared to approximate the system's solution. Actually, we are unable to calculate $S(t)$, which will be the system's necessary solution. We divide $[0, A]$, into P subintervals $[t_j, t_{j+1}]$ of length, i.e., $w = \frac{A}{P}$, using the nodes $t_j = jw$, for $j = 0, 1, 2, ..., P$. We extend the Taylor's theorem at about $t = t_0$, we have a constant $k \in [0, A]$, so that

$$
S(t) = S(t_0) + {}^C_{t_0}D_t^\alpha S(t) \left\{\frac{w^\alpha}{\Gamma(\alpha+1)}\right\} + {}^C_{t_0}D_t^{2\alpha}[S(t)]_{t=k} \left\{\frac{w^{2\alpha}}{\Gamma(2\alpha+1)}\right\}.
$$

Now substitute ${}^C_{t_0}D_t^\alpha S(t) = u_1(t_0, S(t_0), I(t_0))$ and $t = t_0$ in the above equation which provides

$$
S(t_1) = S(t_0) + u_1(t_0, S(t_0), I(t_0)) \left\{\frac{w^\alpha}{\Gamma(\alpha+1)}\right\} + {}^C_{t_0}D_t^{2\alpha}[S(t)]_{t=k} \left\{\frac{w^{2\alpha}}{\Gamma(2\alpha+1)}\right\}.
$$

If m is small, we ignore the higher terms, then

$S(t_1) = S(t_0) + u_1(t_0, S(t_0), I(t_0)) \left\{ \dfrac{w^\alpha}{\Gamma(\alpha+1)} \right\}$. A general formula of expanding about $t_j = t_j + w$,

provides

$S(t_j+1) = S(t_j) + u_1(t_j, S(t_j), I(t_j)) \left\{ \dfrac{w^\alpha}{\Gamma(\alpha+1)} \right\}$.

Similarly, we have

$I(t_j+1) = I(t_j) + u_1(t_j, S(t_j), I(t_j)) \left\{ \dfrac{w^\alpha}{\Gamma(\alpha+1)} \right\}$.

7 Numerical discussion

In this part, we evaluate and verify the analytic results of our model system (1) using detailed numerical simulations. Although the majority of fractional order differential equations lack accurate analytic solutions, approximation, and numerical methods have been devised. Through the mathematical software MATLAB (2018a), we have employed Taylor's theorem in the numerical scheme. Following are several categories for the numerical output of model simulations and the accompanying findings:

Table 2. Parameter values for numerical study

Parameters	Values	Reference
Λ	5	Estimated
μ	0.05	Assumed
β	0.003	Assumed
γ	0.06	Assumed
m	0.03	Assumed
n	0.04	Assumed
δ	0.002	Assumed
r	0.02	Assumed

Case 1: Dynamical features of the whole population for different fractional orders The parameters' values in Table 2 are used to examine people's dynamic behaviour. All individuals' behaviour over time for different fractional orders α is shown in Figure 2 through Figure 4. The number of susceptible people rises as α moves from 0.90 to 0.98, as seen in Figure 2. The number of infected people rises over time as α rises, as seen in Figure 3. When α in Figure 4 goes from 0.90 to 0.98, there are more people who have been found.

Case 2: Stability analysis of the proposed model Figure 5 to Figure 7 depicts the global stability of system (1) at E_1 with different initial condition taking α=0.90, 0.94, 0.98, confirming our theoretical results in Theorem 6. **Case 3: Impact of α on S and I** Figure 8 and Figure 9 show the effects of α on susceptible and infected people. It can be shown from Figure 8 that the number of susceptible persons rises as α increases. Figure 9 shows that the number of infected people first declines but then rises over time.

Case 4: Mean density of S and I under γ values Plotting the mean densities of S and I with respect to γ for different fractional orders is shown in Figure 10 and Figure 11. As seen in Figure 10, the mean density of susceptible people rises as the value of α rises. Figure 11 shows that as the values of α fall, the mean density of infected people rises with regard to γ.

Case 5: Mean density of S and I under δ values Figure 12 and Figure 13 shows the plot of mean density of S and I with respect to δ for various fractional order. Figure 12 shows that the mean density of susceptible people rises as the value of α rises. Figure 13 shows that as the values of α decline, the mean density of infected people rises with regard to δ.
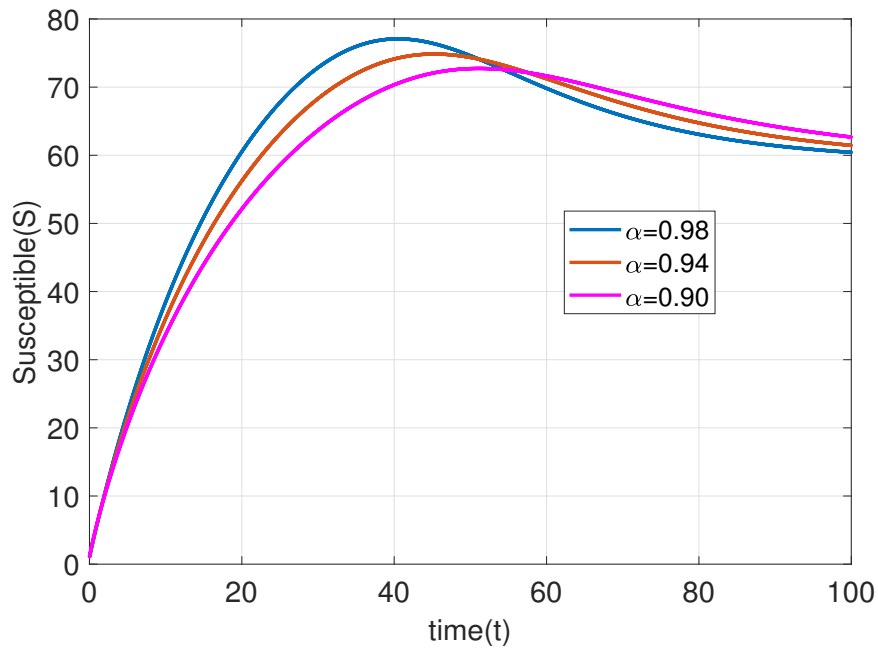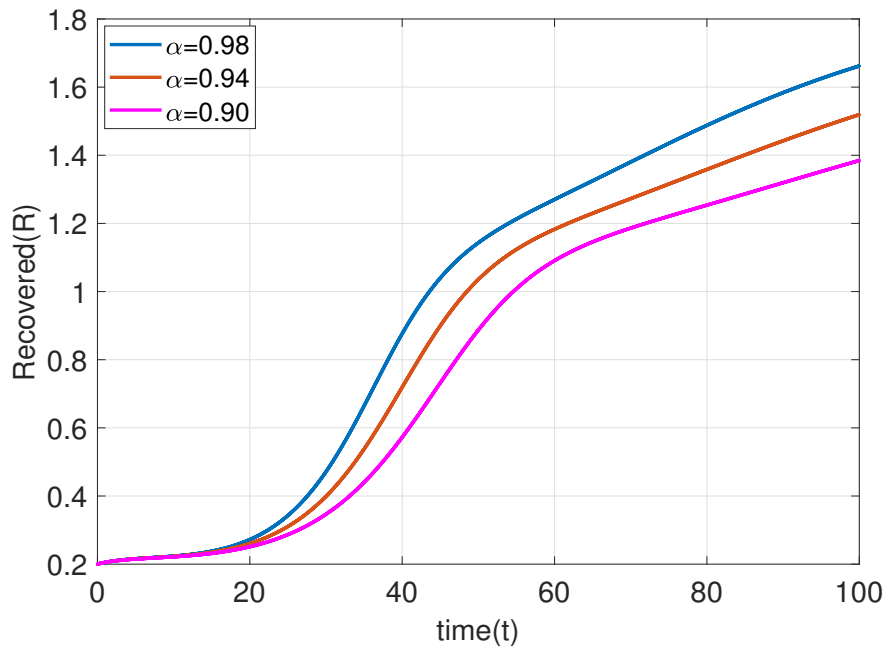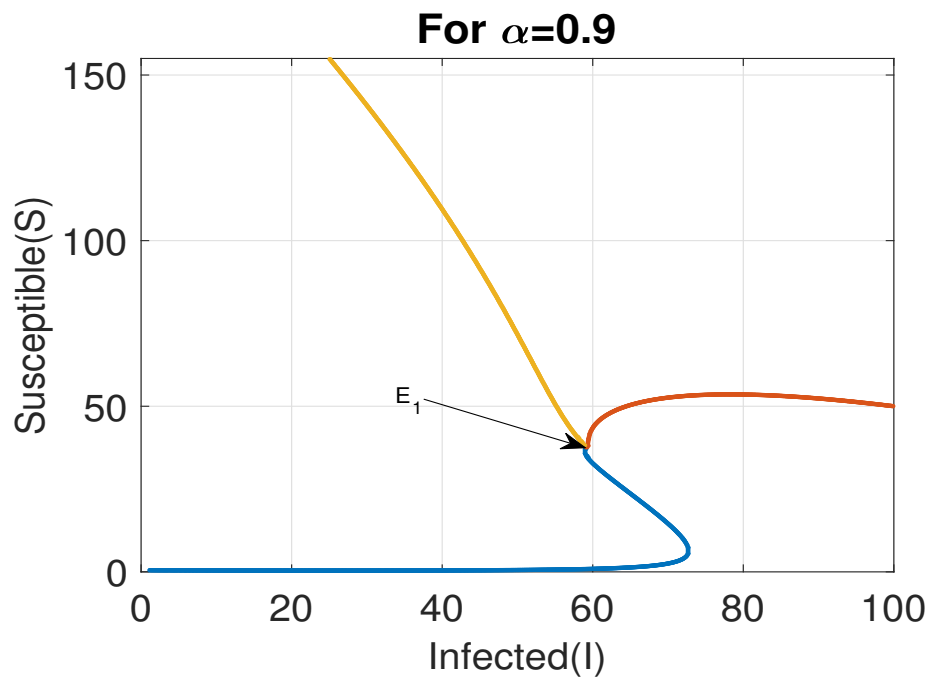
Figure 2. The behavior of Susceptible individuals for values of α = 0.90, 0.94, 0.98
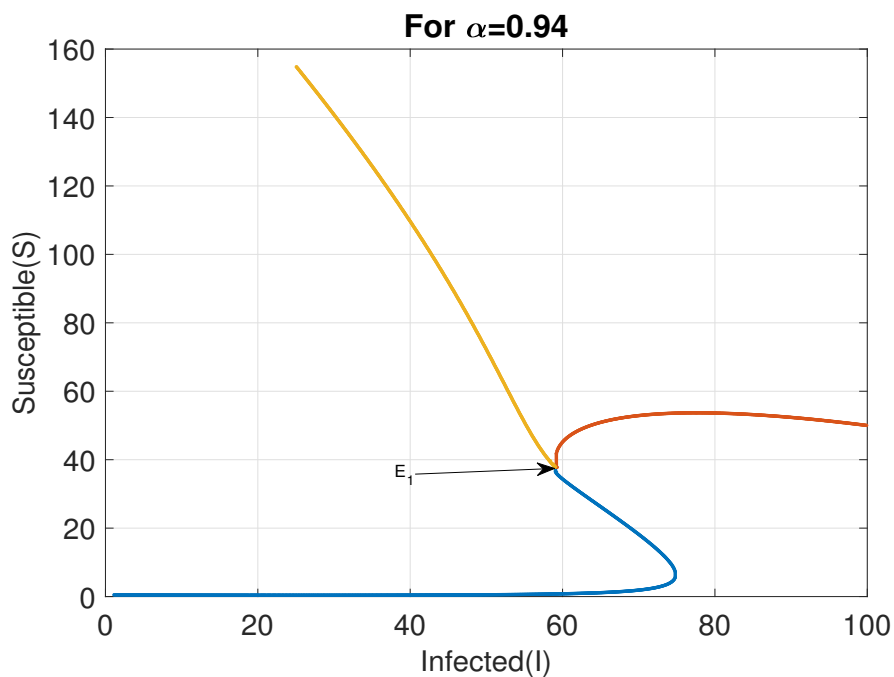

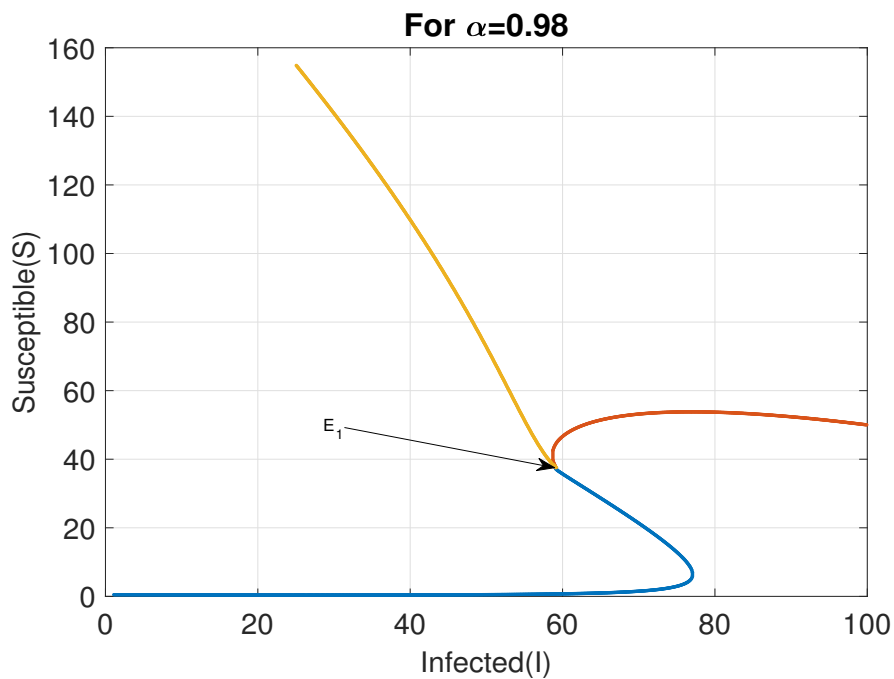**Figure 3.** The behavior of Infected individuals for values of α = 0.90, 0.94, 0.98

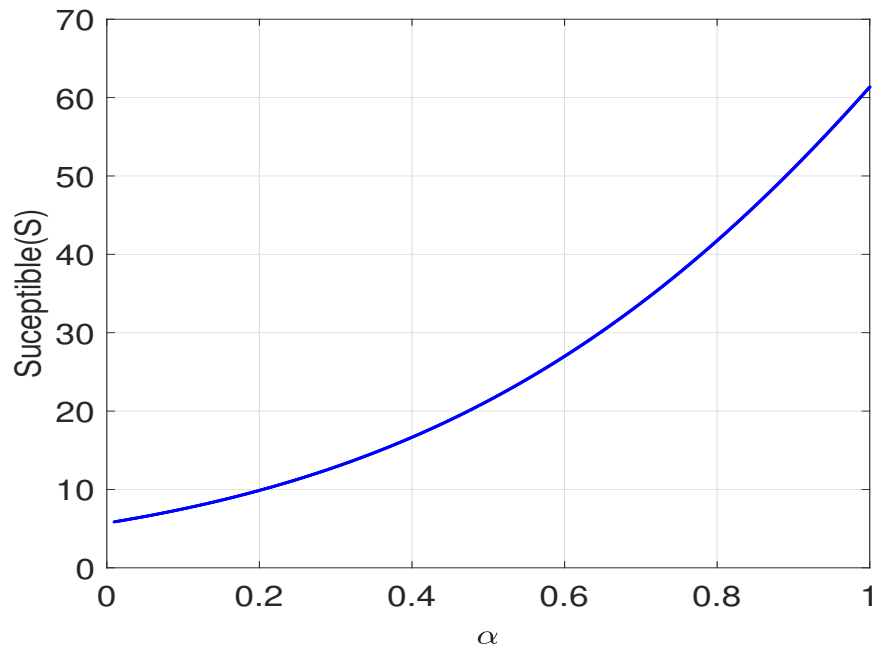**Figure 4.** The behavior of Recovered individuals for values of $\alpha = 0.90, 0.94, 0.98$

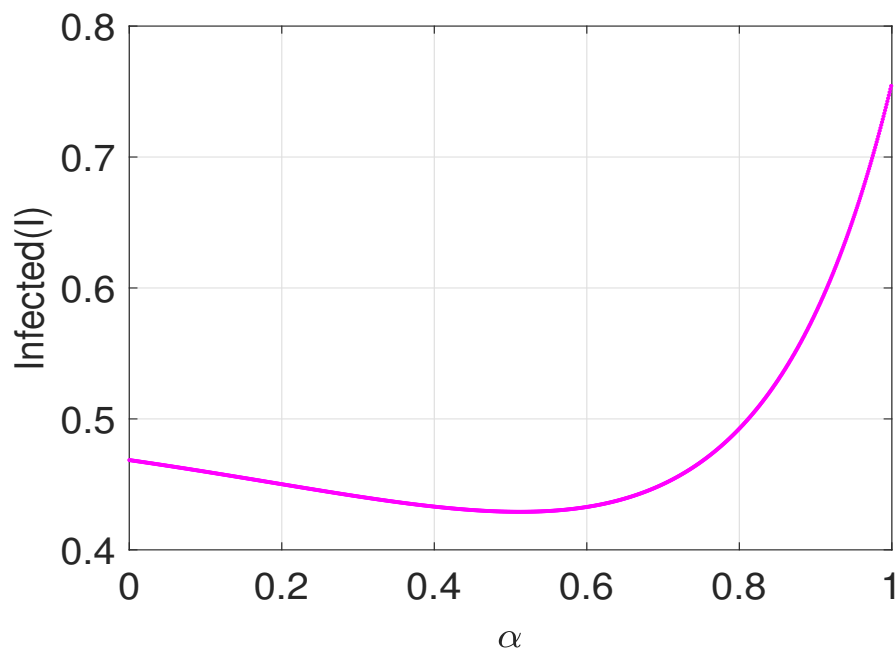**Figure 5.** Phase portrait diagram for values of $\alpha = 0.90$

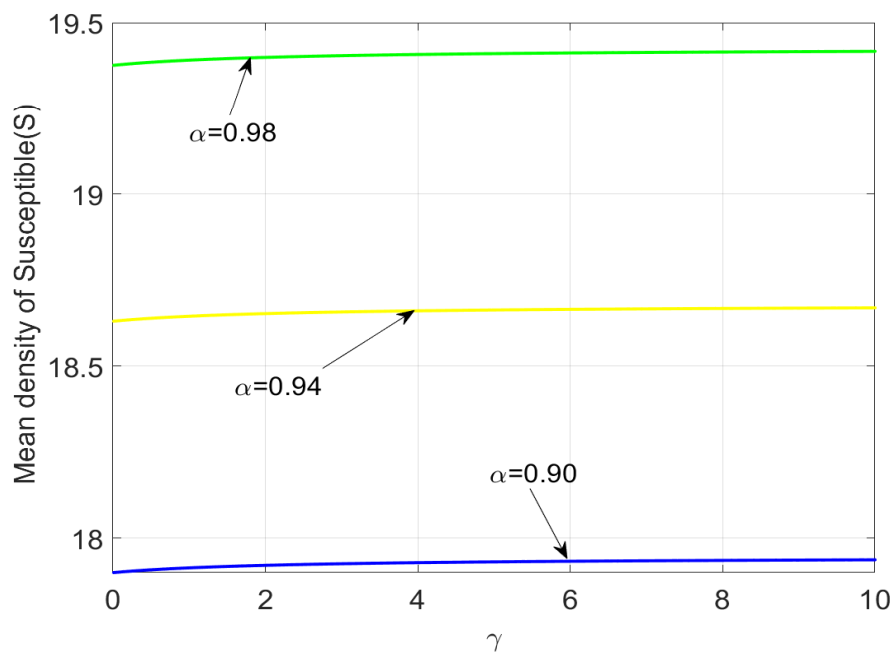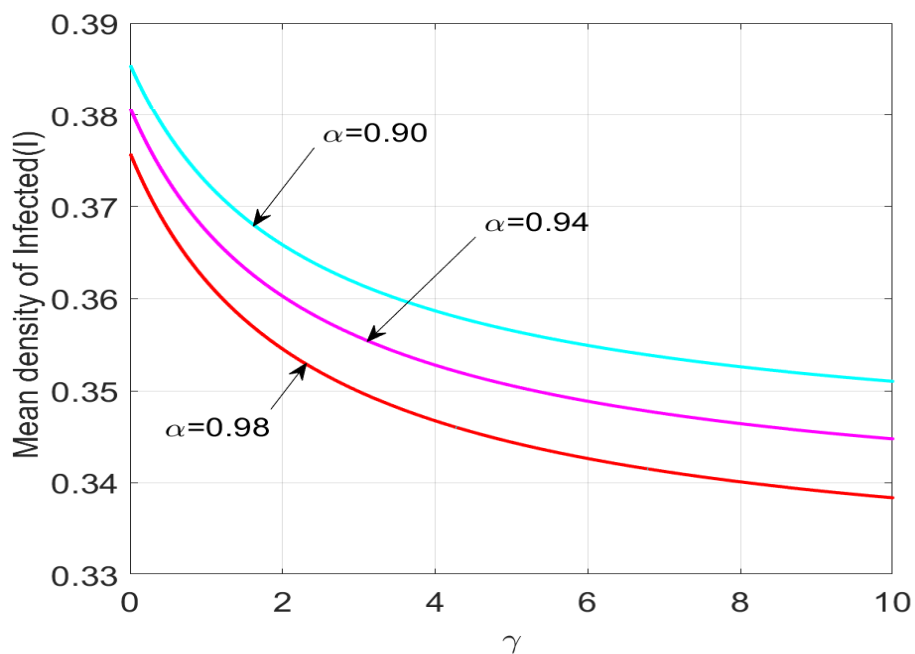**Figure 6.** Phase portrait diagram for values of $\alpha = 0.94$

Figure 7. Phase portrait diagram for values of $\alpha = 0.98$

Figure 8. Dynamics of S under α values

Figure 9. Dynamics of I under α values

Figure 10. Mean density of S under γ for $\alpha = 0.90, 0.94, 0.98$

Figure 11. Mean density of I under γ for $\alpha = 0.90, 0.94, 0.98$
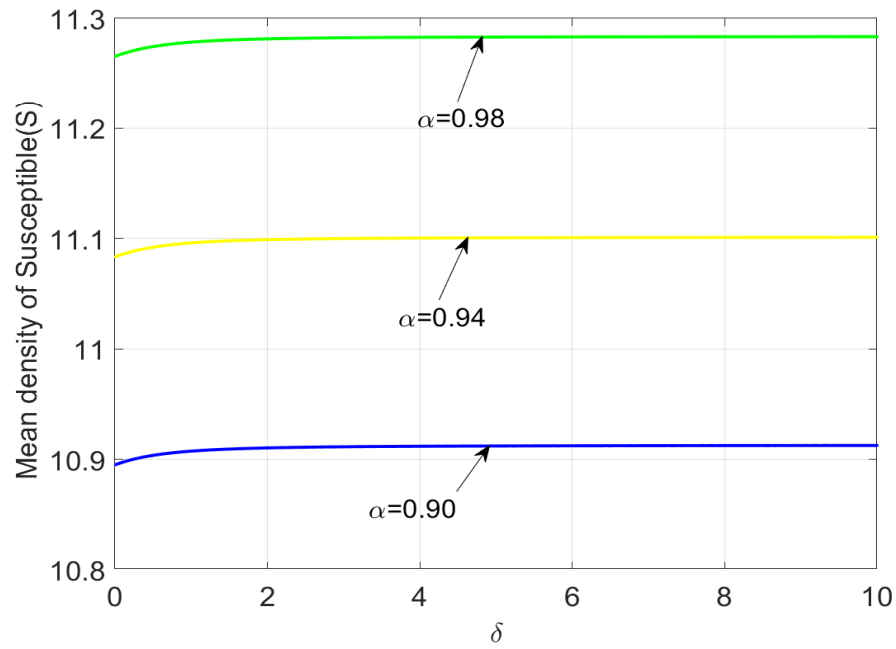
Figure 12. Mean density of S under δ for α=0.90, 0.94, 0.98
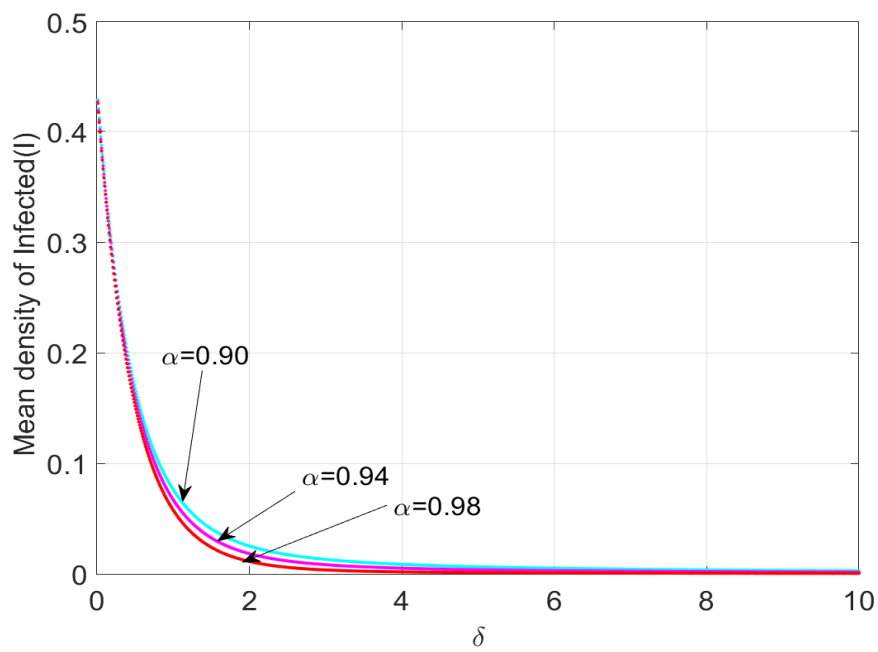
Figure 13. Mean density of I under δ for $\alpha = 0.90, 0.94, 0.98$

Case 6: Variation of γ **under** *S* **and** *I* **for** α = 0.98 Figure 14 and Figure 15 shows that the effect of γ on *S* and *I* with time for α=0.98. Figure 14 demonstrates a rise in the number of vulnerable people as the inhibitory rate γ drops and reaches its stable state, but the illness is not completely eradicated since it will continue to exist at a much lower level. We noticed that the infected population drops when the inhibitory rate γ rises in Figure 15. Thus, it is assumed that preventative actions conducted by vulnerable and sick individuals will aid in reducing the spread of illness.
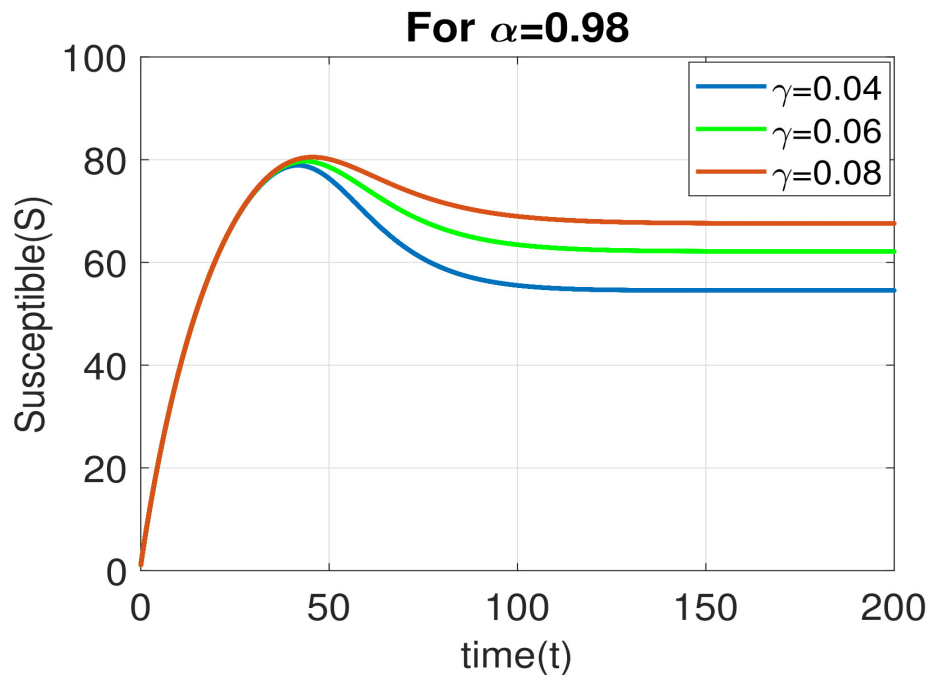
Figure 14. Variation of γ under *S* for α=0.98
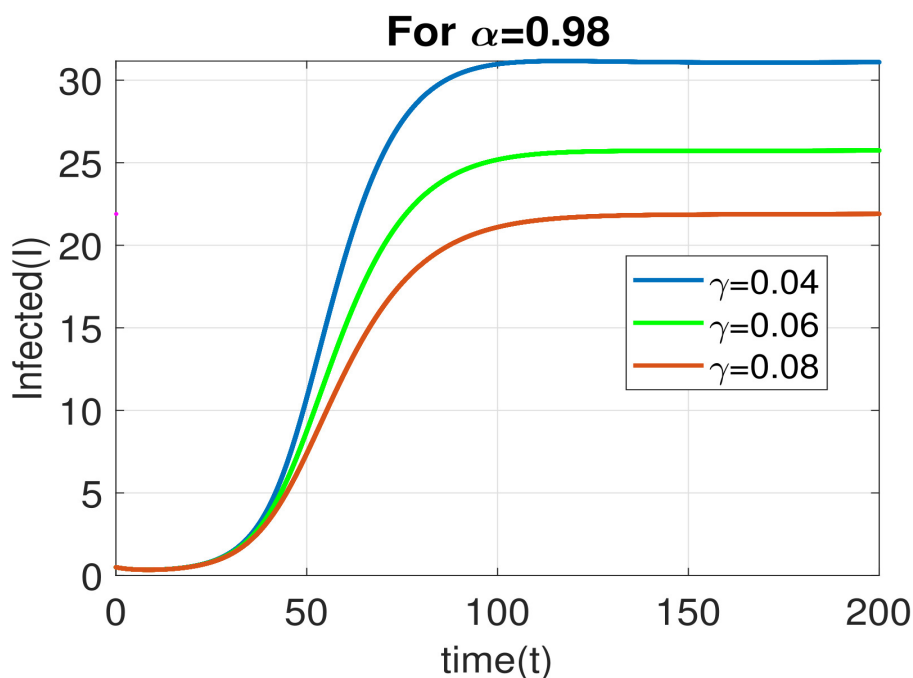
Figure 15. Variation of γ under *I* for α=0.98

Case 7: Variation of δ under S and I for α=0.98. Figure 16 and Figure 17 shows that the effect of δ on S and I with time for α=0.98. As the recovery rate δ declines and reaches its steady state, Figure 16 depicts a rise in the number of sensitive people. In Figure 17, we observed that the infected population decreases when the recovery rate δ changes from 0.001 to 0.003.
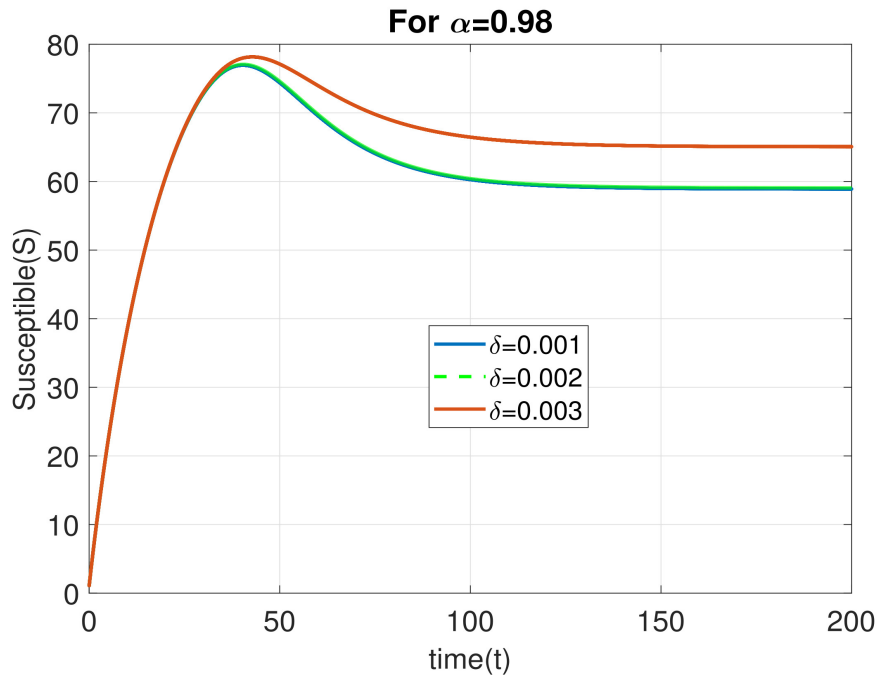
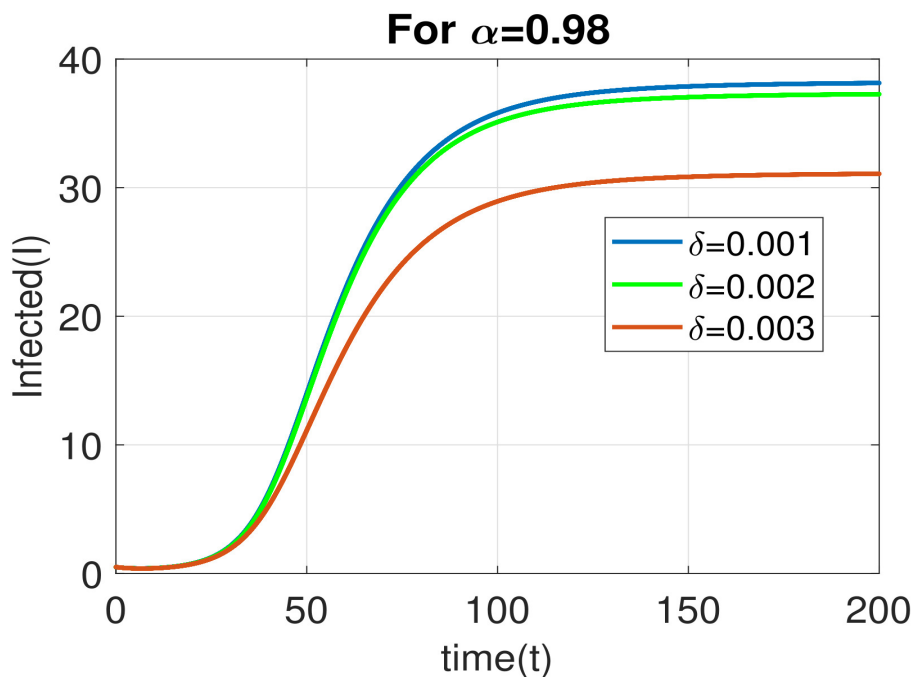

Figure 16. Variation of δ under S for α=0.98


**Figure 17.** Variation of δ under I for α=0.98

Case 8: Optimal control Figure 18 and Figure 19 depict the time series of people who are vulnerable to infection, those who have been infected, and those who have recovered over a time period of $[0, 100]$, with optimum control using fractional order $\alpha=0.9$. Infectious illness prevention depends heavily on treatment rates, and several theories have been put out in which vaccination rates are seen as very advantageous. The reproduction number R_0 falls as a consequence of the inclusion of the treatment rate parameter. We chose a final time of $t_f=100$ for the simulation of the optimum control problem governed by model (1), which corresponds to Table 2. The time series of the ideal cost J^* and the ideal control variable v^* are shown in Figure 20 and Figure 21.
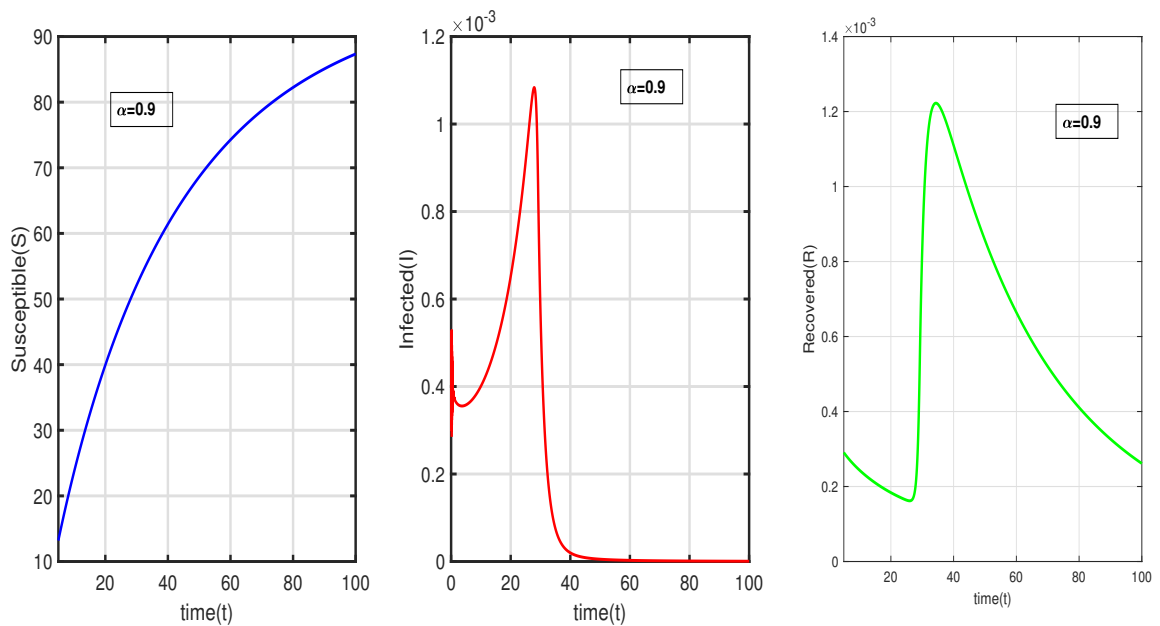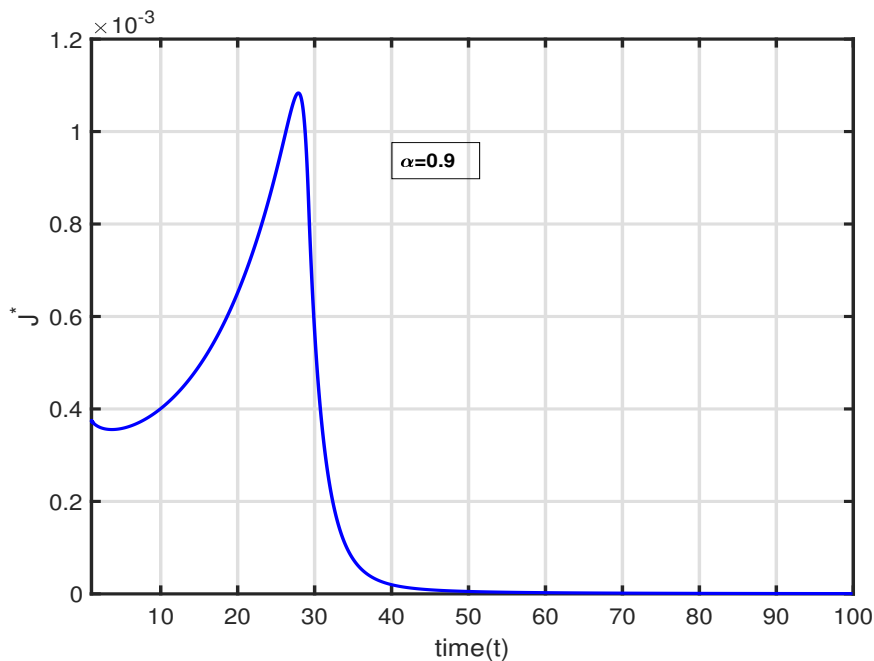

Figure 18. When $\alpha=0.9$, the time series of the model system (1) corresponds to Table 2
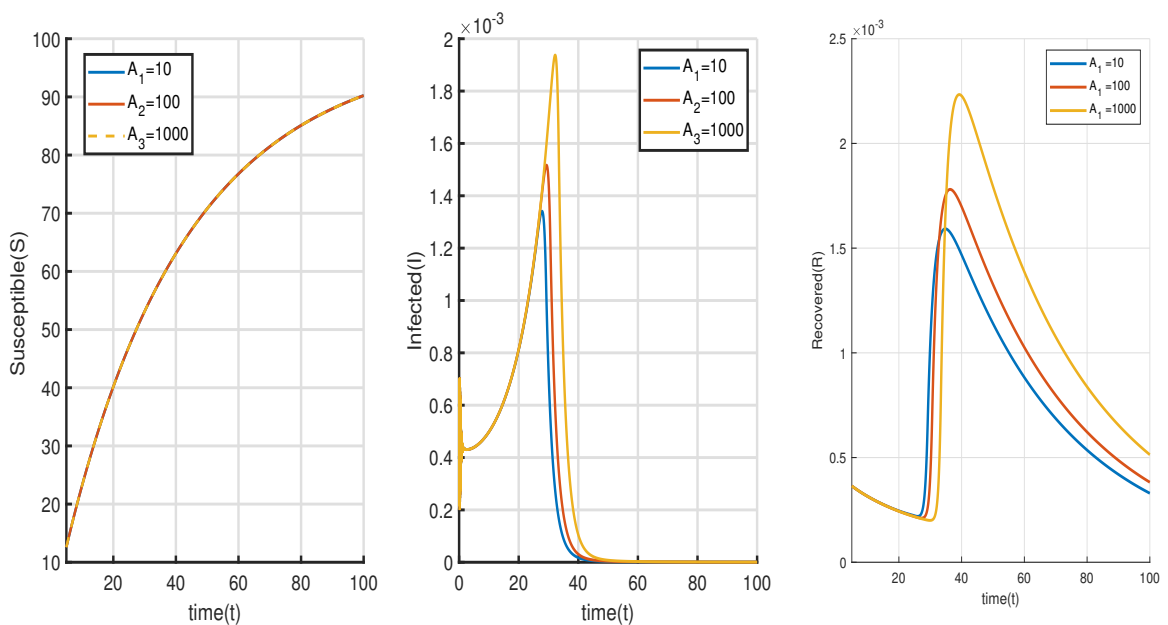
Figure 19. When $\alpha=0.9$, the time series of the model system (1) corresponds to Table 2
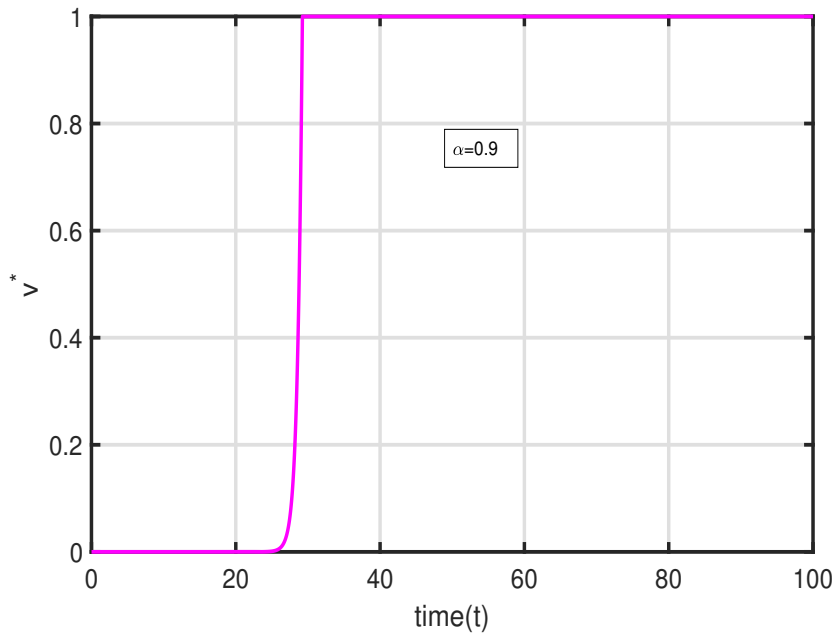
Figure 20. With parameter values matching to Table 2 for $\alpha=0.9$, a time series of the ideal control variable v^* is produced

Figure 21. With parameter values matching to Table 2 for $\alpha=0.9$, a time series of the ideal cost J^* is produced

8   Conclusion

The mathematical model used in this article aims to depict the dynamics of infectious disease when the ratio of infected to susceptible populations is high, taking into account the effects of inhibitory activity, behavioral changes that occur during epidemics, and the limitations of treatment facilities. Analyzing the stability characteristics of equilibrium points corresponding to no infection and

sustained infection states, it is shown that the disease-free equilibrium is locally asymptotically stable when $R_0 < 1$ and unstable when $R_0 > 1$.

The R-H criteria has been used to examine the stability of the model's endemic equilibrium. The simulation results predict that the infection will worsen as the rate of transmission rises, but that it will stabilize due to the accessibility of treatment centres. Furthermore, the prevalence of the infection decreases proportionally when the amount of suppression used by the affected people increases. The results of our simulation also showed that, in order to successfully eradicate the virus, the treatment of the population must be closely coordinated with the resources at hand. Understanding the complexities of disease outbreaks is made possible by the use of epidemic modelling. Numerical simulations provide the visualization of the efficacy of theoretical solutions. Comprehensive information, suitable infectious disease treatment methods, and the availability of healthcare services are required for the successful decrease of infection within society. In addition, we showed the global stability of the equilibrium state by choosing an appropriate Lyapunov function.

The importance of fractional order to population dynamics has also been noted. The optimum solution to the optimal control issue must meet certain requirements, which we have established using Pontryagin's Maximum Principle. It is obvious that the disease's spread can be stopped and eliminated if the control measure v^* is used. Additionally, Theorem 8 has identified the ideal control value v^* to reduce the cost of vaccination, as shown by $J(v) = \left(\int_0^{t_f} [I + A_1 v^2] \, dt \right)$. For optimum control, we presume a final time $t_f = 100$. As a consequence, changing the derivatives' order may change the stability requirements for equilibrium locations without changing any other parametric variables. We are unable to analyze our findings using an integer order method since we have achieved so little theoretical advancement in this fractional order framework. We find a variety of biological modelling outcomes based on fractional differential equations in this work. The proposed model may be analyzed further to explore chaotic solutions and various forms of bifurcations by incorporating time delay parameters. More than one control parameter may be used to better understand the treatment strategies and management of the spread of the disease.

Declarations

Use of AI tools

The authors declare that they have not used Artificial Intelligence (AI) tools in the creation of this article.

Data availability statement

All data generated or analyzed during this study are included in this article.

Ethical approval

The authors state that this research complies with ethical standards. This research does not involve either human participants or animals.

Consent for publication

Not applicable

Conflicts of interest

The authors declare that they have no conflict of interest.

References

[1] Kermack, W.O. and McKendrick, A.G. A contribution to the mathematical theory of epidemics. *Proceedings of the Royal Society of London. Series A,* 115(772), 700–721, (1927). [CrossRef]

[2] Kermack, W.O. and McKendrick, A.G. Contributions to the mathematical theory of epidemics-II: the problem of endemicity. *Proceedings of the Royal Society of London. Series A,* 138(834), 55–83, (1932). [CrossRef]

[3] Mukherjee, D. Stability analysis of an SI epidemic model with time delay. *Mathematical and Computer Modelling,* 24(9), 63–68, (1996). [CrossRef]

[4] Hethcote, H.W. and van den Driessche, P. An SIS epidemic model with variable population size and a delay. *Journal of Mathematical Biology,* 34, 177–194, (1995). [CrossRef]

[5] D'Onofrio, A., Manfredi, P. and Salinelli, E. Vaccinating behaviour, information, and the dynamics of SIR vaccine preventable diseases. *Theoretical Population Biology,* 71(3), 301–317, (2007). [CrossRef]

[6] Buonomo, B., d'Onofrio, A. and Lacitignola, D. Global stability of an SIR epidemic model with information dependent vaccination. *Mathematical Biosciences,* 216(1), 9–16, (2008). [CrossRef]

[7] Hattaf, K., Lashari, A., Louartassi, Y. and Yousfi, N. A delayed SIR epidemic model with a general incidence rate. *Electronic Journal of Qualitative Theory of Differential Equations,* 2023(3), 1–9, (2013). [CrossRef]

[8] Goel, K. and Nilam. Stability behavior of a nonlinear mathematical epidemic transmission model with time delay. *Nonlinear Dynamics,* 98, 1501–1518, (2019). [CrossRef]

[9] Kumar, A., Goel, K. and Nilam. A deterministic time-delayed SIR epidemic model: mathematical modeling and analysis. *Theory in Biosciences,* 139, 67–76, (2020). [CrossRef]

[10] Kumar, A. and Nilam. Dynamic behavior of an SIR epidemic model along with time delay; Crowley–Martin type incidence rate and holling type II treatment rate. *International Journal of Nonlinear Sciences and Numerical Simulation,* 20(7–8), 757–771, (2019). [CrossRef]

[11] Paul, S., Mahata, A., Mukherjee, S., Roy, B., Salimi, M. and Ahmadian, A. Study of fractional order SEIR epidemic model and effect of vaccination on the spread of COVID-19. *International*

Journal of Applied and Computational Mathematics, 8, 237, (2022). [CrossRef]

[12] Dubey, B., Patra, A., Srivastava, P.K. and Dubey, U.S. Modeling and analysis of an SEIR model with different types of nonlinear treatment rates. *Journal of Biological Systems,* 21(03), 1350023, (2013). [CrossRef]

[13] Paul, S., Mahata, A., Ghosh, U. and Roy, B. SEIR epidemic model and scenario analysis of COVID-19 pandemic. *Ecological Genetics and Genomics,* 19, 100087, (2021). [CrossRef]

[14] Tipsri, S. and Chinviriyasit, W. Stability analysis of SEIR model with saturated incidence and time delay. *International Journal of Applied Physics and Mathematics,* 4(1), 42–45, (2014). [CrossRef]

[15] Paul, S., Mahata, A., Mukherjee, S. and Roy, B. Dynamics of SIQR epidemic model with fractional order derivative. *Partial Differential Equations in Applied Mathematics,* 5, 100216, (2022). [CrossRef]

[16] Mahata, A., Paul, S., Mukherjee, S., Das, M. and Roy, B. Dynamics of Caputo fractional order SEIRV epidemic model with optimal control and stability analysis. *International Journal of Applied and Computational Mathematics,* 8, 28, (2022). [CrossRef]

[17] Mahata, A., Paul, S., Mukherjee, S. and Roy, B. Stability analysis and Hopf bifurcation in fractional order SEIRV epidemic model with a time delay in infected individuals. *Partial Differential Equations in Applied Mathematics,* 5, 100282, (2022). [CrossRef]

[18] Henderson, D.A. *Smallpox-The Death of a Disease.* Prometheus Books: Amherst, New York, USA, (2009).

[19] Samui, P., Mondal, J., Ahmad, B. and Chatterjee, A.N. Clinical effects of 2-DG drug restraining SARS-CoV-2 infection: a fractional order optimal control study. *Journal of Biological Physics,* 48, 415-438, (2022). [CrossRef]

[20] Shekhawat, U. and Roy Chowdhury (Chakravarty), A. Computational and comparative investigation of hydrophobic profile of spike protein of SARS-CoV-2 and SARS-CoV. *Journal of Biological Physics,* 48, 399-414, (2022). [CrossRef]

[21] Allegretti, S., Bulai, I.M., Marino, R., Menandro, M.A. and Parisi, K. Vaccination effect conjoint to fraction of avoided contacts for a Sars-Cov-2 mathematical model. *Mathematical Modelling and Numerical Simulation with Applications,* 1(2), 56-66, (2021). [CrossRef]

[22] Nindjin, A.F. and Aziz-Alaoui, M.A. Persistence and global stability in a delayed Leslie-Gower type three species food chain. *Journal of Mathematical Analysis and Applications,* 340(1), 340–357, (2008). [CrossRef]

[23] Iwa, L.L., Nwajeri, U.K., Atede, A.O., Panle, A.B. and Egeonu, K.U. Malaria and cholera co-dynamic model analysis furnished with fractional-order differential equations. *Mathematical Modelling and Numerical Simulation with Applications,* 3(1), 33-57, (2023). [CrossRef]

[24] Barman, D., Roy, J. and Alam, S. Trade-off between fear level induced by predator and infection rate among prey species. *Journal of Applied Mathematics and Computing,* 64, 635–663, (2020). [CrossRef]

[25] Das, P., Nadim, S.S., Das, S. and Das, P. Dynamics of COVID-19 transmission with comorbidity: a data driven modelling based approach. *Nonlinear Dynamics,* 106, 1197–1211, (2021). [CrossRef]

[26] Das, S., Das, P. and Das, P. Optimal control of behaviour and treatment in a nonautonomous SIR model. *International Journal of Dynamical Systems and Differential Equations,* 11(2), 108-130, (2021). [CrossRef]

[27] Das, P., Upadhyay, R.K., Misra, A.K., Rihan, F.A., Das, P. and Ghosh, D. Mathematical model of COVID-19 with comorbidity and controlling using non-pharmaceutical interventions and vaccination. *Nonlinear Dynamics,* 106, 1213-1227, (2021). [CrossRef]

[28] Capasso, V. and Serio, G. A generalization of the Kermack-Mckendrick deterministic epidemic model. *Mathematical Biosciences,* 42(1–2), 43–61, (1978). [CrossRef]

[29] D'Onofrioa, A. and Manfredi, P. Information-related changes in contact patterns may trigger oscillations in the endemic prevalence of infectious diseases. *Journal of Theoretical Biology,* 256(3), 473–478, (2009). [CrossRef]

[30] Wei, C. and Chen, L. A delayed epidemic model with pulse vaccination. *Discrete Dynamics in Nature and Society,* 2008, 746951, (2008). [CrossRef]

[31] Capasso, V., Grosso, E. and Serio, G. Mathematical models in epidemiological studies. I. Application to the epidemic of cholera verified in Bari in 1973. *Annali Sclavo; Rivista di Microbiologia e di Immunologia,* 19(2), 193–208, (1977).

[32] Capasso, V. Global solution for a diffusive nonlinear deterministic epidemic model. *SIAM Journal on Applied Mathematics,* 35(2), 274–284, (1978). [CrossRef]

[33] Zhang, J.Z., Jin, Z., Liu, Q.X. and Zhang, Z.Y. Analysis of a delayed SIR model with nonlinear incidence rate. *Discrete Dynamics in Nature and Society,* 2008, 636153, (2008). [CrossRef]

[34] Anderson, R.M. and May, R.M. Regulation and stability of host-parasite population interactions: I. Regulatory processes. In *Foundations of Ecology II,* (pp. 219–267). USA: University of Chicago Press, (1978). [CrossRef]

[35] Li, X.Z., Li, W.S. and Ghosh, M. Stability and bifurcation of an SIR epidemic model with nonlinear incidence and treatment. *Applied Mathematics and Computation,* 210(1), 141-150, (2009). [CrossRef]

[36] Hammouch, Z., Yavuz, M. and Özdemir, N. Numerical solutions and synchronization of a variable-order fractional chaotic system. *Mathematical Modelling and Numerical Simulation with Applications,* 1(1), 11-23, (2021). [CrossRef]

[37] Daşbaşı, B. Stability analysis of an incommensurate fractional-order SIR model. *Mathematical Modelling and Numerical Simulation with Applications,* 1(1), 44-55, (2021). [CrossRef]

[38] Gholami, M., Ghaziani, R.K. and Eskandari, Z. Three-dimensional fractional system with the stability condition and chaos control. *Mathematical Modelling and Numerical Simulation with Applications,* 2(1), 41-47, (2022). [CrossRef]

[39] Wang, W. and Ruan, S. Bifurcations in an epidemic model with constant removal rate of the infectives. *Journal of Mathematical Analysis and Applications,* 291(2), 775-793, (2004). [CrossRef]

[40] Zhang, X. and Liu, X. Backward bifurcation of an epidemic model with saturated treatment function. *Journal of Mathematical Analysis and Applications,* 348(1), 433-443, (2008). [CrossRef]

[41] Zhonghua, Z. and Yaohong, S. Qualitative analysis of a SIR epidemic model with saturated treatment rate. *Journal of Applied Mathematics and Computing,* 34, 177–194, (2010). [CrossRef]

[42] Zhou, L. and Fan, M. Dynamics of an SIR epidemic model with limited medical resources revisited. *Nonlinear Analysis: Real World Applications,* 13(1), 312-324, (2012). [CrossRef]

[43] Dubey, B., Patra, A., Srivastava, P.K. and Dubey, U.S. Modeling and analysis of an SEIR model with different types of nonlinear treatment rates. *Journal of Biological Systems,* 21(03), 1350023, (2013). [CrossRef]

[44] Kumar, A. and Nilam. Dynamical model of epidemic along with time delay; Holling type II

incidence rate and Monod-Haldane type treatment rate. *Differential Equations and Dynamical Systems,* 27, 299–312, (2019). [CrossRef]

[45] Diethelm, K. and Ford, N.J. Analysis of fractional differential equations. *Journal of Mathematical Analysis and Applications,* 265(2), 229-248, (2002). [CrossRef]

[46] Rahaman, M., Mondal, S.P., Alam, S., Metwally, A.S.M., Salahshour, S., Salimi, M. et al. Manifestation of interval uncertainties for fractional differential equations under conformable derivative. *Chaos Solitons & Fractals,* 165, 112751, (2022). [CrossRef]

[47] Barman, D., Roy, J., Alrabaiah, H., Panja, P., Mondal, S.P. and Alam, S. Impact of predator incited fear and prey refuge in a fractional order prey predator model. *Chaos Solitons & Fractals,* 142, 110420, (2021). [CrossRef]

[48] Nguyen, T.T.H., Nguyen, N.T. and Tran, M.N. Global fractional Halanay inequalities approach to finite-time stability of nonlinear fractional order delay systems. *Journal of Mathematical Analysis and Applications,* 525(1), 127145, (2023). [CrossRef]

[49] Petras, I. *Fractional-Order Nonlinear Systems: Modeling, Analysis and Simulation*. Higher Education Press: Beijing, China, (2011).

[50] Odibat, Z.M. and Shawagfeh, N.T. Generalized Taylor's formula. *Applied Mathematics and Computation,* 186(1), 286-293, (2007). [CrossRef]

[51] Podlubny, I. *Fractional Differential Equations.* Academic Press: San Diego, (1999).

[52] Liang, S., Wu, R. and Chen, L. Laplace transform of fractional order differential equations. *Electronic Journal of Differential Equations,* 2015(139), 1-15, (2015).

[53] Mainardi, F. On some properties of the Mittag-Leffler function $E_\alpha(-t^\alpha)$, completely monotone for $t > 0$ with $0 < \alpha < 1$. *Discrete and Continuous Dynamical Systems Series B,* 19(7), 2267-2278, (2014). [CrossRef]

[54] Li, Y., Chen, Y. and Podlubny, I. Stability of fractional-order nonlinear dynamic systems: Lyapunov direct method and generalized Mittag-Leffler stability. *Computers & Mathematics with Applications,* 59(5), 1810-1821, (2010). [CrossRef]

[55] Javidi, M. and Nyamoradi, N. A fractional-order toxin producing phytoplankton and zooplankton system. *International Journal of Biomathematics,* 7(04), 1450039, (2014). [CrossRef]

[56] Diekmann, O., Heesterbeek, J.A.P. and Roberts, M.G. The construction of next-generation matrices for compartmental epidemic models. *Journal of the Royal Society Interface,* 7(47), 873-885, (2009). [CrossRef]

[57] Kumar, A. and Nilam. Effects of nonmonotonic functional responses on a disease transmission model: modeling and simulation. *Communications in Mathematics and Statistics,* 10, 195–214, (2022). [CrossRef]

[58] Ding, Y., Wang, Z. and Ye, H. Optimal control of a fractional-order HIV-immune system with memory. *IEEE Transactions on Control Systems Technology,* 20(3), 763-769, (2011). [CrossRef]

[59] Agarwal, O.P. A general formulation and solution scheme for fractional optimal control problems. *Nonlinear Dynamics,* 38, 323-337, (2004). [CrossRef]

[60] Kamocki, R. Pontryagin maximum principle for fractional ordinary optimal control problems. *Mathematical Methods in the Applied Sciences,* 37(11), 1668-1686, (2014). [CrossRef]

(https://bulletinbiomath.org)

RESEARCH PAPER

Fractional-order brucellosis transmission model between interspecies with a saturated incidence rate

Dilara Yapışkan [ID] 1,2,‡ and **Beyza Billur İskender Eroğlu** [ID] 1,*,‡

¹Department of Mathematics, Balıkesir University, 10145 Balıkesir, Türkiye, ²Center for Research and Development in Mathematics and Applications (CIDMA), Department of Mathematics, University of Aveiro, 3810-193 Aveiro, Portugal

* Corresponding Author
‡ dilarayapiskan@ua.pt (Dilara Yapışkan); biskender@balikesir.edu.tr (Beyza Billur İskender Eroğlu)

Abstract

In this study, brucellosis dynamics between interspecies are discussed with the Atangana-Baleanu fractional derivative to examine the transmission of brucellosis by its behavior. The recovered compartment, recruitment, and natural death rate for humans are considered for the fractional order model to analyze the transmission dynamics in more detail from an epidemiological point of view. Additionally, the saturated incidence rate is suggested for brucellosis as indirectly transmitted to individuals from the environment. By fixed point theory, it is verified that developed fractional transmission dynamics have a unique solution. The model under consideration employs the Adams-type predictor-corrector method for numerical solution. All comparative results are plotted by MATLAB.

Keywords: Atangana-Baleanu derivative; brucellosis; existence and uniqueness; fixed point theory; mathematical modeling

AMS 2020 Classification: 34A08; 00A71; 47H10; 34A34

1 Introduction

Brucellosis is a zoonotic illness that can be transferred to individuals by direct contact with infected animals or indirectly from Brucella in a contaminated environment [1]. Humans are transmitted by it in various manners. Firstly, humans can contract brucellosis by consuming rare cooked meat or unpasteurized dairy products. Second, researchers studying bacteria in a laboratory environment can become infected by breathing in Brucella. Finally, it can be transmitted to veterinarians or staff working who come into intimate touch with the skin deformation or droppings of infected animals. Furthermore, it is known that human-to-human transmission is extremely uncommon [2]. Even though the mortality from the disease is negligible in humans, brucellosis causes serious organ damage and can continue for several years. Apart from that, the case is not thought to be so

severe in animals. However, the infection can lead to significant financial damage by decreasing infant survival, milk production, reproduction, and prolificacy [3, 4]. To contain these negative results from happening, it is necessary to prevent brucellosis transmission in animals. Vaccination is often the first preferred way for transmissible diseases, and animals can be vaccinated against brucellosis. Still, it is plenty challenging to eradicate the infection by only vaccination [5]. Detection and elimination of infected animals are other significant measures. It is necessary to understand the dynamics of brucellosis in order to apply additional preventive measures.

Epidemiological models can analyze the course of the diseases since they are constructed by considering the characteristics of the infection and the nature of each one [6–8]. On the contrary, fractional derivatives have allowed many real-world problems to be solved, as they can fulfill complex manners due to their definition [9–12]. Therefore, epidemiological models are analyzed according to the transmission dynamics behavior when combined with fractional derivatives [13–20]. In this context, various mathematical models are discussed by researchers for predicting the dynamics of brucellosis, both integer and fractional. Li et al. examined the impact of preventative strategies and different incidence rates on the transmission of Brucella in China via integer-order models [21, 22].

Lolika et al. and Nyerere et al. proposed integer-order dynamical models for the spreading of brucellosis, incorporating the impacts of seasonality [23, 24]. In addition, Nyerere et al. investigated the efficacy of treatment for humans by presenting another integer-order model for brucellosis spread among humans and animals [25]. Sun et al. offered a systematic examination of the transmission dynamics of several brucellosis integer-order mathematical models with their application in China [26]. Lolika and Helikumi proposed and studied two integer-order mathematical models for human brucellosis transmission, in which humans become infected through contact with wildlife and cattle [27]. Another important research topic that has attracted attention recently is the interspecies transmission of brucellosis. Ma et al. posed a discrete model for sheep-human brucellosis transmission dynamics in Jilin, China, and investigated the effectiveness of control measures [28]. Abagna et al. developed a deterministic model to investigate the transmission dynamics and control of bovine brucellosis in a cattle herd [29]. Thongtha and Modnak formulated an interactive bison–human environment mathematical model that contains the impact of human transmission, chronic brucellosis, and control strategy on the brucellosis dynamics [30]. More than that, Peter constructed the fractional model based on hypothetical data, only considering the transmission of brucellosis among cows [31]. Loika and Helikumi describe a fractional model that reveals the transmission of brucellosis among sheep only, utilizing real data from Egypt [32].

As mentioned above, few studies in the literature discuss the fractional-order brucellosis model. Unfortunately, these models do not deal with the transmission of brucellosis among different species of populations. However, since brucellosis increases by showing an exponential behavior depending on the transmission rate of the infection [33], it would be more realistic to study it with a derivative operator that had this behavior. Thanks to the crossover property of the Atangana-Baleanu derivative in terms of Caputo (ABC), it not only allows the explanation of more complex nonlinear phenomena but also does not cause singularity problems at the beginning and end of biological processes. This provides a better insight into the models at their critical points. Due to all these advantages, the ABC derivative has been quite successful in modeling infectious diseases under reality in recent years [34–36].

Incidence rates are another significant element in epidemiological models because they characterize the functional relationship between susceptible and infected people. The incidence rate in epidemiological models is directly proportional to the population's lifestyle and overpopulation and is a consideration that especially impacts the dynamics of transmission. To illustrate the standard incidence rate is expressed based on the total population, while the bi-linear incidence

rate is associated with the law of mass action [37]. The saturated incidence rate improved by Capasso and Serio [38] is frequently favored to describe indirect transmission from bacterial infections such as cholera and brucellosis [22, 26, 39–41], as it causes a saturation level when the exposed (infected) individuals achieve their utmost. Since the amount of Brucella that causes infection by interacting is present at this incidence rate, the interaction rate is controlled with fitting parameters by determining the behavioral change and population density of infected individuals. For bacterial diseases, the saturated incidence rate appears to be closer to reality than the bilinear incidence rate.

Motivated by continuing investigation into this topic, in this study, the deficiencies in the transmission model of brucellosis between sheep and humans proposed by Hou et al. with data from the Inner Mongolia region of China are dealt with and discussed via ABC derivative [42]. As far as we know, the interspecific brucellosis transmission model with ABC derivative has not yet been examined. It is also considered the recovered compartment (with recovery rate) for the human population in the model, the recruitment rate for susceptible humans, and the mortality rate for all humans. Besides, indirect brucellosis transmission is given with a saturated incidence rate instead of the bilinear incidence rate for a more realistic analysis. The unit consistency of the model is also included. It is not always possible to achieve the exact solution of nonlinear fractional-order models. On that account, according to the fixed point theory, it is shown that there exists a unique solution to the fractional brucellosis model. Then, the Adam-type predictor-corrector method is utilized to perform the numerical solution of the model.

The remainder of this article is structured as follows: Section 2 presents some primary concepts of fractional calculus and the developed interspecies fractional-order brucellosis transmission model. Section 3 employs fixed-point theory to demonstrate the existence and uniqueness of the model of solutions. Section 4 is devoted to the numerical solution and discussion. Finally, Section 5 includes conclusions of the analysis work and gives future direction.

Preliminaries

Here, more details and some definitions and concepts necessary for the completion of this study are presented.

Definition 1 ([43]) *For $0 \leq \alpha \leq 1$ and $f \in H^1(a, b)$, the α-order left and right ABC fractional derivatives of the f are expressed as*

$$^{ABC}_{a}D^\alpha_t f(t) = \frac{M(\alpha)}{1-\alpha} \int_a^t \frac{df(\varrho)}{d\varrho} E_\alpha \left[-\frac{\alpha}{1-\alpha} (t-\varrho)^\alpha \right] d\varrho, \tag{1}$$

$$^{ABC}_{t}D^\alpha_b f(t) = \frac{-M(\alpha)}{1-\alpha} \int_t^b \frac{df(\varrho)}{d\varrho} E_\alpha \left[-\frac{\alpha}{1-\alpha} (\varrho-t)^\alpha \right] d\varrho, \tag{2}$$

where E_α is the Mittag-Leffler function and $M(\alpha)$ is the normalization function such as $M(\alpha) = 1 - \alpha + \frac{\alpha}{\Gamma(\alpha)}$ with $M(0) = M(1) = 1$.

Definition 2 ([43]) *The Atangana-Baleanu fractional integral of α-order of the f is expressed as*

$$^{ABC}_{a}I^\alpha_t f(t) = \frac{1-\alpha}{M(\alpha)} f(t) + \frac{\alpha}{M(\alpha)\Gamma(\alpha)} \int_a^t (t-\varrho)^{\alpha-1} f(\varrho) d\varrho. \tag{3}$$

2   Fractional-order brucellosis transmission model

In this section, not only the time derivative is replaced within the ABC sense to examine the brucellosis model by the transmission behavior, but it is also developed by eliminating the deficiencies in the model introduced by Huo et al. [42] for interspecies brucellosis transmission. The brucellosis model as introduced in [42] is given by

$$
\begin{cases}
\dfrac{dS}{dt} = A - \beta S \,(E + I) - \phi SB - (\mu + v)\,S + \delta V, \\[2mm]
\dfrac{dV}{dt} = vS - (\mu + \delta)\,V - \varepsilon\beta V\,(E + I) - \varepsilon\phi VB, \\[2mm]
\dfrac{dE}{dt} = \beta\,(S + \varepsilon V)\,(E + I) + \phi\,(S + \varepsilon V)\,B - (\sigma + \mu)\,E, \\[2mm]
\dfrac{dI}{dt} = \sigma E - (\mu + c)\,I, \\[2mm]
\dfrac{dB}{dt} = k\,(E + I) - (d + n\tau)\,B, \\[2mm]
\dfrac{dS_h}{dt} = -\beta_h S_h\,(E + I) - \phi_h S_h B + \sigma_h\,(1 - p)\,I_{ah}, \\[2mm]
\dfrac{dI_{ah}}{dt} = \beta_h S_h\,(E + I) + \phi_h S_h B - \sigma_h I_{ah}, \\[2mm]
\dfrac{dI_{ch}}{dt} = \sigma_h p I_{ah}.
\end{cases}
\tag{4}
$$

In model (4), susceptible sheep are denoted S, vaccinated sheep by V, exposed sheep by E, and infected sheep by I. The total number of sheep is $N = S + V + E + I$. The number of infectious units in the environment is represented by B. Susceptible humans are signified by S_h, acute infection humans by I_{ah}, and chronic infection humans by I_{ch}. Acute infection humans, if they do not recover, pass into the compartment chronic infection. Total human population $N_h = S_h + I_{ah} + I_{ch}$. The birth and mortality rates for sheep are A and μ, respectively. Susceptible sheep interact with exposed and infected sheep at the rate of β. Brucella is transmitted to susceptible sheep at a rate ϕ. Also, Susceptible sheep are vaccinated at the rate v, whereas ε is an incorrect vaccination rate. The immunity of vaccinated sheep is lost at a rate of δ. Exposed sheep are infected at the rate σ, and infected sheep are culled at a rate c. Brucella from exposed and infected sheep are shed at a rate k. While Brucella decays in the environment at a rate d, it is effectively disinfected at a rate τ. No data are reported on the transmission among humans of brucellosis between 2005 and 2010, so the rate of transmission among humans is assumed to be zero. Additionally, in the model (4), brucellosis transmission humans directly from sheep at a rate of β_h and indirectly from Brucella at a rate of ϕ_h. Acute infection humans become chronic infection at a rate $\sigma_h p$. Chronic infection humans are also susceptible to the $\sigma_h\,(1 - p)$ rate. Since the study of Kermack and McKendrick [44], epidemiological models have been created with the recovered compartment to observe the spread of the infection in more detail. However, in model (4), there is no recovered compartment for humans. Additionally, human birth and death rates are other important parameters to consider when analyzing the population. Note that these parameters are not adapted to model (4). For this reason, the model is developed by considering the mentioned deficiencies and is introduced with the ABC derivative so that it can be discussed realistically.

The classical derivative has the s^{-1} second dimension to represent s seconds, while the ${}^{ABC}_{\;\;0}D^\alpha_t$ fractional derivative has the $s^{-\alpha}$ dimension. The auxiliary parameter θ with second dimension s is employed for unit consistency [45]. The following is the fractional-order brucellosis transmission

model for $0 \leq \alpha \leq 1$ and $t \geq 0$:

$$
\begin{cases}
\theta^{\alpha-1}{}^{ABC}_0D^\alpha_t S = \Lambda_s - \beta S \left(E + I\right) - \phi \frac{SB}{\rho+B} - \left(\mu + \nu\right) S + \delta V, \\
\theta^{\alpha-1}{}^{ABC}_0D^\alpha_t V = \nu S - \left(\mu + \delta\right) V - \varepsilon\beta V \left(E + I\right) - \varepsilon\phi \frac{VB}{\rho+B}, \\
\theta^{\alpha-1}{}^{ABC}_0D^\alpha_t E = \beta \left(S + \varepsilon V\right) \left(E + I\right) + \phi \frac{\left(S+\varepsilon V\right)B}{\rho+B} - \left(\sigma + \mu\right) E, \\
\theta^{\alpha-1}{}^{ABC}_0D^\alpha_t I = \sigma E - \left(\mu + c\right) I, \\
\theta^{\alpha-1}{}^{ABC}_0D^\alpha_t B = k \left(E + I\right) - \left(d + n\tau\right) B, \\
\theta^{\alpha-1}{}^{ABC}_0D^\alpha_t S_h = \Lambda_h - \beta_h S_h \left(E + I\right) - \phi_h \frac{S_h B}{\rho+B} - \mu_h S_h, \\
\theta^{\alpha-1}{}^{ABC}_0D^\alpha_t I_{ah} = \beta_h S_h \left(E + I\right) + \phi_h \frac{S_h B}{\rho+B} - \left(\sigma_h + \mu_h\right) I_{ah}, \\
\theta^{\alpha-1}{}^{ABC}_0D^\alpha_t I_{ch} = \sigma_h p I_{ah} - \left(\gamma_{ch} + \mu_h\right) I_{ch}, \\
\theta^{\alpha-1}{}^{ABC}_0D^\alpha_t R_h = \sigma_h \left(1 - p\right) I_{ah} + \gamma_{ch} I_{ch} - \mu_h R_h,
\end{cases}
\tag{5}
$$

where the initial conditions are

$$
\begin{cases}
S\left(0\right) = S_0, V\left(0\right) = V_0, \ I\left(0\right) = I_0, \ E\left(0\right) = E_0, \ B\left(0\right) = B_0, \\
S_h\left(0\right) = S_{h0}, \ I_{ah}\left(0\right) = I_{ah0}, \ I_{ch}\left(0\right) = I_{ch0}, \ R_h\left(0\right) = R_{h0}.
\end{cases}
\tag{6}
$$
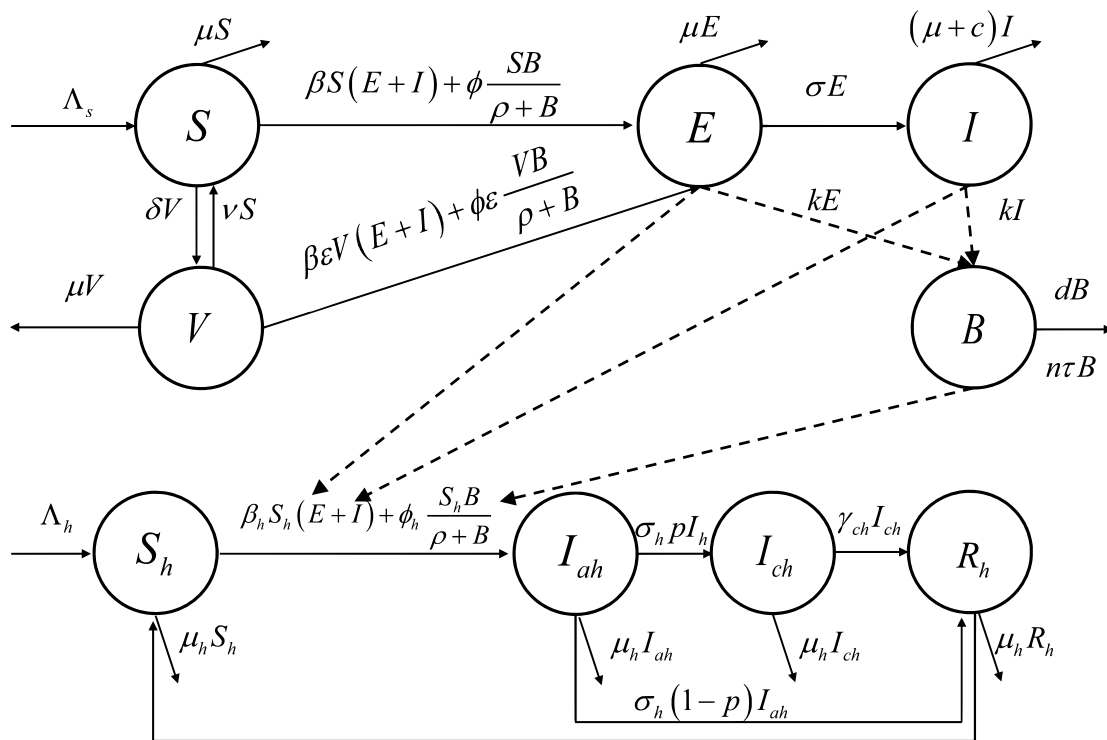
Figure 1. Flowchart of the direct and indirect transmission of the developed fractional brucellosis model

As seen in Figure 1, the human population is separated into four classifications based on their epidemiological stages. The compartment R_h in the model (5) describes recovered humans. To elaborately investigate these stages, it is assumed that there is a recruitment rate Λ_h for compartment S and a natural death rate μ_h for all compartments. Acute and chronic infections are recovered with rates $\sigma_h \left(1 - p\right)$ and γ_{ch}, respectively. Also, susceptible sheep and humans catch infections indirectly at rates $\phi \frac{B}{\rho+B}$ and $\phi_h \frac{B}{\rho+B}$, in which ϕ and ϕ_h represent interaction rates with the bacteria-contaminated environment, ρ is the half-saturation constant of the Brucella

population and $\frac{1}{\rho+B}$ is the inhibition effect as well. Hence, $\frac{B}{\rho+B}$ is the probability of exposed sheep and acute infection in humans owning the infection with symptoms, given interaction with the contaminated environment. Although the saturated incidence rate initially behaves linearly, the probability of infection continues to increase to a specific level as the bacteria reproduce. That is to say that even if Brucella in a contaminated environment is in extraordinary numbers, individuals indirectly interacting with more Brucella will not significantly augment the risk to their already threatened health. In this way, the infection transmission level will saturate at rates ϕ and ϕ_h. The amount of Brucella interacted to begin infection is already within this incidence rate. Thus, the saturated incidence rate appears more sensible than the bilinear incidence rate for indirect transmission of bacterial diseases as it prevents the interaction rate from achieving extraordinary numbers by determining appropriate parameters based on the behavioral change and population density of exposed (infected) individuals.

3   Existence and uniqueness

In this section, the existence of a unique solution for the developed brucellosis model is analyzed. By fixed point theory, it is verified that developed fractional transmission dynamics have a unique solution with the initial conditions (6). Suppose a continuous $\mathbb{R} \to \mathbb{R}$ function described by $\mathcal{H}(\mathcal{J})$ including the sup norm characteristic is a Banach space on $\mathcal{J} = [0, T]$ and

$$\mathcal{Q} = \mathcal{H}(\mathcal{J}) \times \mathcal{H}(\mathcal{J}) \times \mathcal{H}(\mathcal{J}) \times \mathcal{H}(\mathcal{J}) \times \mathcal{H}(\mathcal{J}) \times \mathcal{H}(\mathcal{J}) \times \mathcal{H}(\mathcal{J}) \times \mathcal{H}(\mathcal{J}) \times \mathcal{H}(\mathcal{J}),$$

with norm $\|(S, V, E, I, B, S_h, I_{ah}, I_{ch}, R_h)\| = \|S\| + \|V\| + \|E\| + \|I\| + \|B\| + \|S_h\| + \|I_{ah}\| + \|I_{ch}\| + \|R_h\|$, where $\|S\| = \sup_{t \in \mathcal{J}} |S|$, $\|V\| = \sup_{t \in \mathcal{J}} |V(t)|$, $\|E\| = \sup_{t \in \mathcal{J}} |E(t)|$, $\|I\| = \sup_{t \in \mathcal{J}} |I(t)|$, $\|B\| = \sup_{t \in \mathcal{J}} |B(t)|$, $\|S_h\| = \sup_{t \in \mathcal{J}} |S_h(t)|$, $\|I_{ah}\| = \sup_{t \in \mathcal{J}} |I_{ah}(t)|$, $\|I_{ch}\| = \sup_{t \in \mathcal{J}} |I_{ch}(t)|$, $\|R_h\| = \sup_{t \in \mathcal{J}} |R_h(t)|$. Implementing the fractional integral described in (3) to each side of Eq. (5), the model is written below:

$$S(t) - S(0) = \theta^{1-\alpha}\,{}^{ABC}_0 I^\alpha_t \left\{ \Lambda_s - \beta S(t)(E(t) + I(t)) - \phi \frac{S(t)B(t)}{\rho + B(t)} - (\mu + \nu)S(t) + \delta V(t) \right\},$$

$$V(t) - V(0) = \theta^{1-\alpha}\,{}^{ABC}_0 I^\alpha_t \left\{ \nu S(t) - (\mu + \delta)V(t) - \varepsilon\beta V(t)(E(t) + I(t)) - \varepsilon\phi \frac{V(t)B(t)}{\rho + B(t)} \right\},$$

$$E(t) - E(0) = \theta^{1-\alpha}\,{}^{ABC}_0 I^\alpha_t \left\{ \beta(S(t) + \varepsilon V(t))(E(t) + I(t)) + \phi \frac{(S(t) + \varepsilon V(t))B(t)}{\rho + B(t)} - (\sigma + \mu)E(t) \right\},$$

$$I(t) - I(0) = \theta^{1-\alpha}\,{}^{ABC}_0 I^\alpha_t \left\{ \sigma E(t) - (\mu + c)I(t) \right\},$$

$$B(t) - B(0) = \theta^{1-\alpha}\,{}^{ABC}_0 I^\alpha_t \left\{ k(E(t) + I(t)) - (d + n\tau)B(t) \right\},$$

$$S_h(t) - S_h(0) = \theta^{1-\alpha}\,{}^{ABC}_0 I^\alpha_t \left\{ \Lambda_h - \beta_h S_h(t)(E(t) + I(t)) - \phi_h \frac{S_h(t)B(t)}{\rho + B(t)} - \mu_h S_h(t) \right\},$$

$$I_{ah}(t) - I_{ah}(0) = \theta^{1-\alpha}\,{}^{ABC}_0 I^\alpha_t \left\{ \beta_h S_h(t)(E(t) + I(t)) + \phi_h \frac{S_h(t)B(t)}{\rho + B(t)} - (\sigma_h + \mu_h)I_{ah}(t) \right\},$$

$$I_{ch}(t) - I_{ch}(0) = \theta^{1-\alpha}\,{}^{ABC}_0 I^\alpha_t \left\{ \sigma_h p I_{ah}(t) - (\gamma_{ch} + \mu_h)I_{ch}(t) \right\},$$

$$R_h(t) - R_h(0) = \theta^{1-\alpha}\,{}^{ABC}_0 I^\alpha_t \left\{ \sigma_h(1 - p)I_{ah}(t) + \gamma_{ch}I_{ch}(t) - \mu_h R_h(t) \right\}.$$

$$(7)$$

Exerting the definition given by (3), the following expression is acquired:

$$S(t) - S(0) = \frac{(1-\alpha)\theta^{1-\alpha}}{M(\alpha)}F_1(t, S) + \frac{\alpha\theta^{1-\alpha}}{M(\alpha)\Gamma(\alpha)}\int_0^t (t - \varrho)^{\alpha-1}F_1(\varrho, S)\,d\varrho,$$

$$V(t) - V(0) = \frac{(1-\alpha)\theta^{1-\alpha}}{M(\alpha)}F_2(t, V) + \frac{\alpha\theta^{1-\alpha}}{M(\alpha)\Gamma(\alpha)}\int_0^t (t - \varrho)^{\alpha-1}F_2(\varrho, V)\,d\varrho,$$

$$E(t) - E(0) = \frac{(1-\alpha)\theta^{1-\alpha}}{M(\alpha)}F_3(t, E) + \frac{\alpha\theta^{1-\alpha}}{M(\alpha)\Gamma(\alpha)}\int_0^t (t - \varrho)^{\alpha-1}F_3(\varrho, E)\,d\varrho,$$

$$I(t) - I(0) = \frac{(1-\alpha)\theta^{1-\alpha}}{M(\alpha)}F_4(t, I) + \frac{\alpha\theta^{1-\alpha}}{M(\alpha)\Gamma(\alpha)}\int_0^t (t-\varrho)^{\alpha-1}F_4(\varrho, I)\, d\varrho,$$

$$B(t) - B(0) = \frac{(1-\alpha)\theta^{1-\alpha}}{M(\alpha)}F_5(t, B) + \frac{\alpha\theta^{1-\alpha}}{M(\alpha)\Gamma(\alpha)}\int_0^t (t-\varrho)^{\alpha-1}F_5(\varrho, B)\, d\varrho,$$

$$S_h(t) - S_h(0) = \frac{(1-\alpha)\theta^{1-\alpha}}{M(\alpha)}F_6(t, S_h) + \frac{\alpha\theta^{1-\alpha}}{M(\alpha)\Gamma(\alpha)}\int_0^t (t-\varrho)^{\alpha-1}F_6(\varrho, S_h)\, d\varrho,$$

$$I_{ah}(t) - I_{ah}(0) = \frac{(1-\alpha)\theta^{1-\alpha}}{M(\alpha)}F_7(t, I_{ah}) + \frac{\alpha\theta^{1-\alpha}}{M(\alpha)\Gamma(\alpha)}\int_0^t (t-\varrho)^{\alpha-1}F_7(\varrho, I_{ah})\, d\varrho, \tag{8}$$

$$I_{ch}(t) - I_{ch}(0) = \frac{(1-\alpha)\theta^{1-\alpha}}{M(\alpha)}F_8(t, I_{ch}) + \frac{\alpha\theta^{1-\alpha}}{M(\alpha)\Gamma(\alpha)}\int_0^t (t-\varrho)^{\alpha-1}F_8(\varrho, I_{ch})\, d\varrho,$$

$$R_h(t) - R_h(0) = \frac{(1-\alpha)\theta^{1-\alpha}}{M(\alpha)}F_9(t, R_h) + \frac{\alpha\theta^{1-\alpha}}{M(\alpha)\Gamma(\alpha)}\int_0^t (t-\varrho)^{\alpha-1}F_9(\varrho, R_h)\, d\varrho,$$

where the kernels are described by

$$
\begin{aligned}
F_1(t, S) &= \Lambda_s - \beta S(t)(E(t) + I(t)) - \phi\frac{S(t)B(t)}{\rho+B(t)} - (\mu+\nu)S(t) + \delta V(t),\\
F_2(t, V) &= \nu S(t) - (\mu+\delta)V(t) - \varepsilon\beta V(t)(E(t)+I(t)) - \varepsilon\phi\frac{V(t)B(t)}{\rho+B(t)},\\
F_3(t, E) &= \beta(S(t) + \varepsilon V(t))(E(t)+I(t)) + \phi\frac{(S(t)+\varepsilon V(t))B(t)}{\rho+B(t)} - (\sigma+\mu)E(t),\\
F_4(t, I) &= \sigma E(t) - (\mu+c)I(t),\\
F_5(t, B) &= k(E(t)+I(t)) - (d+n\tau)B(t),\\
F_6(t, S_h) &= \Lambda_h - \beta_h S_h(t)(E(t)+I(t)) - \phi_h\frac{S_h(t)B(t)}{\rho+B(t)} - \mu_h S_h(t),\\
F_7(t, I_{ah}) &= \beta_h S_h(t)(E(t)+I(t)) + \phi_h\frac{S_h(t)B(t)}{\rho+B(t)} - (\sigma_h+\mu_h)I_{ah}(t),\\
F_8(t, I_{ch}) &= \sigma_h p I_{ah}(t) - (\gamma_{ch}+\mu_h)I_{ch}(t),\\
F_9(t, R_h) &= \sigma_h(1-p)I_{ah}(t) + \gamma_{ch}I_{ch}(t) - \mu_h R_h(t).
\end{aligned}
\tag{9}
$$

Theorem 1 *If the below inequality holds*

$$0 \le \beta(\eta_3 + \eta_4) + \phi\frac{\eta_5}{\rho+\eta_5} < 1,$$

so the kernel F_1 provides for Lipschitz condition and contraction.

Proof Assumed S and S_1 are two functions, the undermentioned inequality is obtained:

$$
\begin{aligned}
\|F_1(t, S) - F_1(t, S_1)\| &= \left\| \Lambda_s - \left(\beta(E(t)+I(t)) + \phi\frac{B(t)}{\rho+B(t)} + \mu+\nu\right)S(t) + \delta V(t) \right.\\
&\quad \left. - \left(\Lambda_s - \left(\beta(E(t)+I(t)) + \phi\frac{B(t)}{\rho+B(t)} + \mu+\nu\right)S_1(t) + \delta V(t)\right) \right\|\\
&\le \left(\beta(E(t)+I(t)) + \phi\frac{B(t)}{\rho+B(t)} + \mu+\nu\right)\|S(t) - S_1(t)\|.
\end{aligned}
$$

Let $\varpi_1 = \left(\beta(E(t)+I(t)) + \phi\frac{B(t)}{\rho+B(t)} + \mu+\nu\right)$, where $\|S\| \le \eta_1$, $\|V\| \le \eta_2$, $\|E\| \le \eta_3$, $\|I\| \le \eta_4$, $\|B\| \le \eta_5$, $\|S_h\| \le \eta_6$, $\|I_{ah}\| \le \eta_7$, $\|I_{ch}\| \le \eta_8$, and $\|R_h\| \le \eta_9$, are bounded functions, we have

$$
\begin{aligned}
\|F_1(t, S) - F_1(t, S_1)\| &\le \left(\beta(\eta_3+\eta_4) + \phi\frac{\eta_5}{\rho+\eta_5} + \mu+\nu\right)\|S(t) - S_1(t)\|\\
&\le \varpi_1\|S(t) - S_1(t)\|.
\end{aligned}
$$

Thus, $F_1(t, S)$ supplies the Lipschitz condition with Lipschitz constant

$$\varpi_1 = \left(\beta \left(E(t) + I(t) \right) + \phi \frac{B(t)}{\rho + B(t)} + \mu + \nu \right).$$

Furthermore, $0 \leq \varpi_1 < 1$, then kernel $F_1(t, S)$ is a contraction. In the same manner, the Lipschitz condition and contraction are provided by the kernels $F_2, F_3, F_4, F_5, F_6, F_7, F_8$, and F_9 given below:

$$
\begin{aligned}
\|F_2(t, V) - F_2(t, V_1)\| &\leq \varpi_2 \|V(t) - V_1(t)\|, \\
\|F_3(t, E) - F_3(t, E_1)\| &\leq \varpi_3 \|E(t) - E_1(t)\|, \\
\|F_4(t, I) - F_4(t, I_1)\| &\leq \varpi_4 \|I(t) - I_1(t)\|, \\
\|F_5(t, B) - F_5(t, B_1)\| &\leq \varpi_5 \|B(t) - B_1(t)\|, \\
\|F_6(t, S_h) - F_6(t, S_{h1})\| &\leq \varpi_6 \|S_h(t) - S_{h1}(t)\|, \\
\|F_7(t, I_{ah}) - F_7(t, I_{ah1})\| &\leq \varpi_7 \|I_{ah}(t) - I_{ah1}(t)\|, \\
\|F_8(t, I_{ch}) - F_7(t, I_{ch1})\| &\leq \varpi_8 \|I_{ch}(t) - I_{ch1}(t)\|, \\
\|F_9(t, R_h) - F_9(t, R_{h1})\| &\leq \varpi_9 \|R_h(t) - R_{h1}(t)\|.
\end{aligned}
\tag{10}
$$

The kernels in Eq. (8) can be rewritten as:

$$S(t) = S(0) + \frac{(1-\alpha)\theta^{1-\alpha}}{M(\alpha)} F_1(t, S) + \frac{\alpha\theta^{1-\alpha}}{M(\alpha)\Gamma(\alpha)} \int_0^t (t-\varrho)^{\alpha-1} F_1(\varrho, S) \, d\varrho,$$

$$V(t) = V(0) + \frac{(1-\alpha)\theta^{1-\alpha}}{M(\alpha)} F_2(t, V) + \frac{\alpha\theta^{1-\alpha}}{M(\alpha)\Gamma(\alpha)} \int_0^t (t-\varrho)^{\alpha-1} F_2(\varrho, V) \, d\varrho,$$

$$E(t) = E(0) + \frac{(1-\alpha)\theta^{1-\alpha}}{M(\alpha)} F_3(t, E) + \frac{\alpha\theta^{1-\alpha}}{M(\alpha)\Gamma(\alpha)} \int_0^t (t-\varrho)^{\alpha-1} F_3(\varrho, E) \, d\varrho,$$

$$I(t) = I(0) + \frac{(1-\alpha)\theta^{1-\alpha}}{M(\alpha)} F_4(t, I) + \frac{\alpha\theta^{1-\alpha}}{M(\alpha)\Gamma(\alpha)} \int_0^t (t-\varrho)^{\alpha-1} F_4(\varrho, I) \, d\varrho,$$

$$B(t) = B(0) + \frac{(1-\alpha)\theta^{1-\alpha}}{M(\alpha)} F_5(t, B) + \frac{\alpha\theta^{1-\alpha}}{M(\alpha)\Gamma(\alpha)} \int_0^t (t-\varrho)^{\alpha-1} F_5(\varrho, B) \, d\varrho, \tag{11}$$

$$S_h(t) = S_h(0) + \frac{(1-\alpha)\theta^{1-\alpha}}{M(\alpha)} F_6(t, S_h) + \frac{\alpha\theta^{1-\alpha}}{M(\alpha)\Gamma(\alpha)} \int_0^t (t-\varrho)^{\alpha-1} F_6(\varrho, S_h) \, d\varrho,$$

$$I_{ah}(t) = I_{ah}(0) + \frac{(1-\alpha)\theta^{1-\alpha}}{M(\alpha)} F_7(t, I_{ah}) + \frac{\alpha\theta^{1-\alpha}}{M(\alpha)\Gamma(\alpha)} \int_0^t (t-\varrho)^{\alpha-1} F_7(\varrho, I_{ah}) \, d\varrho,$$

$$I_{ch}(t) = I_{ch}(0) + \frac{(1-\alpha)\theta^{1-\alpha}}{M(\alpha)} F_8(t, I_{ch}) + \frac{\alpha\theta^{1-\alpha}}{M(\alpha)\Gamma(\alpha)} \int_0^t (t-\varrho)^{\alpha-1} F_8(\varrho, I_{ch}) \, d\varrho,$$

$$R_h(t) = R_h(0) + \frac{(1-\alpha)\theta^{1-\alpha}}{M(\alpha)} F_9(t, R_h) + \frac{\alpha\theta^{1-\alpha}}{M(\alpha)\Gamma(\alpha)} \int_0^t (t-\varrho)^{\alpha-1} F_9(\varrho, R_h) \, d\varrho.$$

Going recursively, Eq. (11) yielded

$$S_n(t) = \frac{(1-\alpha)\theta^{1-\alpha}}{M(\alpha)} F_1(t, S_{n-1}) + \frac{\alpha\theta^{1-\alpha}}{M(\alpha)\Gamma(\alpha)} \int_0^t (t-\varrho)^{\alpha-1} F_1(\varrho, S_{n-1}) \, d\varrho,$$

$$V_n(t) = \frac{(1-\alpha)\theta^{1-\alpha}}{M(\alpha)} F_2(t, V_{n-1}) + \frac{\alpha\theta^{1-\alpha}}{M(\alpha)\Gamma(\alpha)} \int_0^t (t-\varrho)^{\alpha-1} F_2(\varrho, V_{n-1}) \, d\varrho,$$

$$E_n(t) = \frac{(1-\alpha)\theta^{1-\alpha}}{M(\alpha)} F_3(t, E_{n-1}) + \frac{\alpha\theta^{1-\alpha}}{M(\alpha)\Gamma(\alpha)} \int_0^t (t-\varrho)^{\alpha-1} F_3(\varrho, E_{n-1}) \, d\varrho,$$

$$I_n(t) = \frac{(1-\alpha)\theta^{1-\alpha}}{M(\alpha)} F_4(t, I_{n-1}) + \frac{\alpha\theta^{1-\alpha}}{M(\alpha)\Gamma(\alpha)} \int_0^t (t-\varrho)^{\alpha-1} F_4(\varrho, I_{n-1}) \, d\varrho,$$

$$B_n(t) = \frac{(1-\alpha)\theta^{1-\alpha}}{M(\alpha)} F_5(t, B_{n-1}) + \frac{\alpha\theta^{1-\alpha}}{M(\alpha)\Gamma(\alpha)} \int_0^t (t-\varrho)^{\alpha-1} F_5(\varrho, B_{n-1}) \, d\varrho,$$

$$S_{h,n}(t) = \frac{(1-\alpha)\theta^{1-\alpha}}{M(\alpha)} F_6(t, S_{h,n-1}) + \frac{\alpha\theta^{1-\alpha}}{M(\alpha)\Gamma(\alpha)} \int_0^t (t-\varrho)^{\alpha-1} F_6(\varrho, S_{h,n-1}) \, d\varrho,$$

$$I_{ah,n}(t) = \frac{(1-\alpha)\theta^{1-\alpha}}{M(\alpha)} F_7(t, I_{ah,n-1}) + \frac{\alpha\theta^{1-\alpha}}{M(\alpha)\Gamma(\alpha)} \int_0^t (t-\varrho)^{\alpha-1} F_7(\varrho, I_{ah,n-1}) \, d\varrho, \tag{12}$$

$$I_{ch,n}(t) = \frac{(1-\alpha)\theta^{1-\alpha}}{M(\alpha)} F_8(t, I_{ch,n-1}) + \frac{\alpha\theta^{1-\alpha}}{M(\alpha)\Gamma(\alpha)} \int_0^t (t-\varrho)^{\alpha-1} F_8(\varrho, I_{ch,n-1}) \, d\varrho,$$

$$R_{h,n}(t) = \frac{(1-\alpha)\theta^{1-\alpha}}{M(\alpha)} F_9(t, R_{h,n-1}) + \frac{\alpha\theta^{1-\alpha}}{M(\alpha)\Gamma(\alpha)} \int_0^t (t-\varrho)^{\alpha-1} F_9(\varrho, R_{h,n-1}) \, d\varrho,$$

along with the initial conditions $S(0) = S_0$, $V(0) = V_0$, $I(0) = I_0$, $E(0) = E_0$, $B(0) = B_0$, $S_h(0) = S_{h0}$, $I_{ah}(0) = I_{ah0}$, $I_{ch}(0) = I_{ch0}$, and $R_h(0) = R_{h0}$. By taking the difference between successive terms, the following equalities are reached:

$$\psi_{1n}(t) = S_n(t) - S_{n-1}(t) = \frac{(1-\alpha)\theta^{1-\alpha}}{M(\alpha)} \{F_1(t, S_{n-1}) - F_1(t, S_{n-2})\}$$
$$+ \frac{\alpha\theta^{1-\alpha}}{M(\alpha)\Gamma(\alpha)} \int_0^t (t-\varrho)^{\alpha-1} \{F_1(\varrho, S_{n-1}) - F_1(\varrho, S_{n-2})\} \, d\varrho, \tag{13}$$

$$\psi_{2n}(t) = V_n(t) - V_{n-1}(t) = \frac{(1-\alpha)\theta^{1-\alpha}}{M(\alpha)} \{F_2(t, V_{n-1}) - F_2(t, V_{n-2})\}$$
$$+ \frac{\alpha\theta^{1-\alpha}}{M(\alpha)\Gamma(\alpha)} \int_0^t (t-\varrho)^{\alpha-1} \{F_2(\varrho, V_{n-1}) - F_2(\varrho, V_{n-2})\} \, d\varrho, \tag{14}$$

$$\psi_{3n}(t) = E_n(t) - E_{n-1}(t) = \frac{(1-\alpha)\theta^{1-\alpha}}{M(\alpha)} \{F_3(t, E_{n-1}) - F_3(t, E_{n-2})\}$$
$$+ \frac{\alpha\theta^{1-\alpha}}{M(\alpha)\Gamma(\alpha)} \int_0^t (t-\varrho)^{\alpha-1} \{F_3(\varrho, E_{n-1}) - F_3(\varrho, E_{n-2})\} \, d\varrho, \tag{15}$$

$$\psi_{4n}(t) = I_n(t) - I_{n-1}(t) = \frac{(1-\alpha)\theta^{1-\alpha}}{M(\alpha)} \{F_4(t, I_{n-1}) - F_4(t, I_{n-2})\}$$
$$+ \frac{\alpha\theta^{1-\alpha}}{M(\alpha)\Gamma(\alpha)} \int_0^t (t-\varrho)^{\alpha-1} \{F_4(\varrho, I_{n-1}) - F_4(\varrho, I_{n-2})\} \, d\varrho, \tag{16}$$

$$\psi_{5n}(t) = B_n(t) - B_{n-1}(t) = \frac{(1-\alpha)\theta^{1-\alpha}}{M(\alpha)} \{F_5(t, B_{n-1}) - F_5(t, B_{n-2})\}$$
$$+ \frac{\alpha\theta^{1-\alpha}}{M(\alpha)\Gamma(\alpha)} \int_0^t (t-\varrho)^{\alpha-1} \{F_5(\varrho, B_{n-1}) - F_5(\varrho, B_{n-2})\} \, d\varrho, \tag{17}$$

$$\psi_{6n}(t) = S_{h,n}(t) - S_{h,n-1}(t) = \frac{(1-\alpha)\theta^{1-\alpha}}{M(\alpha)} \{F_6(t, S_{h,n-1}) - F_6(t, S_{h,n-2})\}$$
$$+ \frac{\alpha\theta^{1-\alpha}}{M(\alpha)\Gamma(\alpha)} \int_0^t (t-\varrho)^{\alpha-1} \{F_6(\varrho, S_{h,n-1}) - F_6(\varrho, S_{h,n-2})\} d\varrho, \tag{18}$$

$$\psi_{7n}(t) = I_{ah,n}(t) - I_{ah,n-1}(t) = \frac{(1-\alpha)\theta^{1-\alpha}}{M(\alpha)} \{F_7(t, I_{ah,n-1}) - F_7(t, I_{ah,n-2})\}$$
$$+ \frac{\alpha\theta^{1-\alpha}}{M(\alpha)\Gamma(\alpha)} \int_0^t (t-\varrho)^{\alpha-1} \{F_7(\varrho, I_{ah,n-1}) - F_7(\varrho, I_{ah,n-2})\} d\varrho, \tag{19}$$

$$\psi_{8n}(t) = I_{ch,n}(t) - I_{ch,n-1}(t) = \frac{(1-\alpha)\theta^{1-\alpha}}{M(\alpha)} \{F_8(t, I_{ch,n-1}) - F_8(t, I_{ch,n-2})\}$$
$$+ \frac{\alpha\theta^{1-\alpha}}{M(\alpha)\Gamma(\alpha)} \int_0^t (t-\varrho)^{\alpha-1} \{F_8(\varrho, I_{ch,n-1}) - F_8(\varrho, I_{ch,n-2})\} d\varrho, \tag{20}$$

$$\psi_{9n}(t) = R_{h,n}(t) - R_{h,n-1}(t) = \frac{(1-\alpha)\theta^{1-\alpha}}{M(\alpha)} \{F_9(t, R_{h,n-1}) - F_9(t, R_{h,n-2})\}$$
$$+ \frac{\alpha\theta^{1-\alpha}}{M(\alpha)\Gamma(\alpha)} \int_0^t (t-\varrho)^{\alpha-1} \{F_9(\varrho, R_{h,n-1}) - F_9(\varrho, R_{h,n-2})\} d\varrho. \tag{21}$$

In addition, it is obvious that $S_n(t) = \sum_{i=0}^n \psi_{1i}(t)$, $V_n(t) = \sum_{i=0}^n \psi_{2i}(t)$, $E_n(t) = \sum_{i=0}^n \psi_{3i}(t)$, $I_n(t) = \sum_{i=0}^n \psi_{4i}(t)$, $B_n(t) = \sum_{i=0}^n \psi_{5i}(t)$, $S_{h,n}(t) = \sum_{i=0}^n \psi_{6i}(t)$, $I_{ah,n}(t) = \sum_{i=0}^n \psi_{7i}(t)$, $I_{ch,n}(t) = \sum_{i=0}^n \psi_{8i}(t)$, and $R_{h,n}(t) = \sum_{i=0}^n \psi_{9i}(t)$. By implementing the norm to both sides of Eq. (13) and utilizing the triangular inequality, it can be expressed as:

$$\|\psi_{1n}(t)\| = \|S_n(t) - S_{n-1}(t)\| = \left\| \frac{(1-\alpha)\theta^{1-\alpha}}{M(\alpha)} \{F_1(t, S_{n-1}) - F_1(t, S_{n-2})\} \right.$$
$$+ \frac{\alpha\theta^{1-\alpha}}{M(\alpha)\Gamma(\alpha)} \int_0^t (t-\varrho)^{\alpha-1} \{F_1(\varrho, S_{n-1}) - F_1(\varrho, S_{n-2})\} d\varrho \bigg\|$$
$$\leq \frac{(1-\alpha)\theta^{1-\alpha}}{M(\alpha)} \|F_1(t, S_{n-1}) - F_1(t, S_{n-2})\|$$
$$+ \frac{\alpha\theta^{1-\alpha}}{M(\alpha)\Gamma(\alpha)} \int_0^t (t-\varrho)^{\alpha-1} \|F_1(\varrho, S_{n-1}) - F_1(\varrho, S_{n-2})\| d\varrho. \tag{22}$$

Due to the fact that the Lipschitz condition is provided for by kernel F_1, the following can be written:

$$\|\psi_{1n}(t)\| = \|S_n(t) - S_{n-1}(t)\| \leq \frac{(1-\alpha)\theta^{1-\alpha}}{M(\alpha)} \varpi_1 \|S_{n-1} - S_{n-2}\|$$
$$+ \frac{\alpha\theta^{1-\alpha}}{M(\alpha)\Gamma(\alpha)} \varpi_1 \int_0^t (t-\varrho)^{\alpha-1} \|S_{n-1} - S_{n-2}\| d\varrho, \tag{23}$$

then obtained as:

$$\|\psi_{1n}(t)\| \leq \frac{(1-\alpha)\theta^{1-\alpha}}{M(\alpha)} \varpi_1 \|\psi_{1(n-1)}(t)\| + \frac{\alpha\theta^{1-\alpha}}{M(\alpha)\Gamma(\alpha)} \varpi_1 \int_0^t (t-\varrho)^{\alpha-1} \|\psi_{1(n-1)}(\varrho)\| d\varrho. \tag{24}$$

Similarly, the following results are acquired

$$
\begin{aligned}
&\|\psi_{2n}(t)\| \leq \tfrac{(1-\alpha)\theta^{1-\alpha}}{M(\alpha)}\varpi_2\left\|\psi_{2(n-1)}(t)\right\| + \tfrac{\alpha\theta^{1-\alpha}}{M(\alpha)\Gamma(\alpha)}\varpi_2\int_0^t (t-\varrho)^{\alpha-1}\left\|\psi_{2(n-1)}(\varrho)\right\|d\varrho,\\
&\|\psi_{3n}(t)\| \leq \tfrac{(1-\alpha)\theta^{1-\alpha}}{M(\alpha)}\varpi_3\left\|\psi_{3(n-1)}(t)\right\| + \tfrac{\alpha\theta^{1-\alpha}}{M(\alpha)\Gamma(\alpha)}\varpi_3\int_0^t (t-\varrho)^{\alpha-1}\left\|\psi_{3(n-1)}(\varrho)\right\|d\varrho,\\
&\|\psi_{4n}(t)\| \leq \tfrac{(1-\alpha)\theta^{1-\alpha}}{M(\alpha)}\varpi_4\left\|\psi_{4(n-1)}(t)\right\| + \tfrac{\alpha\theta^{1-\alpha}}{M(\alpha)\Gamma(\alpha)}\varpi_4\int_0^t (t-\varrho)^{\alpha-1}\left\|\psi_{4(n-1)}(\varrho)\right\|d\varrho,\\
&\|\psi_{5n}(t)\| \leq \tfrac{(1-\alpha)\theta^{1-\alpha}}{M(\alpha)}\varpi_5\left\|\psi_{5(n-1)}(t)\right\| + \tfrac{\alpha\theta^{1-\alpha}}{M(\alpha)\Gamma(\alpha)}\varpi_5\int_0^t (t-\varrho)^{\alpha-1}\left\|\psi_{5(n-1)}(\varrho)\right\|d\varrho,\\
&\|\psi_{6n}(t)\| \leq \tfrac{(1-\alpha)\theta^{1-\alpha}}{M(\alpha)}\varpi_6\left\|\psi_{6(n-1)}(t)\right\| + \tfrac{\alpha\theta^{1-\alpha}}{M(\alpha)\Gamma(\alpha)}\varpi_6\int_0^t (t-\varrho)^{\alpha-1}\left\|\psi_{6(n-1)}(\varrho)\right\|d\varrho,\\
&\|\psi_{7n}(t)\| \leq \tfrac{(1-\alpha)\theta^{1-\alpha}}{M(\alpha)}\varpi_7\left\|\psi_{7(n-1)}(t)\right\| + \tfrac{\alpha\theta^{1-\alpha}}{M(\alpha)\Gamma(\alpha)}\varpi_7\int_0^t (t-\varrho)^{\alpha-1}\left\|\psi_{7(n-1)}(\varrho)\right\|d\varrho,\\
&\|\psi_{8n}(t)\| \leq \tfrac{(1-\alpha)\theta^{1-\alpha}}{M(\alpha)}\varpi_8\left\|\psi_{8(n-1)}(t)\right\| + \tfrac{\alpha\theta^{1-\alpha}}{M(\alpha)\Gamma(\alpha)}\varpi_8\int_0^t (t-\varrho)^{\alpha-1}\left\|\psi_{8(n-1)}(\varrho)\right\|d\varrho,\\
&\|\psi_{9n}(t)\| \leq \tfrac{(1-\alpha)\theta^{1-\alpha}}{M(\alpha)}\varpi_9\left\|\psi_{9(n-1)}(t)\right\| + \tfrac{\alpha\theta^{1-\alpha}}{M(\alpha)\Gamma(\alpha)}\varpi_9\int_0^t (t-\varrho)^{\alpha-1}\left\|\psi_{9(n-1)}(\varrho)\right\|d\varrho.
\end{aligned}
\tag{25}
$$

Considering the results received, the existence of the solution of model (5) is given with the help of the following theorem.

Theorem 2 *If there exists t_0 satisfying the following inequality*

$$
\frac{1-\alpha}{M(\alpha)}\varpi_i + \frac{t_0}{M(\alpha)\Gamma(\alpha)}\varpi_i < 1, \text{ for } i = 1,2,...,9,
\tag{26}
$$

then the model (5) has a solution.

Proof It is established that the functions $S(t), V(t), I(t), E(t), B(t), S_h(t), I_{ah}(t), I_{ch}(t)$, and $R_h(t)$ are bounded, and their kernels are fulfilled the Lipschitz condition. Employing the recursive technique, the following relationship is achieved:

$$
\begin{aligned}
&\|\psi_{1n}(t)\| \leq \|S(0)\|\left[\tfrac{(1-\alpha)\theta^{1-\alpha}}{M(\alpha)}\varpi_1 + \tfrac{t\theta^{1-\alpha}}{M(\alpha)\Gamma(\alpha)}\varpi_1\right]^n,\\
&\|\psi_{2n}(t)\| \leq \|V(0)\|\left[\tfrac{(1-\alpha)\theta^{1-\alpha}}{M(\alpha)}\varpi_2 + \tfrac{t\theta^{1-\alpha}}{M(\alpha)\Gamma(\alpha)}\varpi_2\right]^n,\\
&\|\psi_{3n}(t)\| \leq \|E(0)\|\left[\tfrac{(1-\alpha)\theta^{1-\alpha}}{M(\alpha)}\varpi_3 + \tfrac{t\theta^{1-\alpha}}{M(\alpha)\Gamma(\alpha)}\varpi_3\right]^n,\\
&\|\psi_{4n}(t)\| \leq \|I(0)\|\left[\tfrac{(1-\alpha)\theta^{1-\alpha}}{M(\alpha)}\varpi_4 + \tfrac{t\theta^{1-\alpha}}{M(\alpha)\Gamma(\alpha)}\varpi_4\right]^n,\\
&\|\psi_{5n}(t)\| \leq \|B(0)\|\left[\tfrac{(1-\alpha)\theta^{1-\alpha}}{M(\alpha)}\varpi_5 + \tfrac{t\theta^{1-\alpha}}{M(\alpha)\Gamma(\alpha)}\varpi_5\right]^n,\\
&\|\psi_{6n}(t)\| \leq \|S_h(0)\|\left[\tfrac{(1-\alpha)\theta^{1-\alpha}}{M(\alpha)}\varpi_6 + \tfrac{t\theta^{1-\alpha}}{M(\alpha)\Gamma(\alpha)}\varpi_6\right]^n,\\
&\|\psi_{7n}(t)\| \leq \|I_{ah}(0)\|\left[\tfrac{(1-\alpha)\theta^{1-\alpha}}{M(\alpha)}\varpi_7 + \tfrac{t\theta^{1-\alpha}}{M(\alpha)\Gamma(\alpha)}\varpi_7\right]^n,\\
&\|\psi_{8n}(t)\| \leq \|I_{ch}(0)\|\left[\tfrac{(1-\alpha)\theta^{1-\alpha}}{M(\alpha)}\varpi_8 + \tfrac{t\theta^{1-\alpha}}{M(\alpha)\Gamma(\alpha)}\varpi_8\right]^n,\\
&\|\psi_{9n}(t)\| \leq \|R_h(0)\|\left[\tfrac{(1-\alpha)\theta^{1-\alpha}}{M(\alpha)}\varpi_9 + \tfrac{t\theta^{1-\alpha}}{M(\alpha)\Gamma(\alpha)}\varpi_9\right]^n.
\end{aligned}
\tag{27}
$$

Hence, the solutions exist and are provided continuously for the model (5). For the sake of clarity,

to exhibit that the functions $S(t)$, $V(t)$, $I(t)$, $E(t)$, $B(t)$, $S_h(t)$, $I_{ah}(t)$, $I_{ch}(t)$, and $R_h(t)$ have a solution to model (5), suppose that

$$
\begin{aligned}
S(t) - S(0) &= S_n(t) - \Phi_{1n}(t), \\
V(t) - V(0) &= V_n(t) - \Phi_{2n}(t), \\
E(t) - E(0) &= E_n(t) - \Phi_{3n}(t), \\
I(t) - I(0) &= I_n(t) - \Phi_{4n}(t), \\
B(t) - B(0) &= B_n(t) - \Phi_{5n}(t) \\
S_h(t) - S_h(0) &= S_{h,n}(t) - \Phi_{6n}(t), \\
I_{ah}(t) - I_{ah}(0) &= I_{ah,n}(t) - \Phi_{7n}(t), \\
I_{ch}(t) - I_{ch}(0) &= I_{ch,n}(t) - \Phi_{8n}(t), \\
R_h(t) - R_h(0) &= R_{h,n}(t) - \Phi_{9n}(t).
\end{aligned}
\tag{28}
$$

Accordingly, the expression $\|\Phi_{1n}(t)\|$ is acquired as:

$$
\begin{aligned}
\|\Phi_{1n}(t)\| &= \left\| \frac{(1-\alpha)\theta^{1-\alpha}}{M(\alpha)} \{F_1(t,S) - F_1(t,S_{n-1})\} \right. \\
&\quad \left. + \frac{\alpha\theta^{1-\alpha}}{M(\alpha)\Gamma(\alpha)} \int_0^t (t-\varrho)^{\alpha-1} \{F_1(\varrho,S) - F_1(\varrho,S_{n-1})\} d\varrho \right\| \\
&\leq \frac{(1-\alpha)\theta^{1-\alpha}}{M(\alpha)} \|F_1(t,S) - F_1(t,S_{n-1})\| \\
&\quad + \frac{\alpha\theta^{1-\alpha}}{M(\alpha)\Gamma(\alpha)} \int_0^t (t-\varrho)^{\alpha-1} \|F_1(\varrho,S) - F_1(\varrho,S_{n-1})\| d\varrho \\
&\leq \frac{(1-\alpha)\theta^{1-\alpha}}{M(\alpha)} \omega_1 \|S - S_{n-1}\| + \frac{t\theta^{1-\alpha}}{M(\alpha)\Gamma(\alpha)} \omega_1 \|S - S_{n-1}\|.
\end{aligned}
\tag{29}
$$

After using this process recursively, then yields at t_0

$$
\|\Phi_{1n}(t)\| \leq \left[\frac{(1-\alpha)\theta^{1-\alpha}}{M(\alpha)} + \frac{t_0\theta^{1-\alpha}}{M(\alpha)\Gamma(\alpha)} \right]^{n+1} \omega_1^{n+1} P_1.
\tag{30}
$$

As n approaches infinity, taking the limit to both sides of Eq. (30), it is obtained as $\|\Phi_{1n}(t)\| \to 0$. Consequently, the existence of the solution of the model (5) is verified. Similarly, it is found $\|\Phi_{2n}(t)\| \to 0$, $\|\Phi_{3n}(t)\| \to 0$, $\|\Phi_{4n}(t)\| \to 0$, $\|\Phi_{5n}(t)\| \to 0$, $\|\Phi_{6n}(t)\| \to 0$, $\|\Phi_{7n}(t)\| \to 0$, $\|\Phi_{8n}(t)\| \to 0$, and $\|\Phi_{9n}(t)\| \to 0$. Now, the uniqueness of the solution is given by the following theorem.

Theorem 3 *The model* (5) *has a unique solution, provided that*

$$
\frac{(1-\alpha)\theta^{1-\alpha}}{M(\alpha)} \omega_i + \frac{t_0\theta^{1-\alpha}}{M(\alpha)\Gamma(\alpha)} \omega_i < 1, \text{ for } i = 1, 2, ..., 9.
$$

Proof Assumed that $S_1(t)$, $V_1(t)$, $E_1(t)$, $I_1(t)$, $B_1(t)$, $S_{h1}(t)$, $I_{ah1}(t)$, $I_{ch1}(t)$, and $R_{h1}(t)$ are also solutions of the model (5). Then,

$$
\begin{aligned}
S(t) - S_1(t) &= \frac{(1-\alpha)\theta^{1-\alpha}}{M(\alpha)} \{F_1(t,S) - F_1(t,S_1)\} \\
&\quad + \frac{\alpha\theta^{1-\alpha}}{M(\alpha)\Gamma(\alpha)} \int_a^t (t-\varrho)^{\alpha-1} \{F_1(\varrho,S) - F_1(\varrho,S_1)\} d\varrho.
\end{aligned}
\tag{31}
$$

Considering that the kernel fulfills the Lipschitz condition, implementing the norm to both sides

of Eq. (31), it reaches the inequality presented below:

$$\|S(t) - S_1(t)\| \leq \frac{(1-\alpha)\theta^{1-\alpha}}{M(\alpha)}\varpi_1 \|S(t) - S_1(t)\| + \frac{t\theta^{1-\alpha}}{M(\alpha)\Gamma(\alpha)}\varpi_1 \|S(t) - S_1(t)\|. \quad (32)$$

It gives

$$\|S(t) - S_1(t)\| \left(1 - \frac{(1-\alpha)\theta^{1-\alpha}}{M(\alpha)}\varpi_1 - \frac{t\theta^{1-\alpha}}{M(\alpha)\Gamma(\alpha)}\varpi_1\right) \leq 0. \quad (33)$$

As $\left(1 - \frac{(1-\alpha)\theta^{1-\alpha}}{M(\alpha)}\varpi_1 - \frac{t\theta^{1-\alpha}}{M(\alpha)\Gamma(\alpha)}\varpi_1\right) > 0$, then $\|S(t) - S_1(t)\| = 0$. As a result, it is attained $S(t) = S_1(t)$. Similarly, it is seen that $V(t) = V_1(t)$, $E(t) = E_1(t)$, $I(t) = I_1(t)$, $B(t) = B_1(t)$, $S_h(t) = S_{h1}(t)$, $I_{ah}(t) = I_{ah1}(t)$, $I_{ch}(t) = I_{ch1}(t)$, and $R_h(t) = R_{h1}(t)$. Thus, it is concluded that model (5) has a unique solution.

4 Numerical solutions and discussion

In this section, numerical solutions of the improved fractional brucellosis model are obtained using the parameter values in Table 1 for $t = 12$ years. The initial conditions are $S(0) = 4.341 \times 10^7$, $V(0) = 8.44 \times 10^6$, $E(0) = 0$, $I(0) = 1.33 \times 10^6$, $B(0) = 6 \times 10^6$, $S_h(0) = 2.384 \times 10^7$, $I_{ah}(0) = 8663$, $I_{ch}(0) = 0$, and $R_h(0) = 0$ [42]. The Adams-type predictor-corrector method is applied to solve the fractional-order brucellosis model [46]. All numerical results are given by means of MATLAB.

Table 1. Interpretation of parameters in model (5)

Parameter	Value & Units & References
Λ_s	11629200 (sheep year^{-1}), [42]
β	1.48×10^{-8} (sheep^{-1}year^{-1}), [42]
ϕ	1.7×10^{-10} (bacteria^{-1} year^{-1}), [42]
ρ	10^7 (bacteria), Assumed
μ	0.22 (year^{-1}), [42]
ν	0.316 (year^{-1}), [42]
δ	0.4 (year^{-1}), [42]
ε	0.18 (year^{-1}), [42]
σ	1 (year^{-1}), [42]
c	0.15 (year^{-1}), [42]
k	15 (bacteria sheep^{-1} year^{-1}), [42]
d	3.6 (year^{-1}), [42]
n	0 (year^{-1}), [42]
τ	0 (year^{-1}), [42]
Λ_h	0.0057 (human year^{-1}), [47]
β_h	1.58×10^{-10} (sheep^{-1}year^{-1}), [42]
ϕ_h	1×10^{-11} (bacteria^{-1}year^{-1}), [42]
μ_h	0.0054 (year^{-1}), [47]
$\sigma_h p$	0.6 (year^{-1}), [42]
$\sigma_h(1-p)$	0.4 (year^{-1}), [42]
γ_{ch}	0.5 (year^{-1}), [48]

Figure 2 compares the developed fractional brucellosis model with the integer model over a 12-year period. The fractional brucellosis model demonstrates a slight reduction in the transmission of bacteria to sheep and humans with a saturated incidence rate. This reduction is observed due
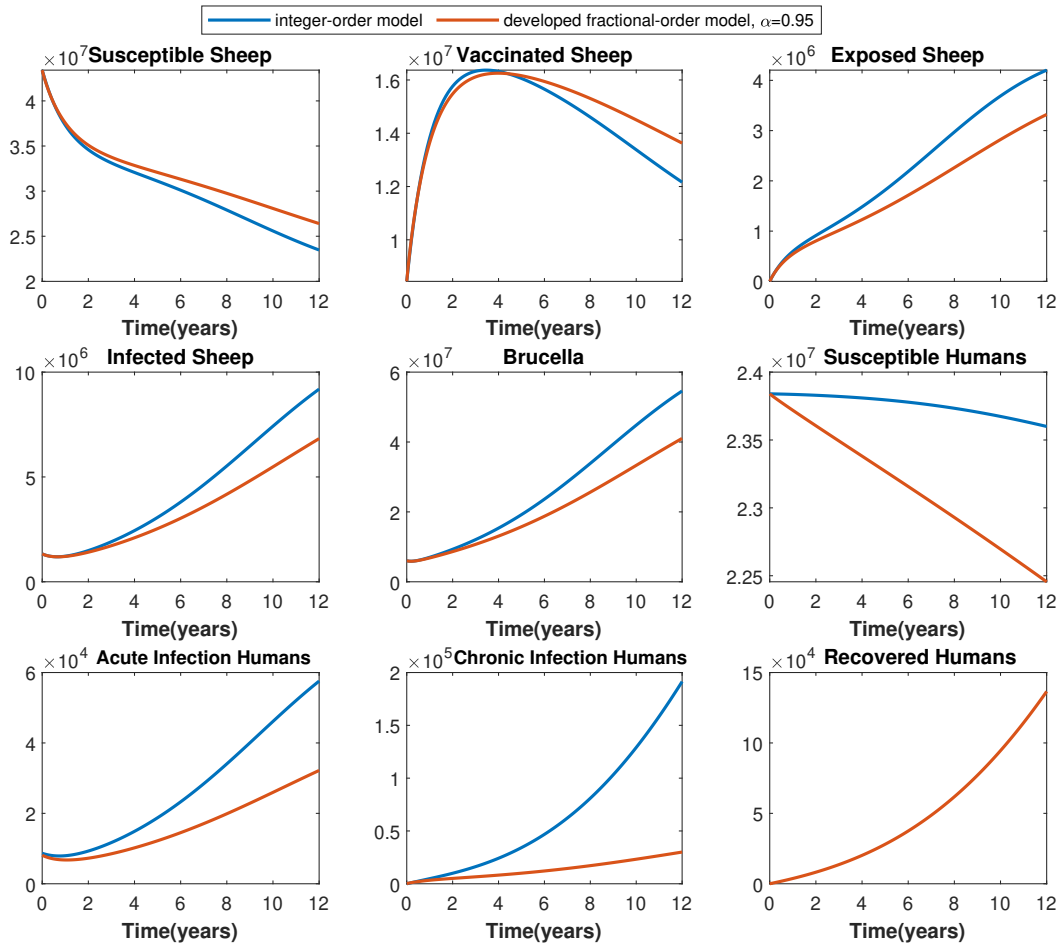
Figure 2. The comparison of the integer-order model with the developed fractional derivative model

to various factors, including the human birth and death rates and the existence of a recovered compartment. The inclusion of a recovered compartment of humans into the model resulted in a reduction in the number of susceptible individuals. In the integer order brucellosis model, chronically infected humans become susceptible upon recovery. In contrast, in the developed fractional brucellosis model, the behavior of susceptible and recovered humans in the process can be clearly examined with the addition of the recovered compartment of humans. This allows for the review of the transmission process with greater specificity. Moreover, a reduction in the rate of transmission is observed due to the continued shedding of Brucella bacteria from exposed and infected sheep throughout the process. Figure 3, the developed fractional brucellosis model is compared in different orders and this change is reflected in the graphical results as flexibility. In other words, the behavior appears to fade as the order of derivatives decreases. Nevertheless, it is evident from the graphs that an interspecies brucellosis epidemic has initiated. Consequently, it is imperative to implement various control strategies to eliminate the infection.

5   Conclusions

Brucellosis is an interspecies infectious disease that influences people and animal health, as well as financial growth in affected areas. Hence, figuring out the transmission dynamic of brucellosis has become crucial. For this purpose, a fractional-order model for interspecies transmission of brucellosis was developed. First, the current brucellosis transmission model with integer order
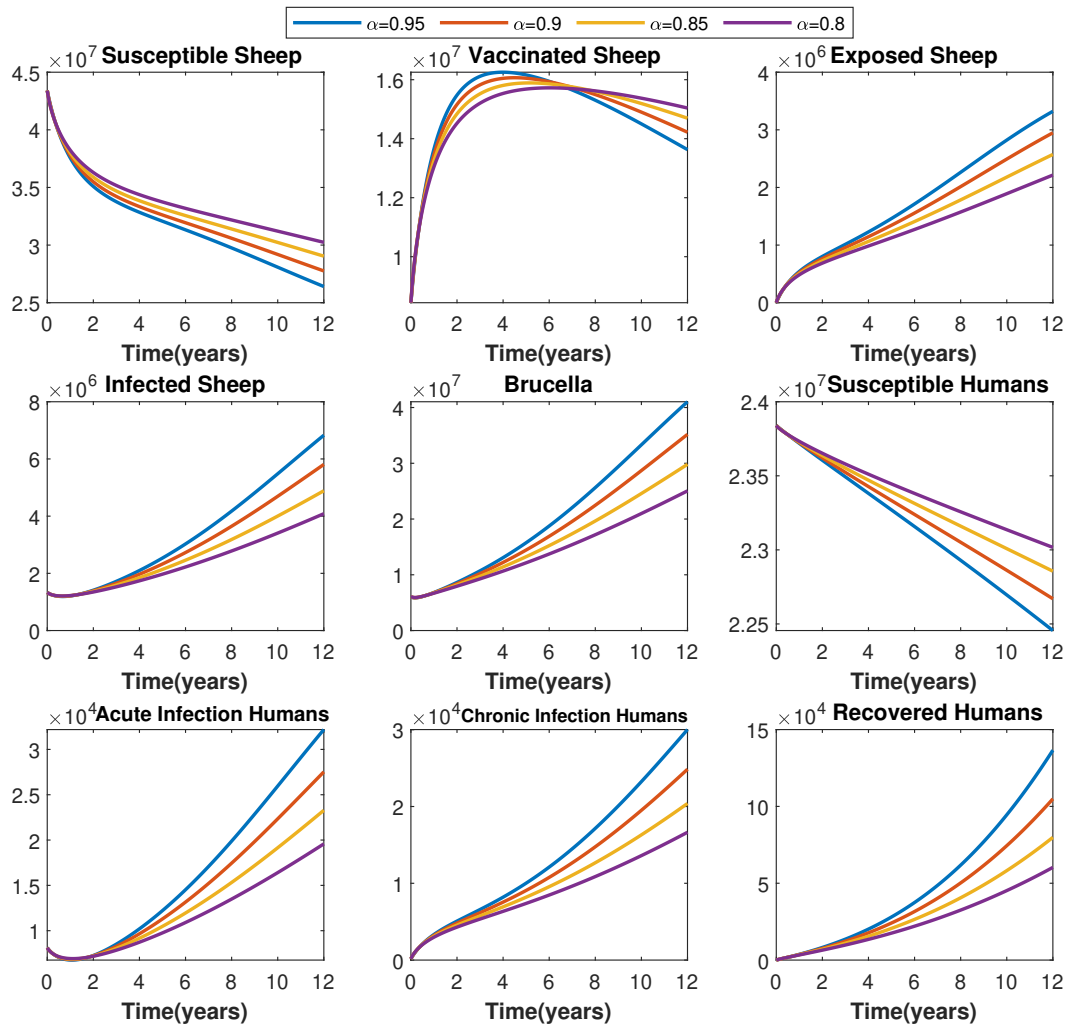
Figure 3. The comparison of the developed fractional derivative model with different fractional orders

was incorporated with the ABC fractional derivative to examine the transmission by its behavior. Then, to observe more specifically, the model was discussed with the recovered compartment, recruitment, and natural mortality rate for humans. Also, the saturated incidence rate was proposed for brucellosis as indirectly transmitted to individuals from the environment. The fixed-point theory was used to reveal the existence and uniqueness of solutions to the developed model. The model has been numerically solved using Adams-type predictor-corrector method with help of the MATLAB. Graphically, the effect of fractional derivatives of different orders on the model behavior was examined. It was observed that the interspecies brucellosis epidemic increased in the process. For this reason, an analysis of the dynamics and sensitivity of the developed fractional brucellosis model is planned for future work. Thus, we hope that the factors that cause brucellosis transmission, which adversely affects the community, could be determined.

Declarations

Use of AI tools

The authors declare that they have not used Artificial Intelligence (AI) tools in the creation of this article.

Data availability statement

All data generated or analyzed during this study are included in this article.

Ethical approval

The authors state that this research complies with ethical standards. This research does not involve either human participants or animals.

Consent for publication

Not applicable

Conflicts of interest

The authors declare that they have no conflict of interest.

Funding

Author's contributions

D.Y.: Investigation, Methodology, Formal Analysis, Writing-Original draft preparation, Visualization, Software. B.B.İ.E.: Project administration, Conceptualization, Validation, Supervision, Writing-Reviewing and Editing, Software. The authors have read and agreed to the published version of the manuscript.

Acknowledgements

Not applicable

References

[1] Pappas, G., Akritidis, N., Bosilkovski, M. and Tsianos, E. Brucellosis. *The New England Journal of Medicine*, 352, 2325-2336, (2005). [CrossRef]

[2] Doganay, M. and Aygen, B. Human brucellosis: an overview. *International Journal of Infectious Diseases*, 7(3), 173-182, (2003). [CrossRef]

[3] Roth, F., Zinsstag, J., Orkhon, D., Chimed-Ochir, G., Hutton, G., Cosivi, O. et al. Human health benefits from livestock vaccination for brucellosis: case study. *Bulletin of the World Health Organization*, 81, 867-876, (2003).

[4] Moreno, E. Retrospective and prospective perspectives on zoonotic brucellosis. *Frontiers in Microbiology*, 5, 213, (2014). [CrossRef]

[5] Li, M.T., Sun, G.Q., Wu, Y.F., Zhang, J. and Jin, Z. Transmission dynamics of a multi-group brucellosis model with mixed cross infection in public farm. *Applied Mathematics and Computation*, 237, 582-594, (2014). [CrossRef]

[6] Bonyah, E., Khan, M.A., Okosun, K.O. and Gómez-Aguilar, J.F. On the co-infection of dengue fever and Zika virus. *Optimal Control Applications and Methods*, 40(3), 394-421, (2019). [CrossRef]

[7] Ghaffari, P., Silva, C.J. and Torres, D.F.M. Mathematical models and optimal control in

mosquito transmitted diseases. In *Bio-Mathematics, Statistics, and Nano-Technologies: Mosquito Control Strategies* (pp. 143-156). New York, USA: Chapman and Hall/CRC, (2023). [CrossRef]

[8] Yapışkan, D., Yurtoğlu, M., Avcı, D., Eroğlu, B.B.İ. and Bonyah, E. A novel model for Monkeypox disease: system analysis and optimal preventive strategies. *Iranian Journal of Science*, 47, 1665-1677, (2023). [CrossRef]

[9] Tajani, A., El Alaoui, F.Z. and Boutoulout, A. Regional boundary controllability of semilinear subdiffusion Caputo fractional systems. *Mathematics and Computers in Simulation*, 193, 481-496, (2022). [CrossRef]

[10] Özaltun, G., Konuralp, A. and Gümgüm, S. Gegenbauer wavelet solutions of fractional integro-differential equations. *Journal of Computational and Applied Mathematics*, 420, 114830, (2023). [CrossRef]

[11] Tunç, O. and Tunç, C. Ulam stabilities of nonlinear iterative integro-differential equations. *Revista de la Real Academia de Ciencias Exactas, Físicas y Naturales. Serie A. Matemáticas,* 117(3), 118, (2023). [CrossRef]

[12] Wanassi, O.K. and Torres, D.F.M. An integral boundary fractional model to the world population growth. *Chaos, Solitons & Fractals,* 168, 113151, (2023). [CrossRef]

[13] Goyal, M., Baskonus, H.M. and Prakash, A. Regarding new positive, bounded and convergent numerical solution of nonlinear time fractional HIV/AIDS transmission model. *Chaos, Solitons & Fractals,* 139, 110096, (2020). [CrossRef]

[14] Veeresha, P., Malagi, N.S., Prakasha, D.G. and Baskonus, H.M. An efficient technique to analyze the fractional model of vector-borne diseases. *Physica Scripta,* 97(5), 054004, (2022). [CrossRef]

[15] Zaitri, M.A., Zitane, H. and Torres, D.F.M. Pharmacokinetic/Pharmacodynamic anesthesia model incorporating psi-Caputo fractional derivatives. *Computers in Biology and Medicine,* 167, 107679, (2023). [CrossRef]

[16] Eroğlu, B.B.İ and Yapışkan, D. Optimal strategies to prevent COVID-19 from becoming a pandemic. In *Mathematical Modeling and Intelligent Control for Combating Pandemics, Springer Optimization and Its Applications* (pp. 39-55). Cham, Switzerland: Springer, (2023). [CrossRef]

[17] Hussain, S., Tunç, O., ur Rahman, G., Khan, H. and Nadia, E. Mathematical analysis of stochastic epidemic model of MERS-corona & application of ergodic theory. *Mathematics and Computers in Simulation,* 207, 130-150, (2023). [CrossRef]

[18] Yapışkan, D. and Eroğlu, B.B.İ. Fractional optimal control of a generalized SIR epidemic model with vaccination and treatment. In *Fractional Dynamics in Natural Phenomena and Advanced Technologies* (pp. 131-150). Newcastle upon Tyne, UK: Cambridge Scholars Publishing, (2024).

[19] Yurtoğlu, M. and Avcı, D. Optimal antivirus strategies for a virus propagation modelled with Mittag-Leffler Kernel. In *Fractional Dynamics in Natural Phenomena and Advanced Technologies* (pp. 113-130). Newcastle upon Tyne, UK: Cambridge Scholars Publishing, (2024).

[20] Musafir, R.R., Suryanto, A. and Darti, I. Optimal control of a fractional-order Monkeypox epidemic model with vaccination and rodents culling. *Results in Control and Optimization*, 14, 100381, (2024). [CrossRef]

[21] Li, M., Sun, G., Zhang, J., Jin, Z., Sun, X., Wang, Y. et al. Transmission dynamics and control for a brucellosis model in Hinggan League of Inner Mongolia, China. *Mathematical Biosciences and Engineering*, 11(5), 1115-1137, (2014). [CrossRef]

[22] Li, M.T., Sun, G.Q., Zhang, W.Y. and Jin, Z. Model-based evaluation of strategies to control

brucellosis in China. *International Journal of Environmental Research and Public Health,* 14(3), 295, (2017). [CrossRef]

[23] Lolika, P.O., Mushayabasa, S., Bhunu, C.P., Modnak, C. and Wang, J. Modeling and analyzing the effects of seasonality on brucellosis infection. *Chaos, Solitons & Fractals,* 104, 338-349, (2017). [CrossRef]

[24] Nyerere, N., Luboobi, L.S., Mpeshe, S.C. and Shirima, G.M. Modeling the impact of seasonal weather variations on the infectiology of brucellosis. *Computational and Mathematical Methods in Medicine,* 2020, 8972063, (2020). [CrossRef]

[25] Nyerere, N., Luboobi, L.S., Mpeshe, S.C. and Shirima, G.M. Mathematical model for brucellosis transmission dynamics in livestock and human populations. *Communications in Mathematical Biology and Neuroscience,* 2020(3), 1-29, (2020). [CrossRef]

[26] Sun, G.Q., Li, M.T., Zhang, J., Zhang, W., Pei, X. and Jin, Z. Transmission dynamics of brucellosis: mathematical modelling and applications in China. *Computational and Structural Biotechnology Journal,* 18, 3843-3860, (2020). [CrossRef]

[27] Lolika, P.O. and Helikumi, M. An intrinsic analysis of human brucellosis dynamics in Africa. *Asian Research Journal of Mathematics,* 18(11), 1-26, (2022). [CrossRef]

[28] Ma, X., Sun, G.Q., Wang, Z.H., Chu, Y.M., Jin, Z. and Li, B.L. Transmission dynamics of brucellosis in Jilin province, China: Effects of different control measures. *Communications in Nonlinear Science and Numerical Simulation,* 114, 106702, (2022). [CrossRef]

[29] Abagna, S., Seidu, B. and Bornaa, C.S. A mathematical model of the transmission dynamics and control of bovine brucellosis in cattle. *Abstract and Applied Analysis,* 2022, 9658567, (2022). [CrossRef]

[30] Thongtha, A. and Modnak, C. The bison–human–environment dynamics of brucellosis infection with prevention and control studies. *International Journal of Dynamics and Control,* 12, 551-570, (2024). [CrossRef]

[31] Peter, O.J. Transmission dynamics of fractional order brucellosis model using Caputo-Fabrizio operator. *International Journal of Differential Equations,* 2020, 2791380, (2020). [CrossRef]

[32] Lolika, P.O. and Helikumi, M. Dynamics and analysis of chronic brucellosis in sheep. *Journal of Advances in Mathematics and Computer Science,* 37(7), 61-81, (2022). [CrossRef]

[33] Guan, P., Wu, W. and Huang, D. Trends of reported human brucellosis cases in mainland China from 2007 to 2017: an exponential smoothing time series analysis. *Environmental Health and Preventive Medicine,* 23, 23, (2018). [CrossRef]

[34] Jajarmi, A., Yusuf, A., Baleanu, D. and Inc, M. A new fractional HRSV model and its optimal control: a non-singular operator approach. *Physica A: Statistical Mechanics and its Applications,* 547, 123860, (2020). [CrossRef]

[35] Biswas, A.S., Aslam, B.H. and Tiwari, P.K. Mathematical modeling of a novel fractional-order Monkeypox model using the Atangana-Baleanu derivative. *Physics of Fluids,* 35(11), (2023). [CrossRef]

[36] Slimane, I., Nieto, J.J. and Ahmad, S. A fractional-order bovine babesiosis epidemic transmission model with nonsingular Mittag-Leffler law. *Fractals,* 31(02), 2340033, (2023). [CrossRef]

[37] Hussain, G., Khan, A., Zahri, M. and Zaman, G. Stochastic permanence of an epidemic model with a saturated incidence rate. *Chaos, Solitons & Fractals,* 139, 110005, (2020). [CrossRef]

[38] Capasso, V. and Serio, G. A generalization of the Kermack-Mckendrick deterministic epidemic

model. *Mathematical Biosciences,* 42(1-2), 43-61, (1978). [CrossRef]

[39] Mwasa, A. and Tchuenche, J.M. Mathematical analysis of a cholera model with public health interventions. *Biosystems,* 105(3), 190-200, (2011). [CrossRef]

[40] Lemos-Paião, A.P., Silva, C.J. and Torres D.F.M. An epidemic model for cholera with optimal control treatment. *Journal of Computational and Applied Mathematics,* 318, 168-180, (2017). [CrossRef]

[41] Zhang, J., Jin, Z., Li, L. and Sun, X.D. Cost assessment of control measure for brucellosis in Jilin province, China. *Chaos, Solitons & Fractals,* 104, 798-805, (2017). [CrossRef]

[42] Hou, Q., Sun, X., Zhang, J., Liu, Y., Wang, Y. and Jin, Z. Modeling the transmission dynamics of sheep brucellosis in Inner Mongolia Autonomous Region, China. *Mathematical Biosciences,* 242(1), 51-58, (2013). [CrossRef]

[43] Atangana, A. and Baleanu, D. New fractional derivatives with nonlocal and non-singular kernel: theory and application to heat transfer model. *Thermal Science,* (20)2, 763-769, (2016). [CrossRef]

[44] Kermack, W.O. and McKendrick, A.G. A contribution to the mathematical theory of epidemics. *Proceedings of the Royal Society of London. Series A,* 115(772), 700-721, (1927). [CrossRef]

[45] Gómez-Aguilar, J.F., Rosales-García, J.J., Bernal-Alvarado, J.J., Córdova-Fraga, T. and Guzmán-Cabrera, R. Fractional mechanical oscillators. *Revista Mexicana de Física,* 58(4), 348-352, (2012).

[46] Baleanu, D., Jajarmi, A., Sajjadi, S.S. and Mozyrska, D. A new fractional model and optimal control of a tumor-immune surveillance with non-singular derivative operator. *Chaos: An Interdisciplinary Journal of Nonlinear Science,* 29(8), 083127, (2019). [CrossRef]

[47] Ma, J. National Bureau of Statistics of China. In *China Statistical Yearbook.* Beijing, China: China Statistics Press, (2010).

[48] Bosilkovski, M., Keramat, F. and Arapović, J. The current therapeutical strategies in human brucellosis. *Infection,* 49, 823-832, (2021). [CrossRef]

Bulletin of Biomathematics (BBM)

(https://bulletinbiomath.org)